DISPLACEMENT MONITORING BY INTEGRATING ON-LINE PHOTOGRAMMETRIC OBSERVATIONS WITH DYNAMIC INFORMATION

C. ARMENAKIS

November 1987

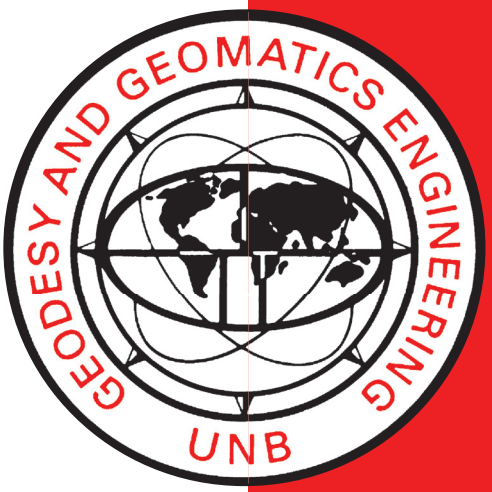

TECHNICAL REPORT
NO. 133

PREFACE

In order to make our extensive series of technical reports more readily available, we have scanned the old master copies and produced electronic versions in Portable Document Format. The quality of the images varies depending on the quality of the originals. The images have not been converted to searchable text.

DISPLACEMENT MONITORING BY INTEGRATING ON-LINE PHOTOGRAMMETRIC OBSERVATIONS WITH DYNAMIC INFORMATION

Constadinos Armenakis

Department of Surveying Engineering
University of New Brunswick
P.O. Box 4400
Fredericton, N.B.
Canada
E3B 5A3

November 1987

ABSTRACT

Data collection and -processing in photogrammetric monitoring are thoroughly investigated.

The determination of displacements by photogrammetry requires multiple photographic campaigns and therefore photo-measurements on multi-temporal photographs. An on-line semi-automatic photogrammetric system for targetted and natural object points using the analytical stereo-plotter has been developed. In the case of targetted points, the analytical plotter has been utilized as an on-line mono-comparator with the measuring mark driven automatically to predetermined photo-locations. For natural points an integrated "cross-identification" and measuring procedure has been designed and implemented. The combination of comparator/stereo-plotter mode allows the point-transfer operation to be done "digitally". In both cases image positioning is performed under computer control, and on-line editing capabilities are provided.

A combined sequential photogrammetric approach was developed for data processing. The dynamic characteristics of the object position vectors are introduced in both the functional and stochastic models. Thus, the single-epoch static photogrammetric model has been extended to incorporate the additional object information where the object parameter vector is updated not only as new observations become available but also as a function of time.

Examples with real and simulated data are given which demonstrate the usefulness of the newly developed methodologies.

That is, a) the time required for the photo-measurements is significantly reduced while their accuracy has been improved, and b) the integration of photogrammetric and dynamic information provides better estimation for the location and accuracy of the unknown parameters.

TABLE OF CONTENTS

TABLE OF CONTENTS (Cont'd)

TABLE OF CONTENTS (Cont'd)

LIST OF TABLES

LIST OF FIGURES

LIST OF FIGURES (Cont'd)

LIST OF FIGURES (Cont'd)

ACKNOWLEDGEMENTS

A number of individuals and organizations contributed to the completion of this research work. Without their support the end would still be just a dream.

The financial support from the University of New Brunswick and the Natural Science and Engineering Research Council of Canada is thankfully acknowledged.

I am grateful to my supervisor, Dr. Wolfgang Faig, for his continuous assistance, guidance, and interest in this work. Our discussions were always fruitful, constructive, and enjoyable.

For reviewing the original manuscript and for their constructive criticism and remarks, Dr. E. Derenyi, Dr. A. Chrzanowski and Dr. Y.C. Lee of the Department of Surveying Engineering, Dr. L. Garey of the University of New Brunswick in Saint John, Dr. T. Needhanm of the Department of Forest Engineering, and Dr. V. Kratky of Energy, Mines and Resources Canada are gratefully acknowledged.

I wish to thank Dr. S. Masry for providing useful information on the analytical stereo-plotter. For introducing me to the PDP 11/60 computer, Dr. Y.C. Lee and Mr. T. McCarthy and Mr. R. Mullin of Universal Systems Ltd. are thankfully acknowledged.

I owe an awful lot to my wife Anne and to my son Lee. Anne's continuous encouragment and patience bolstered my morale during the difficult periods of this work. I am also grateful to her for the excellent and diligent typing work she did in order to transfer my

handwritten manuscript to its final typed form. Lee offered me the most enjoyable breaks from my work during this research.

My brother Antonis Armenakis of the Department of Mathematics and Statistics deserves credit for his cheerful attitude and his valuable advice on mathematical and statistical subjects.

My parents never stopped supporting me, even from a distance. My parents-in-law also provided constant encouragement in my work.

Kathy Stratton's contribution to the typing part of this work is very much appreciated.

The presence of Marinos Kavouras, Stelios Mertikas, Kostas Papanikolaou, Stratis and Despina Tsamouras, and Panos and Maria Hourdakis has given me many unforgettable happy memories.

I also wish to thank my graduate colleagues for their co-operation. In particular, I wish to mention the members of the Photogrammetric group, and especially Peter Shih for our many nocturnal discussions. Zhengdong Shi is thanked for providing the raw data for the laboratory test.

The assistance provided by the faculty members of the Department while attending their lectures is appreciated.

Finally, I must thank Mrs. Noreen Bonnell, Mrs. Theresa Pearce, and Mrs. Debbie Smith for the pleasant atmosphere I always found in the Office of Surveying Engineering and for the cheerful assistance they provided during my stay here.

Στην Αννα και στον Λη μας

1. INTRODUCTION

The Greek philosopher Heracletos, in his effort to answer the cosmogony questions of his times, said in 500 BC that "All is flux". In archaic terms this means that everything is variable or unstable. This is confirmed by the physical model known as "cause"- "transmission" - "effect" under which almost every part of the earth's surface and even man-made structures are subject to variations of size, shape and position with time. The period of these changes differs from case to case depending on the individual characteristics of the deformable body. The determination and sometimes also the interpretation of these movements is the objective of deformation surveys.

The necessity of detecting, monitoring, and interpreting displacements is dictated by four major concerns: a) safety, b) scientific, c) economic, and d) environmental. A great number of lives have been lost because of dam failures, mining catastrophes, land slides, collapsed buildings, -bridges, or -tunnels. It is obvious that continuous and rigorous monitoring of the natural or man-made environment is vital in predicting and preventing a future disaster. The precise determination of variations of a body can support and aid in improving new design theories by providing information about the load-deformation relationship. The body of

knowledge on deformation mechanisms can also be enhanced, which leads to the development of more sophisticated and refined procedures. Capital losses also strongly support deformation studies. Infrastructure failures such as bridges and dams can cause damages of thousands to millions of dollars even if no lives are lost. Subsidence phenomena cause property damages, disruption of operations and of general communications. Furthermore, environmental awareness has grown in recent decades. Concerns have been raised about the sinking of cities (e.g., Venice, Bangkok, Mexico City) and about reclamation of damaged lands. As has been stated by Faig, (1986) "Deformation measurements, if properly conducted, provide the best preventative medicine and as such are well worth the investment for society".

Historically, surveying engineers have been involved in the field of measuring and evaluating movements because of their professional expertise. The different methodologies and techniques used are presented in Chapter 2 together with their associated advantages and limitations. In the same chapter, the displacement transformation matrix is derived and the relationship between displacement and deformation is proven by the author. Factors affecting the significance of the estimated displacements are also analysed.

Photogrammetry is one of the methods used by surveying engineers to determine position, shape, and size of objects related to a spatial reference system. In Chapter 3, the advantages of photogrammetry in the area of monitoring displacements are examined, and at the same time several limitations of the photogrammetric

systems are discussed. Emphasis is given to the design aspects of the photogrammetric monitoring networks so that possible optimal results are obtained. The different photogrammetric approaches are presented and examined. Various photogrammetric examples demonstrate the capabiltiy of photogrammetry to successfully complete monitoring projects.

However, the photogrammetric potential in this area has not yet been fully exploited. For example, at the IIIrd International Symposium of Deformation Measurements by Geodetic Methods held in Budapest in 1982, the following recommendations were adopted:

"In accordance with the resolutions of the Montreux FIG Congress, more attention must be paid to the applications of remote sensing technology in the field of deformation measurements in cooperation with the ISPRS Commission 5. It is justified to increase research in complex photogrammetric systems for use in deformation measurements. The international cooperation, connected with these complex systems, should be expanded".

A photogrammetric monitoring system consists of three parts: data acquisition (photography), data collection (photo-measurements), and data processing (computations, results, and evaluation). Attention was focused on the last two aspects based on previous experience (e.g., Armenakis, 1983) and practical considerations. Thus, the objectives of this research were set to be in the improvement of the photogrammetric monitoring systems by contributing to the phases of data collection and -processing (Chapters 4 and 5). The purpose of this research is twofold: a) to design and implement a data collection system which will accelerate the measuring process while at the same time improving the quality of the photo-measurements; and b) to enhance the photogrammetric mathematical model by combining it with external dynamic object information in order to

improve the estimation of both the position and the accuracy of the unknown parameters.

For the photogrammetric determination of displacements, multiple photo-observation campaigns are necessary which require measurements on multi-temporal photographs. While the conventional procedures do not contain inherent critical problems with targetted points other than the lack of automation, the situation changes drastically when natural object points are involved. Their quality, the elimination of possible misidentifications during point-transfer operations, the ease of storage, retrieval, editing, and measuring are all aspects of major importance in a modern photogrammetric monitoring system.

One of the prerequisites was the introduction of automation to replace several manual operations and their inherent errors. Automated procedures are more cost effective as they are faster, more accurate, less expensive and also help to generate new products, e.g., in data editing and data management. The analytical photogrammetric stereo-plotter was chosen as the most suitable type of instrumentation. Its on-line capabilities and analytical solutions are described, together with its limitations for this specific research. These limitations were circumvented by designing new procedures, which along with the developed analytical measuring methods, led to the development and implementation by the author of an on-line semi-automatic photogrammetric measuring system for targetted and natural photo-points.

In the case of targetted points, the analytical plotter is utilized as an on-line mono-comparator. For the natural points, the

combination of stero-comparator/plotter mode allows the point-transfer operations to be performed "digitally". For both types of object points, the measurements (or image positioning) are performed under computer control.

Until now, most of the deformation models were of a static type aiming for a statistical statement showing the existence or non-existence of movements in the space domain. Present developments focus on dynamic models (Gerstenecker et al., 1978; Papo, 1985), where displacements are studied with respect to time and frequency of occurence and moreover, as functions of causative parameters (Welsch, 1981).

As a direct three-dimensional monitoring scheme, photogrammetry has rarely used the time factor extensively as the fourth dimension. Monitoring photogrammetry has merely been used as a single frame in a movie film, one out of a series of frames which together present the complete four-dimensional picture of the behaviour of the moving object. That is, each new position of the object points determining the trajectories of the points in motion is estimated independently of the preceding one. What is needed then, is a connecting factor for all these single frames. The time factor can serve this purpose if it can be expressed as a parameter of functions representing a dynamic state.

In order to study the dynamic characteristics of the displacements, where the actual positions of the object points change not only as new observations become available but also progressively as a result of a cause, the photogrammetric observation model can be supported and improved by a functional

relationship between the object points at successive epochs. Thus, the dynamic characteristics of the displacements are not ignored because this information can be directly incorporated into the photogrammetric evaluation model. These principles are described, examined, analysed, discussed, and further developed in Chapter 5. As a result, a combined photogrammetric and prediction approach has been designed and implemented by the author. The developed mathematical model of a sequential photogrammetric procedure for monitoring displacements is based on the principles of sequential least squares adjustments. Attention is also paid to practical, numerical and computational considerations and restrictions. The final iterated extended linearized formulae derived for the updated estimation of the object information (position and accuracy) can be considered equivalent to the principle of Bayes or Kalman filtering which is found in the theory of optimal estimation. (Swerling, 1971; Krakiwsky, 1975; Junkins, 1978; Vanicek and Krakiwsky, 1986).

The developments in the data collection and data processing phases which constitute the core of this research were implemented in two main software packages. These packages provided the means for the application, verification and evaluation of the solutions proposed by the author. In Chapter 6 three examples are utilized to examine the potential of these ideas. Simulated and real data are incorporated.

The findings of this research are summarized in Chapter 7. The performance of the proposed methods is evaluated and recommendations are made based on the knowledge and experience gained through this study.

2. DISPLACEMENTS AND DEFORMATION

Usually, for monitoring purposes the entire deformable body is represented by a number of properly distributed discrete points called detail points. Under certain circumstances, forces applied either by the surrounding matter or by direct contact or by gravity cause the body to alter position and shape. The determination of these changes can be done by monitoring the position of the detail points with respect to a reference system at time intervals depending on the frequency and rate of motion. Therefore, each detail point is considered to be in a continuous motion in the space and time domain.

2.1 Expressions of Displacements

As has been stated earlier, our objective is to monitor the trajectories of the points representing the deformable object. The study of the geometry of motion (change in the position of a particle) ignoring the force action that produces it, is referred to as kinematics. Kinematics deals with four basic concepts: position (and displacement), velocity, acceleration and jerk. We concentrate on the aspect of position since the remaining three terms can be

defined as functions of position through time.

The position of a detail point P with respect to a Cartesian coordinate system may be defined in terms of magnitude (length) and direction of the radius vector **p**. That is, the position vector OP = **p** (Fig. 2.1) is determined as

$$\mathbf{p} = x\mathbf{i} + y\mathbf{j} + z\mathbf{k} \qquad (2.1)$$

where **i**, **j**, and **k** are the unit vectors along the positive direction of the orthogonal X, Y, and Z axes. Vector **p** can also be expressed as a function of the unit vector $\mathbf{p}_u$ along **p** as

$$\mathbf{p} = || \mathbf{p} || \, \mathbf{p}_u \qquad (2.2)$$

where

$$|| \mathbf{p} || = (x^2 + y^2 + z^2)^{1/2} \qquad (2.3)$$

is the length or Euclidean norm of vector **p**.

The direction of the vector **p** can be defined in terms of the direction of the unit vector $\mathbf{p}_u$. By equating equs.(2.1) and (2.2) we get

$$\mathbf{p}_u = \frac{x}{|| \mathbf{p} ||}\mathbf{i} + \frac{y}{|| \mathbf{p} ||}\mathbf{j} + \frac{z}{|| \mathbf{p} ||}\mathbf{k} \qquad (2.4a)$$

or

$$\mathbf{p}_u = \mathbf{i} \cos\alpha + \mathbf{j} \cos\beta + \mathbf{k} \cos\gamma \qquad (2.4b)$$

where α, β, and γ are the angles between **p** and the positive directions of the OX, OY and OZ axes. Since, $\cos\alpha = x/||\mathbf{p}||$, $\cos\beta = y/||\mathbf{p}||$ and $\cos\gamma = z/||\mathbf{p}||$ are associated with the direction of a line; they are called the direction cosines of the line and are often denoted by l, m, and n respectively.

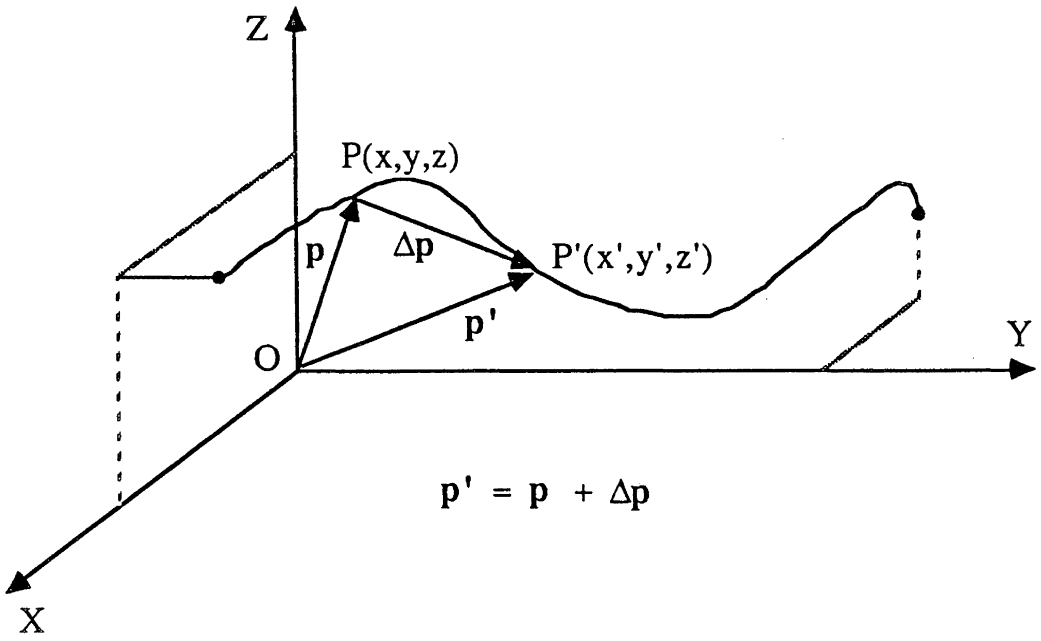

Figure 2.1: Position vectors $\mathbf{p}$ and $\mathbf{p}'$ and displacement vector $\Delta\mathbf{p}$.

Consider that point P is moving along a path in space and that after time δt is displaced from P to its new position P' through a distance $\Delta\mathbf{p}$. The trajectory of P can then be described by the position vector

$$\mathbf{p}(t) = x(t)\ \mathbf{i} + y(t)\ \mathbf{j} + z(t)\ \mathbf{k} \qquad (2.5)$$

We can now define that displacement is a change in position of a point within a time period δt. Although that displacement is expressed by the displacement vector $\Delta\mathbf{p} = OP' - OP$, the motion which governs the change may occur along any of an infinite number of paths.

A general displacement is expressed as the difference of the coordinates between the two positions of point P. Thus,

$$\Delta \mathbf{p} = \mathbf{p}' - \mathbf{p} = (x'-x \quad y'-y \quad z'-z)^T = (\delta x \quad \delta y \quad \delta z)^T \quad (2.6)$$

However, sometimes it is convenient to define a displacement in terms of the simplest motion which could produce it. Based on Chasles' theorem for rigid bodies (Beggs, 1983), the most general displacement of a point P is composed of a change (extension or contraction) of the length of the position vector by k and a simultaneous rotation Θ about an axis Oe through the origin of the coordinate system (Fig. 2.2).

This is analysed to be a scale change of the coordinate components of the position vector along the axes followed by three sequential rotations of the position vector around the axes.

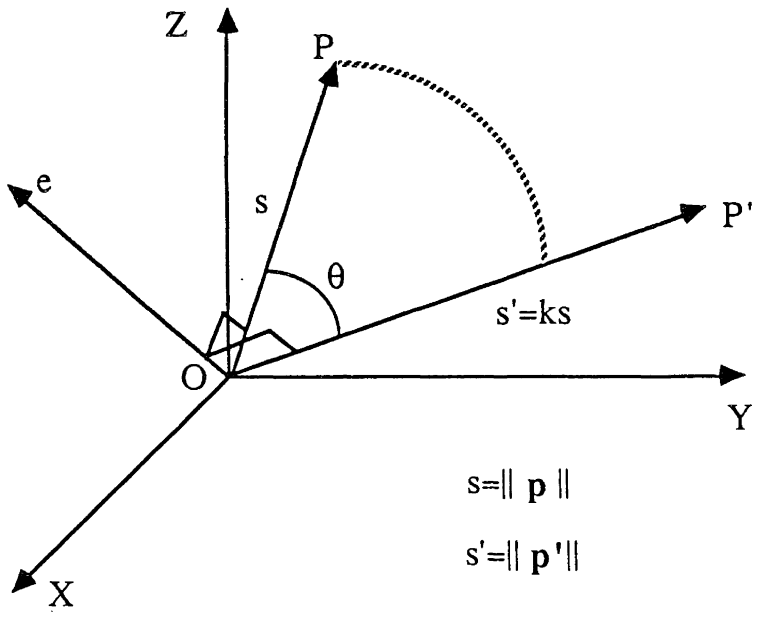

Figure 2.2: Displacement components of the simplest path motion.

Generally, we can say that the new position vector **p'** of **p** is represented by

$$\mathbf{p'} = \mathbf{Tp} + \mathbf{h} \qquad (2.7)$$

where **T** is the displacement transformation matrix and **h** is the translation vector. However, since the rotation axis Oe passes through the origin O, then $\mathbf{h} = \mathbf{0}$ and equ.(2.7) becomes

$$\mathbf{p'} = \mathbf{T} \cdot \mathbf{p} \qquad (2.8)$$

The displacement matrix **T** represents the effects of the causes, which displace **p** to **p'**. In this case the displacement $\Delta\mathbf{p}$ is defined as

$$\Delta\mathbf{p} = \mathbf{p'} - \mathbf{p} = \mathbf{Tp} - \mathbf{p} = (\mathbf{T} - \mathbf{I})\mathbf{p} = \mathbf{Dp} \qquad (2.9)$$

where $\mathbf{D} = (d_{ij})$ is the matrix of actual displacement with

$$d_{ij} = t_{ij} - \delta_{ij},$$

with δ_{ij} being the Kronecker symbol.

To compare the two approaches (equs.(2.6) and (2.9)) expressing the displacement vector $\Delta\mathbf{p}$, the new position vector **p'** in equ.(2.6) is expressed by incorporating the translation vector **p** into a general 4 by 4 matrix as

$$\begin{bmatrix} 1 \\ \hline \mathbf{p'} \end{bmatrix} = \left[\begin{array}{c|c} 1 & \mathbf{O}^T \\ \hline \Delta\mathbf{p} & \mathbf{I} \end{array}\right] \begin{bmatrix} 1 \\ \hline \mathbf{p} \end{bmatrix} \qquad (2.10)$$

where **p**, **p'**, $\Delta\mathbf{p}$ are 3 by 1 vectors, **O** is a 3 by 1 zero vector and **I** is a 3 by 3 identity matrix.

Consequently, both expressions of displacements describe the relation between the new and the old position vectors using a transformation - or transition matrix. In this study equ.(2.8) has been chosen to express the displacement of point P to its new position P' for the following reasons.

1) As will be shown in the next sections, the matrix **T** provides direct information about the deformity and the attitude of the position vector **p**. Hence, **p** can be defined at any time t. In contrast, equ.(2.10) requires knowledge of the final result $\Delta\mathbf{p}$ regardless of cause.
2) It offers the possibility to group certain areas of the deformable body for which there are strong indications that they have the same (or even similar) displacement and deformation effects.
3) If certain deformation properties of the body are known, the displacement vector $\Delta\mathbf{p}$ can be estimated directly from the actual displacement matrix **D** and the initial position vector **p** (equ.(2.9)) without having to estimate the final position vector $\mathbf{p}'$ (equ.(2.6)).
4) The state of vector $\mathbf{p}'$ is related to the one of **p** by a more familiar 3 by 3 matrix and not by a 4 by 4 hypermatrix as in equ.(2.10).

Nevertheless, both representations of displacements are equivalent. This can be easily proved by expressing the position vector in cartesian and polar coordinates respectively. Either form can be adopted depending on the specific application and problem.

2.2 Derivation of the Displacement Transformation Matrix T

The displacement of a point using the simplest path motion given by equ.(2.8) may be produced by a special family of linear transformations called affine transformations (Wells and Frankich,

1983; Martin, 1982; Anton, 1984).

For a deformable body the change of its position and shape is due to the individual effect of the next affine transformations: orthogonal rotation, scalar transformation, elongation (expansion) or compression, and shear. These transformations express geometrically how a point P moves to its new position P'. Their effects on the position vector **p** are:

1) Three-dimensional rotation. The length of **p** remains unchanged, while its direction changes (Fig. 2.3a)

$$\mathbf{p}' = \mathbf{M}\,\mathbf{p} = \begin{bmatrix} m_{11} & m_{12} & m_{13} \\ m_{21} & m_{22} & m_{23} \\ m_{31} & m_{32} & m_{33} \end{bmatrix} \begin{bmatrix} x \\ y \\ z \end{bmatrix} \qquad (2.11)$$

where $\mathbf{M} = \mathbf{M}_x \cdot \mathbf{M}_y \cdot \mathbf{M}_z$ and $\mathbf{M}_x$, $\mathbf{M}_y$, $\mathbf{M}_z$ are othogonal matrices representing the rotation of the vector **p** about three axes respectively.

2) Three-dimensional scaling. The direction of **p** remains unchanged, while its length is changed linearly along the three coordinate axes (Fig.2.3b).

$$\mathbf{p}' = s\,\mathbf{I}\,\mathbf{p} = s \begin{bmatrix} 1 & 0 & 0 \\ 0 & 1 & 0 \\ 0 & 0 & 1 \end{bmatrix} \begin{bmatrix} x \\ y \\ z \end{bmatrix} \qquad (2.12)$$

where s is the scale factor.

3) Three-dimensional expansion or compression (strain). The length of vector **p** is changed differently along the three coordinate axes (Fig.2.3c)

$$\mathbf{p}' = \mathbf{E}\,\mathbf{p} = \begin{bmatrix} e_x & 0 & 0 \\ 0 & e_y & 0 \\ 0 & 0 & e_z \end{bmatrix} \begin{bmatrix} x \\ y \\ z \end{bmatrix} \qquad (2.13)$$

where e_x, e_y, and e_z are the scale factors along the corresponding axes.

If $0 < e_i < 1$ we have compression,

if $e_i > 1$ we have expansion, and

if $e_i = 1$ there is no change of scale along the i^{th} direction $(i = x,y,z)$.

4) Three-dimensional shearing. This is the lateral displacement of the position vector along planes parallel to the coordinate axes. According to Faux and Pratt, (1983) and from Figure (2.3d) we can see that for a point P with position vector **p** the inner product

$$\tau = \mathbf{u}^T \mathbf{p} \qquad (2.14)$$

is the length of the perpendicular distance between point P and a plane parallel to the slip plane (ε) passing through the origin. In the case of two dimensions, this expresses the distance between slip line ε and the OX axis with **u** being the unit vector at P normal to the line ε. If P slides along line ε then the new position vector **p'** can be defined as (ibid)

$$\mathbf{p}' = \mathbf{p} + \Delta\mathbf{p} = \mathbf{p} + \beta\,\tau\,\mathbf{s} \qquad (2.15)$$

where the displacement vector $\Delta\mathbf{p}$ is expressed as a quantity proportional to τ. β is a scalar constant and **s** is the direction of line ε.

Because of equ.(2.14), equ.(2.15) becomes

$$\mathbf{p}' = \mathbf{p} + \beta\,(\mathbf{u}^T \mathbf{p})\,\mathbf{s} = \mathbf{p} + \beta\,\mathbf{s}\,(\mathbf{u}^T \mathbf{p}) =$$

$$= (I + \beta \, s \, u^T) \, p \qquad (2.16)$$

Based on equ.(2.16) the new position vector p' of p after shearing is expressed generally as

$$p' = S \; p = \begin{bmatrix} 1 & a & b \\ c & 1 & d \\ e & f & 1 \end{bmatrix} \begin{bmatrix} x \\ y \\ z \end{bmatrix} \qquad (2.17)$$

where a, b, c, d, e, and f result by multiplying β by the elements of the vector product su^T, with $s = (s_i \; s_j \; s_k)^T$ and $u = (u_i \; u_j \; u_k)^T$.

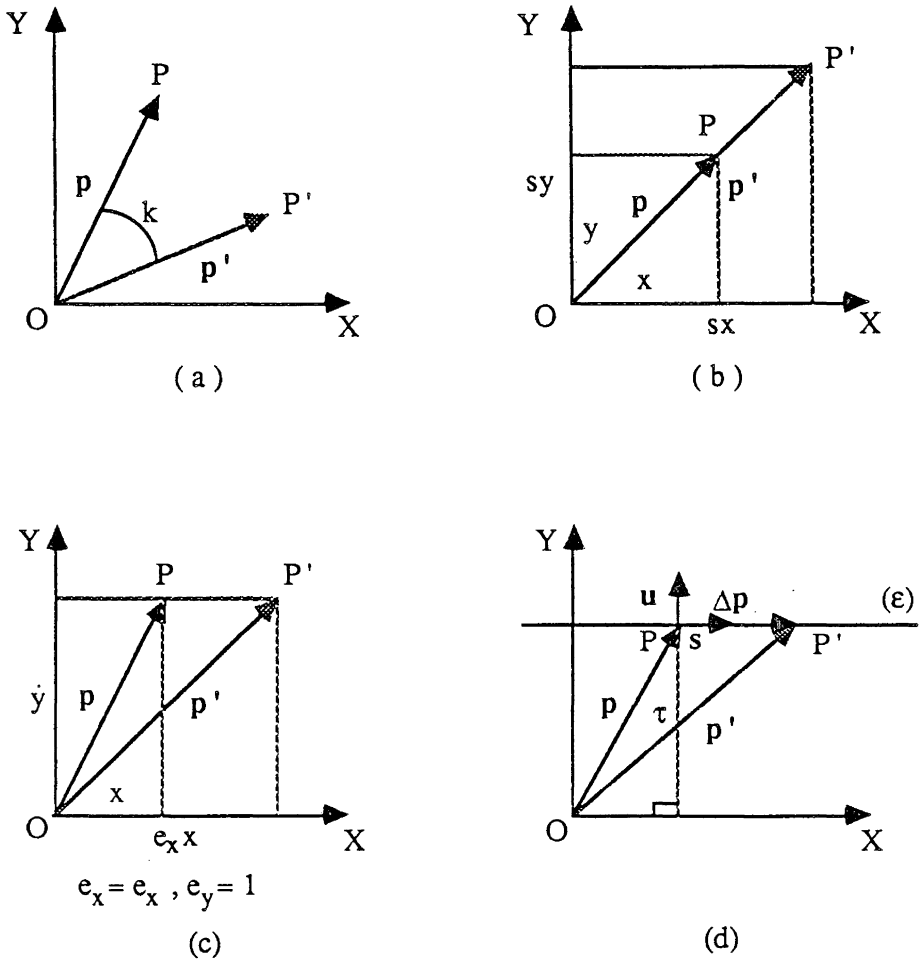

Figure 2.3: Affine transformations in two dimensions.

Combining all the above effects on the position of point P we derive the final form of the compound transformation matrix **T** as

$$\mathbf{T} = s\ \mathbf{I}\cdot\mathbf{S}\cdot\mathbf{E}\cdot\mathbf{M} = \begin{bmatrix} t_{11} & t_{12} & t_{13} \\ t_{21} & t_{22} & t_{23} \\ t_{31} & t_{32} & t_{33} \end{bmatrix} \qquad (2.18)$$

The elements t_{ij} of **T** are

$$\begin{aligned}
t_{11} &= s\,(\ e_x m_{11} + a\, e_y m_{21} + b\, e_z m_{31}) \\
t_{12} &= s\,(\ e_x m_{12} + a\, e_y m_{22} + b\, e_z m_{32}) \\
t_{13} &= s\,(\ e_x m_{13} + a\, e_y m_{23} + b\, e_z m_{33}) \\
t_{21} &= s\,(c\, e_x m_{11} + \ e_y m_{21} + d\, e_z m_{31}) \\
t_{22} &= s\,(c\, e_x m_{12} + \ e_y m_{22} + d\, e_z m_{32}) \\
t_{23} &= s\,(c\, e_x m_{13} + \ e_y m_{23} + d\, e_z m_{33}) \\
t_{31} &= s\,(e\, e_x m_{11} + f\, e_y m_{21} + \ e_z m_{31}) \\
t_{32} &= s\,(e\, e_x m_{12} + f\, e_y m_{22} + \ e_z m_{32}) \\
t_{33} &= s\,(e\, e_x m_{13} + f\, e_y m_{23} + \ e_z m_{33})
\end{aligned}$$

The final form of the displacement matrix **T** shows that we are only interested in the geometric components of the motion of a point and not in the causes of the motion.

2.3 Factorization of the Displacement Matrix T according to the Simplest Path Theorem

According to the simplest path theorem the displacement matrix should represent an extension (or contraction) along the three orthogonal axes and three rotations about these axes. This means that the matrix **T** must be decomposed as

$$\mathbf{T} = k \cdot \mathbf{Q} \qquad (2.19)$$

where

k : is a scale factor

Q : is a three-dimensional orthogonal rotation matrix

Based on the properties of orthogonal matrices, the elements of the displacement matrix are necessary to fulfil the following conditions:

$$A = B = C = k^2 \tag{2.20a}$$

$$D = E = F = 0 \tag{2.20b}$$

where

$$A = \sum_{i=1}^{3} t_{i1}^2 \tag{2.21a}$$

$$B = \sum_{i=1}^{3} t_{i2}^2 \tag{2.21b}$$

$$C = \sum_{i=1}^{3} t_{i3}^2 \tag{2.21c}$$

$$D = \sum_{i=1}^{3} t_{i1} \cdot t_{i2} \tag{2.21d}$$

$$E = \sum_{i=1}^{3} t_{i1} \cdot t_{i3} \tag{2.21e}$$

$$F = \sum_{i=1}^{3} t_{i2} \cdot t_{i3} \tag{2.21b}$$

Proof of $\mathbf{T} = k \cdot \mathbf{Q}$

Let k be the scale factor and $\mathbf{Q}$ the orthogonal rotation matrix between the two position vectors $\mathbf{p}$ and $\mathbf{p'}$, then according to equs.(2.8) and (2.19) $\mathbf{p'}$ is expressed as

$$\mathbf{p'} = \mathbf{T} \cdot \mathbf{p} = k \cdot \mathbf{Q} \cdot \mathbf{p} \tag{2.22}$$

Taking the square of the norm of $\mathbf{p}'$, we have

$$\begin{aligned} || \mathbf{p}' ||^2 = \mathbf{p}'^T \cdot \mathbf{p}' &= \mathbf{p}^T \cdot \mathbf{Q}^T \cdot k \cdot k \cdot \mathbf{Q} \cdot \mathbf{p} = \\ &= k^2 \cdot \mathbf{p}^T \cdot \mathbf{Q}^T \cdot \mathbf{Q} \cdot \mathbf{p} = k^2 \cdot \mathbf{p}^T \cdot \mathbf{p} = \\ &= k^2 \, || \mathbf{p} ||^2 \end{aligned} \tag{2.23}$$

Therefore, from equ.(2.23)

$$k^2 = \frac{|| \mathbf{p}' ||^2}{|| \mathbf{p} ||^2} \tag{2.24a}$$

or

$$k^2 = \frac{Ax^2 + By^2 + Cz^2 + 2Dxy + 2Exz + 2Fyz}{x^2 + y^2 + z^2} \tag{2.24b}$$

An affine transformation is a special case of collineation and preserves parallelism (Martin, 1982). That is, this type of linear transformation is independent of the slope of the position vectors, and the slope of a line connecting two transformed points depends only on the slope of the line joining the detail points and not on the position vectors (Thompson, 1969). Also, the coefficients A, B, C, D, E, F are constant quantities across the entire space domain, since they are derived from the elements of the matrix **T** and their values depend only on the parameters determining **T**.

Consequently, it is possible to arbitrarily choose position vectors $\mathbf{p}$ and $\mathbf{p}'$ at any location of the coordinate system. The following six cases are examined to determine the coefficients A, B, C, D, E, and F.

Case 1. The position vectors are located on the X-axis. Dividing the numerator and denominator of the right hand side (rhs) of equ.(2.24b) by x^2 and taking into the account that $x \neq 0$, $y = z = 0$ results in

$$A = k^2 \tag{2.25}$$

Case 2. The position vectors are located on the Y-axis. Dividing the numerator and the denominator of the rhs of equ.(2.24b) by y^2 and taking into account that $y \neq 0$, $x = z = 0$ we have

$$B = k^2 \tag{2.26}$$

Case 3. The position vectors are located on the Z-axis. Dividing the numerator and the denominator of the rhs of equ.(2.24b) by z^2 and taking into account that $z \neq 0$, $x = y = 0$ we get

$$C = k^2 \tag{2.27}$$

Case 4. The position vectors are defined as the section between the plane defined by two of the coordinate axes and the bisecting plane containing the third axis. Considering that $x = y$, $z = 0$ and dividing the numerator and denominator of the rhs of equ.(2.24b) by x^2 we have

$$k^2 = \frac{A + B + 2D}{2}$$

or $2k^2 = A + B + 2D$

which, because of equs.(2.25) and (2.26), becomes

$$2k^2 = 2k^2 + 2D$$

which leads to

$$D = 0 \qquad (2.28)$$

Case 5. The position vectors are defined similarly to the previous case with the conditions $z = x$, $y = 0$. Dividing the numerator and denominator of the rhs of equ.(2.24b) by z^2 we have

$$k^2 = \frac{A + C + 2E}{2}$$

or $2k^2 = A + C + 2E$

which, because of equs.(2.25) and (2.27), becomes

$$2k^2 = 2k^2 + 2E$$

which leads to

$$E = 0 \qquad (2.29)$$

Case 6. The position vectors are defined similar to the previous case with the conditions $y = z$, $x = 0$. Dividing the numerator and denominator of the rhs of equ.(2.24b) by y^2 we have

$$k^2 = \frac{B + C + 2F}{2}$$

or $2k^2 = B + C + 2F$

which, because of equs.(2.26) and (2.27), results in

$$2k^2 = 2k^2 + 2F$$

which leads to

$$F = 0 \qquad (2.30)$$

Equations (2.25) to (2.30) prove that the necessary conditions (2.20a) and (2.20b) respectively are satisfied. Therefore, it has been shown that the displacement matrix can be factorized in the form of equ.(2.19) and the new position vector $\mathbf{p}'$ is now expressed as

$$\mathbf{p}' = k \cdot \mathbf{Q} \cdot \mathbf{p} \qquad (2.31)$$

It can be determined if the four displacement parameters are known. These are: the scale factor k and the three Euler's angles about the axes.

2.4 Relationship between the Displacements and Deformation

It was previously mentioned that the displacements of the detail points with the use of matrix **T** determine completely the change in position and shape of the deformable body. Based on equ.(2.31), the change in position of a point is represented by the orthogonal rotation matrix **Q**, which leaves the length of every position vector unchanged. Thus, from each new position vector of the detail points we can infer about the total motion of the body. Similarly, the scale factor k represents the variation in the length of the position vector, and therefore its total effect at each detail point will provide information about the change in the shape of the deformable body.

The expansion (or contraction) of the position vector by a scale factor k without any change in its direction is the geometric interpretation of the eigenvalue-eigenvector problem. (e.g., Wells, 1971; Wells and Frankich, 1983; Anton, 1984). It means that there

are some mutually orthogonal axes, so-called principal axes, along which this deformation occurs. These axes remain orthogonal after a deformation has taken place (Chen, 1983). Thus, the deformation can be expressed by a matrix **Z**. The direction of the principal axes are determined by the normalized eigenvectors of **Z** while the eigenvalues express the total deformation along the principal axes.

According to the above, the transition matrix **T** can be given as

$$\mathbf{T} = k\,\mathbf{Q} = \mathbf{Z} \cdot \mathbf{Q} \qquad (2.32)$$

where the matrix **T** is decomposed into the product of the orthogonal matrix **Q**, which rotates the position vector and of a symmetric matrix **Z** representing the deformation (Khachaturyan, 1983). The matrix **Z** should be symmetric due to the nature of the problem. For a symmetric matrix all the eigenvalues are real numbers, while its eigenvectors corresponding to different eigenvalues are orthogonal to each other (Strang, 1980). Therefore, matrix **Z** can always be reduced to a diagonal matrix **D** by an orthogonal matrix **U**.

According to the spectral decomposition (ibid) the symmetric matrix **Z** may be written in the following form

$$\mathbf{Z} = \mathbf{U}\,\mathbf{D}\,\mathbf{U}^{\mathbf{T}} = d_1 \cdot \mathbf{e}_1 \cdot \mathbf{e}_1^{\mathrm{T}} + d_2 \cdot \mathbf{e}_2 \cdot \mathbf{e}_2^{\mathrm{T}} + d_3 \cdot \mathbf{e}_3 \cdot \mathbf{e}_3^{\mathrm{T}} \qquad (2.33)$$

where $\mathbf{e}_1$, $\mathbf{e}_2$, and $\mathbf{e}_3$ are the normalized eigenvectors of matrix **Z** and the corresponding columns of matrix **U**.

An application to the above analysis would be to determine the deformation and the rotation matrices **Z** and **Q** respectively, given the displacement matrix **T**. The sequence of the computations is (Khachaturyan, 1983):

1. Compute the symmetric matrix Z^2

$$
\begin{aligned}
Z^2 &= Z\ Z^T && (Z^T = Z, \text{ since } Z \text{ is symmetric}) \\
&= Z\ Q\ Q^T\ Z^T && (Q \cdot Q^T = I \text{ since } Q \text{ is orthogonal}) \\
&= Z\ Q(Z\ Q)^T && (Z\ Q = T, \text{ according to equ.(2.32)}) \\
&= T\ T^T
\end{aligned}
$$

2. Compute the eigenvalues d_1^2, d_2^2, d_3^2 and the normalized eigenvectors $\mathbf{e}_1$, $\mathbf{e}_2$, and $\mathbf{e}_3$ of matrix Z^2. (Note: If Z^2 has eigenvalues d_1^2, d_2^2, d_3^2 and corresponding eigenvectors $\mathbf{e}_1$, $\mathbf{e}_2$, $\mathbf{e}_3$, then Z has eigenvalues d_1, d_2, d_3 and eigenvectors $\mathbf{e}_1$, $\mathbf{e}_2$, $\mathbf{e}_3$ (Strang, 1980)).

3. Compute the eigenvalues d_i of Z from $d_i = (d_i^2)^{1/2}$, i=1,2,3.

4. Compute the deformation matrix Z using the spectral theorem (equ.(2.33)).

5. Compute the rotation matrix Q using equ.(2.32)

$$Q = Z^{-1}\ T$$

where the inverse Z^{-1} of matrix Z can be computed either directly or from equ.(2.33) after replacing d_i by d_i^{-1} (i=1,2,3) (since $Z^{-1}\mathbf{x} = d^{-1}\mathbf{x}$ if $Z\mathbf{x} = d\mathbf{x}$).

It is understandable that the final displacement matrix T can be estimated after the displacement vector $\Delta\mathbf{p}$ has been determined properly. Figure (2.4) provides an illustration of the general monitoring problem and the relationship between displacements and deformations. The complexity of the problem requires interdisciplinary cooperation as in many engineering tasks.

2.5 Methods of Monitoring Displacements

The aim of the monitoring campaign is to determine the magnitude and the direction of motion of the detail points representing the object. There are three major factors upon which the selection of a measuring method highly depends:

- magnitude of displacements
- frequency (rate) of movements
- accuracy requirements

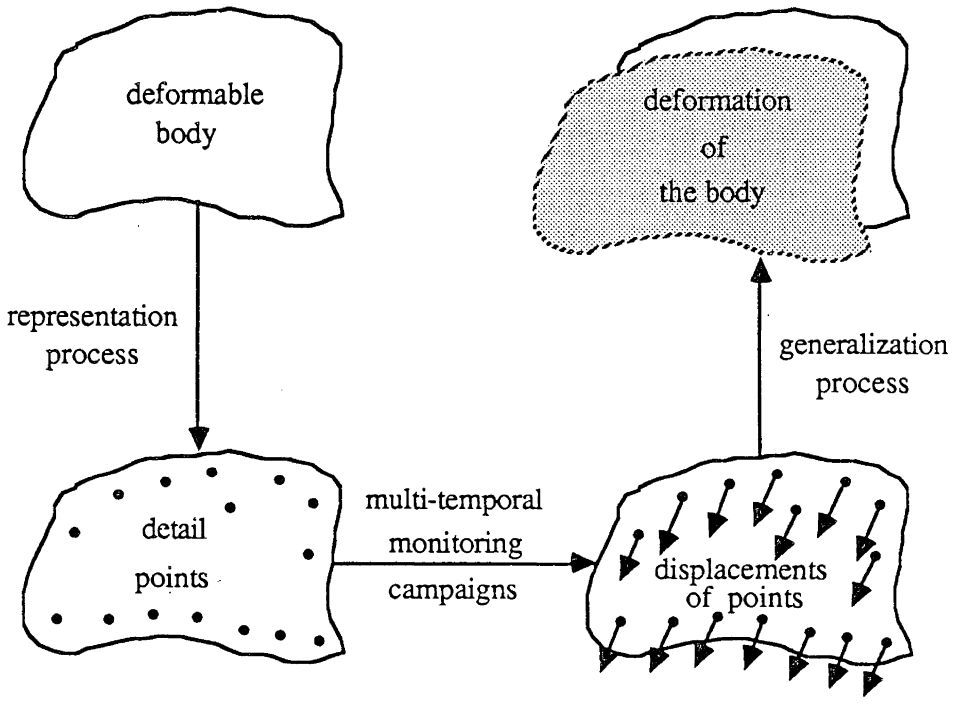

Figure 2.4: Relation between displacements and deformations (after Niemeier, 1982).

Furthermore, the intended monitoring scheme must be capable of

satisfying the following distinctive necessities (Chen, 1983):

- higher accuracy requirements than for networks established for point positioning
- repeatability of measurements
- integration of different types of measurements
- specialized analysis and evaluation of the gathered information.

The diagram in Figure (2.5) illustrates contemporary methods for detecting and monitoring movements.

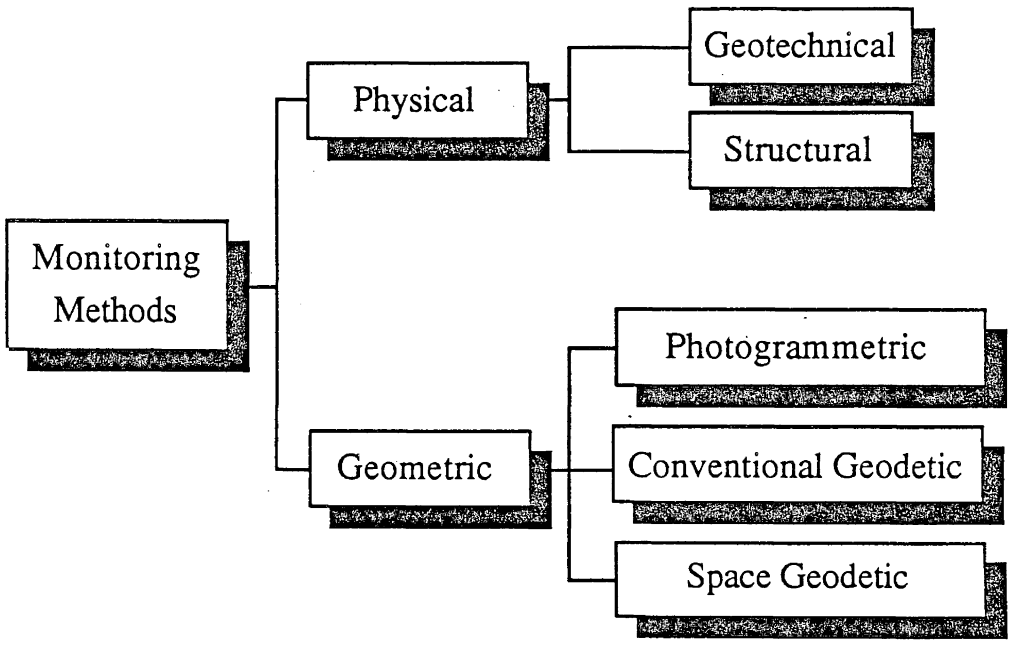

Figure 2.5: Methods for monitoring displacements.

These methods can be divided into two basic groups: physical and geometric (Chrzanowski, 1981). Physical methods are used to measure -usually unidimensional- relative displacements using various linear

mechanical instruments in contact with the object. Geotechnical methods measure changes in elevation with settlement gauges, changes in length with extensometers, changes in slope with inclinometers, etc. Structural methods measure changes in strain with strainmeters, changes in tilt with tiltmeters, and changes in inclination with inverted pendula. Although the precision of geotechnical and structural measurements is very high, the information is incomplete because of its local (or even point related) characteristics. It is therefore desirable to associate the physical monitoring system with geometric methods.

Geometric methods are capable of monitoring both relative and absolute movements with respect to a given reference datum. Depending on the design criteria, these methods range from photogrammetric approaches to conventional- and space geodetic techniques. Photogrammetric methods employ measurements on aerial and/or terrestrial photographs of the object. Conventional geodetic methods are based on observables to form horizontal and/or vertical networks. Space geodetic methods require extra-terrestrial reference information and include systems such as: Transit Doppler Positioning, Satellite Laser Ranging (SLR), Very Long Base-Line Interferometry (VLBI) and the Global Positioning System (GPS). The Inertial Surveying Systems (ISS), a special category of modern 3-dimensional positioning systems, must be included here for the sake of completeness. An overview of the monitoring methods and their relevant accuracies can be found in Chen, (1983) and Krakiwsky, (1986).

The selection of a particular method is a matter of design

considerations to obtain an optimal monitoring scheme. Each method has advantages and disadvantages. Physical methods connected to a recording device can provide continuous monitoring of the information (Chrzanowski et al., 1982). Conventional geodetic methods have achieved very high accuracies, but are point dependent and require extended field operations. They are inappropriate in cases where the object deforms continuously as is every point dependent method. Thus, they can be applied only during intermediate time intervals of relevant equilibrium, that is only before or after the occurrence of displacements. If this is impossible, small movements are absorbed into the observations thereby reducing the apparent accuracy. Space geodetic systems are based on very expensive equipment and are limited by visibility conditions and controllability of the signals. Their accuracy generally deteriorates as the base-line length increases (Krakiwsky, 1986). Photogrammetric methods utilize specialized hardware and software, while their accuracy is directly related to the scale of the photography.

Because each monitoring method has advantages and disadvantages, the author believes that integration of different systems is required to provide a more complete and more accurate picture of the deformable body. Thus, this study focuses on the improvement of the status of photogrammetry as a monitoring method.

2.6 Factors Affecting the Significance of Displacements

The main objective of any monitoring method is to detect and

determine accurately the displacements of the detail points. In this context, the significance of resulting displacements has to be established in order to determine whether their cause is actual deformation or just a reflection of shortcomings of the monitoring approach. Thus, certain aspects are addressed here.

The type of monitoring networks affects the analysis of the results. There are two types of geometric monitoring networks: absolute and relative (Chrzanowski et al., 1981). If the detail points are connected to stable (reference) points outside the deformable body, then we have a so-called absolute or reference network. The main concern in this kind of geometric network is the affirmative verification of the stability of the reference points. If however, the limits of the deformation effects are vague then all points are subject to movements. This type of geometric network is called a relative or object network. The main problems here are the identification of the deformation model and the definition of the reference datum.

The displacement vectors and their accuracy do not depend on the causative factors only, but also on the design of the networks and the observational errors. In each monitoring campaign, random- and systematic errors as well as outliers in the observations will affect the estimated parameters. Weak geometric configuration contributes to poor accuracies.

Consequently, the following factors must be considered for the evaluation of the significance of displacements:

- stability of points
- determination of the accuracies of the observations

- elimination of systematic errors
- detection, elimination and accomodation of outliers
- reliability of the network
- sensitivity of the network.

The identification of stable points is a problem related to the definition of the reference datum. Particularly in relative networks an artificial datum can be defined by using inner minimal constraints (e.g., Perelmuter, 1979; Blaha, 1982; Vanicek and Krakiwsky, 1986) to overcome the singularity inherent in the coefficient matrix of normal equations. Despite their desirable properties, that is the minimization of the Eucledian norm ($|| \delta x ||$ = minimum) and of the trace of the covariance matrix (tr $C_{\hat{x}}$ = minimum), their application in monitoring displacements has certain disadvantages. If some detail points have been displaced, the inner constraint solution will smooth the actual movements and bias the datum (Chen, 1983). On the other hand, the imposition of mathematical constraints can make the solution with singular inverse techniques physically meaningless, unless there is a physical justification (Vanicek and Krakiwsky, 1986). Of course this method can be applied on a subset of detail points whose stability has been established and thus the zero variance computational base can be defined (Fraser and Gruendig, 1985).

Solutions to the datum problem have also been described in Koch and Fritch (1981), where a symmetric reflexive generalized inverse of the singular matrix of normal equations is used and in van Mierlo (1978), where special similarity transformations (S-transformations) are applied. A general solution to the same problem is given in

Chen (1983) using the projection theory in the parameter space.

The datum can be also defined by the so-called explicit minimal constraints. Here the rank deficient design matrix can be augmented by a matrix whose rank is equal to the rank defect of the matrix of normal equations (Vanicek and Krakiwsky, 1986; Secord, 1985). Of course the observation vector is extended accordingly. This approach can be considered much more favourable in photogrammetric networks because the reference (control) points are introduced as weighted constraint equations in most of the modern photogrammetric adjustment procedures. Thus, the datum defect of seven can be removed.

There are several statistical tests (van Mierlo, 1978; Chrzanowski et al, 1981; Niemeier, 1981; Koch and Fritch, 1981; Krakiwsky, 1986) to examine the stability of certain points. That is, H_O: $\mathbf{d} = \mathbf{0}$ against H_A: $\mathbf{d} \neq \mathbf{0}$, where $\mathbf{d}$ is the vector of displacements. Some of the geodetic methods are based on invariant quantities such as angles (Tobin, 1983; Secord, 1985; Janusz, 1983). Although they can be applied in terrestrial photogrametric networks, their use in purely photogrammetric networks involving aerial photography however, is very difficult due to different camera locations for each monitoring campaign.

A possible general photogrammetric approach can be based on a trial and error method. The datum for both epochs is defined according to external information about the physical behaviour of the object. Afterwards the datum is redefined with explicit minimal constraints based on those control points which showed minimum displacements. Next, each remaining control point contributes to

the definition of the datum for each epoch. Again all common control points are statistically tested on the assumption of stability. If the point passes the test then it is considered stable and contributes to the reference datum. Detail points can also be examined and if they pass the stability test, they are then considered as additional control points. The contribution of each point is weighted according to the amount of displacement.

This concept has been presented in Fritch, (1986) where photogrammetry has been selected as the monitoring method. The datum definition in this application is based on an S-transformation instead of explicit minimal constraints, while equal weighting of the participating points has been applied.

The previously mentioned projection theory (Chen, 1983) is also a significant tool in identifying stable points. The displacement vectors $\mathbf{d_i}$ can be determined using the same minimal constraints for both epochs. Then $\mathbf{d_i}$ is mapped to $\mathbf{d_{i+1}}$ using a weighted projection operator (Chen, 1983; Secord, 1985). The weighting scheme is inversely proportional to the displacement occurred. Thus the contribution of a point to the datum defined by the weighted projection is heavier if the point has moved less. While the weighted projection minimizes the first norm of displacement ($\Sigma|\mathbf{d_j}|$ = minimum) the unit weight projection is equivalent to the inner constraints approach, which minimizes the Eucledian norm of $\mathbf{d}$ ($||\mathbf{d}||$ = minimum).

The accuracy of the observations affects both the estimation of the unknown parameters and their covariance matrices. Hence, systematic errors may be included in the determined movements and

their accuracies, if the observations have been introduced with erroneous weights. So far, empirical and trial and error methods as well as the measuring accuracies of the instruments used have been the main sources for the determination of the variances (and/or the covariances) of the observations. However, some analytical methods are available. Förstner and Schroth, (1981) have applied multivariate analysis for the estimation, approximation and evaluation of covariance matrices for reseau photo-images. A more general approach has been proposed and developed by Chen, (1983) where variance components of different types of observables can be estimated with the Minimum Norm Quadratic Unbiased Estimation (MINQUE) principle.

The presence of systematic errors will obviously bias the displacements of points. In photogrammetric networks, compensation of systematic errors, such as atmospheric correction and image distortions due to the imperfectness of interior orientation must be a prerequisite for the adjustment.

Another concern in every monitoring campaign is the detection and elimination of outlying observations. Perhaps it is even more important to determine the influence of undetectable outliers on the estimated parameters. The need for a diagnostic mechanism was always there and dates back to early attempts to infer on sets of statistical data. In the surveying community it was first introduced by Baarda (1968). The concept of reliability distinguishes between internal reliability which describes the lower bounds for gross error that can be detected by a statistical test, and external reliability which indicates the effect of non-

detectable gross-errors on the final results. Since then, much research has been performed within the geodetic and photogrammetric community to refine the blunder detection techniques, e.g., Pope (1976), Förstner (1979) and (1985), Grün (1979), Kavouras (1982), El-Hakim (1982), and Chen (1983). However, the main purpose of these studies was to identify the outliers for further examination. Protection against outliers and even accomodation of them (Beckman and Cook, 1983; Barnet and Lewis, 1984; Mertikas, 1987) are also very significant aspects and should be investigated by the surveying engineers.

No matter which monitoring method is used, it is critical to have a measure to detect the minimum magnitude of movements. This is expressed by the sensitivity criterion (Niemeier, 1982).

The final product of a number of monitoring campaigns will be the displacement vectors at the detail points and their accuracies expressed by their variance-covariance matrix. There are two ways to obtain this information: either by separate single-epoch or by simultaneous multiple epoch network adjustment. Further elaboration on these two approaches will be given in the next chapter.

Finally, the popular global congruency test (Niemeier, 1981) is presented here for the case of an absolute type network. The null hypothesis

$$H_o: E\{\hat{\mathbf{x}}_2\} - E\{\hat{\mathbf{x}}_1\} = \mathbf{0} \qquad (2.34)$$

examines whether the coordinates of the detail points $\hat{\mathbf{x}}_1$ and $\hat{\mathbf{x}}_2$ respectively are identical within their error ellipsoids. The displacement vector is

$$\mathbf{d} = \hat{\mathbf{x}}_2 - \hat{\mathbf{x}}_1 \qquad (2.35)$$

and its estimated covariance matrix $\mathbf{C}_d$ is

$$\mathbf{C}_d = \mathbf{C}_{\hat{x}1} + \mathbf{C}_{\hat{x}2} \tag{2.36}$$

assuming that there is no correlation between $\hat{\mathbf{x}}_1$ and $\hat{\mathbf{x}}_2$. The test statistic Y is

$$Y = \frac{\hat{\sigma}_d^2}{\sigma_o^2} \tag{2.37}$$

where

$$\hat{\sigma}_d^2 = \frac{\mathbf{d}^T \cdot \hat{\mathbf{C}}_d^{-1} \cdot \mathbf{d}}{\text{rank}(\mathbf{C}_d)} \tag{2.38a}$$

and

$$\hat{\sigma}_o^2 = \frac{df_1 \cdot \hat{\sigma}_{o1}^2 + df_2 \cdot \hat{\sigma}_{o2}^2}{df_1 + df_2} \tag{2.38b}$$

$\hat{\sigma}^2_{oi}$ (i=1,2) are the estimated variance factors of the adjustments.

Y has an F-distribution with u and df degrees of freedom, that is

$$Y \approx F_{u,\ df} \tag{2.39}$$

where

$$u = \text{rank}\ (\ \hat{\mathbf{C}}_d\ )$$

$$df = df_1 + df_2$$

If $Y \leq F_{u,\ df,\ 1-\alpha}$ then H_o is accepted, otherwise H_o is rejected (α is the significance level).

While this test statistically examines the existence of group movements, it can also be applied to investigate displacements of a single point P. In this case $\mathbf{d}$ becomes a 3 by 1 vector $\mathbf{d}_p$ = [dx dy dz]^T, $\hat{\mathbf{C}}_d$ becomes a 3 by 3 matrix $\hat{\mathbf{C}}_{dp}$ and u is equal to 3. Another

test to check for single point displacement is to determine whether vector $\mathbf{d}_p$ lies outside the error ellipsoid defined by $\hat{\mathbf{C}}_{dp}$. That is, if

$$\mathbf{d}_p^T \hat{\mathbf{C}}^{-1}_{dp} \mathbf{d}_p > 3 \cdot F_{3,\, df,\, 1-\alpha} \qquad (2.40)$$

then a single point movement is indicated.

For all aspects mentioned in this section, proper statistical tests can be applied to examine the corresponding null hypotheses. However, it is not within the scope of this study to mention all these tests. The interested reader is referred to the pertinent literature. It must be emphasized that the prudent use of statistical tests has made them a useful and powerful tool of inference in examining the importance of displacements.

3. PHOTOGRAMMETRY AS A MONITORING METHOD

Photogrammetric methods can be used to monitor the visible surface of a deformable object. The basic unit is the photograph- aerial or terrestrial - on which an image of the object is recorded. Measuring the photographic images of the detail points we can obtain reliable information about the status of the object. Detailed steps of a photogrammetric monitoring procedure are described in Armenakis, (1983).

3.1 Advantages and Limitations of Photogrammetry

Photogrammetric methods are suitable for monitoring displacements, because a photograph represents a remote, complete and instantaneous record of an object. An instantaneous record of a particular situation which may be changing in time, together with a complete coverage, is most appropriate for a phenomenon such as a moving object.

The ability to measure natural detail points using the on-line "cross-identification" procedure (Chapter 4) makes the photogrammetric approaches independent of pre-established targetted points, except for a limited number of control points. Thus, by

being a point independent system, virtually an infinite number of object points are recorded and can be measured. Of course this requires no extra cost and time for field work. A series of successive photographs of the object provides an archival record. Therefore, it is possible to go back in time and to establish new natural points in areas where displacements had not been anticipated or to recover lost points and thus enhancing the displacement history of the deformable body.

As a non-contact monitoring method, photogrammetry can safely measure inaccessible or dangerous areas as well as objects in hostile environments. The data acquisition time ranges from short to instantaneous, thus allowing the capture of even high frequency displacements because all points are recorded simultaneously.

As far as the accuracy is concerned, sub-centimetre (with aerial photogrammetry; Fraser and Stoliker, 1983) and sub-millimetre (with close-range photogrammetry; Brown, 1980; Fraser and Brown, 1986) accuracies are achievable. The object-to-camera distance is the decisive factor for the accuracies obtained photogrammetrically. Due to the nature of the photogrammetric networks (for example symmetric distribution of object points) the accuracy of point determination is homogeneous, while the large number of degrees of freedom increases the reliability of the estimated object coordinates.

At little additional expense more photographs (observations) of the object can be taken and also - if preferable - a wider coverage of the area can be achieved. The measuring phase of the image points does not impose major time constraints (Chapter 4).

Finally, the photography can be utilized for other purposes such as qualitative examination (photo-interpretation), mapping, and digital terrain modelling.

Despite of all these welcome advantages, the photogrammetric methods are not the panacea for every monitoring project. There are certain limitations which in a number of occasions prevent the efficient use of photogrammetry.

The application of photogrammetry does not provide direct on-site measurements. There is a lapse of time until the evaluation of data is completed. Therefore it is not the proper method for real-time monitoring of active situations. However, this need has been realized and thoroughly addressed at the Symposium on 'Real-Time Photogrammetry - A New Challenge' held in Ottawa in June 1986.

The obtainable high accuracies require the use of high precision photogrammetry. This involves sophisticated and expensive software and hardware as well as highly trained and specialized personnel. The high capital cost that needs to be invested for photogrammetric applications, often prohibits cost-effective solutions, particularly for small projects.

The quality of the photographs is not always very good, and inappropriate exposure, light and weather conditions and also image motion effects reduce the overall accuracies.

Natural detail points may be aggravated by deterioration of the surface of the object. Precise location of these points can also be difficult due to shadow combinations which change with time. The problems with the conventional methods for point transfer and measurement are given in Chapter 4.

The reference coordinate system on which the photogrammetric network depends, can create problems, such as questionable quality of the control points or even lack of control points due to disorganization of activities.

Photographic coverage of very large areas is also not suggested for economical and practical reasons. Keeping in mind that nobody or nothing is perfect, the author believes that the advantages demonstrated by photogrammetry make this method an invaluable member of the family of monitoring techniques.

3.2 Design Aspects of Photogrammetric Monitoring Networks

In the previous chapter the main characteristics of monitoring networks were presented. In this section the significant aspect of optimal design for a photogrammetric monitoring network is underlined. This enables us to set the requirements for the observations in order to estimate the unknown parameters and achieve the desired accuracy within reasonable cost limits. Thus, methodology guide-lines are given accompanied with the pertinent literature on the subject.

The design methodology is governed by the following six aspects:

- unknown parameters and their accuracies
- mathematical model
- type of observations with their accuracies and the multi-temporal measuring campaigns (data collection)
- data processing

- evaluation and presentation of the results
- optimization of the design.

In every project the end product has to be clearly defined, in order to develop specifications. Next comes the mathematical modelling and the designation of parameters and observables. At the present time the extended collinearity equations are the most appropriate functional model for photogrammetry.

The observations consist of photo-measurements from aerial and/or terrestrial photographs while geodetic and other geometric measurements or constraints can also be included. The frequency of the monitoring campaigns depends on the nature of the displacements. The distribution of the detail points usually relies on predicted active displacement zones.

Data processing as well as evaluation and presentation of the results are based on contemporary specialized photogrammetric equipment, computer software and hardware, and professional expertise.

While the first aspects of methodology are more or less straight-forward, the last aspect of optimizing the design procedure requires special attention. The criteria of optimization are (Torlegard, 1981; Schmitt, 1982):

- Accuracy, which is expressed as
  - precision: measure of the variances and covariances of the estimated parameters
  - fidelity: measure of the existence of systematic errors in the mathematical model
  - reliability: measure of the ability to detect, localize and

eliminate outlying observations

- Testability: measure of the significance level of the hypotheses tested
- Economy: measure of cost and benefit of the project.

These criteria must be fulfilled and optimized for the four design problems (preanalysis) of a monitoring photogrammetric network. The widely accepted classification scheme of these problems is (Grafarend, 1974):

1) Zero-order design (ZOD) problem. It is concerned with the optimal definition of the reference datum.
2) First-order design (FOD) problem. It is concerned with the optimal configuration of the network.
3) Second-order design (SOD) problem. It is concerned with the optimal designation of weights to the observations.
4) Third-order design (TOD) problem. It is concerned with the optimal improvement of a network if extra points or observations are added to it.

To the above design problems a fifth one can be added, called the combined design problem where, with a preassigned covariance matrix of the parameters, both first- and second-order design problems have to be optimally solved (Vanicek and Krakiwsky, 1986).

We dealt with the zero order design problem in the previous chapter and it will be beyond the scope of this work to further elaborate on it here.

The first-order design problem is significant for a photogrammetric monitoring network. The configuration problem is characterized by a given weight matrix of the observations and an

ideal or desired variance-covariance matrix of the estimated parameters and pursues an optimal design matrix. The photogrammetric aspects which have to be examined in order to solve this optimization problem are those which affect the formulation and structure of the design submatrices. These are:

- intersection of optical rays at the object points (bundle geometry)
- number of camera stations
- number of photographs on which a point appears (overlap)
- base-to-object distance ratio
- image scale and focal length
- additional parameters for interior orientation
- density and distribution of detail- and of control points
- target clusters
- multi-control constraints.

The general aspects of the second-order design problem have been addressed in the previous chapter. From the photogrammetric point of view the following parameters contribute to the improvement of the weight matrix of the observations:

- images of high photographic quality
- size, shape and reflectance properties of targets
- multiple exposures from each camera station
- multiple measurements of image points
- use of high precision comparators.

For the photogrammetric monitoring networks the third order design problem can generally be reduced and solved for as the configuration problem (FOD).

Excellent theoretical analyses on the photogrammetric network design and optimization can be found in Fraser (1984a), Torlegard (1981) and Förstner (1985).

The optimization of the criteria set for each problem is not an easy task. At the beginning, the proper functions have to be derived expressing each criterion and their subsequent optimization has to be performed under certain constraints. The latter is solved either directly or by trial and error procedures (Vanicek and Krakiwsky, 1986). Linear and quadratic programming techniques are required. Photogrammetric network design can be performed also interactively with the advent of computer graphics technology (Gustafson and Brown, 1985).

The subject of optimal design and its complexity for geodetic networks has been addressed during the International Symposium on Geodetic Networks and Computations of the International Association of Geodesy held in Munich in August 1982. The proceedings of this symposium contain much useful information for the interested reader.

3.3 Various Photogrammetric Approaches and Applications

The advantageous characteristics of photogrammetry contribute to its use as a significant monitoring method. It can be applied both qualitatively and quantitatively, provided that the deformable object has been captured photographically at least at two different instants in time. The first aspect is used to detect and record changes. This includes all types of remote sensing. When numerical

values of displacements have to be determined, then the quantitative properties of photogrammetry are utilized.

A single photograph provides a one-to-one correspondence between the photographic coordinates of the image points and the coordinates of the object points. This relationship is expressed by a projective transformation of the three-dimensional object space to the two-dimensional image space. In this case, the scale differs from one image point to another, providing the recovery of only two dimensions of the object space from image measurements. The retrieval of the third dimension is possible through a spatial intersection of photographic rays, only when the object points appear with non-zero parallactic angles on at least two photographs.

Consequently, photogrammetric methods can be used to determine two- or three-dimensional displacements. They are classified into four general categories (Cooper, 1984; Torlegard, 1978) according to the different approaches used for the photogrammetric restitution.

I. Use of a single photograph (time parallax method).

This approach is suitable for monitoring planar displacements due to lack of information along the camera-to-object direction. This restriction is very critical because it is very difficult to assume that an object deforms only along a plane. Therefore, the next three approaches are mostly utilized.

II. Use of photogrammetric stereo-models.

The analytical or analogue restitution of stereo-models can provide graphical or digital information. The former consists of contour

lines and other graphical features generated by an analogue or analytical stereo-plotter. The latter type of information is in the form of X, Y, Z object coordinates for single points, regular or irregular digital elevation models (DEM) and profiles. The comparison of the corresponding type of data from two different epochs provides the actual displacements.

The direct determination of object displacement vectors from model displacement vectors (Armenakis, 1983; Faig, 1984b) can be considered as a special case of this category. This approach requires control points only in one epoch plus well-identified images of stable object points among the different observation campaigns.

III. Use of resection/intersection method.

This is a two-step analytical approach to solve the photogrammetric point densification problem. First the control points are utilized to determine the elements of exterior orientation (space resection) of the cameras involved. Then, the positions of the object detail points are estimated by the spatial intersection of two or more photographic rays.

IV. Use of the simultaneous bundle adjustment method.

This is the most rigorous photogrammetric approach (with the extended collinearity equations) capable of providing the highest point positioning accuracies. The complete variance-covariance information for each object point is extremely useful for statistical analysis to determine the significance of resulting

displacements. This approach also allows the combination of aerial and terrestrial photographs for the estimation of the point positioning.

The incorporation of dynamic information related to the movements of the object in a photogrammetric bundle adjustment defines the sequential photogrammetric approach for monitoring displacements. Its definition and the derivation of the appropriate mathematical model are presented in this study (Chapter 5).

The achievable accuracies vary from 1:10,000 for category I, to about 1:20,000 of the object size for category II, to less than 1:50,000 of the object size for category III and to 1:500,000 of the object's principal dimension for category IV (Fraser, 1986b).

The basic configurations of the camera positions with respect to the object for monitoring purposes are illustrated in Figure (3.1).

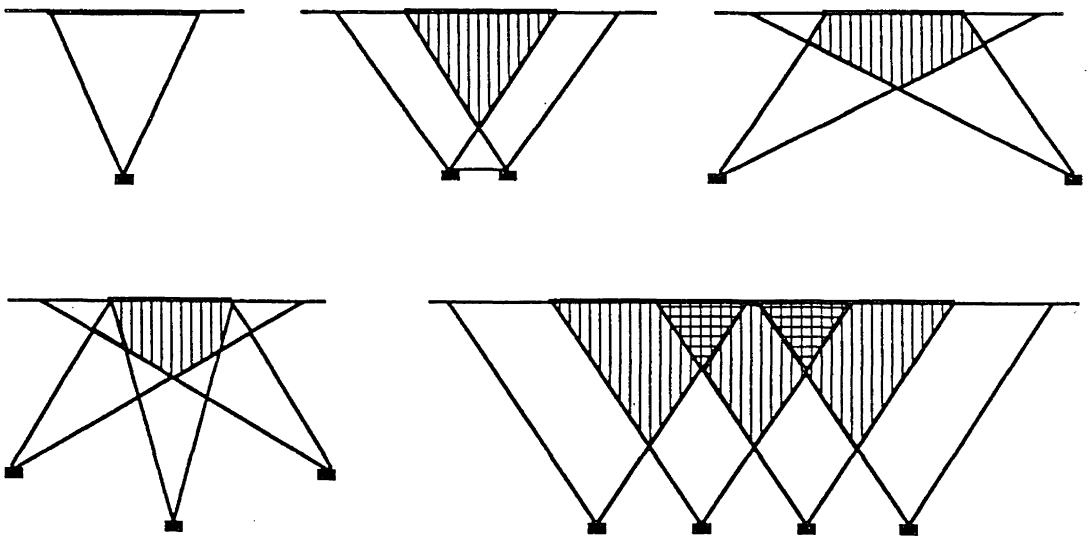

Figure 3.1: Basic configurations of camera positions for monitoring purposes.

As previously mentioned, the displacement vector **dx** of the detail points is determined by comparing the results from multi-temporal photogrammetric campaigns. The comparison is based on either differences of point positions (indirect approach) or differences of observations (direct approach) between two observation epochs (Chrzanowski et al., 1981; Vanicek and Krakiwsky, 1986), i.e.

$$\mathbf{dx}' = f_1 (\mathbf{x}_2, \mathbf{x}_1) \qquad (3.1)$$

or $$\mathbf{dx}'' = f_2 (\mathbf{l}_2, \mathbf{l}_1) \qquad (3.2)$$

The existence of a common reference datum between the two epochs is a prerequisite condition.

Intuitively, both approaches should yield the same displacement vector **dx** (= **dx'** = **dx''**). The conditions under which the two approaches are equivalent or not are discussed explicitly in Vanicek and Krakiwsky, (1986).

The direct approach requires the preservation of the same configuration between the epochs which means that not only the same detail points must be maintained but also the same observables. Systematic errors can be eliminated if the same conditions exist and the same instruments are used during the different campaigns. Although this method has been applied to horizontal and vertical geodetic networks (e.g., Tobin, 1983; Vanicek and Krakiwsky, 1986; Secord, 1985) its photogrammetric applications are limited to terrestrial photography only, where the camera stations can be kept fixed. In the case of aerial photography the displacements cannot be expressed directly as differences of either raw or adjusted photo-observations.

On the other hand, the indirect approach offers certain advantages (Chrzanowski, 1981; Chen, 1983). It removes the restriction for a common network of object points and observables between the campaigns, it allows more effective elimination of systematic errors and detection of outliers, it permits a rigorous analysis of the results, and it provides a more meaningful picture of the deformable body for identifying deformation trends since the displacements are expressed as coordinate differences.

If the displacements are determined with the indirect approach then the positions of the points can be estimated either by a simultaneous multi-epoch adjustment or by separate single-epoch adjustments. The former is recommended if correlation exists between the observations from the different campaigns. If there is no correlation or if the correlation is assumed to be zero as in most present applications, then the two adjustment techniques are equivalent. It is obvious that the computational burden increases in the combined multi-epoch adjustment with additional measuring campaigns. Nevertheless its adoption can increase the geometric strength of the bundle configuration if there are common stable object points between two photogrammetric campaigns (cf. Fraser and Gruendig, 1985).

The photogrammetric approaches alluded to have been applied widely in the field of monitoring displacements, as evident from the following representative list of projects taken from photogrammetric literature.

Monitoring of the earth crustal movements due to its importance is perhaps one of the most popular areas where photogrammetry is

utilized. Fields of particular monitoring interest are: landslides: Peterson, (1976); Kölbl and Stuby, (1982); Veress, (1982a); Fraser, (1982); Fraser and Stoliker, (1983), glacial fluctuations: Faig, (1965); Stirling, (1982); Reinhardt and Rentsch, (1986), volcanic hazards: Johnson, (1982).

In mining operations photogrammetric monitoring of displacements has been applied in: subsidence: Brown, (1973); Crossfield, (1979); Somogyi, (1982); Armenakis (1983) and (1984); Faig, (1984b) and (1984c); Fraser, (1984b), open-pit mines for: volume changes: Fenton, (1982); Johnson and Grube, (1982); Toomey, (1982); monitoring mine slopes: Robertson et al. (1982); Fritsch, (1986), monitoring rock faces: Dauphin and Torlegard, (1977).

Photogrammetric techniques have also been applied in determining structural movements of: buildings: Erlandson and Veress, (1975); Torlegard and Dauphin, (1976); Fraser et al., (1984); Uzi, (1984), dams: Brandenberger and Erez, (1972): Brandenberger et al., (1983), bridges: Veress, (1980); Christensen, (1980); Cooper et al., (1984), transmission line towers and light standards: Veress, (1982b); Florek, (1975), construction areas: Veress and Hatzopoulos, (1981); Shortis et al., (1986), models and materials in laboratory tests: Bernini et al., (1968); Mehto and Viitanen, (1976); van Wijk and Ziemann, (1976); Wrobel and Weise, (1980); Jacobi, (1980); Wong and Vanderohe, (1981).

Recently, the use of photogrammetry has increased very rapidly in the field of industrial monitoring projects (Fraser and Brown, 1986). Some examples are given here: ship industry: Faig, (1978); Haggren et al., (1978); Szczechowski, (1980), automobile industry:

Cooper and Shortis, (1978); Borutta and Peipe, (1986); aerospace industry: Kilburg and Rathburn, (1984); tools, machinery and parts inspections: Faig, (1980); Robertson, (1982); Reichenbach, (1984); Fraser, (1985); telecommunication industry: Brown, (1980); El-Hakim, (1985); Fraser, (1986a).

4. PHOTO-OBSERVATIONS OF MULTI-TEMPORAL PHOTOGRAPHS USING THE ANALYTICAL STEREO-PLOTTER

4.1 Data Acquisition

Independent of the monitoring method, the same specific points representing a deformable body must be repetitively measured in order to determine their motion with respect to a stable reference system. For the photogrammetric determination of displacements, multiple photo-observation epochs are therefore necessary. This requires measurements of the images of the object points on different photographs taken at different periods of time. Both metric and non-metric cameras can be used. However, the selection of either one depends on several factors, such as: accuracy requirements, photo-scale, location and size of the deformable object, available hardware components for measurements and evaluation, and the degree of sophistication of the software.

Since the photo-images of the same points must be well and clearly identified without ambiguity, the detail points are categorized as:

a) Targetted (or signalized) points. These points are marked artificially on the object prior to photographic coverage of it. Painted patterns of square or circular targets are most commonly

used in an effort to reduce pointing errors. This type of point is preferred for high accuracy requirements, and usually restricted to accessible areas and laboratory environments. The disadvantage lies in the higher cost involved in constructing, establishing and maintaining the targets over time.

b) Natural (or physical) points. These are distinct points and form part of the surface pattern of the deformable body. Street intersections, building corners and discrete object details are usually chosen. Due to ambiguities which may arise with respect to their true position, physical points are selected for medium to low ranges of accuracies, remote areas or areas with on-site difficulties, but also because of their lower cost. They are particularly useful in the monitoring of areas of the object where displacements had not been predicted and therefore targets had not been placed.

It is of major importance that all aspects related to the design of a photogrammetric monitoring campaign (section 3.2) should also be carefully considered during the phase of data acquisition.

4.2 Conventional Procedures for Photogrammetric Data Collection

In every photogrammetric application with high accuracy requirements, it makes common sense to use the rigorous analytical photogrammetric methodology. In such an approach, the basic unit is the photograph and the measurements required are sets of x, y photo-coordinates of the images of the points of interest measured on each

photograph. Depending on the type of points, the images can be measured with mono- and stereo-comparators. In addition, point transfer and marking instruments are often needed to identify corresponding images on different overlapping photographs and to mark them permanently on the diapositives.

Having referred to the equipment employed in the photogrammetric data collection phase, the mensuration steps are given next. They consist of:

a) Locating, that is the identification and selection of the images of the detail points.
b) Marking, that is the transfer of the point locations to the corresponding overlapping photographs.
c) Measuring, that is the determination of the photo-coordinates of the image points with respect to a two-dimensional cartesian photo-coordinate system, and
d) Recording, that is the storage of the x, y sets of photo-coordinates together with their associated point- and photograph identification numbers.

The conventional mensuration procedure of targetted points involves the locating-, measuring-, and recording stages. Because the images of these points appear distinctively on photographs taken at different periods, and identification errors can be kept to a minimum, mono-comparators and stereo-comparators in one photo-mode are used. Binocular vision of the photograph is desirable since it reduces eye fatigue and improves pointing accuracy. All modern comparators are equipped with encoders for digital output of the x,

y photo-coordinates. It is possible therefore, through an interface and an alphanumeric terminal unit, to send directly to the computer --in sequential form-- the measured photo-coordinates along with their identification- and photograph numbers. This saves time and avoids typing errors, while the information transmitted can be organized in such a manner so to be ready for subsequent computations.

However, this setup still represents a manual operation, in that the operator has to visit each point using the handwheels, and a paper print as a guide. This is also an open-loop system. The latter is very important and means that there is no flow of information in the opposite direction, that is from the computer to the interface and then to the comparator. This missing closed-loop link would provide some advantageous characteristics to the measuring system. For example, the operations could be accelerated by automatic positioning on the photographs at predetermined locations under computer control, while the availability of on-line editing capabilities could increase flexibility and improve the reliability of the observations.

The situation changes drastically when natural points instead of signalized ones have to be measured. The identification of physical details on the surface of the object may turn out to be a difficult and laborious task as their appearance in various photographs from different epochs may be radically different due to changes in perspective projections and in illumination. Consequently, the point transfer operation, which is the most

important step in the case of physical points, becomes problematic. The use of only a stereo-comparator, where point identification/selection, stereo-point transfer, measurements and recording are all combined, as in aerotriangulation situations, is no longer possible. Although it is possible to transfer and measure points on reference photographs from different epochs, it is extremely difficult to transfer the same points on to the overlapping photographs from the same epoch. This would be feasible if there was an easy way to reconstruct the same interior orientation (centering of the photographs on the photo-stage) for the reference photograph-- because it has been removed from the photo-stage-- and to revisit the same selected points.

To overcome this major difficulty, the mensuration procedure is separated into two operations (Armenakis, 1983). In the first, a verification is made that the images of the same natural points appear on photographs taken at different epochs. This is achieved with a "cross-identification" of the image points between two multi-temporal photographs. The "pseudo"-pair of these reference photographs is placed on the stages of a point transfer- and marking device, such as the Wild PUG3. Then location (identification and selection) and marking (drilling holes into the emulsion of both diapositives) of the physical points are performed.

In the second operation the actual measurements of the photo-coordinates takes place. "Real" photo-pairs, that is the reference photograph and the corresponding overlapping photograph both from the same epoch are placed on the stages of a stereo-comparator.

Since the points are marked on one diapositive, their homologous images on the matching diapositive are easily determined stereoscopically, and all four photo-coordinates can be measured and recorded.

The preservation of stereoscopic perception in both operations is highly desireable because there is an improvement of the stereoscopic acuity of the human eyes over the monocular acuity by a factor of approximately 2 (Manual of Photogrammetry, 1980; Trinder, 1984). Therefore, better results are obtained in locating and measuring the physical points of interest using stereo methods.

Although this approach is conceptually correct and has been applied, (Armenakis, 1983 and 1984) shortcomings have been observed in two areas. At the production level this process is slow and tedious for the operator, while the quality of the measurements may be not as good as it should be to meet the accuracy requirements. These limitations are due to the following reasons (cf. Okang, 1971; Schoeler, 1978):

A) For the operations on the point transfer and marking device:

--Poor stereoscopic perception since photographic positions and orientations may deviate significantly from the normal case. Thus, point transfer may be tedious and even questionable especially on instruments which lack optical image rotation and continuous magnification.

--Lack of flatness if film is used instead of glass plates.

--Various sizes of the drilled holes due to variable pressure on the drilling levers and due to the wear of the drilling

heads.

--Manual coarse motion of the photographs leading to poor handling.

--Possible misalignment between viewing ray path and marking tools.

--Loss of information, since the mechanical marking of points in the emulsion destroys photographic information. Although drilling can be performed in the near vicinity of the physical point, questions arise related to the point identification during the measuring phase.

--Storage and labelling problems. The points are marked on the diapositives, which become the reference photographs for each epoch but also are the media for consecutive measurements. However, there is no identification number next to each point, and the large number of marked points may confuse the operator, not to mention the damage to the emulsion. In addition, destruction of the marking through time is possible as remainders of the removed emulsion layer may fill in the hole.

--Lack of editing capabilities. Deletion or replacement of points is impossible because the points are marked permanently. Addition of a point at a later time cannot easily be performed without creating extra work for the operator during both the transferring and measuring operations.

B) For the actual mensuration phase on the stereo-comparator:

--Emulsion deposits on the periphery of the marks (holes) due to drilling and cleaning prohibit sharp stereoscopic perception for precise measurements.

--Difference in size between the measuring marks and the drilled holes may cause centering errors.

--Lack of the ability to randomize the identification errors by repetitive measurements, since the holes made in the emulsion make the initial identification the final one.

--Difficulties in numbering the points due to lack of an identification number unless detail sketches on paper prints are kept, which results in time consuming delays.

--As in the case of the mono-comparator, it is also a manual operation, an open-loop system, and lacks editing capabilities.

Although modern point transfer and marking instruments are equipped with optical image rotation, continuous magnification, encoders for digital output and laser beams which evaporate the emulsion at the target spot, a number of these problems remain. The combination of the above mentioned shortcomings in the critical phase of data collection contributes to: a) a reduced accuracy and reliability of the measurements due to larger pointing errors, and b) a lower productivity and flexibiltiy due to the number of manual operations involved.

4.3 On-Line Analytical Photogrammetric Systems

The design and implementation of techniques and approaches for data collection and data processing depends to a large extent on the available hardware and software components. The inherent mathematical rigour of the analytical photogrammetric methods may not be fully exploited without a precise photogrammetric system which is automated to a certain degree.

The precision can be obtained by using mono- and/or stereo-comparators, while partial automation is possible by connecting an optico-mechanical photogrammetric instrument with a digital processor. Either the same processor or another host computer can handle the computational aspects. Relevant to the above two major functions are two modes of operation: the off-line mode, where the different steps of data collection and processing are separated both physically and timewise, and the so-called on-line mode based on the principle of simultaneous data collection and processing (Kratky, 1976).

The photogrammetric systems are generally classified as analogue, hybrid and digital (Kratky, 1976; Konecny, 1980). Totally digital or integrated systems which combine certain photogrammetric functions with editing and data base management (Dowman, 1977; Manual of Photogrammetry, 1980) are beyond the scope of this research. The conventional stereo-plotters and comparators belong to the analogue category because a mechanical computer performs the photogrammetric restitution while the human operator plays the role

of a correlator for the image matching operations. If the conventional instrument is interfaced with a computer to assist in certain operations, then we have a hybrid system. In this case the interface allows information to flow only in one direction, namely from the instrument to the computer forming an open-loop on-line system (Fig. 4.1a). If, however, there is not only processing of the information, but also a feed-back from the computer to the measuring device which supervises and controls the measuring operations, the system is a closed-loop on-line digital system (Fig. 4.1b).

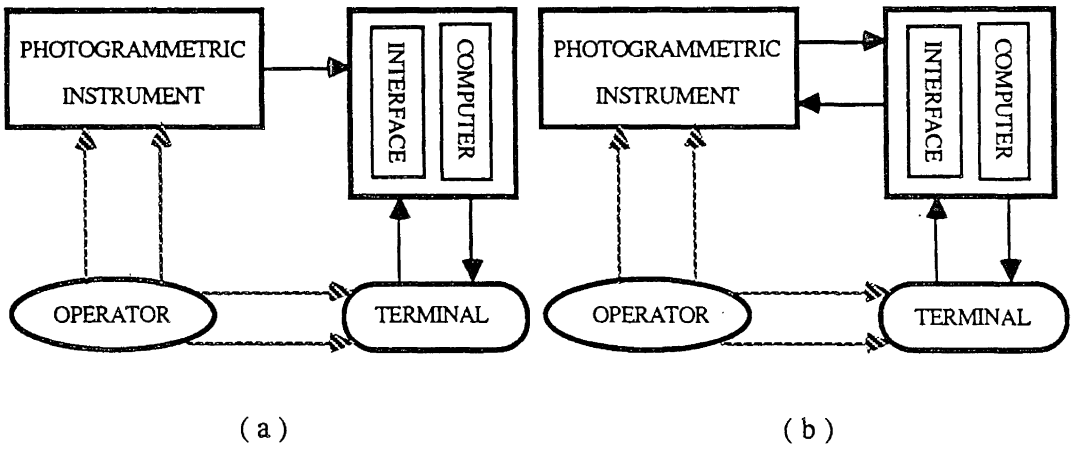

Figure 4.1: Open- and closed-loop on-line systems.

Digital systems are based on purely analytical solutions and direct communication between a photograph measuring device and the computer through an interface. This two-way communication is usually carried out in a real- or near real-time environment. This means that the time elapsed between activating the handwheels and/or the footdisk and the response of the measuring mark is less than 1/25th of a

second.

A very important part of digital photogrammetric systems is the interface (Fig. 4.1) The interface serves two main purposes (Seymour, 1980): firstly, it allows the computer to control the movements of the measuring device via its servo-system and secondly it is the communication link between the operator and the computer. The trend today is towards including microprocessors into interface design.

The computer-assisted comparators and the analytical stereo-plotters belong to the category of digital photogrammetric systems. Obviously, the closed-loop on-line photogrammetric systems are the most versatile since they are based on purely analytical principles, and any modification is done mainly through the software.

Several other aspects should be considered for the on-line mode of operations. A variety of computers supporting the digital systems must be examined with respect to different performance characteristics such as processing time (or speed), storage capacity and input/output times. An available on-line computer should be utilized to physically control the measuring process and- whenever required- to perform the necessary computations (Kratky, 1980). Both operations are done as soon as the minimum information is available.

Another factor is the capability for on-line data editing. Points can be remeasured, deleted or added. Because of the sequential nature of photogrammetric mensuration, there is a need for sequential and recursive computational techniques. The

algorithms used must incorporate the continuous change of the information without ignoring the computer power and the critical response time. A solution to the design of the system would be its division into smaller units; once solved, and after the results have been evaluated, one can proceed to more complex formations (Kratky, 1979 and 1984; Dorrer, 1981 and 1986; Molenaar, 1981).

Computational efficiency and numerical accuracy should be preserved, and the mathematical rigour should not be sacrificed. There are two fundamental algorithmic methods: simultaneous and sequential solutions (Gruen, 1985). While simultaneous processes can be applied when all data are available, the on-line interactive nature of the photogrammetric functions favours sequential techniques. The latter can be further classified into stepwise, semi-sequential and truly sequential algorithms (Fig. 4.2)

In stepwise methods the basic photogrammetric units are added one after the other. Changes in the data are possible at the latest stage, and the final results are not exactly identical to those obtained from a direct simultaneous solution. The semi-sequential algorithms permit editing of the data at previous stages. Updating of the solution is performed only between the point of intervention and the final stage. Finally, there are the truly sequential solutions which allow intervention at any stage, and the solution is computed taking into the account all the changes. The solution obtained by this method is rigorous and equivalent to the simultaneous direct solution (Mikhail and Helmering, 1973; Rosculet, 1980; Dowideit, 1980; Gruen, 1985). Consequently, the last approach

is the most preferable for on-line digital photogrammetric systems.

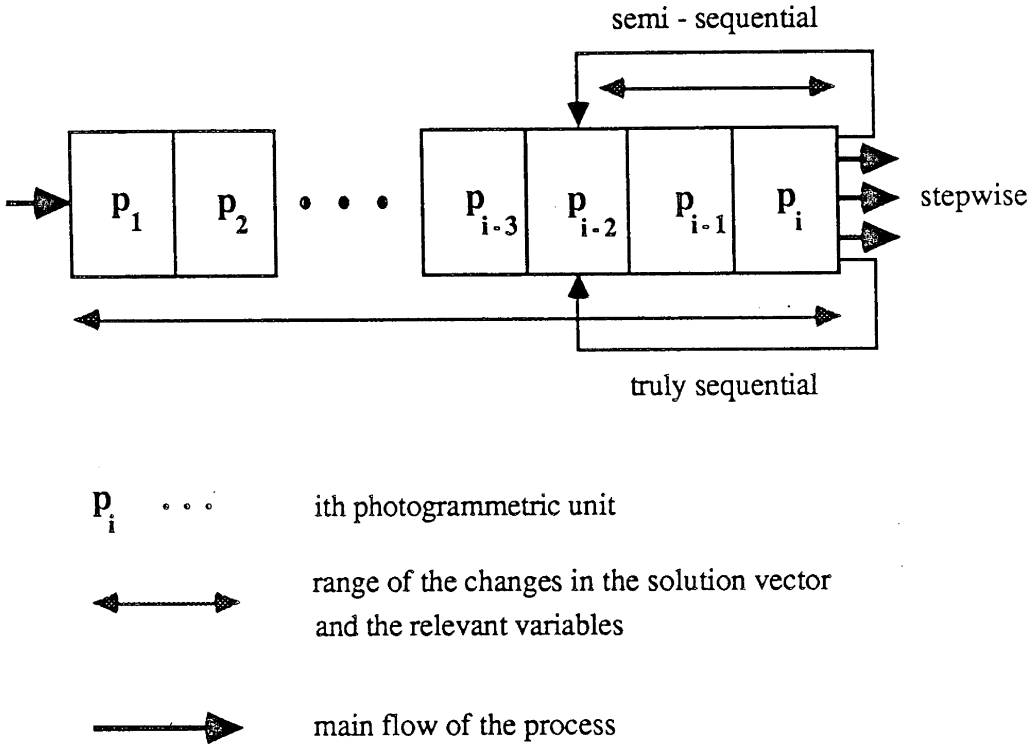

Figure 4.2: Stepwise, semi- and truly sequential algorithms (after Gruen, 1985).

As illustrated in Figure (4.1), the operator is part of the loop system. Considerations, therefore, should be given to the man/machine interaction by including into the system optimal communications, ergonomics, safeguards for human errors and machine failures and, finally, user-friendly hardware and software (Dorrer, 1986).

In recent years there has been a continuous evolution in digital photogrammetric systems which are most suitable for on-line

photogrammetric measurements.

4.4 The Analytical Photogrammetric Stereo-Plotter OMI AP-2C and its Control Computer PDP 11/60

From the discussion on conventional photogrammetric data collection it is evident that the approach used is separated physically and timewise into different phases. That is, an off-line mode governs the mensuration of photo-coordinates of the targetted and natural points. Furthermore, in the case of natural points, the point transfer operation is questionable and one of the requirements of the measuring conditions is that of stereoscopic observations. A digital photogrammetric system, such as the analytical stereo-plotter, is the most suitable for on-line photogrammetric measurements. It can be used in three modes of operation: mono-, stereo-comparator and stereo-plotter.

The Department of Surveying Engineering at the University of New Brunswick acquired in 1968 an analytical stereo-plotter model AP-2C from Ottico Meccanica Italiana (OMI). In 1978 its Bendix control computer was replaced by a Digital Equipment Corporation (DEC) PDP 11/60.

The operational concept of the analytical plotters can be described as a stereo-comparator connected to a computer with a feed-back link. The analytical reconstruction principle introduced by U.V. Helava replaces the analogue space restitution with digitally projecting rays. In other words, the transformation between object and image spaces is carried out analytically by the

digital control computer on-line with the photogrammetric instrument. The handwheels and/or the footdisk connected with shaft encoders generate pulses and the accumulated pulses define the spatial (model or object) coordinates X, Y, Z, which are transmitted to the computer via the interface. The photo-coordinates are computed using the collinearity equations. The elements of the interior and exterior orientations are known and already stored in the computer together with known X, Y, Z values. Corrections to the image coordinates due to various distortions can also be applied (with opposite signs). Using the interface, these photo-coordinates are transferred into carriage coordinates via the secondary feed-back loop. That is, the computed photo-coordinates are compared with the actual position of the carriers. The magnitude and the direction of the difference is transmitted to the servo-motors which cause the stages to move. There is a continuous comparison of the actual position of the carrier with its final destination. When the difference becomes zero, the movement stops. The computation of the photo-coordinates via the collinearity equations and the secondary feed-back loop comprise the real-time program. More details about it can be found in Masry, (1972) and in Jaksic, (1967) and (1979).

The main components of the analytical-plotter AP-2C are (Fig. 4.3):

a) The optical-mechanical unit, which consists of the viewing and measuring devices, the control panel and the operator's control parts. The viewing systems move in the x-direction while the photo-carriers move in the y-direction. The measuring devices are rotary

spindle encoders providing a precision of 2μm. The optical system is equipped with continuous magnification from 8x to 16x (although this may be changed), common and individual image rotation and ortho/pseudo observation capability. The format of the stages is 240mm x 240 mm, the travelling speed of the picture carriers is about 12 mm/s, and the size of the floating mark is 40 μm. The control panel consists of buttons which control the movement of the stages and the plotting table as well as initiate certain actions. The operator introduces the movements with the two handwheels, the footdisk and a joy-stick located on the control panel.

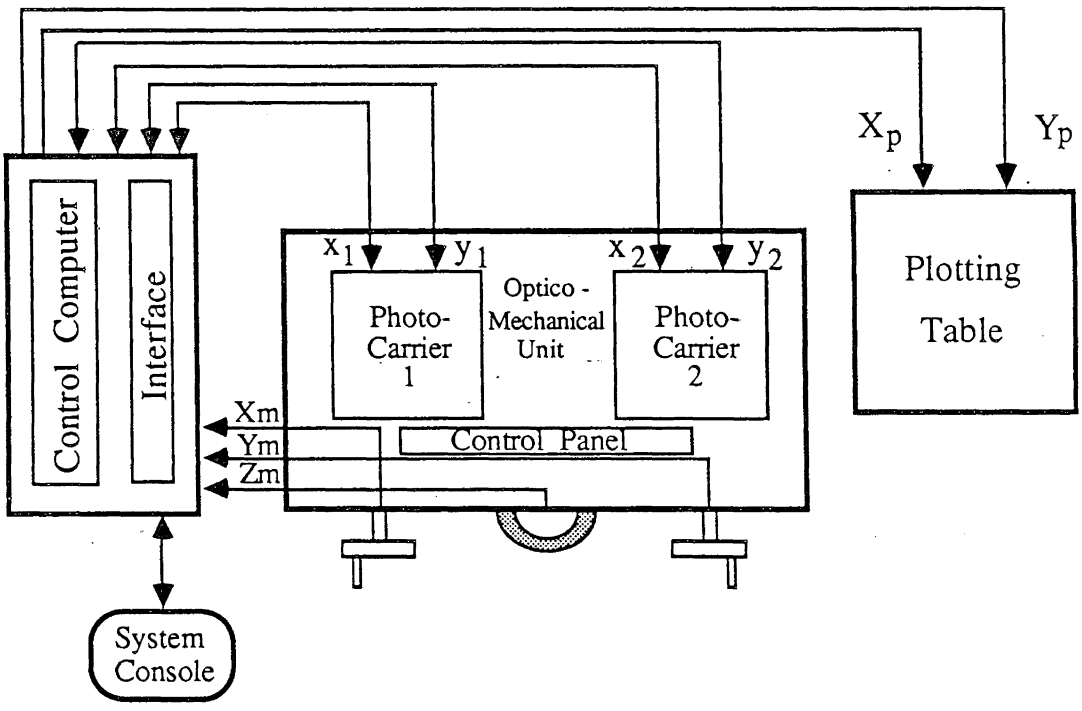

Figure 4.3: Components of the analytical-stereo plotter OMI AP-2C.

b) The control processor is a mini-computer. It runs under the DEC's RSX-11M operating system in a real-time, multi-user, time-sharing environment. The PDP 11/60 can address only 32K (=32768) words - the address limit of 16 bits - at any one time. Therefore, a task cannot reference more than 32K words at one time. The analytical plotter uses for its real-time program, two shared common regions of 4K words each. The first one is related to the 33 word buffer area in the memory to/from which the interface actually writes/reads. The second requires a "device common" be specified for direct access to the interface registers (a "device common" is a special type of shared region that occupies a physical address on the I/O page. When mapped into the virtual address space of a task, a device common permits the task to manipulate peripheral device registers directly).

Consequently, only 24K words are then available. To reduce the memory space requirement, a conventional task is divided into segments and can access more code (or data) than can fit within the address limits. This technique uses a tree-like overlay structure. An overlaid program is a program which has been broken down into parts, which are loaded into memory automatically during execution. Therefore, the overlays are task segments (branches) that can run independently. Since they do not have to be available to the task at the same time, they can share the same address space. When a segment is needed, the operating system makes it available by replacing (overlaying) a segment that is no longer being used. By

interchanging its parts, a task can run even though it is too large to be executed as one piece. The common part of the program which permanently resides in memory during the execution of the task is called the root of the tree. In our case, for example, the real-time program is always part of the root since it continuously controls the movements of the carriages.

There are two major software parts: a) The real-time dependent programs which consist of interrupt level hardware control routines, and b) the user level programs which are not subjected to critical execution time and are called system application software, i.e., relative and absolute orientations, etc. The two types of software communicate between each other via a common block (Fig. 4.4).

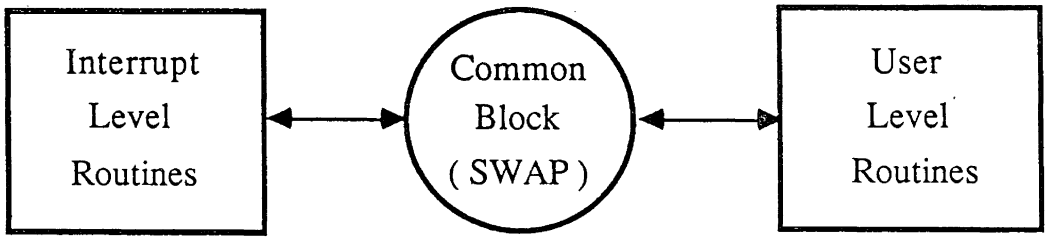

Figure 4.4: Communication between real-time programs and application programs.

The interrupt mechanism related to the sequence of several calculation tasks according to predetermined priorities must be disabled and reenabled when the variables in the common block are changed. The shut off of the interrupts should not be longer than 20 ms, otherwise the movements of the photo-carriers will be jerky.

c) The interface used has a microprocessor which is connected by a Direct Memory Access (DMA) transfer of data between the PDP 11/60 mini-computer and the optical-mechanical unit. The DMA property provides high baud rates, making the data exchange very fast compared to parallel or serial type of interfaces.

d) The system console is an alpha-numeric CRT terminal and provides a conversational, interactive, instructed and editing mode of communication between the operator and the system.

e) The plotting table is a flatbed plotter with plotting dimensions of 1.20m x 1.40m. The positioning system of the plotting table is activated by buttons located on the control panel. The corresponding table coordinates are calculated as part of the real-time program. The difference lies on the secondary loop for the plotting table which is of an open-loop type and on the positioning accuracy of the plotting coordinates.

4.5 On-Line Semi-Automatic Photogrammetric Data Collection using the Analytical Stereo-Plotter

For the design and implementation of the data collection system using the analytical stereo-plotter, certain factors were considered and examined in order to set the basis for the development of the new system.

The basic photogrammetric unit is set to be the photograph itself. Therefore, all the operations involved are based on the photo-coordinates. This also serves the purpose for fully analytical procedures. The original basic real-time program (Masry

and Konecny, 1970) was kept unchanged. The image coordinates are computed for both photographs in the coordinate system of each photo-carrier through the collinearity equations as function of: a) XM, YM, ZM (model or machine coordinates), b) position and attitude of both cameras with respect to the fictitious machine reference system (XC_i, YC_i, ZC_i, w_i, φ_i, k_i, i=1,2), and c) basic interior orientation elements (x_{oi}, y_{oi}, c_i, i=1,2) that is,

$$x_1 = x_{o1} - c_1 \frac{V_1W_1}{V_3W_1}, \quad y_1 = y_{o1} - c_1 \frac{V_2W_1}{V_3W_1} \tag{4.1a}$$

$$x_2 = x_{o2} - c_2 \frac{U_1W_2}{U_3W_2}, \quad y_2 = y_{o2} - c_2 \frac{U_2W_2}{U_3W_2} \tag{4.1b}$$

where,

i = 1,2: refers to the left and right photograph, respectively

V_j, U_j (j=1, 2, 3): the row elements of the corresponding rotation matrices $\mathbf{R}_1 = f(w_1, \varphi_1, k_1)$ and $\mathbf{R}_2 = f(w_2, \varphi_2, k_2)$, respectively

$W_1 = [XM - XC_1, YM - YC_1, ZM - ZC_1]^T$

$W_2 = [XM - XC_2, YM - YC_2, ZM - ZC_2]^T$

Three important aspects were discovered and investigated by the author. The first concerns the real-time program which does <u>not</u> compute photo-coordinates, that is coordinates referenced to the fiducial system, but rather stage coordinates for each individual photograph. The latter are referred to a coordinate system whose origin is the fiducial centre and its X- and Y-axes are parallel to the axes of the photo-stage (Fig. 4.5). It is self-explanatory that each stage has its own coordinate system.

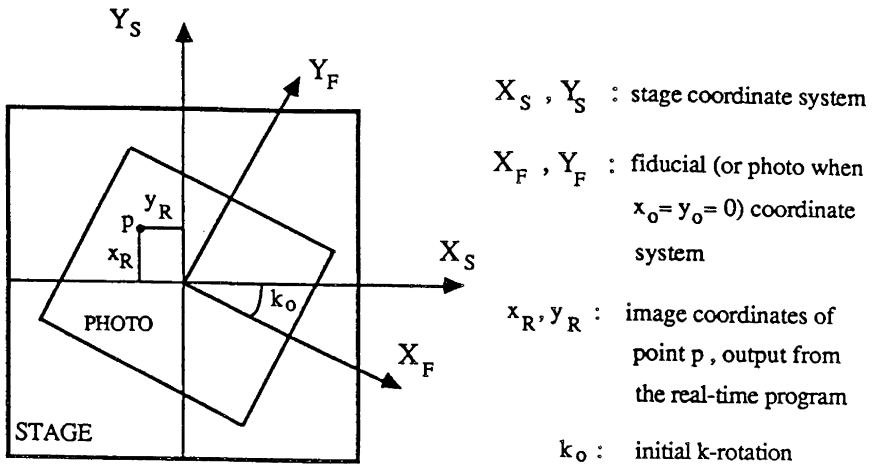

Figure 4.5: Geometry between stage and fiducial coordinate systems as related to the real-time program.

The second aspect is related to the first one. It was discovered that during the process of interior orientation the existing software was performing only a centering operation, that is the coincidence of the stage centre with the fiducial centre. The existence of the initial k_o-rotation (Fig. 4.5) is neglected (k_o = 0) and its influence is absorbed in the total k-rotation of the exterior orientation of the photograph. That is,

$$\text{total } k_{\text{exterior}} = \text{actual } k_{\text{exterior}} + \text{initial } k_o \quad (4.2)$$

Also, in the case of dependent pair relative orientation the final value of k_2 has contributions from the initial k_{o1} and k_{o2}. Of course, these problems do not appear when conventional work is done on the analytical-plotter using a photo-pair in regular stereo-photogrammetric applications.

But as a result of the first and second aspects we never have the interior orientation as normally defined, and even more important, it is impossible to achieve the same orientation of a

photograph on the photo-carrier if the photograph is removed and reset again. That means we cannot relocate photo-points with known photo-coordinates using the computer-controlled capabilities of the analytical-plotter, unless the k_o-rotation is known.

The third aspect concerns the origin of the stage system as set in the real-time program and its physical realization. Since the photo-stages and the optics have the ability to move in y and x independently for the left and the right image respectively, the departure of each carrier from its zero position is called offset (Fig. 4.6) and should be considered during the calculation of the image coordinates by the real-time program. When the offsets are not equal to zero they affect the XC_i, YC_i coordinates of the perspective centres. The offsets play an important role during certain operations, such as interior orientation, image measurements for relative orientation and fine pointing operation in the case of data collection for natural points. More details are given in the pertinent sections. Of course, if the offsets become zero, the origin (zero position) of the stage system is shifted accordingly.

In this study the origin of the machine coordinate system shifted from the machine space to the perspective centre of the fixed photograph (when XC=YC=ZC=0, **R**=**I**). This serves the purpose of locating image coordinates indirectly from model coordinates using the plotter-mode existing real-time program and a scale of 1:1 between image and model space (Fig. 4.7).

Therefore, the image coordinates are computed and located on the photo-carriers as:

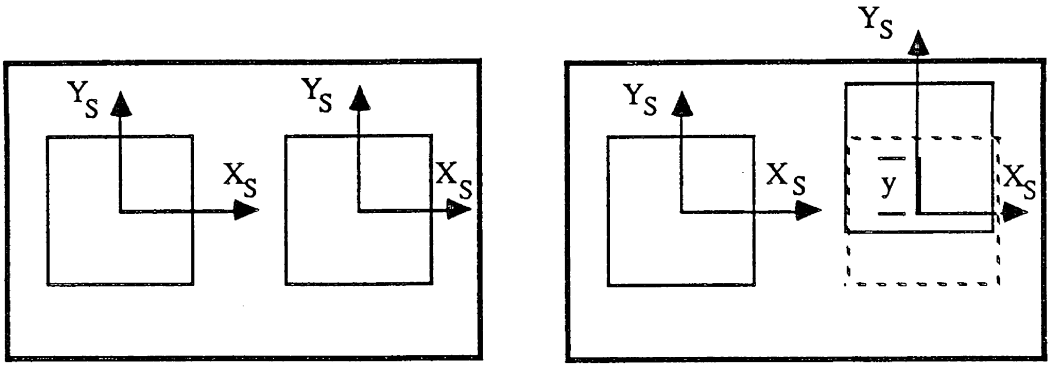

Figure 4.6: Offsets of photo-carriers.
(a) x-, y-offsets of both stages are zero.
(b) x-offsets are zero, y-offset of the left carrier is y.

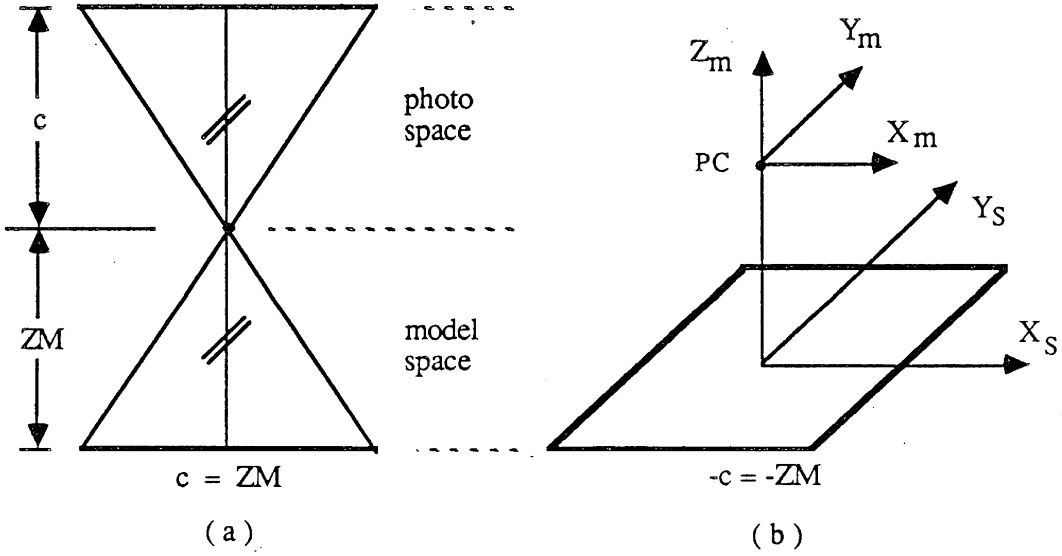

Figure 4.7: Geometric configurations between photo- and model spaces.
(a) actual situtation.
(b) conceptual representation for the real-time program.

$$sc = -c / -ZM = 1 \qquad (4.3a)$$

$$x_s = sc \cdot XM = XM \qquad (4.3b)$$

$$y_s = sc \cdot YM = YM \qquad (4.3c)$$

With this analysis we can proceed to the description of the developed on-line semi-automatic photogrammetric data collection system for monitoring object displacements using targetted and natural points, respectively. The effects and their compensation of the above mentioned problems are further discussed.

4.5.1 Measurements of Signalized Points

The mensuration of targetted points does not have any inherent difficulties. The main disadvantage of the conventional approach using a comparator is lack of mechanization. The use of the computer-controlled analytical-plotter offers the advantage of automating the measuring process to a certain extent, while at the same time incorporating on-line editing options. The system that has been developed works as on-line mono-comparator where either the left or the right photo-carrier can be used for this single image operation. Furthermore, the measuring mark can be driven automatically to predetermined image locations. Depending on how well these a-priori locations are known, the only remaining steps will be fine-pointing (centering) and recording of the information.

Because these last two steps require the operator's involvement, the system is classified as semi-automatic.

A fully automated system incorporating target-recognition devices is described in Brown, (1984). Precise mensuration is completely automatic by means of image processing of the output of solid-state video cameras. This system uses special targets, called retro-targets, which are many hundred times brighter than conventional ones, thus providing high contrast within the photograph. The automatic centering device is based on a Charge Couple Device (CCD) array interfaced with a dedicated microprocessor to provide the determination of the offset of the target centroid within 0.30 μm. Since this system requires specialized equipment and is applicable for laboratory environments with ultra high precision specifications, it was decided for this research to develop a more general system based on more commonly available instrumentation, i.e., use the instrumentation installed at the Department of Surveying Engineering at the University of New Brunswick. Due consideration was given to recent evolutions in surveying engineering and mapping.

The data needed for the automatic positioning of the photograph at predetermined locations are "approximate" photo-coordinates. They can normally be obtained in two ways (cf. Jacobsen, 1984 and Perry, 1984).

a) With the use of a digitizer. The signalized points together with reference marks (fiducial marks for metric cameras, or the edges of the image for non-metric cameras) are digitized, usually from an enlarged paper-print. A file with these digitized table coordinates is created on disk.

In the analytical plotter the same reference marks are measured in a stage coordinate system whose origin is at their centre of gravity and whose axes are parallel to the photo-carrier axes.

This provides the parameters for a two-dimensional similarity transformation, which is then used to transfer the digitized coordinates into approximate stage-coordinates. These stage-coordinates are stored in the control computer. Rather than just using the minimum of two reference points required for the transformation, three or four points are normally used in a linear parametric least squares adjustment, in order to detect possible blunders. In addition to the solution vector, residuals, the a-posteriori variance factor and the variance-covariance matrix of the four unknown parameters are computed.

b) With the use of "approximate" object coordinates. In many cases the displacement of the object is moderate in magnitude. Therefore, after the absolute positions of the detail points have been determined in one epoch, their coordinates can be stored in a file and used as approximations for the next photogrammetric campaign. The photograph can be placed on either of the photo-carriers of the analytical-plotter where the centering operation is performed. Measuring consequently the stage-coordinates of at least three fully coordinated three dimensional object points, which can be easily retrieved, and applying a space resection, the elements of exterior orientation can be estimated. Now that approximate values for interior- and exterior orientation parameters as well as for the object coordinates are available and stored in the computer, the

stage-coordinates can be approximated by applying the collinearity equations. Again these coordinates are stored for future retrieval. The subroutine for the simple space resection handles up to nine points. First approximations for the six unknown parameters can be either entered directly or else computed with initial $w = \varphi = 0$. The final solution is obtained by updating these values using the method of non-linear parametric least squares adjustment. The computed statistical information includes the residual vector of the observations, the a-posteriori variance factor and the variance-covariance matrix of the unknown paramenters.

At this point the already stored approximate stage-coordinates are recalled and placed into the interface registers as output model (machine) coordinates. The measuring mark is then automatically driven to the corresponding image positions in plotter-mode according to equations (4.3). Fine setting and recording of the final stage-coordinates and assigning them to corresponding photograph and point identification numbers follows.

The system provides the options of either automatic sequential or operator specified point numbering, the capabilities to revisit a previously measured point, to add a new point by transferring the control to the operator for scanning the photograph manually in mono-comparator mode, to delete a point and to change (or keep) the point identification number. For metric imagery (format of 230mm x 230 mm) the measuring mark is automatically driven to the locations of the four corner or side fiducial marks. For non-metric cameras

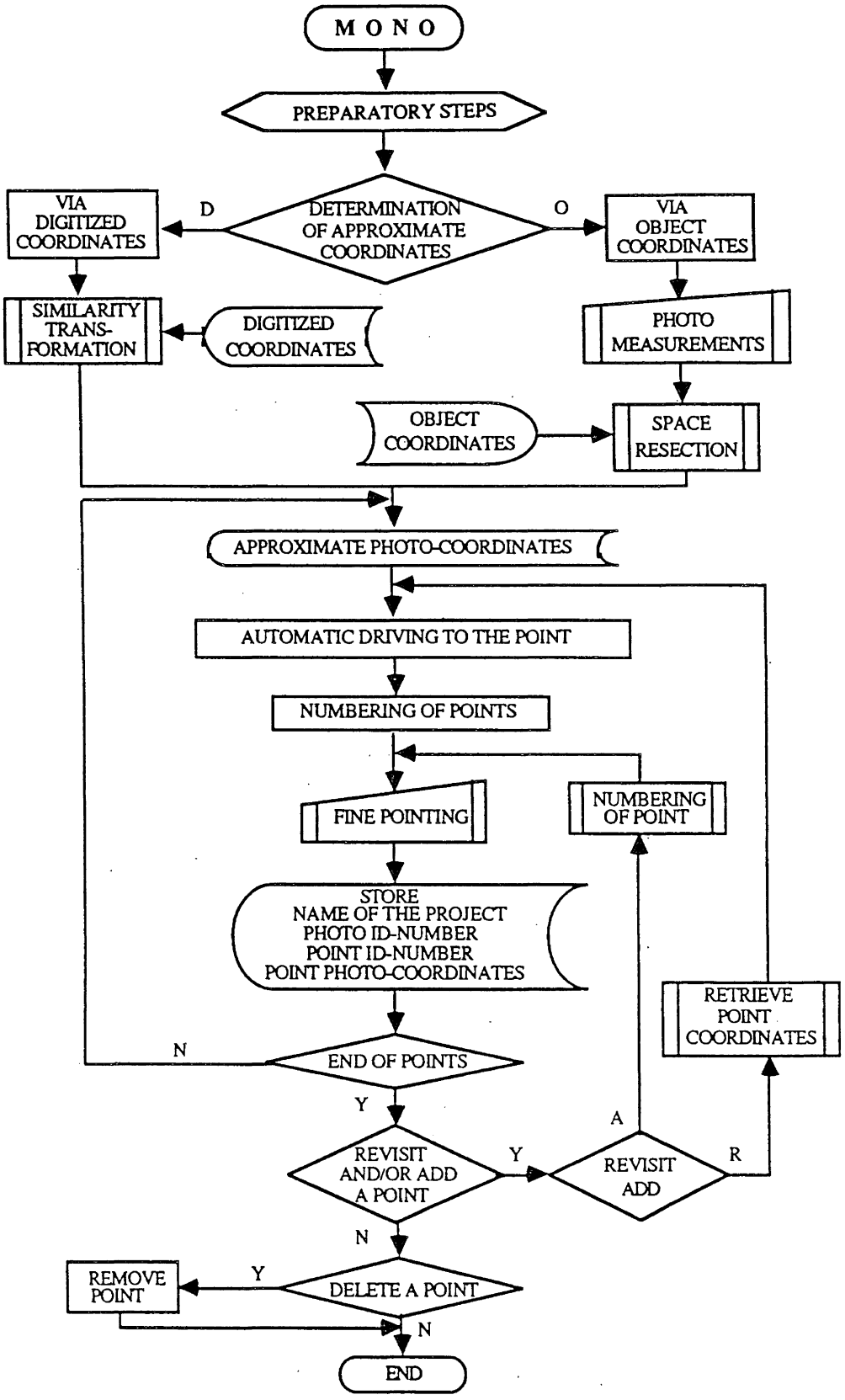

Figure 4.8: Functional diagram of the MONO-mode.

the operator drives manually to the appropriately selected reference marks on the photograph. In both cases the final stage-coordinates of the reference marks are stored. Up to one hundred ten (110) points per photograph can be measured.

The functions of this on-line semi-automatic measuring system for discrete targetted points are illustrated in Figure (4.8). The preparatory steps include operations, such as: calling of certain initialization routines, selection of left/right photo-carrier, type of camera, diapositives or negatives, input of the basic parameters of interior orientation, title of the project, file operations.

4.5.2 Measurements of Natural Points

The measurements of the images of physical details of the object on multi-temporal photographs were found to be a tiresome operation, as mentioned in the discussion of the conventional approach (section 4.2). Besides the lack of automation, dubious accuracies and operator's strain heavily contribute to the shortcomings of the existing procedure. Therefore, the following aspects have been considered by the author:

a) introduction of automation to speed up the entire process;
b) introduction of objective criteria to improve the final accuracies, and;
c) the combination of a) and b) must be beneficial to the operator.

The unique characteristics of the analytical-plotter are

utilized again. Using the instrument as the common link, the previously described "cross-identification" and measuring phases for physical points can be integrated. Thus, all the mensuration steps in this case are combined while the point-transfer operation is performed "digitally". That is, the photo-coordinates will be the means for locating the same natural points on various multi-temporal photographs. The implementation of these considerations led to the design and development of an on-line semi-automatic measuring system for natural points, which satisfies to a great extent the above addressed aspects. The principles of this system are described next.

The implied analytical method employs the formation of "real" and "pseudo" photogrammetric models, based on the relative spatial positions of the photographs at the same or different time (epoch) respectively (Fig. 4.9a). "Pseudo" models are used to locate, measure and record photo-coordinates from overlapping multi-temporal photographs. "Real" models are formed for the same purpose, but for the homologous points on the overlapping photographs of the same photographic campaign.

According to this method, the location of the photopoints at various periods is based on a more objective criterion --the photo-coordinates-- than solely on the human perception, which is not excluded. Thus, after locating the points of interest at this preliminary stage of mensuration, their photo-coordinates are stored in the computer. Then, whenever these points are requested, the measuring mark is automatically and accurately driven to their

location and the immobility of the photo-carrier is ensured. The requirement for a stationary photograph in conjunction with the need of photogrammetric model formation for establishing relative positions of the photographs, leads to the principle of dependent pair analytical relative orientation. The origin of the reference system for the analytical-plotter is set to be at the perspective centre of the fixed photograph for both "pseudo" and "real" models.

Considering the image point location on different photographs taken at different time periods using the "cross-identification" procedure, a solution needs to be:

i) independent of the absolute positions and attitudes of the camera stations; and

ii) independent of the object space.

This independence from external reference systems provides the ability to proceed to the mensuration procedures without preliminary computations.

Consequently, the problem is defined as: At the first epoch a point P is recorded on the pair of photographs L1/R1. This same point P is displaced to a new position P' at the second epoch, which is then recorded on the second pair of photographs L2/R2 (Fig. 4.9a). To ensure that point P exists and is imaged in both epochs, photographs L1 and R2 are used initially (Fig. 4.9b).

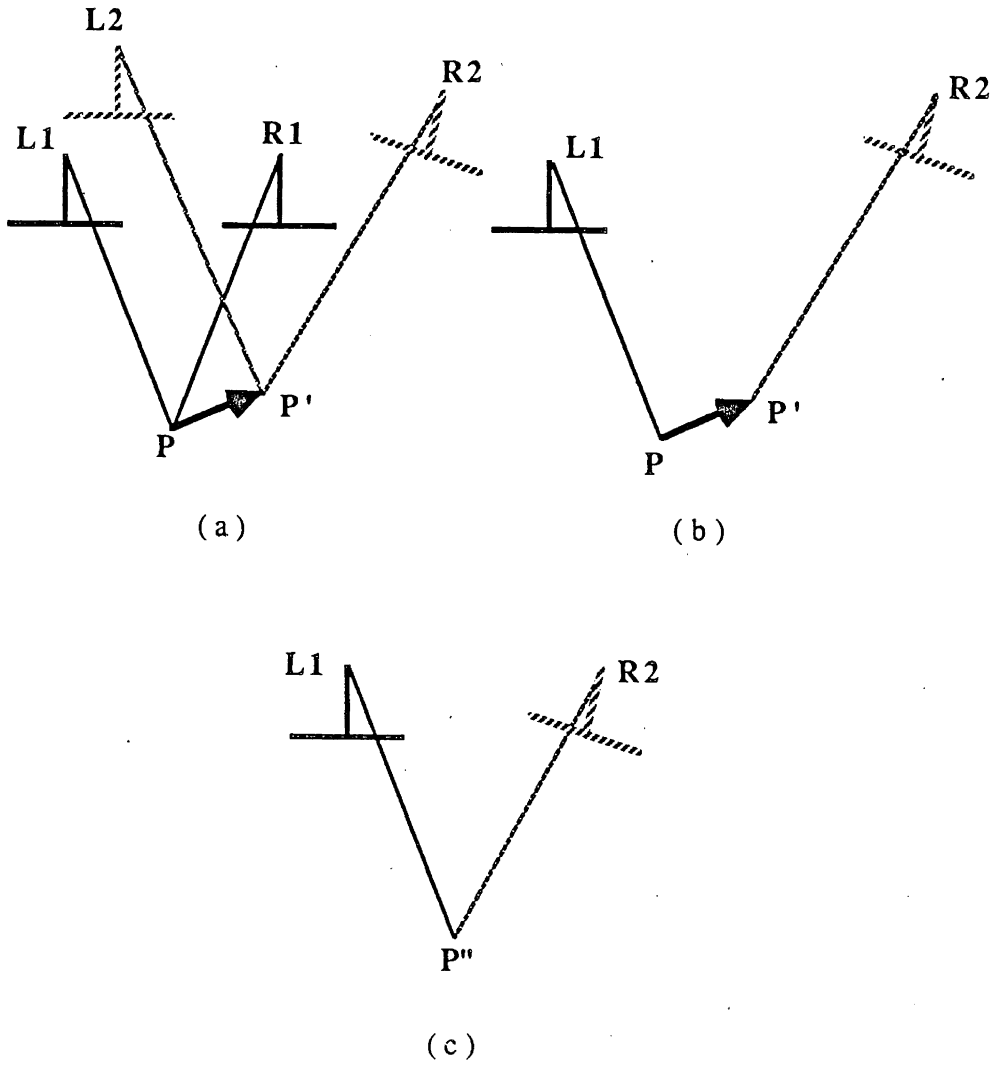

Figure 4.9: Determination of corresponding photo-points using "real" and "pseudo" models.
(a) Actual situation ("real" models L1, R1 and L2, R2)
(b) Non-intersection of corresponding photo-vectors from different epochs
(c) "Pseudo" model formation (L1, R2)

The non-intersection of the corresponding rays L1P and R2P' is overcome by the formation of the "pseudo" model L1/R2 (Fig. 4.9c). This is accomplished by using the analytical-plotter in stereo-comparator mode, where the image coordinates of at least five pairs

of corresponding points have to be measured. Actually, the measuring mark is driven automatically by the developed software to the six von Gruber locations, and the operator eliminates the x- and y-parallaxes so that the proper stage-coordinates of these points are recorded. Assuming L1 to be the reference photograph, the position and orientation (bx), by_2, bz_2, w_2, φ_2, k_2 of the dependent photograph R2 with respect to the fixed L1 are computed with the coplanarity equations. The combined method of least squares adjustment has been applied to estimate the five unknown parameters of relative orientation. The residual vector, as well as the a-posteriori variance factor and the estimated variance-covariance matrix of the parameters are computed for the statistical evaluation of this relative orientation. It is expected that residual y-parallaxes will remain due to two reasons: a) poor geometric intersection of the photographic rays depending on camera positions and attitudes, and b) varying magnitudes of displacements at different zones within the overlapping area. Having established an "approximate" relative orientation of the "pseudo" model, the operator locates well identified natural detail points on the two photographs from different epochs. Existing parallaxes are manually removed, x-parallax with the Z-footdisk and y-parallax by moving the carrier of the dependent photograph with the Y-handwheel.

At this stage it is very important and worth mentioning these points, namely:

1) The stage-coordinates --output of the real-time program-- have to be transferred to the fiducial photo-system defined by the

calibrated fiducial marks.

This is necessary because of the unknown initial k_o-rotation. As soon as the photograph is removed from the photo-carrier, it is impossible to relocate the image points by their stage-coordinates after the photograph has been placed on the photo-carrier again. The physical nature of the measuring system of the analytical-plotter suggested the choice of an affine transformation (Appendix IV). The calibrated fiducial marks, which are held fixed, and the coordinates of the fiducial marks measured in the stage-system are used to determine the six parameters of this transformation. The final photo-coordinates are then stored, since they will be recalled in the second phase of the measuring process.

2) The elimination of the y-parallax at each point during fine pointing introduces (additional) y-parallaxes at all the other points. This offset of the dependent photograph from its initial position after the relative orientation has been completed, affects the output of the real-time program. This is not overly important since we are only interested in the image-coordinates and already have an "approximate" relative orientation. However, the y-offsets are recorded at each point along with the corresponding model (machine) coordinates. Thus, whenever there is a request to revisit any of the previously measured points for verification, the model coordinates together with the y-offset of this point (XM, YM, ZM, y-offset) are needed to precisely relocate the point on both photographs.

At the initial phase, where the two photographs are from

different epochs, the stereoscopic perception might need to be improved. This can be achieved by controlling the lateral magnification and rotation of the images. Large kappa (k) rotation between the two photographs can be eliminated by optical rotation of the individual images after they were placed on the stages. Differential and simultaneous continuous (zoom) magnification for both the left and the right photographs is obtained by adjusting the optical train. Although both operations can be computer-controlled (Masry and Faig, 1977) the additional computations do not seem to be justified for the photogrammetric normal case i.e., for near vertical aerial photographs. Otherwise, it may overload the computer and thus delay the measuring process.

The formation of the "pseudo" model between photographs L1 and R2 provides the means for selecting, measuring and storing the photo-coordinates of natural detail points for one photograph of each epoch. The corresponding homologous coordinates on photographs of the same epoch are then determined by restituting analytically the "real" photogrammetric models L1/R1 and L2/R2, respectively. The evaluation of the relative orientation is based on the computed statistical information as previously mentioned. Photographs L1 and R2 are treated as stationary for this phase. During the interior orientation procedure, the relation between photo-system and stage-system is explicitly defined, again by an affine transformation. The fiducial marks are usually characterized as high quality targets and therefore the transformation parameters are mainly influenced by unavoidable random measuring errors (Kratky, 1972 and 1980).

However, since the transformation used conforms as best as possible to the physical measuring system of the analytical-plotter, preliminary tests showed that the effect of the random pointing errors is usually well within the measuring accuracy of the instrument. The six affine parameters are determined with the method of linear least squares adjustment. The computed statistical information consists of the residual vector and the estimated variance-covariance matrix of the unknown elements. The latter can be used to determine the effect of the uncertainty of the parameters on to the photo-coordinates according to the law of error propagation.

Having established this reliable relationship between photo- and stage-systems, the photo-coordinates x_1, y_1 of the reference point p_1 on the stationary photograph transferred to the stage-coordinates can be automatically and accurately relocated by the software. The procedure is similar to the one used in the case of targetted points. The goal is then to determine the corresponding photo-coordinates on the dependent photograph.

The investigation of this problem under the plotter-mode real-time program led to two alternative solutions. For both of them an important constraint was set. It enforces that the model coordinates must correspond to the recorded relocateable reference photo-coordinates x_1, y_1, since they can be restored through the servo-motors of the stationary stage. This constraint is materialized by the spatial direction of the original projected ray O_1p_1 (Figures 4.10 and 4.11) emanating from the fixed photograph,

where $x_1, y_1, -c_1$ are the coordinates of the photo-point p_1 with the origin of the coordinate system at O_1 ($XC_1=0$, $YC_1=0$, $ZC_1=0$).

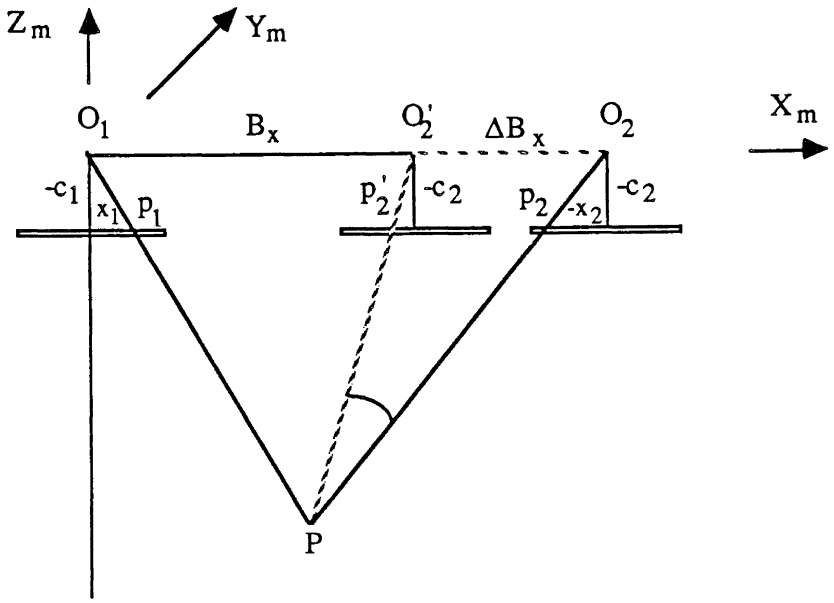

Figure 4.10: Tested geometry for the location of the homologous point p_2.

In the first method (Fig. 4.10) the model point P is determined arbitrarily along the ray O_1p_1. In order to determine the corresponding photo-coordinates of point p_2 on the dependent photograph, point P is kept fixed and the optical ray PO'_2 is rotated about it. At the same time the system of the dependent photograph moves along the direction of the base component B_x until the ray passes through the homologous point p_2. This approach was disregarded as it has two major disadvantages. In the first, the continuous change of B_x for each point results in a continuous

change of the model scale, thus requiring continuous adjustment of the operator's vision. In the second, the continuous updating of the B_x parameter in the common block (SWAP) area for the real-time program causes jerky movements of the carriage due to continuous calling of the interrupt mechanism. That also is not pleasant for the operator's eyes since it causes additional strain.

Subsequently, a second method was studied and a new solution to the problem was found by the author (Fig. 4.11). It was decided that the camera parameters were to be left unchanged. Thus, in order to determine the corresponding coordinates x_2, y_2 of point p_2 the proper model coordinates XM, YM, ZM along the ray O_1p_1 have to be defined, since the elements of interior and exterior orientations of both photographs are known. The previously mentioned constraint holds again in this case. Point p_2 is located and its photo-coordinates are determined and recorded by introducing a model movement in Z direction, enforcing the constraint by having the servo-motors materializing the initial direction O_1p_1 and stop when perfect stereovision is achieved. Therefore, an iterative positioning process has been designed, which consists of the following steps:

1. Drive automatically to point p_1 on the reference photograph, since its photo-coordinates are known from the initial phase and lock on it, by setting:

   $$XM = x_1 \ , \quad YM = y_1 \ , \quad ZM = -c_1 \qquad (4.4)$$

2. Enter new ZM values through the footdisk, so that:

   $$ZM_i = ZM_{i-1} + \Delta Z_i \ (i=\text{number of iteration}) \qquad (4.5)$$

3. Extend the ray O_1p_1 along its original direction by calculating new values for XM, YM:

$$sc = ZM_i/-c_1 \qquad (4.6a)$$

$$XM_i = sc \cdot x_1 \qquad (4.6b)$$

$$YM_i = sc \cdot y_1 \qquad (4.6c)$$

4. Eliminate any remaining local y-parallax, which might exist due to imperfections of relative orientation, by moving the non-stationary photograph.

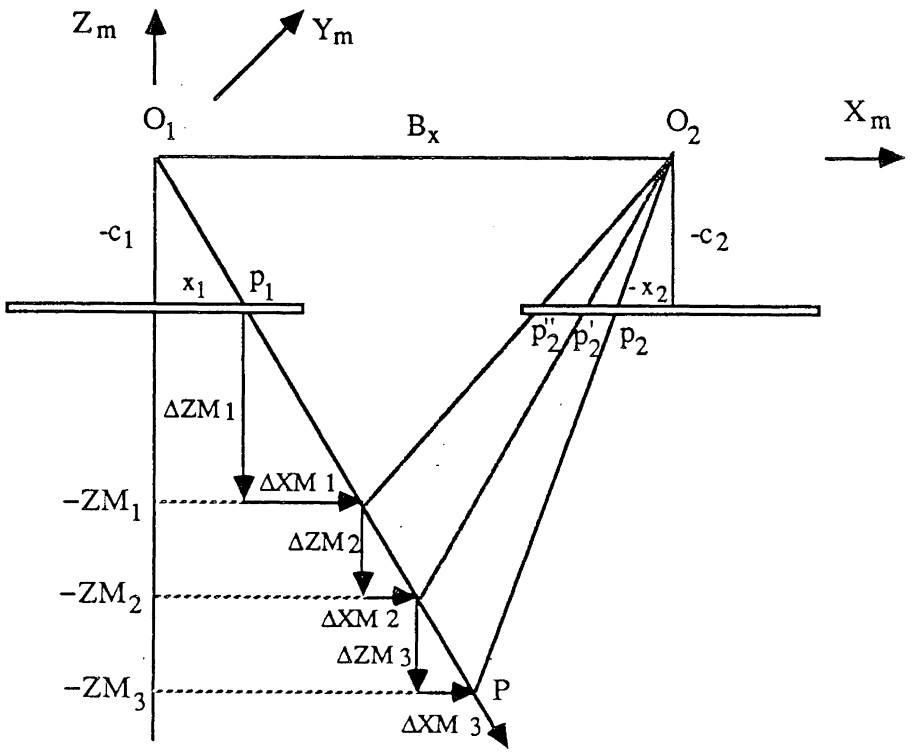

Figure 4.11: Final geometry for the location of the homologous point p_2.

5. Verify whether the correct value of x-parallax has been determined so that the two measuring marks are fused into one floating mark which contacts the virtual model of the object at the correct point.
6. Examine if the conditions of steps 4 and 5 are fulfilled. If yes, then the intersection of ray PO_2 with the image plane of the dependent photograph determines the coordinates x_2,y_2 of point p_2. If not, go to step 2.

It is obvious that with this iterative positioning procedure the introduced vertical motion ZM does not affect --although it does momentarily due to the time-cycle of the real-time program-- the position of the measuring mark on the reference photograph so that the already selected detail point is not lost. Figure (4.12) shows diagramatically this iterative procedure.

The entire procedure is the same for both pairs of photographs L1/R1 and L2/R2, respectively. However, for the second pair it works in reverse, that is the reference (or fixed) photograph is R2, which is placed on the right photo-carriage. The final stage-coordinates are transferred to the photo-system by the inverse affine transformation.

The stereo-mode data acquisition system is capable of measuring up to forty (40) natural points per model. It drives the measuring mark to the approximate locations of the fiducial marks (corner or side) for interior orientation, and to the six characteristic locations for relative orientation. These von Gruber locations can

be also visited in manual mode, while up to forty (40) pairs of photo-observations can be handled by the program of relative orientation. The initial phase provides options to number the points either sequentially or by the operator, and offers editing

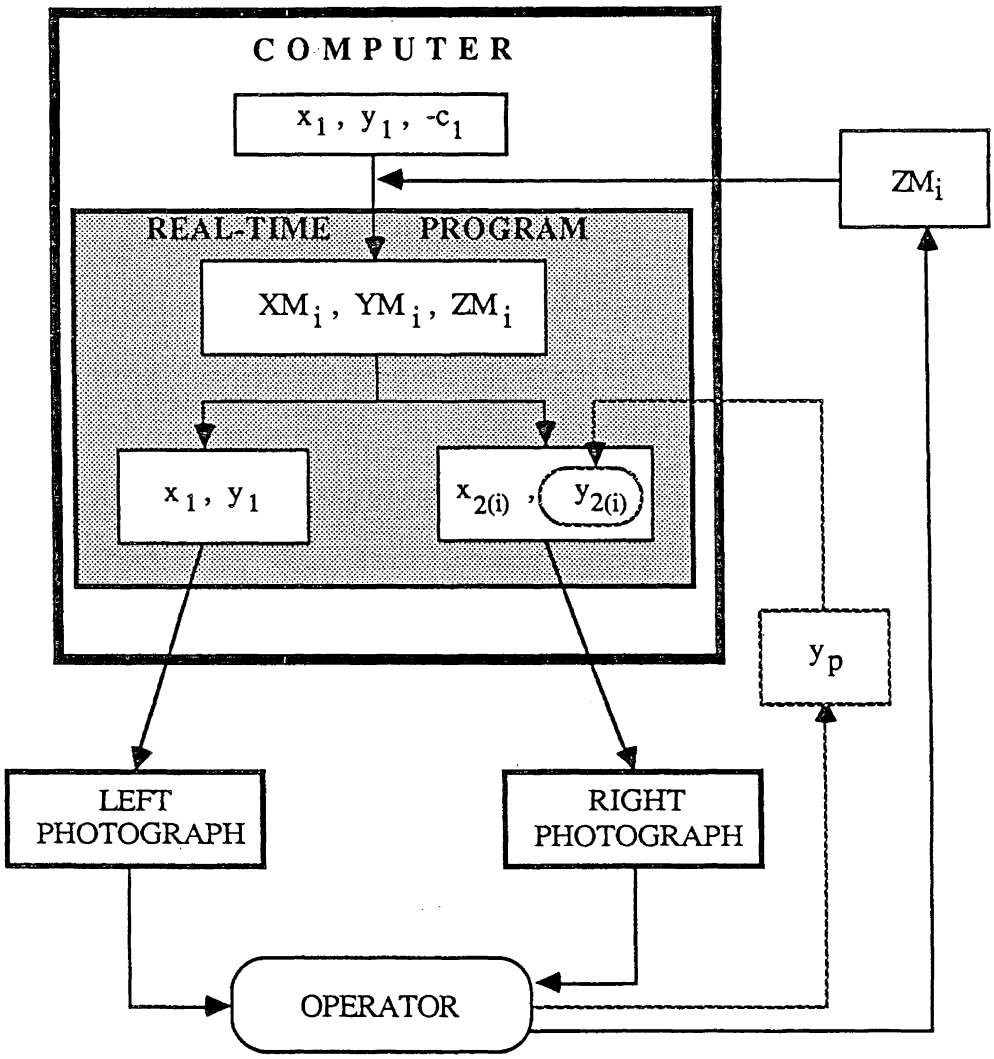

Figure 4.12: Diagram of the positioning routine.

capabilities, such as: revisit, delete, replace a point or change its identification number. If a "real" model is measured during this phase, the system operates as on-line stereo-comparator and an exit option is available before the program enters the next phase. In the second phase it drives the measuring mark automatically to the already selected points on the reference photograph, keeps it on them and determines the corresponding points on the dependent photograph under operator's supervision. The preservation of continuous stereoscopic perception increases the reliability of the observations and eases the operator's task.

The entire procedure of measuring images of non-targetted points between two or more different epochs, in on-line semi-automatic manner using the analytical-plotter, is illustrated in Figure (4.13). The preparatory steps include: calling of certain initialization routines, entering information related to the stationary photograph, the "real"/"pseudo" model, diapositives or negatives, basic interior orientation parameters, identification numbers for the photographs, title of project and simple operations related to files.

4.6 Outline and Organization of the Software

While the control-computer is the heart of the analytical photogrammetric stereo-plotter, the software provides the intelligence that makes the instrument function. The Analytical Photogrammetric On-Line Observations (APOLO) system is a software

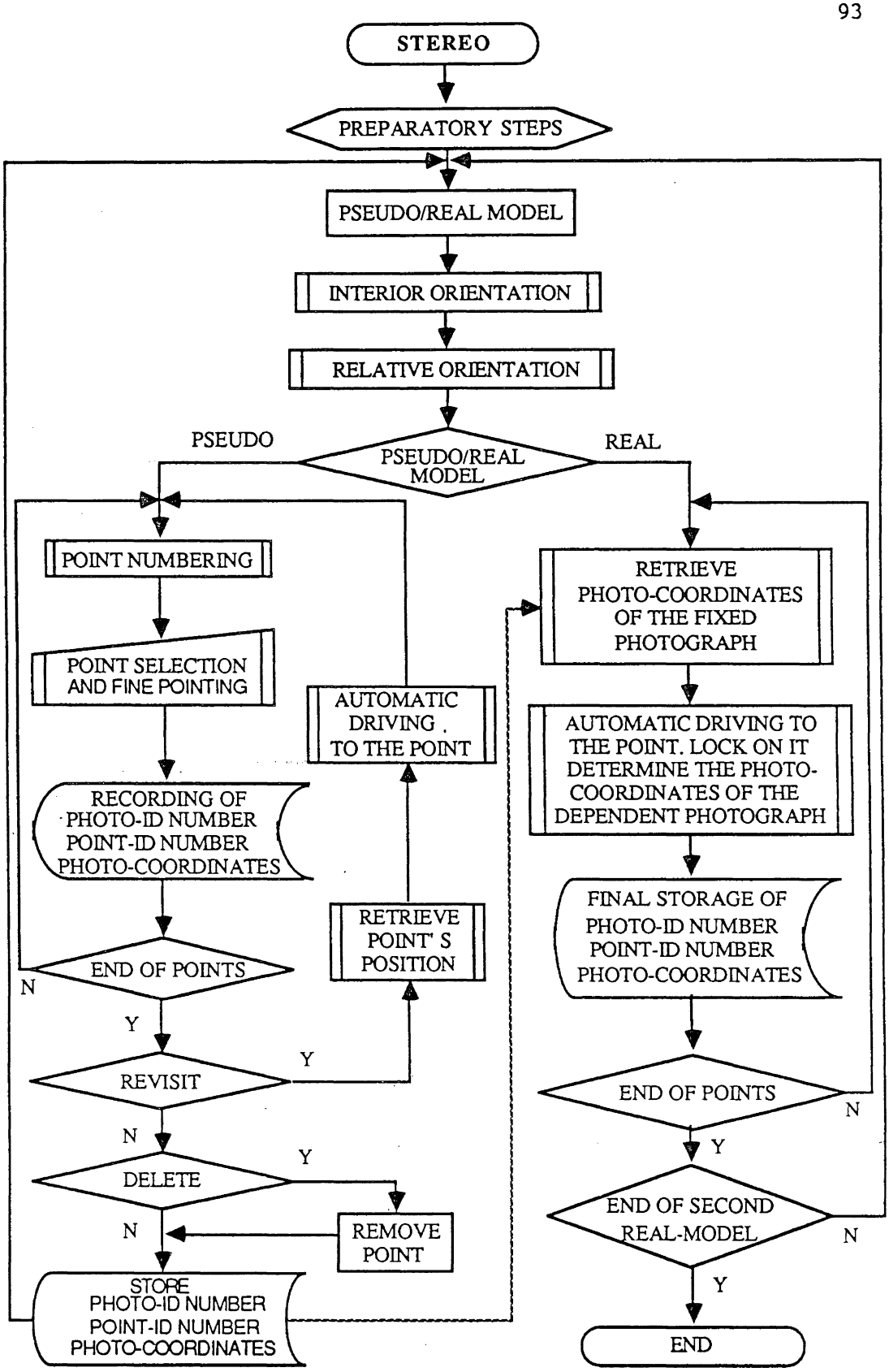

Figure 4.13: Functional diagram of the STEREO-mode.

package designed and developed by the author to perform the on-line semi-automatic measurements of the images of either targetted or natural object points from uni- and multi-temporal photographs. The software, written in PDP FORTRAN 77 is in modular form and the entire task is built by using the overlay technique. It is integrated with the existing basic real-time program, called SUPORT, and the driver which are written in PDP ASSEMBLER language.

The root of the overlaid tree structure consists of APOLO's main program and of SUPORT. The two main branches are the subprograms MONO and STEREO (Fig. 4.14).

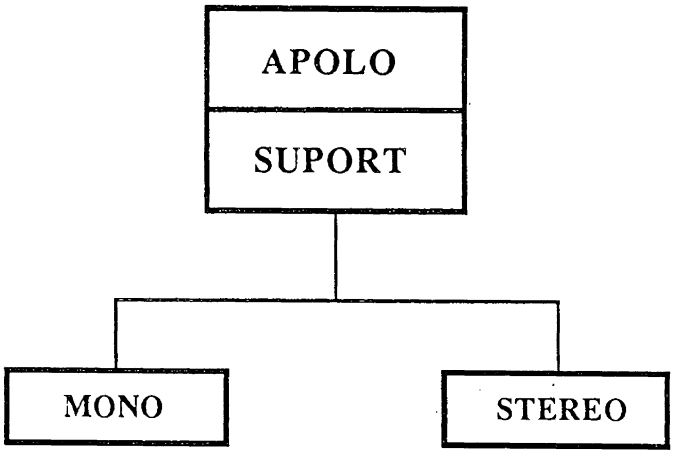

Figure 4.14: General overlay structure of the APOLO system.

The size of the longest segment in APOLO is 24480 words (maximum available size is 24576 words), while the required size of contiguous space on disk for running APOLO is 118 Kbytes. The entire task is built (linked) in approximately 4.8 minutes and uses 5 logical units and 4 active files.

The overlay structures of the subprograms MONO and STEREO for the photo-measurements is illustrated in Figures (4.15) and (4.16). A brief description of the routines used is presented, while detailed flow charts are given in Appendix I.

For the MONO-mode:

QIKDIG :Digitizes and records table-coordinates.

MONO :Main subprogram for the targetted points.

INIL1[1] :Initializes certain parameters of the analytical-plotter. Sets origin at the perspective centre of the fixed photograph.

IOREN1[1] :Performs the centering of the photograph and drives the measuring mark automatically to the location of the reference marks.

LOCST1[1] :Initializes certain parameters and sets up the coordinate system.

DRIVE/VISIT :Drives the measuring mark to the approximate photo-locations of the selected points.

WAINT1[1] :Allows manual operations.

AMATER :Allows fine centering on the fiducial marks and records the measurements.

NUMBER :Performs point-numbering.

SEARCH :Finds the location of points and their coordinates based on their ID number.

STRAN :Performs the similarity transformation.

---

[1]Modified versions of existing routines

LIPADJ :Performs the linear parametric least squares adjustment.

RESECT :Performs the space resection.

ROTMAT :Forms the rotation matrix.

NLPADJ :Performs the non-linear parametric least squares adjustment.

STAT/STATL :Computes statistical information related to the non-linear and linear least squares estimation.

SPIN[2] :Computes the inverse of a symmetric positive-definite matrix using the Cholesky decomposition.

MMULS[2] :Performs matrix multiplication.

TRNSS[2] :Transposes a matrix.

MINVS[2] :Computes the inverse of a matrix.

SLAMP[2] :Activates the lamps of the projectors.

APCIO[2] :Starts the driver for the analytical-plotter.

APCC[2] :Locates the physical centres of the carriages.

APCMK[2] :Masks the interface interrupt.

APCUK[2] :Unmasks the interface interrupt.

APCHLT[2] :Sets a specific position as the origin of the measuring system.

IBUTN[2] :Checks the buttons on the control panel.

---

[2]Existing routines

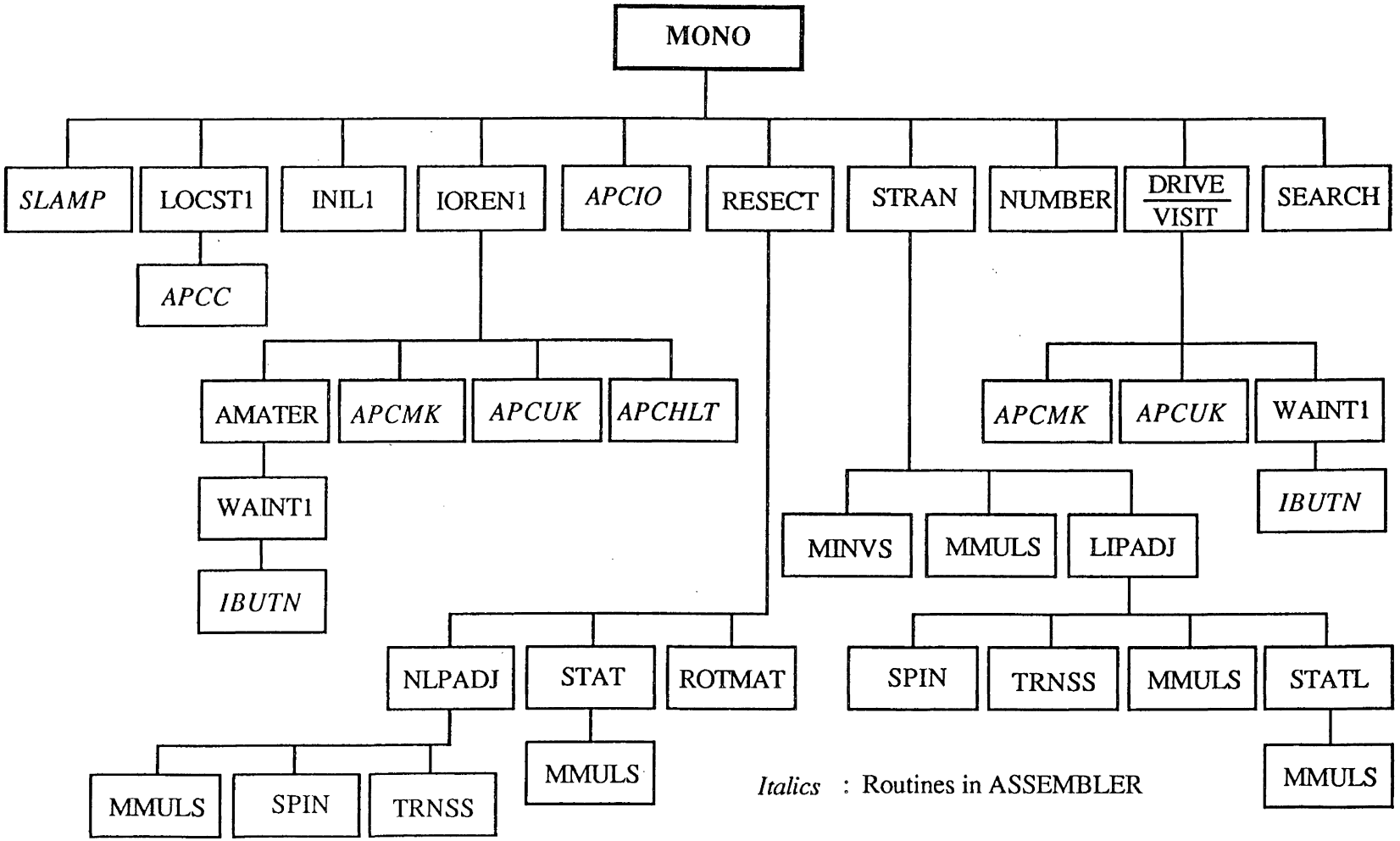

Figure 4.15: Overlay Structure for the On-Line Data Collection in Mono-Comparator Mode.

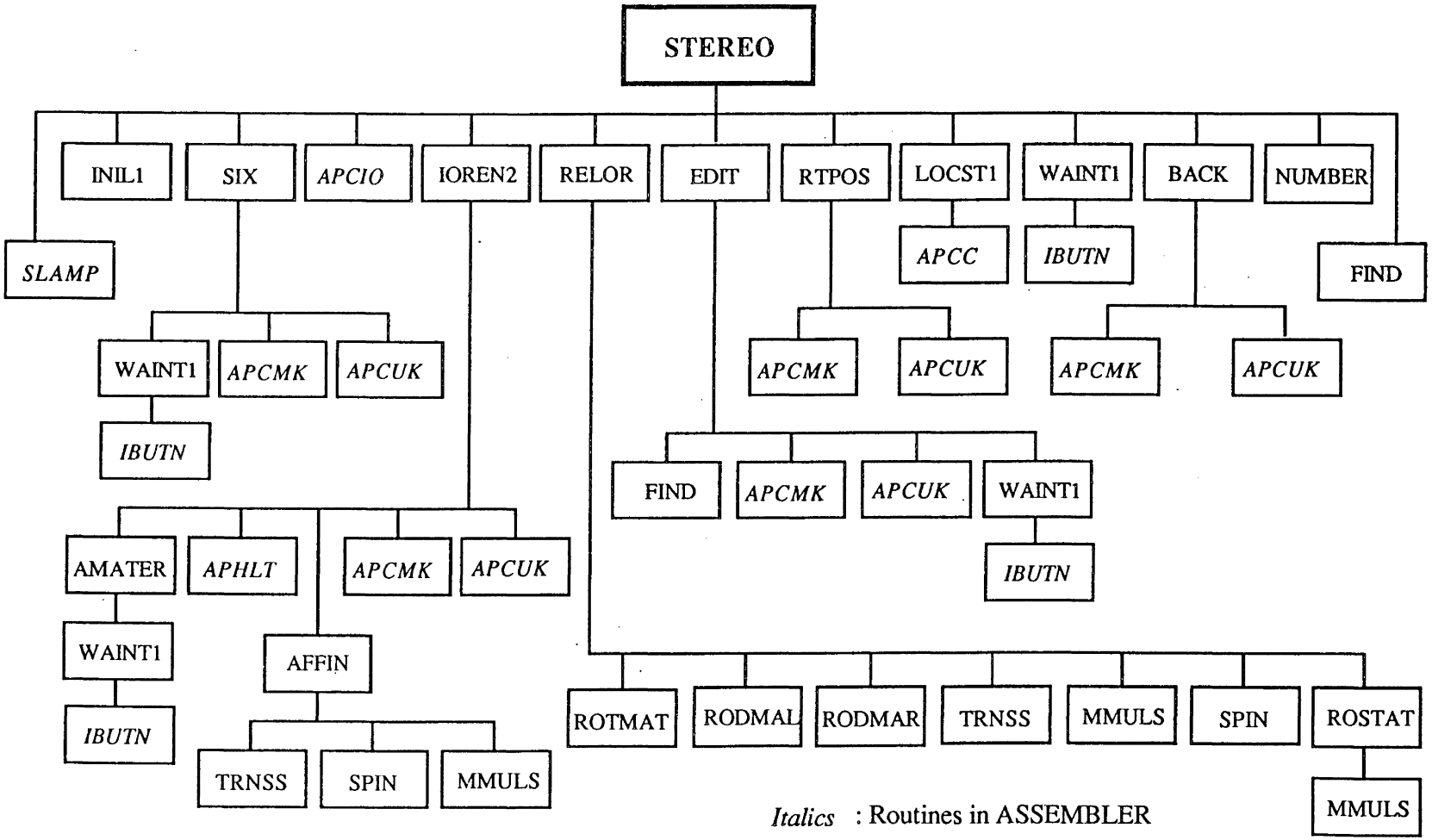

Figure 4.16: Overlay Structure for the On-Line Data Collection in Stereo-Comparator/Plotter Mode.

For the STEREO-mode:

STEREO :Main subprogram for the natural points.

INIL1 :As in MONO-mode.

LOCST1 :As in MONO-mode.

IOREN2 :Performs the interior orientation of the photographs using the affine transformation to transfer stage-coordinates to photo-coordinates and vice-versa.

AMATER :As in MONO-mode.

WAINT1 :As in MONO-mode.

NUMBER :As in MONO-mode.

FIND :As routine SEARCH in MONO-mode.

SIX :Calculates approximate values for the base components, drives the measuring marks to the von Gruber locations, allows elimination of parallaxes and records the corresponding stage-coordinates.

RELOR :Performs analytically the dependent pair relative orientation.

BACK :Passes the computed elements of relative orientation to the real-time program.

RODMAL/RODMAR:Form design matrices for the relative orientation when the stationary photograph is on the left or right carrier, respectively.

ROSTAT :Computes the statistical information of the combined least squares adjustment for the relative orientation.

EDIT :Performs the editing functions.

RTPOS :Performs the positioning operations for the homologous points, in the case of real-models.

AFFIN :Performs the affine transformation.

SPIN: :As in MONO-mode.

MMULS :As in MONO-mode.

TRNSS :As in MONO-mode.

4.7 Evaluation of the Quality of the Measured Photo-Coordinates

The determination of the accuracy C_{OB} of the position of the object points or their trajectories by photogrammetric means is a direct function of the accuracy C_p of the measured photo-coordinates. That is,

$$C_{OB} = f\ (C_p) \qquad (4.7)$$

where the function f is defined by the photogrammetric system, the functional model and the geometric configuration. Therefore, it is important to assess the quality of the photo-observations.

A number of factors affect the measuring precision (Trinder, 1986). They are mainly related to the photogrammetric system and are:

1) image quality (sharp versus blurred images)

2) type of camera

3) type of film

4) target characteristics (size, shape, colour)

5) measuring system

6) optical magnification

7) quality of the optics

8) type of observational procedure (monocular, binocular, stereoscopic)

9) physical and psychological conditions of the observer, as well as his experience.

The evaluation of photo-observations can be performed in three interrelated spaces. The photo-space is related directly to the measuring instrument and to the rest of the above mentioned factors and thus, inference on the quality of the measured images can be made directly. However, it is possible to use either the model- or the object spaces and then, according to certain mathematical relationships to indirectly evaluate the accuracy of the photo-coordinates.

Due to lack of control over most of the above elements, the evaluation of the measurements was performed independently of the object space as follows:

-- For the targetted points:

The performance of the measuring system was assessed with the aid of calibrated grid plates. The mensuration principle is based on the motion of the optics and of the photo-carriages along the x- and y-directions, respectively. The precision of positioning and measuring devices is limited by the manufacturing restrictions of the mechanical, optical and electronic parts. This imperfectness causes systematic linear and non-linear errors (Manual of Photogrammetry, 1980). Two aspects were investigated.

a) The precision (repeatability) of the measurements, where the grid

intersections were observed three (3) times. The statistical measure of repeatability was defined to be the mean value of the individual standard deviations of the observations at each point.

b) The accuracy of the measurements, where the linear systematic errors were considered. The effect of non-linear measuring errors due to dynamic behaviour of the analytical-plotter were not investigated as their magnitude is of lower order and would require grid plates of very high accuracy (Fritz, 1982). The linear systematic errors are composed of different but uniform scale changes along the x- and y-axes and of the non-orthogonality of these axes. The functional model expressing this physical situation is the affinity transformation (Appendix I) between the measured and the calibrated coordinates of the grid points. Due to overdetermination the principle of least squares is applied. The assessment of the accuracy is based on post adjustment tests of the a posteriori estimate of the reference variance factor, the estimated variance-covariance matrix of the unknown parameters, and on visual inspection of the plotted residuals of the observations at each grid point.

-- For the natural points:

The evaluation of the natural points was performed indirectly using the well-established coplanarity equation as functional model. Dependent pair relative orientation was performed for stereo-pairs of photographs with both x, y coordinates from each photograph being treated as observables. The linearization of the condition equation $F(\mathbf{x},\mathbf{l}) = \mathbf{0}$, ($\mathbf{x}$, $\mathbf{l}$ are the vectors of the five unknown relative

orientation parameters and of the photo-observations, respectively), leads to the combined least squares adjustment (adjustment of observations and functionally independent parameters). The stochastic model was based on precision acquired from preliminary photo-observations. The quality of the collected photo-coordinates was assessed with the aid of post adjustment tests of the variance factor and the residuals of the observations, as well as of the residual parallaxes computed for each model point.

The first test was performed on the a-posteriori estimate $\hat{\sigma}_o^2$ of the reference variance factor. This value was compared to the a-priori value σ_o^2 which is considered known since the inverse of the diagonal variance-covariance matrix of the observations was scaled to obtain or weight matrix **P** approximately equal to unity. Since σ_o^2 is considered known, the statistic

$$\frac{df \cdot \hat{\sigma}_o^2}{\sigma_o^2} \qquad (4.8)$$

has a chi-square (X^2) distribution (Mikhail, 1976) where df is the degrees of freedom in the adjustment. The two tailed confidence region for σ_o^2 was computed as:

$$\frac{df \cdot \hat{\sigma}_o^2}{X^2_{df,\alpha/2}} < \sigma_o^2 < \frac{df \cdot \hat{\sigma}_o^2}{X^2_{df,1-\alpha/2}} \qquad (4.9)$$

with α being the confidence level.

The difficult stereoscopic conditions which were encountered during measurements of pre-marked natural points led to the examination of the collected photo-coordinates for possible

blunders. The "data snooping" technique proposed by W. Baarda (1968) was incorporated to test the observations against outliers. This test considers the different precision of the residuals, and therefore their cofactor matrix was computed as (Vanicek and Krakiwsky, 1986):

$$Q_{vv} = P^{-1}B^{T}M(I-A(A^{T}MA)^{-1}A^{T}M)BP^{-1} \qquad (4.10)$$

where

Q_{vv} : the cofactor matrix of the residuals **v**

$$\mathbf{A} = \frac{\partial F(\mathbf{x},\mathbf{l})}{\partial \mathbf{x}} \text{ : the first design matrix}$$

$$\mathbf{B} = \frac{\partial F(\mathbf{x},\mathbf{l})}{\partial \mathbf{l}} \text{ : the second design matrix}$$

P : the weight matrix

$\mathbf{M} = (\mathbf{B}\mathbf{P}^{-1}\mathbf{B}^{T})^{-1}$

The test now consists of comparing the absolute values of the standardized residual w_i with the critical value c. That is,if

$$|w_i| = \frac{|v_i|}{\sigma_{vi}} = \frac{|v_i|}{(\sigma_o\sqrt{q_{vvi}})} > c \qquad (4.11)$$

then the corresponding observation l_i is suspected to be contaminated by a blunder. The critical value c is defined as (Kavouras, 1982):

$$c = \sqrt{F_{1-\alpha o;1,\infty}} = t_{1-\alpha o,\infty} \qquad (4.12)$$

where F and t are the Fisher and Student distributions respectively with degrees of freedom $v_1 = 1$ and $v_2 = \infty$ and α_o is the significance level for the one-dimensional test of the standardized residuals.

Relevant to the residuals are the redundancy numbers $r_{jx,y}$ (j refers to the point, x and y refer to the corresponding photo-observations), which represent the effect of a gross error $\nabla l_{jx,y}$ on the residual $v_{jx,y}$ of the corresponding observation $l_{jx,y}$. They were computed as (Förstner, 1985)

$$r_{jx,y} = (Q_{vv} \cdot P)_{jjx,y} \qquad (4.13)$$

The computation of the r- values served as:

i) a check since

$$\Sigma r_{jx,y} = df \text{ , and} \qquad (4.14)$$

ii) an indicator of the controllability of the observations and of the geometric strength of the configuration of the intersecting rays.

It is worth mentioning here that the redundancy numbers corresponding to the x component of the photo-coordinates always have extremely small values indicating a very weak local geometry and that these observations cannot be checked at all. The reason for this is that variations in the x photo-coordinates influence the z coordinate of the model points and not the parameters of the relative orientation. On the contrary, the redundancy numbers corresponding to the y coordinates being larger than zero indicate a much stronger geometry. Hence, the y-observations are much more controllable as they are related directly to the estimated five parameters and possible gross errors can be detected there (Kratky and El-Hakim, 1983). Nevertheless, an indication of the existence of an outlying y-observation strongly suggests the possibility of a point misidentification.

Another aspect examined to assess the photo-measurements was the vector representing the non-intersection of the two conjugate rays at each model point. The model coordinates and their residual parallaxes with their mean values and standard deviations were computed for each stereo-model.

Software has been developed by the author to evaluate the measurements of both types of image points. The software for the qualitative assessment of the targetted points is written in FORTRAN 77 and runs on the DEC PDP 11/60. The evaluation of the quality of the measured natural points was performed with the corresponding software written in VS FORTRAN for the IBM 3090-180 VF main frame computer.

5. MONITORING OF THE SPATIAL TRAJECTORIES OF OBJECTS WITH THE SEQUENTIAL PHOTOGRAMMETRIC APPROACH

5.1 Introduction to the Sequential Photogrammetric Model

At present, photogrammetric observations are performed at discrete time intervals in order to provide an instantaneous record of the state of the object under examination at particular moments of time. No consideration has been given to the positional properties of the object due to its kinematic behaviour following certain dynamic principles.

Therefore, an attempt has been made by the author to integrate with the photogrammetric functional model additional information stemming from a-priori estimates of the position of the detail points with respect to a spatial reference system. This integration of information for the combined determination of the trajectories of the points is related directly with the phase of data processing.

We can now distinguish two modes of evaluation:

a) The static mode (Fig. 5.1), where monitoring of displacements is carried out in separate campaigns which are independent of each other. The position vectors $\mathbf{r}(t)$ and $\mathbf{r}(t+1)$ at epochs t and t+1 respectively are determined solely from the individual photogrammetric campaigns without any interrelation between the two

observation epochs. The final position vector at each time is estimated by adding the solution corrections to the initial approximate values of the unknown parameters. These corrections depend on the number and configuration of the observations. The final positioning accuracy at each epoch is also a function of the individual observation scheme. The displacement vector, that is the spatial difference between the two position vectors is simply calculated by subtracting the corresponding coordinate elements. No consideration is given on how the position vector **r**(t) moved to its new position **r**(t+1) or on how much **r**(t+1) depends on **r**(t).

b) The sequential mode (Fig. 5.2), where in a time varying situation, positions of the detail points change not only as new

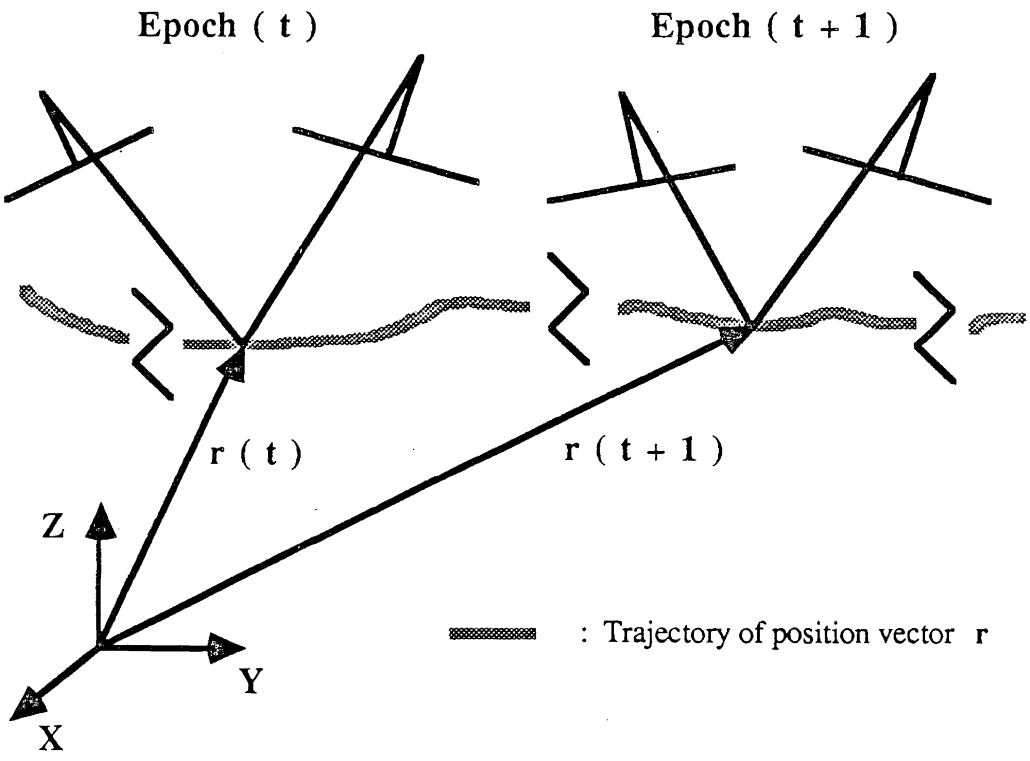

Figure 5.1: Static mode of monitoring displacements.

observations become available but also progressively as a result of a cause. If the cause is adequately known, it is possible to compute a preliminary estimate of the position vector $\mathbf{r}(t)$ based on its previous spatial position $\mathbf{r}(t-1)$. Also, the variance-covariance matrix of $\mathbf{r}(t)$ can be estimated due to the uncertainties of the functional parameters expressing the transition from stage $\mathbf{r}(t-1)$ to stage $\mathbf{r}(t)$. This dynamic information has been directly incorporated into the photogrammetric evaluation model. Consequently, the photogrammetric point determination can be supported and improved by the functional relationship between the object points at successive epochs. An improvement of the accuracies of the determined point positions can also be expected because of the contribution of this additional information.

The term "sequential" was adopted to express the two areas of investigation. The first one is related to the combination of the consecutive photogrammetric campaigns in a sequential order, while the second is associated with the potential application of sequential techniques of the least squares adjustment.

5.2 Sequential Processing of Photogrammetric and Object Observations

The sequential photogrammetric mode for monitoring displacements is developed according to the following scenario that describes a physical situation at an instant of time t. This instant of time is characterized by two events:

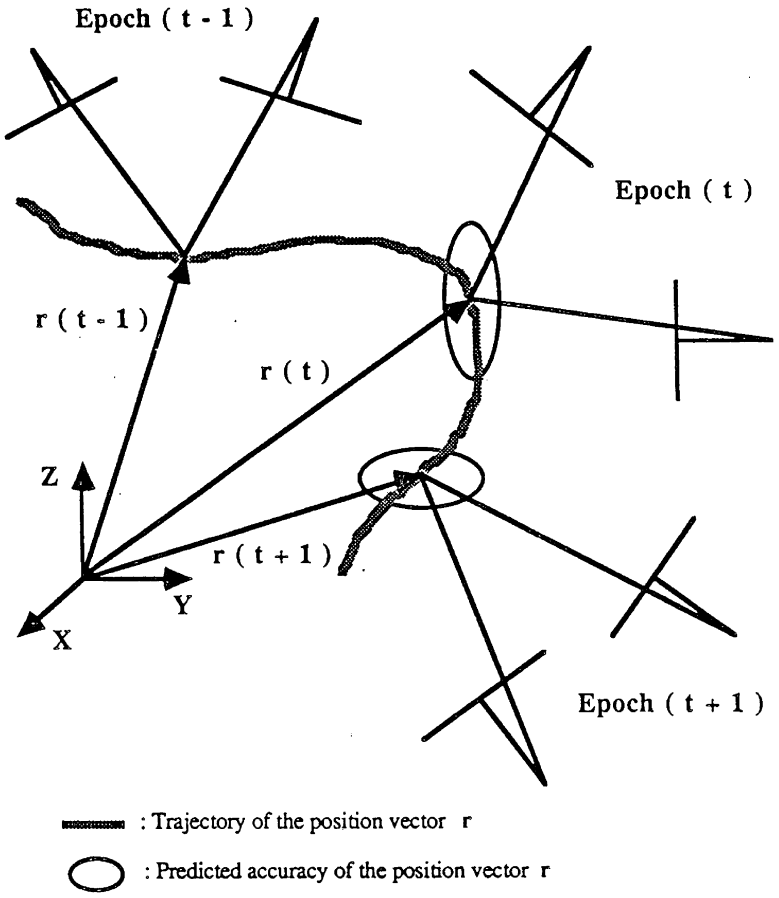

Figure 5.2: Sequential mode of monitoring displacements.

a) Estimated values $\mathbf{x}_{l(t)}$ of the unknown parameter vector $\mathbf{x}_{(t)}$ representing the spatial position of the detail points together with their corresponding covariance matrix $\mathbf{C}_{xl(t)}$ are known. This information is usually available from prediction theories or physical laws affecting the deformable body. Thus, we have

$$\mathbf{x}_{(t)} = \mathbf{x}_{l(t)} \quad , \quad \mathbf{C}_{xl(t)} \tag{5.1}$$

b) At the same discrete time t, photogrammetric observations $\mathbf{l}_{(t)}$ are made. The covariance matrix $\mathbf{C}_{l(t)}$ of the associated observation errors is known. The measured quantities are functions of the parameter vector $\mathbf{x}_{(t)}$ and are expressed as

$$\mathbf{f}_{(t)} (\mathbf{x}_{(t)}) = \mathbf{l}_{(t)} \quad , \quad \mathbf{C}_{l(t)} \tag{5.2}$$

While case b) represents a classical adjustment problem with zero a-priori values of $C^{-1}_{x(t)}$, case a) represents an example where the a-priori weight matrix $C^{-1}_{xl(t)}$ of the unknown parameters is non-zero. This information is usually neglected and not treated in a least squares solution although approximate values of the unknown parameters are required for linearization to form the design matrices, and these initial values are known to a certain degree.

The incorporation of this additional a-priori information is possible with a more generalized perception of the least squares problem. This permits the consideration of all variables involved in the mathematical formulation as observations (Mikhail, 1976) with the unknown parameters becoming quasi-observations. Thus, different types of data can be handled as observables, and any distinction between them is made with the aid of the covariance (or weight) matrix. There are usually two techniques to derive a solution for this general approach (Mikhail, 1976; Vanicek and Krakiwsky, 1986):

In the first one, the designated parameters $\mathbf{x}_1(\equiv \mathbf{x}_{1(t)})$ are treated as observations. Therefore, a new observation vector $\mathbf{l}'$ is formed whose elements are the two discrete observation vectors $\mathbf{x}_1$ and $\mathbf{l}_2(\equiv \mathbf{l}_{(t)})$. The partition of $\mathbf{l}'$ is then

$$\mathbf{l}' = [\ \mathbf{x}_1^T \ |\ \mathbf{l}_2^T]^T \qquad (5.3)$$

For simplicity's sake, the time subscript is dropped from these formulations since at present we refer to the same time t. Also, the subscripts 1 and 2 are introduced and correspond to equs. (5.1) and (5.2) respectively.

Assuming that the two sets of observations are statistically independent, the corresponding covariance- and weight matrices $\mathbf{C}_1$,

and $P_{1'}$ will be

$$C_{1'} = \left[\begin{array}{c|c} C_{x1} & 0 \\ \hline 0 & C_{12} \end{array}\right] \text{ and } P_{1'} = \left[\begin{array}{c|c} C^{-1}{}_{x1} & 0 \\ \hline 0 & C^{-1}{}_{12} \end{array}\right] \quad (5.4)$$

The mathematical model is therefore equivalent to the adjustment of observations or commonly known as the condition approach. Thus

$$g(1') = 0, \quad (5.5)$$

or in linearized form:

$$B'v' + w = 0 \quad (5.6)$$

where

$$B' = [A \mid B] \ , \ v' = [v_1{}^T \mid v_2{}^T]^T \ , \ w = g(1'_o)$$

$$\text{and } A = \left.\frac{\partial g(1')}{\partial x}\right|_{\substack{x=x_o \\ 1=1_o}} \ , \ B = \left.\frac{\partial g(1')}{\partial 1}\right|_{\substack{x=x_o \\ 1=1_o}}$$

In the second approach the two models expressed in equations (5.1) and (5.2) maintain their individuality. This aspect is considered essential in the development of the sequential model, where the mathematical model consists of the two component models. The first component model (equ. (5.1) is of the condition type, with the following linearization:

$f_1(\hat{x}) = 0$ becomes $f_1(x_1 + v_1) = 0$ or

$$f_1(\hat{x})_o + \left.\frac{\partial f_1(\hat{x})}{\partial x}\right|_{x=x_1} \delta x_1 = 0 \quad (5.7a)$$

which is commonly expressed as:

$$A_1 \delta x_1 + w_1 = 0 \quad (5.7b)$$

where

$$A_1 = \frac{\partial f_1(\hat{x})}{\partial x} \quad (5.7c)$$

which becomes $A_1 = I$,

and

$$\mathbf{w}_1 = f_1(\hat{\mathbf{x}})_o \quad \text{or} \quad \mathbf{w}_1 = \mathbf{x}_1 = \mathbf{x}_1 \tag{5.7d}$$

and

$$\delta\mathbf{x}_1 = \delta\mathbf{x}_1 = \mathbf{v}_1 \tag{5.7e}$$

The corresponding weight matrix is

$$\mathbf{P}_1 = \mathbf{C}_{x1}^{-1} \quad \text{or} \quad \mathbf{P}_1 = \mathbf{C}_1^{-1} \tag{5.8}$$

The second component model is of the non-linear parametric type with the following linearization:

$$f_2(\hat{\mathbf{x}}) = \mathbf{l}_2 + \mathbf{v}_2 \text{ or } f_2(\hat{\mathbf{x}})_o + \left.\frac{\partial f_2(\hat{\mathbf{x}})}{\partial \mathbf{x}}\right|_{\mathbf{x}=\mathbf{x}_1} \delta\mathbf{x}_1 - \mathbf{l}_2 - \mathbf{v}_2 = \mathbf{0} \tag{5.9a}$$

which again is expressed in standard terms as

$$\mathbf{A}_2\delta\mathbf{x}_1 + \mathbf{w}_2 - \mathbf{v}_2 = \mathbf{0} \tag{5.9b}$$

where

$$\mathbf{A}_2 = \left.\frac{\partial f_2(\hat{\mathbf{x}})}{\partial \mathbf{x}}\right|_{\mathbf{x}=\mathbf{x}_1} \tag{5.9c}$$

and

$$\mathbf{w}_2 = f_2(\hat{\mathbf{x}})_o - \mathbf{l}_2 \tag{5.9d}$$

The corresponding weight matrix is

$$\mathbf{P}_2 = \mathbf{C}_1^{-1} \quad \text{or} \quad \mathbf{P}_2 = \mathbf{C}_2^{-1} \tag{5.10}$$

The combined linearized mathematical model of equs. (5.7b) and (5.9b) can be considered to be of the parametric form

$$\mathbf{A}\delta\mathbf{x} + \mathbf{w} - \mathbf{v} = \mathbf{0} \tag{5.11a}$$

where

$$\mathbf{A} = \begin{bmatrix} \mathbf{A}_1 \\ \hline \mathbf{A}_2 \end{bmatrix} = \begin{bmatrix} \mathbf{I} \\ \hline \mathbf{A}_2 \end{bmatrix}, \quad \mathbf{w} = \begin{bmatrix} \mathbf{x}_1 \\ \hline \mathbf{w}_2 \end{bmatrix}, \quad \mathbf{v} = \begin{bmatrix} \mathbf{0} \\ \hline \mathbf{v}_2 \end{bmatrix} \tag{5.11b}$$

Assuming logically that there is no correlation between the two sets

of measurements, the combined weight matrix for the model of equ. (5.11) is

$$\mathbf{P} = \begin{bmatrix} \mathbf{P}_1 & \mathbf{0} \\ \mathbf{0} & \mathbf{P}_2 \end{bmatrix} \tag{5.12}$$

$\boldsymbol{\delta x}$ is estimated by applying the least squares criterion

$$\mathbf{v}^T\mathbf{P}\mathbf{v} = \mathbf{v}_1^T\mathbf{P}_1\mathbf{v}_1 + \mathbf{v}_2^T\mathbf{P}_2\mathbf{v}_2 = \text{minimum} \tag{5.13}$$

where $\mathbf{v}_1 = \boldsymbol{\delta}\mathbf{x}_1$ is the residual vector of the observations $\mathbf{x}_1$ and $\mathbf{v}_2$ is the residual vector of the observations $\mathbf{l}_2$. The hypermatrix representing the normal equations for the parametric case (method of indirect observations) of least squares adjustment is (Wells and Krakiwsky, 1971).

$$\begin{bmatrix} \mathbf{P} & -\mathbf{I} & \mathbf{0} \\ -\mathbf{I} & \mathbf{0} & \mathbf{A} \\ \mathbf{0} & \mathbf{A}^T & \mathbf{0} \end{bmatrix} \begin{bmatrix} \mathbf{v} \\ \mathbf{k} \\ \boldsymbol{\delta}\mathbf{x} \end{bmatrix} + \begin{bmatrix} \mathbf{0} \\ \mathbf{w} \\ \mathbf{0} \end{bmatrix} = \mathbf{0} \tag{5.14a}$$

where

$$\mathbf{A}^T = [\mathbf{I} \mid \mathbf{A}_2^T] \ , \ \mathbf{k} = \begin{bmatrix} \mathbf{k}_1 \\ \hline \mathbf{k}_2 \end{bmatrix} \tag{5.14b}$$

and the other hypermatrices or vectors are as defined in equs. (5.11b) and (5.12). The solution (correction) vector $\boldsymbol{\delta x}$ is not partitioned because both subsets of observations are related to the same unknown parameters. It is determined by applying partitioning and elimination techniques to equ. (5.14a). Thus,

$$\boldsymbol{\delta}\mathbf{x} = -(\mathbf{P}_1 + \mathbf{A}_2^T\mathbf{P}_2\mathbf{A}_2)^{-1} (\mathbf{P}_1\mathbf{x}_1 + \mathbf{A}_2^T\mathbf{P}_2\mathbf{w}_2) \tag{5.15}$$

This solution has been derived under the assumption that both observation sets are available simultaneously. However, in reality, measurements become available sequentially or else a-priori estimates of the solution vector may be available (e.g., equ. (5.1)). Therefore, it is preferable and practical to determine new

estimations based on new measurements (e.g., equ. (5.2)), in terms of previous solutions. This approach is possible by deriving sequential expressions of the least squares solution. By arranging the computations in this manner, the estimated $\delta\mathbf{x}$ (or $\hat{\mathbf{x}}$) of the parameter vector is equal to the estimated solution resulting from the first model (equ. (5.1)) plus a correction term from the contribution of the second model (equ. (5.2)). Using again the rules for inverting partitioned matrices plus elementary row and column operations on the partitioned normal equations matrix (equ. (5.14a)), it is possible to obtain a sequential solution for $\delta\mathbf{x}$ through successive eliminations by eliminating $\mathbf{v}$ and $\mathbf{k}$ (Wells and Krakiwsky, 1971; Junkins, 1978). Hence,

$$\delta\mathbf{x} = -\mathbf{N}_1^{-1}\mathbf{q}_1 - \mathbf{N}_1^{-1}\mathbf{A}_2^T\mathbf{k}_2 \qquad (5.16a)$$

where

$$\mathbf{k}_2 = (\mathbf{P}_2^{-1} + \mathbf{A}_2\mathbf{N}_1^{-1}\mathbf{A}_2^T)^{-1}\,(-\mathbf{A}_2\mathbf{N}_1^{-1}\mathbf{q}_1 + \mathbf{w}_2) \qquad (5.16b)$$

$$\mathbf{N}_1^{-1} = (\mathbf{A}_1^T\mathbf{P}_1\mathbf{A}_1)^{-1} = \mathbf{P}_1^{-1}\ , \text{ because } \mathbf{A}_1=\mathbf{I} \qquad (5.16c)$$

$$\mathbf{q}_1 = \mathbf{A}_1^T\mathbf{P}_1\mathbf{w}_1 = \mathbf{P}_1\mathbf{w}_1\ , \text{ because } \mathbf{A}_1=\mathbf{I} \qquad (5.16d)$$

It is also known that

$$-\mathbf{N}_1^{-1}\mathbf{q}_1 = \delta\mathbf{x}_1 \qquad (5.17)$$

where $\delta\mathbf{x}_1$ is the solution for the parameter vector when the first component model f_1 is used only. If we set $\delta\mathbf{x}_2 \hat{=} \delta\mathbf{x}$, which means that the unknown parameters are estimated after considering the second component model f_2 and using equs. (5.16b)- (5.17), then equ. (5.16a) becomes

$$\delta\mathbf{x}_2 = \delta\mathbf{x}_1 + \Delta\mathbf{x} \qquad (5.18a)$$

where

$$\Delta\mathbf{x} = -\mathbf{N}_1^{-1}\mathbf{A}_2^T(\mathbf{P}_2^{-1}+\mathbf{A}_2\mathbf{N}_1^{-1}\mathbf{A}_2^T)^{-1}(\mathbf{A}_2\delta\mathbf{x}_1+\mathbf{w}_2) \text{ or}$$

$$\Delta \mathbf{x} = -\mathbf{P}_1^{-1}\mathbf{A}_2^T(\mathbf{P}_2^{-1}+\mathbf{A}_2\mathbf{P}_1^{-1}\mathbf{A}_2^T)^{-1}(\mathbf{A}_2\delta\mathbf{x}_1+\mathbf{w}_2) \qquad (5.18b)$$

This sequential expression is very significant since it efficiently takes advantage of computations performed in processing previous component observation models. Also, the size of the matrices to be inverted is smaller since it only refers to the indivdual subset of observation equations and not to all observation equations.

However, the solution correction $\delta\mathbf{x}_2$ in equ.(5.18a) is a function of the solution correction $\delta\mathbf{x}_1$. In cases where the initial approximate values $\mathbf{x}_o$ of the parameter vector (usually $\mathbf{x}_o=\mathbf{x}_1=\mathbf{x}_1$) are not very close to the estimated value $\hat{\mathbf{x}}$ or where highly non-linear models are involved, it is desirable to pre-eliminate $\delta\mathbf{x}_1$ from equ.(5.18a). Furthermore, in order to cover situations where the final estimate $\hat{\mathbf{x}}_1=\hat{\hat{\mathbf{x}}}$ is available when the first model has been solved independently but there is no information available for $\mathbf{x}_o$ and $\delta\mathbf{x}_1$, it is practical to change the structure of equ.(5.18a).

Since we have assumed non-linear models for the sake of generalization, the final solution $\hat{\mathbf{x}}$ is determined from both the first and the merged model.

When the first model is used, then

$$\hat{\mathbf{x}} = \hat{\hat{\mathbf{x}}}_1 = \mathbf{x}_o + \sum_{i=1}^{n} \delta\mathbf{x}_{1i} \qquad (5.19)$$

where n is the number of iterations needed to reach convergence.

When the merged model is used, then

$$\hat{\mathbf{x}} = \hat{\hat{\mathbf{x}}}_2 = \mathbf{x}_o + \sum_{i=1}^{m} \delta\mathbf{x}_{2i} = \mathbf{x}_o + \sum_{i=1}^{m} (\delta\mathbf{x}_{1i} + \Delta\mathbf{x}_i) \quad \text{or}$$

$$\hat{\mathbf{x}} \hat{=} \hat{\mathbf{x}}_2 = \mathbf{x}_o + \sum_{i=1}^{m} \delta\mathbf{x}_{1i} + \sum_{i=1}^{m} \Delta\mathbf{x}_i = \hat{\mathbf{x}}_1 + \sum_{i=1}^{m} \Delta\mathbf{x}_i \qquad (5.20)$$

with m being the required number of iterations.

If we substitute the expression $\Delta\mathbf{x}$ from equ.(5.18b) into equ.(5.20) and linearize each time about the most recent estimate, we obtain a very important recursive formula for the ith iteration.

$$\hat{\mathbf{x}}_{2,i} = \hat{\mathbf{x}}_1 - \mathbf{P}_1^{-1}\mathbf{A}_2^T[\mathbf{P}_2^{-1} + \mathbf{A}_2\mathbf{P}_1^{-1}\mathbf{A}_2^T]^{-1}[\mathbf{A}_2(\hat{\mathbf{x}}_{2,i-1}-\hat{\mathbf{x}}_1)+\mathbf{w}_2] \qquad (5.21a)$$

or

$$\hat{\mathbf{x}}_{2,i} = \hat{\mathbf{x}}_1 - \mathbf{C}_1\mathbf{A}_2^T[\mathbf{C}_2 + \mathbf{A}_2\mathbf{C}_1\mathbf{A}_2^T]^{-1}[\mathbf{A}_2(\hat{\mathbf{x}}_{2,i-1}-\hat{\mathbf{x}}_1)+\mathbf{w}_2] \qquad (5.21b)$$

where

$\hat{\mathbf{x}}_{2,o} \hat{=} \hat{\mathbf{x}}_1$

and

$\hat{\mathbf{x}}_1 \hat{=} \mathbf{x}_o$ (value at which the linearization occurs).

The expressions (5.21) state clearly that when a new set of observations is added for the determination of the parameter vector, the resulting new parameter vector is equal to the parameter vector estimated from all previous observation equations plus a correction term. This term is the effect of the new observation equations.

The term $\mathbf{A}_2(\hat{\mathbf{x}}_{2,i} - \hat{\mathbf{x}}_1)$ needs to be clarified at this point. It resulted from equ.(5.18b) and (5.20) as

$$\mathbf{A}_2\delta\mathbf{x}_{1,i} = \mathbf{A}_2(\hat{\mathbf{x}}_{1,i} - \mathbf{x}_o) \qquad (5.22)$$

The terms $\delta\mathbf{x}_1$ and $\delta\mathbf{x}_2$ have been interchanged because the correction

term refers now to the linearization of the second mathematical model and the value at which this linearization occurs can be changed in order to minimize the correction term $\delta\mathbf{x}_i$ at each iteration. Therefore, the initial value $\mathbf{x}_o$ in equ.(5.22) can be improved to become equal to $\hat{\mathbf{x}}_1$. Similarly, the term $\hat{\mathbf{x}}_1$ in equ.(5.22) is replaced by $\hat{\mathbf{x}}_{2,i-1}$ because $\hat{\mathbf{x}}_1$ is no longer the final solution which now is $\hat{\mathbf{x}}_2$ due to the contribution of the second observation set.

Consequently, this substitution yields better accuracy because for each iteration the linearization occurs about values which are closer to the actual value $\hat{\mathbf{x}} \doteq \hat{\mathbf{x}}_2$. The above interchange of correction terms will obviously lead to $A_2(\hat{\mathbf{x}}_{2,i-1} - \hat{\mathbf{x}}_1) = \mathbf{0}$ for i=1. The second term in brackets in equ.(5.21) will therfore be equal to $\mathbf{w}_2 = f_2(\hat{\mathbf{x}}_1) - \mathbf{l}_2$. Together with the known value at location $\hat{\mathbf{x}}_1$ the derivation of this misclosure will participate in the computation of $\hat{\mathbf{x}}_{2,1}$, which will become the new location at which the function f_2 is linearized.

Following the derivation of the solution formula (equs.5.21) for the unknown parameters, is the estimation of their precision. Again, a sequential form of the variance-covariance matrix $\mathbf{C}_{\hat{\mathbf{x}}}$ of the estimated parameters $\hat{\mathbf{x}}$ is derived by applying the law of error propagation to equs.(5.21) (Wells and Krakiwsky, 1971). Therefore, we have

$$\begin{aligned} \mathbf{C}_{\hat{\mathbf{x}}} \doteq \mathbf{C}_{\hat{\mathbf{x}}_2} &= \mathbf{P}_1^{-1} - \mathbf{P}_1^{-1}\mathbf{A}_2^T(\mathbf{P}_2^{-1} + \mathbf{A}_2\mathbf{P}_1^{-1}\mathbf{A}_2^T)^{-1}\mathbf{A}_2\mathbf{P}_1^{-1} \\ &= [\mathbf{I} - \mathbf{P}_1^{-1}\mathbf{A}_2^T(\mathbf{P}_2^{-1} + \mathbf{A}_2\mathbf{P}_1^{-1}\mathbf{A}_2^T)^{-1}\mathbf{A}_2]\mathbf{P}_1^{-1} \end{aligned} \qquad (5.23a)$$

or

$$\mathbf{C}_{\hat{\mathbf{x}}} = [\mathbf{I} - \mathbf{C}_1\mathbf{A}^T{}_2(\mathbf{C}_2 + \mathbf{A}_2\mathbf{C}_1\mathbf{A}^T{}_2)^{-1}\mathbf{A}_2]\mathbf{C}_1 \qquad (5.23b)$$

Equation (5.23b) was derived from equ. (5.23a) given that $\mathbf{P}_1=\mathbf{C}_1^{-1}$ and $\mathbf{P}_2=\mathbf{C}_2^{-1}$. That means that the variance-covariance matrices of the two different observation sets were used unscaled and the weight matrices were simply obtained as their inverses. Two questions may arise:

What will happen if we use relative weight matrices? and

How will this affect the solution and the covariance matrix of the unknown parameters?

The answer to both is related to the preservation of the units of the scaled covariance matrices. Within this context we distinguish four different cases (Vanicek and Krakiwsky, 1986):

i) the a-priori variance factors $\sigma^2_{o,1}$ and $\sigma^2_{o,2}$ are both known and may, but do not have to be equal. ($\mathbf{P}_1 = \mathbf{C}_1^{-1}$, $\mathbf{P}_2 = \mathbf{C}_2^{-1}$).

ii) both $\sigma^2_{o,1}$ and $\sigma_o^2{}_{,2}$ are equal and unknown. In this case only one common factor has to be solved for to provide the relationship between the different weight matrices ($\mathbf{P}_1 = \sigma_o^2\mathbf{C}_1^{-1}$, $\mathbf{P}_2 = \sigma_o^2\mathbf{C}_2^{-1}$).

iii) one variance factor is known, the other unknown. This case is a combination of i) and iii), i.e., $\mathbf{P}_1 = \mathbf{C}_1^{-1}$, $\mathbf{P}_2 = \sigma_o^2{}_{,2}\mathbf{C}_2^{-1}$ or $\mathbf{P}_1 = \sigma_o{}_{,1}^2\mathbf{C}_1^{-1}$, $\mathbf{P}_2 = \mathbf{C}_2^{-1}$ and the corresponding unknown factor has to be determined.

iv) both variance factors are unknown and probably different. Thus, both have to be determined within the solution ($\mathbf{P}_1 = \sigma_o{}_{,1}^2\mathbf{C}_1^{-1}$, $\mathbf{P}_2 = \sigma_o{}_{,2}^2\mathbf{C}_2^{-1}$).

No particular problem arises for case i) and equs. (5.21) and (5.23) can be used as they are.

Case ii) is similar to the usual least squares procedures, where the a-posteriori estimate $\hat{\sigma}_o^2$ of the a-priori variance factor σ_o^2 needs to be computed. The difference here is that the complete quadratic form $\mathbf{v}^T\mathbf{P}\mathbf{v}$ from both models must be calculated. Thus,

$$\hat{\sigma}_o^2 = \frac{\mathbf{v}_1^T\mathbf{P}_1\mathbf{v}_1 + \mathbf{v}_2^T\mathbf{P}_2\mathbf{v}_2}{df} \qquad (5.24)$$

where df if the number of degrees of freedom of the adjustment and equals the total number of equations minus the number of unknowns. In this case the solution equations (5.21) are not affected, but equs. (5.23) have to be premultiplied by $\hat{\sigma}_o^2$ in order to obtain the estimated covariance matrix $\hat{\mathbf{C}}_{\hat{x}}$.

In case iii) the unknown $\hat{\sigma}_{o,i}^2$ (i=1 or 2) can be estimated by using only the corresponding model. The homologous covariance matrix $\mathbf{C}_i$ in equ. (5.23b) has to be scaled prior to combining it with the other terms to form $\mathbf{C}_{\hat{x}}$. However, this only leads to an approximate estimated covariance matrix of the unknown parameters (ibid).

Problems also exist for case iv), where an exact solution is not possible (ibid), although the minimum norm quadratic unbiased estimation (MINQUE) principle (Chen, 1983) provides an alternative approach. These two last cases should be further investigated as they may result in different solutions and different precisions due to different and unknown scale factors.

From this analysis it is evident that the first two cases are more appropriate for consideration in this study. This is in agreement with Mikhail, (1976), who stated that only one common factor must be chosen.

5.3 The Kinematic State of the Object and the Sequential Processing

So far the situation examined has been related to a certain instant in time. Nevertheless, the presented approach is applicable to situation where the deformable body and thus the parameter vector **x** moves at a "slow" rate between discrete time intervals. This state also enables us to form the equality constraint condition of equ. (5.1) and the conventional photogrammetric measurement model of equ. (5.2) at a specific instant of time t_k. The mechanism by which the estimated parameter vector $\hat{\mathbf{x}}$ is affected due to these two models is illustrated in Fig. (5.3).

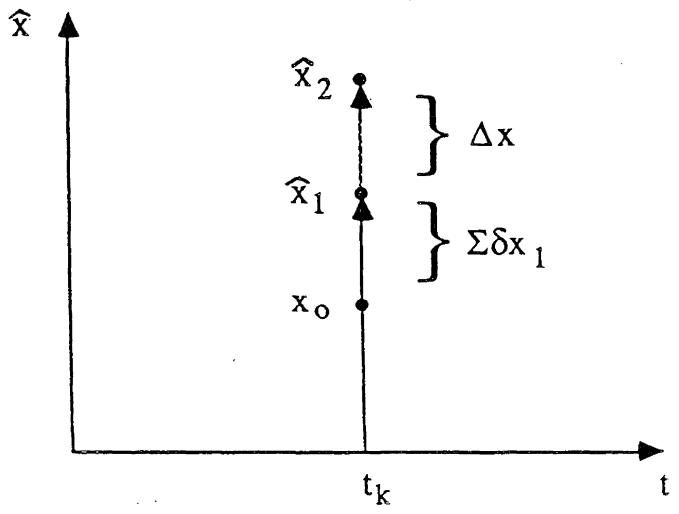

Figure 5.3: Sequential estimation of the parameter vector at time t_k.

If now the time dependence of the parameter vector can be introduced to the first mathematical model f_1, a recursive estimation process

of the unknown vector of parameters results through time (Fig. 5.4). Each instant of time provides a subset t_k (k=1, 2, 3,...), which represents the situation presented in Fig. (5.3).

In this sequential approach with time consideration, the parameter vector changes not only as new observations become available, but also as a function of time because of movement. In terms of modern optimal estimation theory, the processing in such circumstances can be performed with the aid of dynamic filtering techniques (Junkins, 1978), such as Kalman filtering (Kalman, 1960). Filtering is an estimation process that gives an optimal estimate of the current parameter vector based upon all previous observations (measurements). The criterion of optimality continues to be the minimization of the sum of squares of the weighted residuals of the observations (least squares criterion).

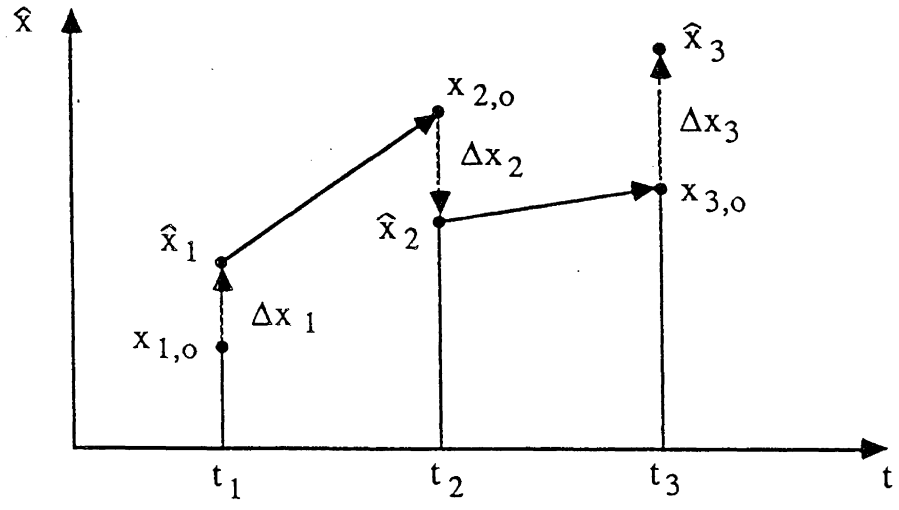

Figure 5.4: Recursive sequential estimation of the parameter vector over time.

Introducing the time factor into the first model (equ. (5.1)) we obtain a dynamic prediction model. If we set

$$\mathbf{x} \hat{=} \mathbf{x}_{(t)} \quad \text{and} \quad \mathbf{x}_{1(t)} = \mathbf{T}(\delta t) \cdot \mathbf{x}_{(t-1)} \tag{5.25}$$

which means that the observations for the parameter vector can be predicted values, then equ.(5.1) becomes

$$\mathbf{x}_{(t)} = \mathbf{T}(\delta t) \cdot \mathbf{x}_{(t-1)} \tag{5.26}$$

$\mathbf{T}(\delta t)$ is the transition (or displacement) matrix, which maps $\mathbf{x}_{(t-1)}$ onto $\mathbf{x}_{(t)}$ in the time interval $\delta t = (t) - (t-1)$. In other words, if a previous estimate $\mathbf{x}_{(t-1)}$ of the parameter vector is known, a current estimate $\mathbf{x}_{(t)}$ can be determined by means of the displacement matrix $\mathbf{T}(\delta t)$. This matrix is very important for the prediction process because it is defined according to physical laws governing the kinematic behaviour of the object. Therefore, the matrix $\mathbf{T}$ is also a function of deterministic parameters $\mathbf{p}$, which due to modelling uncertainties introduce stochastic properties into $\mathbf{T}$. These inaccuracies affect the precision of the location of the predicted parameter vector and must be included in its covariance matrix. The application of the law of covariance to equ.(5.26) results in the derivation of the predicted variance-covariance matrix $\mathbf{C}_{x(t)}$ based on the precision $\mathbf{C}_{x(t-1)}$ of the previous location $\mathbf{x}_{(t-1)}$ and on the precision $\mathbf{C}_p$ of the displacement matrix $\mathbf{T}(\mathbf{p},\delta t)$. Consequently,

$$\mathbf{C}_{x(t)} = \left[\frac{\partial \mathbf{x}_{(t)}}{\partial \mathbf{x}_{(t-1)}} \;\middle|\; \frac{\partial \mathbf{x}_{(t)}}{\partial \mathbf{p}}\right] \left[\begin{array}{c|c} \mathbf{C}_{x(t-1)} & \mathbf{0} \\ \hline \mathbf{0} & \mathbf{C}_p \end{array}\right] \left[\frac{\partial \mathbf{x}_{(t)}}{\partial \mathbf{x}_{(t-1)}} \;\middle|\; \frac{\partial \mathbf{x}_{(t)}}{\partial \mathbf{p}}\right]^T =$$

$$= \left(\frac{\partial \mathbf{x}_{(t)}}{\partial \mathbf{x}_{(t-1)}}\right) \mathbf{C}_{x(t-1)} \left(\frac{\partial \mathbf{x}_{(t)}}{\partial \mathbf{x}_{(t-1)}}\right)^T + \left(\frac{\partial \mathbf{x}_{(t)}}{\partial \mathbf{p}}\right) \mathbf{C}_p \left(\frac{\partial \mathbf{x}_{(t)}}{\partial \mathbf{p}}\right)^T =$$

$$= T(p,\delta t)C_{x(t-1)}T(p,\delta t)^T + \sum_{j=1}^{m}\left[\left(\frac{\partial T(p,\delta t)}{\partial p_j}\, x_{(t-1)}\right) C_{p_j}\left(x_{(t-1)}^T\left(\frac{\partial T(p,\delta t)}{\partial p_j}\right)^T\right)\right] \qquad (5.27)$$

where m is the number of statistically independent parameters.

The summation in equ.(5.27) represents the effect of the uncertainty of the deterministic parameters p on the predicted estimates $x_{(t)}$. Denoting this uncertainty of the prediction model by $Q_{(t)}$, the predicted covariance matrix $C_{x(t)}$ given by equ.(5.27) is expressed in a shorter form as

$$C_{x(t)} = T(p,\delta t) \cdot C_{\hat{x}(t-1)} \cdot T(p,\delta t)^T + Q_{(t)} \qquad (5.28)$$

This analysis shows that equs.(5.21) and (5.23) remain valid after considering the kinematic state of the object. A careful examination of these two equations derived from the sequential weighted least squares adjustment with time consideration reveals that they have the same appearance and therefore are mathematically equivalent to the expressions given for the iterated extended Kalman filter for non-linear dynamic systems (Gelb, 1974). For a better understanding of the time factor involved, and particularly for a more explicit distinction between predicted and updated estimates, equs.(5.21b) and (5.23b) were rewritten with changed notations to conform with Gelb's (1974) formulation. The subscript t implies the final estimation at time t, which is obtained after the contribution from the measurements of the second model. The symbol (-) indicates predicted values based on the dynamic (prediction) model immediately prior to time t (Fig.5.5). The symbol (+) indicates updated values

due to the contribution of the observations immediately following the time t (Fig.5.5).

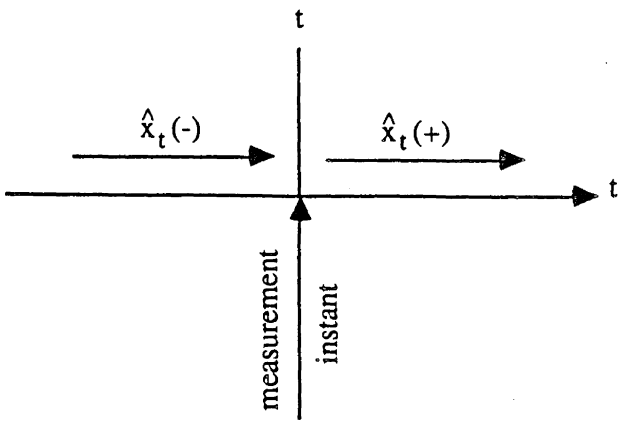

Figure 5.5: Illustration of the predicted and updated values at time t.

Thus, the updated estimated parameter vector (equ.5.21b) becomes

$$\hat{x}_{t,i}(+) = \hat{x}_t(-) - C_t(-)A_t^T[C_t + A_t C_t(-) A_t^T]^{-1}[A_t(\hat{x}_{t,i-1}(+) - \hat{x}_t(-)) + w_t] \tag{5.29}$$

and the updated covariance matrix (equ.5.23b) of the parameter vector becomes

$$C_t(t) = [I - C_t(-)A_t^T(C_t + A_t C_t(-) A_t^T)^{-1} A_t] C_t(-) \tag{5.30}$$

This iterative scheme is executed in vertical- and in horizontal directions, which means updating of the parameter vector due to the correction term from the observations but also updating the correction term itself.

The interaction between the prediction and measurement models is defined with the so-called gain matrix **G**. If we set

$$\mathbf{G} = \mathbf{C}_t(-)\mathbf{A}_t^T[\mathbf{C}_t + \mathbf{A}_t\mathbf{C}_t(-)\,\mathbf{A}_t^T]^{-1} \qquad (5.31)$$

then equ.(5.29) becomes

$$\hat{\mathbf{x}}_{t,i}\,(+) = \hat{\mathbf{x}}_t\,(-) - \mathbf{G}\cdot\mathbf{v}_t \qquad (5.32)$$

with $\mathbf{v}_t$ being the residual vector of the observation model at time t.

Equation (5.32) expresses the updated estimate $\hat{\mathbf{x}}_t(+)$ in terms of the predicted estimate $\hat{\mathbf{x}}_t(-)$ plus the correction term $\mathbf{G}\cdot\mathbf{v}_t$. This term is the product of the gain matrix times the residual vector of the linearized observation model. It indicates therefore, how the measurements:

a) fit to the functional model as expressed by their residuals, and

b) improve the predicted values of the parameters.

Their influence is controlled by the gain matrix **G**, which plays the role of a weight matrix. Small (or large) values of **G** mean small (or large) influences of the observation model on the estimation of the unknown parameters. It is also obvious that the measurements will have no effect in updating the predicted parameters if $\mathbf{v}_t=0$, which renders that either model can be used satisfactorily to estimate the updated parameter vector.

From equ.(5.31) we can see that the predicted covariance matrix $\mathbf{C}_t(-)$ has a major impact on the computation of the gain matrix **G**. If the estimation of $\hat{\mathbf{x}}_{t-1}$ is very accurate, that is $\mathbf{C}_{\hat{\mathbf{x}}(t-1)}$ is small, and if the deterministic parameters **p** of the displacement matrix **T** are well known, that is $\mathbf{Q}_t$ is small, then the computed $\mathbf{C}_t(-)$ will also be small (equ.(5.28)). This causes **G** to approach

zero, and the effect of the measured data will be reduced accordingly. If it happened to be the case that the parameters **p** were not well defined or that there were still unmodelled effects not included in the determination of **T**, then the now predominant predicted value $\hat{\mathbf{x}}_t(-)$ will be erroneous. Although this will show in the residual $\mathbf{v}_t$ the term $\mathbf{G}\cdot\mathbf{v}_t$ will have an insignificant effect on $\hat{\mathbf{x}}_t(-)$ due to a very small **G**. As a result, the estimation process will be based on the prediction model, that is $\hat{\mathbf{x}}_t(+) = \hat{\mathbf{x}}_t(-)$. This problem is known as divergence of the estimation process (Sorenson, 1970; LeMay, 1984). Usually this can be controlled by the examination of the residuals or by accepting the reality and assume that the **T** matrix is imperfect ($\mathbf{Q}_t \neq 0$).

Before we proceed to the application of equs.(5.29) and (5.30) to the estimation process, it is essential to examine their structure with respect to:

a) existing familiar forms of the simultaneous least squares adjustment, and

b) computation aspects involved.

We shall concentrate on a specific term of these two formulae which is rewritten here for the sake of reference.

$$[\mathbf{C}_t + \mathbf{A}_t\mathbf{C}_t(-)\mathbf{A}_t^T]^{-1} \qquad (5.33)$$

where $\mathbf{A}_t$ is the first design matrix of -in our case- the photogrammetric model, $\mathbf{C}_t$ is the covariance matrix of the observables involved, and $\mathbf{C}_t(-)$ is the predicted covariance matrix of the unknown parameters. These matrices have the following dimensions.

$\mathbf{A}_t$ is an n x u matrix;

$\mathbf{C}_t$ is an n x n matrix, usually diagonal;

$\mathbf{C}_t(-)$ is an u x u matrix;

where n is the number of observations and u is the number of unknown parameters to be estimated.

We observe the following:

Firstly, the sequence of matrices involved does not resemble the well known form of the coefficient matrix $\mathbf{A}_t^T\mathbf{C}_t^{-1}\mathbf{A}_t$ of the unknown parameters in a usual simultaneous least squares solution, where only one functional model exists. Consequently, it is difficult to use sections of software developed for the adjustment of the measurement model (see section 5.5).

Secondly, the size of the final matrix in (5.33) to be inverted is n by n. However, the number n of the observation equations is larger than the number u of the unknown parameters. For example, in the case of a photogrammetric bundle block adjustment with an object point appearing on three photographs, the number of observation equations is six, for the three unknown object coordinates of the points (keeping in mind the ratio 2mn to 3n where m is the number of photographs on which a point appears and n is the number of object points, not to mention any additional observation schemes used or the unknown orientation parameters of the photographs).

It will be computationally impractical to apply equs.(5.29) and (5.30) to the sequential monitoring of object displacements by photogrammetric means. In order to develop a new form of the term under examination, (equ.(5.33)), we invoke at this point a matrix inversion expression given in Henderson and Searle (1981). It can

also be found in (Mikhail and Helmering, 1973; Mikhail, 1976; Helmering, 1977; Kratky, 1980) and its proof is given in Appendix V.

Let $\mathbf{C}_t$, $\mathbf{A}_t$, $\mathbf{C}_t(-)$ be non-singular matrices. Then

$$(\mathbf{C}_t+\mathbf{A}_t\mathbf{C}_t(-)\mathbf{A}_t^T)^{-1} = \mathbf{C}_t^{-1}-\mathbf{C}_t^{-1}\mathbf{A}_t(\mathbf{C}_t(-)^{-1}+\mathbf{A}_t^T\mathbf{C}_t^{-1}\mathbf{A}_t)^{-1}\mathbf{A}_t^T\mathbf{C}_t^{-1} =$$
$$= \mathbf{C}_t^{-1}[\mathbf{I}-\mathbf{A}_t(\mathbf{C}_t(-)^{-1}+\mathbf{A}_t^T\mathbf{C}_t^{-1}\mathbf{A}_t)^{-1}\mathbf{A}_t^T\mathbf{C}_t^{-1}] \quad (5.34)$$

By using this property of matrix inversion, the following has been achieved:

a) The familiar form $\mathbf{A}_t^T\mathbf{C}_t^{-1}\mathbf{A}_t$ is preserved and thus the individuality of the measured model is maintained.

b) The matrix in parenthesis $(\mathbf{C}_t(-)^{-1} + \mathbf{A}_t^T\mathbf{C}_t^{-1}\mathbf{A}_t)$ to be inverted has smaller dimensions -equal to the number of unknown parameters- and always will be a 3 x 3 matrix as illustrated in section 5.5.

c) An additional matrix inversion $\mathbf{C}_t(-)^{-1}$ is added, but $\mathbf{C}_t(-)$ as also explained in section 5.5 is a symmetric 3x3 matrix. The matrix inversion $\mathbf{C}_t^{-1}$ usually can be avoided if the weights of the observations are used directly.

d) With respect to the remaining matrix operations, from the original two multiplications and one addition, we now end up with six multiplications, one addition and one subtraction. However, the number of operations involved is considerably smaller than the analogous to n^3 operations required to invert the matrix in equ.(5.33). That particularly holds when the number of observation equations n becomes "large" compared to the number of unknown parameters u.

Substituting now equ.(5.34) into equs.(5.29) and (5.30), the final formulae have been developed for the combined sequential approach, in which the photogrammetric measurements and the kinematic properties of the object are used simultaneously for a direct and rigorous determination of the object trajectory over time.

Thus, the final updated estimated parameter vector is determined as:

$$\hat{\mathbf{x}}_{t,i}(+) = \hat{\mathbf{x}}_t(-) - \mathbf{C}_t(-)\mathbf{A}_t^T\mathbf{C}_t^{-1}[\mathbf{I}-\mathbf{A}_t(\mathbf{C}_t(-)^{-1}+\mathbf{A}_t^T\mathbf{C}_t^{-1}\mathbf{A}_t)^{-1}\mathbf{A}_t^T\mathbf{C}_t^{-1}] \cdot$$

$$\cdot[\mathbf{A}_t(\hat{\mathbf{x}}_{t,i-1}(+) - \hat{\mathbf{x}}_t(-)) + \mathbf{w}_t] \qquad (5.35)$$

and the final updated covariance matrix of the parameter vector will be:

$$\mathbf{C}_t(+) = [\mathbf{I}-\mathbf{C}_t(-)\mathbf{A}_t^T\mathbf{C}_t^{-1}[\mathbf{I}-\mathbf{A}_t(\mathbf{C}_t(-)^{-1}+\mathbf{A}_t^T\mathbf{C}_t^{-1}\mathbf{A}_t)^{-1}\mathbf{A}_t^T\mathbf{C}^{-1}_t]\mathbf{A}_t]\mathbf{C}_t(-) \qquad (5.36)$$

These equations constitute another form of the so-called Bayes filter expressions. They differ from the formulae given in Morrison, (1969), in Krakiwsky, (1975), and in Vanicek and Krakiwsky, (1986) because of the use of different matrix identities in equs.(5.29) and (5.30).

In the case where relative weight matrices are employed, the following relations must be considered in equs.(5.35) and (5.36). The predicted covariance matrix $\mathbf{C}_t(-)$ is replaced by the relative predicted covariance matrix ${}_R\mathbf{C}_t(-)$, given as

$${}_R\mathbf{C}_t(-) = \frac{1}{\sigma_o^2}\,\mathbf{C}_t(-) \qquad (5.37)$$

The inverse $\mathbf{C}_t^{-1}$ of the covariance matrix $\mathbf{C}_t$ of the observations is

replaced by the relative weight matrix ${}_R P_t$, given as

$$ {}_R P_t = \sigma_o^2 \, C_t^{-1} \qquad (5.38) $$

5.4 Prediction and Observation Models

5.4.1 Prediction Model

The prediction model is defined by two equations dealing with the propagation of the parameter vector and its errors. The first equation determines the propagation of the parameter vector through time.

The motion of an object can be generally expressed by a system of usually non-linear first-order differential equations of the form (Liebelt, 1967; Junkins, 1978)

$$ \dot{\mathbf{x}} \equiv \frac{d\mathbf{x}}{dt} = F(\mathbf{x}(t), \mathbf{u}(t), t) \qquad (5.39) $$

where

$\mathbf{x}(t)$: is the state- or parameter vector

$\mathbf{u}(t)$: is the control- or forcing vector

F : is the matrix of non-linear functions

t : is the time factor

Integrating equ. (5.39) and using a known initial condition $\mathbf{x}(t_o)=\mathbf{x}_o$, the trajectory of the parameter vector is estimated over time. In recursive form this trajectory can be estimated at certain instants of time by the transition- or prediction equation

$$ \hat{\mathbf{x}}_{(t+1)} = \mathbf{T}(t+1, t) \cdot \hat{\mathbf{x}}_{(t)} + \mathbf{z}(t+1, t) \qquad (5.40) $$

where

$\hat{\mathbf{x}}_{(t+1)}$: is the estimated parameter vector at time t+1 (current state);

$\hat{\mathbf{x}}_{(t)}$: is the estimated parameter vector at time t (previous state);

$\mathbf{T}(t+1,t)$: is the transition matrix, previously described in equ. (5.26);

$\mathbf{z}(t+1,t)$: is the vector describing the uncertainty (noise) of the system.

If the moving object follows a deterministic trajectory, such as in navigation, projectile motion, etc., the transition matrix can be derived from equ. (5.39) (Morrison, 1969; Grant, 1976; Junkins, 1978; Schwarz, 1983; LeMay, 1984). However, in situations such as in monitoring of ground displacements, where the factors causing the motion are not explicitly known, prediction theories based on certain hypotheses can be used (Kratzsch, 1983). The displacement matrix **T** (section 2.2) has been derived to serve as a general form of the transition matrix because every motion in space can be analysed geometrically.

The transition equation maintains its recursive characteristics if the transition matrix has the following properties (Junkins, 1978):

$$\mathbf{T}(t,t) = \mathbf{I} \tag{5.41a}$$

$$\mathbf{T}(t_2, t_1) = \mathbf{T}(t_1, t_2)^{-1} \tag{5.41b}$$

$$\mathbf{T}(t_3, t_1) = \mathbf{T}(t_3, t_2) \cdot \mathbf{T}(t_2, t_1) \tag{5.41c}$$

The second equation determines the propagation of errors of the parameter vector through time. The expected value of the noise- or residual vector $\mathbf{z}(t+1,t)$ is zero, which conforms with least squares

estimation of $\hat{x}_{(t+1)}$, (sections 5.2 and 5.3). That is the estimator $\hat{\mathbf{x}}_{(t+1)}$ is unbiased if

$$\mu_z = E[\ \mathbf{z}(t+1,\ t)\ ] = \mathbf{0} \tag{5.42}$$

The covariance matrix of $\mathbf{z}(t+1,t)$ is equal to the uncertainty of the prediction model, i.e.

$$E\ [(\mathbf{z}(t+1,t)-\mu_z)(\mathbf{z}(t+1,t)-\mu_z)^T] = E\ [\mathbf{z}(t+1,t)\cdot\mathbf{z}(t+1,t)^T] = \mathbf{Q}_t \tag{5.43}$$

This can be confirmed if we apply the law of error propagation to equ. (5.40) in order to determine the accuracy of the estimated parameters. The resulting predicted covariance matrix $\mathbf{C}_{\hat{x}(t+1)}$ of $\hat{\mathbf{x}}_{(t+1)}$ is the same as the one defined earlier by equ. (5.27) or (5.28). Of course, the analysis of the accuracy as performed in section 5.3 is valid here as well.

5.4.2 Observation Model

The photogrammetric measurement model consists of three types of observation equations together with the relevant weight matrices. **1)** The photo-coordinate measurements are related to the unknown parameters through the extended collinearity equations. The collinearity equations with additional parameters were chosen as the functional model because such a bundle block adjustment provides the most rigorous analytical photogrammetric solution. The general form is

$$F_1\ (\hat{\mathbf{x}}_I,\ \hat{\mathbf{x}}_E,\ \hat{\mathbf{x}}_O;\ \mathbf{l}_p) = \mathbf{0}\ \ ,\ \mathbf{P}_P \tag{5.43}$$

which is written explicitly for one object point P appearing on one photograph as:

$$x_p = x_o + dx\text{-}c\ \frac{r_{11}(XP\text{-}XC) + r_{12}(YP\text{-}YC) + r_{13}(ZP\text{-}ZC)}{r_{31}(XP\text{-}XC) + r_{32}(YP\text{-}YC) + r_{33}(ZP\text{-}ZC)}$$

$$y_p = y_o + dy - c\,\frac{r_{21}(XP-XC) + r_{22}(YP-YC) + r_{23}(ZP-ZC)}{r_{31}(XP-YC) + r_{32}(YP-YC) + r_{33}(ZP-ZC)} \qquad (5.44)$$

where

l_p : is the vector of observables

$\hat{x}_I$: is the vector of the unknown elements of interior orientation

$\hat{x}_E$: is the vector of the unknown elements of exterior orientation

$\hat{x}_O$: is the vector of the unknown object coordinates

P_p : is the weight matrix of the observations

x_p, y_p : are the photo-coordinates of point P

x_o, y_o : are the photo-coordinates of the principal point

c : is the camera constant

dx,dy : are the effects of systematic image errors expressed by additional parameters

XC,YC,ZC : are the coordinates of the camera station in the object space system

XP,YP,ZP : are the object coordinates of point P

$r_{ij}(i=1,2,3;\ j=1,2,3)$: are the elements of the rotation matrix R ($R = R_k R_\varphi R_w$).

The choice of additional parameters is governed by two important principles (Faig, 1984a):

-- to avoid over-parameterization and to minimize the computations, the number of parameters must be as small as possible;

-- to avoid ill-conditioning or singularity of the coefficient matrix of the unknown parameters in the least squares solution, the correlation among the additional parameters and their correlation

with the other unknowns must be negligibly small.

Also , according to Kilpelä (1980) "no single additional parameter set is found to be superior to the others".

The Kilpelä-Salmenperä group of additional parameters which models the causes of image deformation was adopted. The systematic errors dx and dy are expressed as

$$dx = a_1(x_p-x_o) + a_2(y_p-y_o) + (a_3r^2 + a_4r^4 + a_5r^6)(x_p-x_o)(1 - \frac{r_o}{r}) + a_6 2(x_p-x_o)(y_p-y_o) + a_7(r^2 + 2(x_p-x_o)^2)$$

(5.45)

$$dy = -a_1(y_p-y_o) + a_2(x_p-x_o) + (a_3r^2 + a_4r^4 + a_5r^6)(y_p-y_o)(1 - \frac{r_o}{r}) + a_6(r^2 + 2(y_p-y_o)^2) + a_7 2(x_p-x_o)(y_p-y_o)$$

where r_o is a given constant (first non-zero radial distance, where radial distortion is expected to be zero), and r is the radial distance equal to $r = [(x_p-x_o)^2 + (y_p-y_o)^2]^{1/2}$.

By setting r_o equal to zero, equs. (5.45) are reduced to the form used in this study:

$$dx = a_1(x_p-x_o) + a_2(y_p-y_o) + (a_3r^2 + a_4r^4 + a_5r^6)(x_p-x_o) + + a_6 2(x_p-x_o)(y_p-y_o) + a_7(r^2 + 2(x_p-x_o)^2)$$

(5.46)

$$dy = -a_1(y_p-y_o) + a_2(x_p-x_o) + (a_3r^2 + a_4r^4 + a_5r^6)(y_p - y_o) + + a_6(r^2 + 2(y_p-y_o)^2) + a_7 2(x_p-x_o)(y_p-y_o)$$

This additional parameter formulation models systematic errors due

to film deformation (differential scale along the photo-axes and shearing of the photo-axes), radial (symmetric) lens distortion, and decentering lens distortion. The set of additional parameters (equs. (5.46)) is equivalent to the one proposed by Moniwa (1977), and is referred to as "physical model". It is used because it includes only seven (7) parameters ($a_1,.....a_7$) and performed well according to (Murai et al., 1984; Ziemann, 1985; Shih, 1987). An additional reason is its non-algebraic modelling, that is the estimation of the additional parameters does not depend on well distributed image points. The latter is very crucial in photogrammetric monitoring surveys, because the detail points are distributed unevenly most of the time.

A "photo-variant" approach was employed where different additional parameters are assigned for each individual photograph. Although the number of unknown camera parameters increases linearly with the number of photographs (in our case, total of sixteen (16) unknowns per exposure station), the approach is more general because is suitable for both metric and non-metric cameras.

In order to control possible strong correlations among the camera parameters (Moniwa, 1981) which cause ill-conditioning of the normal equations system, weighting of the elements of interior orientation and of the coordinates of the object points has been applied. This then leads to the second and third type of observation equations.

2) The ten (10) elements defining the interior orientation, namely x_o, y_o, c, $a_1,.....,a_7$ are introduced as weighted parameter constraints and are expressed in general form as:

$$F_2(\hat{\mathbf{x}}_I) = \mathbf{l}_I \quad \text{with } \mathbf{l}_I \equiv \mathbf{x}_I^{(o)} \,,\, \mathbf{P}_I \tag{5.47}$$

where

$\mathbf{l}_I$: is the observation vector equal to the initial value $\mathbf{x}_{IO}^{(o)}$ of the unknown parameters of interior orientation

$\hat{\mathbf{x}}_I$: is the vector of the unknown elements of interior orientation

$\mathbf{P}_I$: is the weight matrix of the observations

This scheme ensures that the least squares estimates of the parameters of interior orientation will be within a desirable range.

3) The coordinates of the object points are also treated as weighted parameter constraints. Although this is necessary for the required control points to avoid datum indeterminancies, all the points can be utilized as such to reduce the effect of a weak geometric configuration. The latter reduces also the magnitude of the condition number of the coefficient matrix of the unknown parameters in the normal equations (section 6.2.1).

The observation equations of the object coordinates are in general form

$$F_3(\hat{\mathbf{x}}_O) = \mathbf{l}_O \quad \text{with } \mathbf{l}_O \equiv \mathbf{x}_O^{(o)},\, \mathbf{P}_O \tag{5.48}$$

If only the control points are constrained while the other object points are not, then the relation (5.48) becomes

$$F_3(\hat{\mathbf{x}}_{CN}) = \mathbf{l}_{CN} \quad \text{with } \mathbf{l}_{CN} \equiv \mathbf{x}_{CN}^{(o)} \,,\, \mathbf{P}_{CN} \tag{5.49}$$

and $\hat{\mathbf{x}}_{CN} \varepsilon \hat{\mathbf{x}}_O$

In equs. (5.48) and (5.49):

$\mathbf{l}_O$, $\mathbf{l}_{CN}$: are the observation vectors equal to the initial values $\mathbf{x}_{OB}^{(o)}$ and $x_{OBC}^{(o)}$ respectively, of the unknown object coordinates

$\hat{\mathbf{x}}_O$: is the vector of the unknown coordinates of all

object points

$\hat{\mathbf{x}}_{CN}$: is the vector of the unknown coordinates of the object points used as control

P_O, P_{CN} : are the corresponding weight matrices.

Again, the estimated unknown object coordinates will fall within the boundaries defined by the variances of the initial values $\mathbf{x}_O^{(o)}$ or $\mathbf{x}_{CN}^{(o)}$.

5.5 Initial Estimation of the State Information

The sequential process estimates the updated parameters and their covariance matrices based on their predicted values combined with the new observations. According to their dynamic model, the determination of the current predicted values is a function of their previous state. It is therefore necessary to estimate the parameters and their accuracies at an initial moment of time, referred to as zero epoch, prior to activating the updating mechanism. This a-priori information is usually obtained via the photogrammetric observation model given in the previous section. Although the dynamic model provides the same information, it was decided not to use it for ground displacements because of the uncertainties involved. The estimation process of the overdetermined observation model is based on the least squares principle. The corresponding software for the initial estimation of the state information has been developed by the author.

5.5.1 Estimation of the Unknown Parameters

The three observation equations (5.43), (5.47) and (5.48) are linearized using Taylor's series linear approximation. The extended collinearity observation equation is of the implicit or combined model type. Its linearized form is

$$\mathbf{A}_1\delta\mathbf{x}_1 + \mathbf{B}_1\mathbf{v}_1 + \mathbf{w}_1 = \mathbf{0} \qquad (5.50)$$

where

$\mathbf{A}_1 = -\frac{\partial \mathbf{F}_1}{\partial \mathbf{x}}\Big|_{\mathbf{x}^{(o)},1}$: is the first design matrix

$\mathbf{B}_1 = -\frac{\partial \mathbf{F}_1}{\partial \mathbf{l}}\Big|_{\mathbf{x}^{(o)},1}$: is the second design matrix

$\mathbf{w}_1 = F_1\,(\mathbf{x}_I^{(o)}, \mathbf{x}_E^{(o)}, \mathbf{x}_O^{(o)}; \mathbf{l}_p)$: is the misclosure vector

$\delta\mathbf{x}_1$: is the correction (solution) vector of the unknown parameters $\mathbf{x}_I$, $\mathbf{x}_E$, $\mathbf{x}_O$

$\mathbf{v}_1$: is the vector of the observation residuals

Before we proceed, we examine the elements of the second design matrix **B** for one set of collinearity equations. The elements of matrix **B** are defined as

$$\mathbf{B} = \begin{bmatrix} \frac{\partial F_1}{\partial x_p} & \frac{\partial F_1}{\partial y_p} \end{bmatrix} = \begin{bmatrix} \frac{\partial x_p}{\partial x_p} + \frac{\partial dx}{\partial x_p} & \frac{\partial x_p}{\partial y_p} + \frac{\partial x_p}{\partial y_p} \\ \\ \frac{\partial y_p}{\partial x_p} + \frac{\partial dy}{\partial x_p} & \frac{\partial y_p}{\partial y_p} + \frac{\partial dy}{\partial y_p} \end{bmatrix} =$$

$$= \begin{bmatrix} 1 + \varepsilon_{11} & 0 + \varepsilon_{12} \\ \\ 0 + \varepsilon_{21} & 1 + \varepsilon_{22} \end{bmatrix} \qquad (5.51)$$

The terms ε_{ij} (i=1,2; j=1,2) are very small quantities because they are functions of the additional parameters $a_1,\ldots a_7$ whose numerical magnitude is generally small. When multiplied by the residual vector $\mathbf{v}_1$ they become even smaller (second order terms), and therefore their contribution to the term $\mathbf{B}_1\mathbf{v}_1$ becomes insignificant. Hence without loss of generality they may be neglected (Brown, 1969). Consequently, the second design matrix $\mathbf{B}_1$ can be replaced by the unit matrix. Equ.(5.43) can thus be treated as being of the explicit or non-linear parametric type

$$F_1\ (\hat{\mathbf{x}}_I,\ \hat{\mathbf{x}}_E,\ \hat{\mathbf{x}}_O) = \mathbf{l}_p \qquad ,P_P \qquad (5.52)$$

whose linearization leads to

$$\mathbf{A}_1\delta\mathbf{x}_1 + \mathbf{w}_1 - \mathbf{v}_1 = \mathbf{0} \qquad (5.53)$$

The misclosure vector is now defined as

$$\mathbf{w}_1 = F_1\ (\mathbf{x}_I,\ \mathbf{x}_E,\ \mathbf{x}_O)\ \Big|_{x(o)} - \mathbf{l}_p$$

The observation equation (5.47) of the parameters of interior orientation is of the explicit or non-linear parametric type and its linearized form is

$$\mathbf{A}_2\delta\mathbf{x}_2 + \mathbf{w}_2 - \mathbf{v}_2 = \mathbf{0} \qquad (5.54)$$

where

$$A_2 = \left.\frac{\partial F_2}{\partial \hat{x}_I}\right|_{x_I^{(o)}} = I$$: is the first design matrix and is equal to the unit matrix because initial approximate values $x_I^{(o)}$ are treated as observations.

δx_2 : is the correction (solution) vector of the unknown parameters x_{IO}

v_2 : is the vector of the observation residuals

$w_2 = F_2(\hat{x}_I)\Big|_{x_I^{(o)}} - l_I$: is the misclosure vector

The observation equation (5.48) of the coordinates of the object points is also of the explicit or non-linear parametric type and is linearized as

$$A_3\delta x_3 + w_3 - v_3 = 0 \qquad (5.55)$$

where

$$A_3 = \left.\frac{\partial F_3}{\partial \hat{x}_0}\right|_{x_0^{(o)}} = I$$: is the first design matrix and is equal to unit matrix because the initial approximate values $x_0^{(o)}$ are treated as observations.

δx_3 : is the correction (solution) vector of the unknown parameters x_{OB}

v_3 : is the vector of the observation residuals

$w_3 = F_3(\hat{x}_0)\Big|_{x_0^{(o)}} - l_0$: is the misclosure vector

The compact linear form of equs.(5.53), (5.54) and (5.55) after the partitioning the matrices is

$$A_{PI}\delta x_I + A_{PE}\delta x_E + A_{PO}\delta x_O + w_P - v_P = 0, \quad P_P \qquad (5.56a)$$

$$A_{OB}\delta x_O + w_O - v_O = 0, \quad P_O \qquad (5.56b)$$

$$A_{II}\delta x_I + w_I - v_I = 0, \quad P_I \qquad (5.56c)$$

The hyper matrix of equs.(5.56) is $A\delta x + w - v = 0$ or

$$\begin{bmatrix} A_{PI} & A_{PE} & A_{PO} \\ 0 & 0 & A_{OB} \\ A_{II} & 0 & 0 \end{bmatrix} \begin{bmatrix} \delta x_I \\ \delta x_E \\ \delta x_O \end{bmatrix} + \begin{bmatrix} w_P \\ w_O \\ w_I \end{bmatrix} - \begin{bmatrix} v_P \\ v_O \\ v_I \end{bmatrix} = \begin{bmatrix} 0 \\ 0 \\ 0 \end{bmatrix} \qquad (5.57)$$

and the weight matrix P for all the observations will be

$$P = \begin{bmatrix} P_P & 0 & 0 \\ 0 & P_O & 0 \\ 0 & 0 & P_I \end{bmatrix} \qquad (5.58)$$

While matrices A_{II} and A_{OB} have been defined earlier, the structures of the design matrices A_{PI}, A_{PE}, A_{PO} of the extended collinearity equations are illustrated in Fig. 5.6. A basic assumption is that each point i appears on each photograph j. If a point does not appear on a specific photograph, the corresponding element location is set to zero.

The non-zero locations of the design matrices refer to two object points appearing on three photographs.

The least squares estimates of the unknown parameters are obtained under the condition that

$$(v_P^T P_P v_P + v_O^T P_O v_O + v_I^T P_I v_I) \text{ becomes minimum.} \qquad (5.59)$$

The normal equations are obtained using Lagrange's method for equality constrained parameter optimization. The variation function Φ is formed first:

$$\begin{aligned} \Phi = {} & v_P^T P_P v_P + v_O^T P_O v_O + v_I^T P_I v_I + \\ & + 2k_1^T(A_{PI}\delta x_I + A_{PE}\delta x_E + A_{PO}\delta x_O + w_P - v_P) + \\ & + 2k_2^T(A_{OB}\delta x_O + w_O - v_O) + \\ & + 2k_3^T(A_{II}\delta x_I + w_I - v_I) \end{aligned} \qquad (5.60)$$

where k_1, k_2, k_3 are the vectors of Lagrange multipliers.

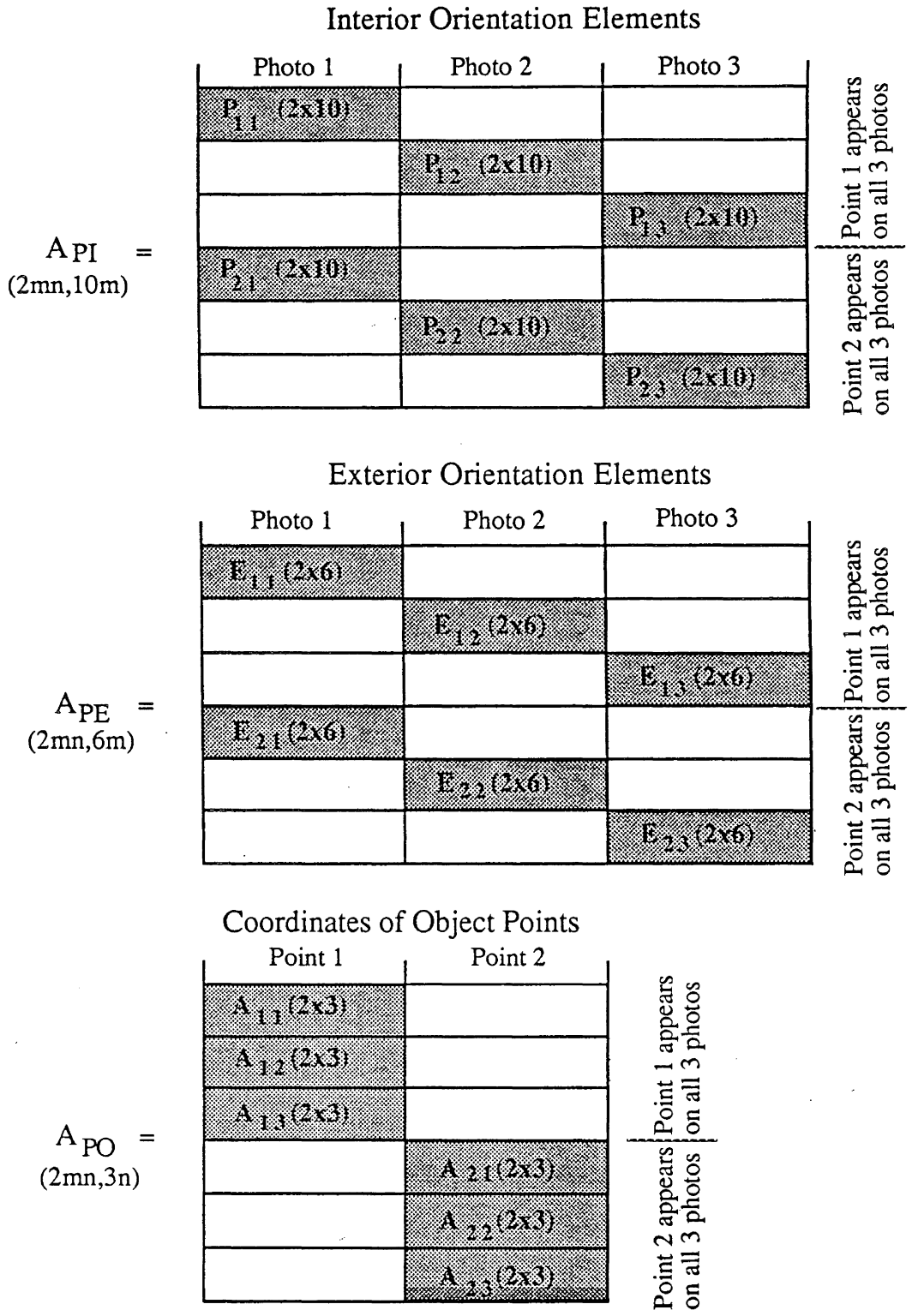

Figure 5.6: Structure of the design matrices of the extended collinearity equations (m is the total number of photographs, n is the total number of points).

To obtain the extremum -minimum in the case- of equ. (5.59) subject to the constraints of equs. (5.56), the necessary conditions are

$$\begin{bmatrix} \partial \Phi \\ \hline \partial \hat{\mathbf{v}} \end{bmatrix}^T = \mathbf{0} \tag{5.61a}$$

$$\begin{bmatrix} \partial \Phi \\ \hline \partial \hat{\mathbf{x}} \end{bmatrix}^T = \mathbf{0} \tag{5.61b}$$

$$\begin{bmatrix} \partial \Phi \\ \hline \partial \mathbf{k} \end{bmatrix} = \mathbf{0} \tag{5.61c}$$

Equations (5.61) constitute the system of normal equations, namely,

$$\left[\begin{array}{ccc|ccc|ccc} P_P & 0 & 0 & -I & 0 & 0 & 0 & 0 & 0 \\ 0 & P_O & 0 & 0 & -I & 0 & 0 & 0 & 0 \\ 0 & 0 & P_I & 0 & 0 & -I & 0 & 0 & 0 \\ \hline -I & 0 & 0 & 0 & 0 & 0 & A_{PI} & A_{PE} & A_{PO} \\ 0 & -I & 0 & 0 & 0 & 0 & 0 & 0 & A_{OB} \\ 0 & 0 & -I & 0 & 0 & 0 & A_{II} & 0 & 0 \\ \hline 0 & 0 & 0 & A_{PI}{}^T & 0 & A_{II}{}^T & 0 & 0 & 0 \\ 0 & 0 & 0 & A_{PE}{}^T & 0 & 0 & 0 & 0 & 0 \\ 0 & 0 & 0 & A_{PO}{}^T & A_{OB}{}^T & 0 & 0 & 0 & 0 \end{array}\right] \left[\begin{array}{c} v_P \\ v_O \\ v_I \\ \hline k_1 \\ k_2 \\ k_3 \\ \hline \delta_{xI} \\ \delta_{xE} \\ \delta_{xO} \end{array}\right] + \left[\begin{array}{c} 0 \\ 0 \\ 0 \\ \hline 0 \\ 0 \\ 0 \\ \hline 0 \\ 0 \\ 0 \end{array}\right] = \left[\begin{array}{c} 0 \\ 0 \\ 0 \\ \hline 0 \\ 0 \\ 0 \\ \hline 0 \\ 0 \\ 0 \end{array}\right] \tag{5.61}$$

The expressions for the correction parameter $\delta\mathbf{x}$ are derived through successive elimination processes. Elimination of $[\mathbf{v}_P{}^T \ \mathbf{v}_O{}^T \ \mathbf{v}_I{}^T]^T$ from equ. (5.61) results in

$$\left[\begin{array}{ccc|ccc} -P_P{}^{-1} & 0 & 0 & A_{PI} & A_{PE} & A_{PO} \\ 0 & -P_O{}^{-1} & 0 & 0 & 0 & A_{OB} \\ 0 & 0 & -P_I{}^{-1} & A_{II} & 0 & 0 \\ \hline A_{PI}{}^T & 0 & A_{II}{}^T & 0 & 0 & 0 \\ A_{PE}{}^T & 0 & 0 & 0 & 0 & 0 \\ A_{PO}{}^T & A_{OB}{}^T & 0 & 0 & 0 & 0 \end{array}\right] \left[\begin{array}{c} k_1 \\ k_2 \\ k_3 \\ \hline \delta_{xI} \\ \delta_{xE} \\ \delta_{xO} \end{array}\right] + \left[\begin{array}{c} w_P \\ w_O \\ w_I \\ \hline 0 \\ 0 \\ 0 \end{array}\right] = \left[\begin{array}{c} 0 \\ 0 \\ 0 \\ \hline 0 \\ 0 \\ 0 \end{array}\right] \tag{5.62}$$

In the next step, the elimination of $\mathbf{k} = [\mathbf{k}_1{}^T \ \mathbf{k}_2{}^T \ \mathbf{k}_3{}^T]^T$ takes place which gives

$$\begin{bmatrix} A_{11_T} & A_{12} & A_{13} \\ A_{12}{}^T & A_{22_T} & A_{23} \\ A_{13}{}^T & A_{23}{}^T & A_{33} \end{bmatrix} \begin{bmatrix} \delta x_I \\ \delta x_E \\ \delta x_O \end{bmatrix} + \begin{bmatrix} u_1 \\ u_2 \\ u_3 \end{bmatrix} = \begin{bmatrix} 0 \\ 0 \\ 0 \end{bmatrix} \tag{5.63}$$

where

$$A_{11} = A_{PI}{}^{T}P_{P}A_{PI}, \quad A_{12} = A_{PI}{}^{T}P_{P}A_{PE}, \quad A_{13} = A_{PI}{}^{T}P_{P}A_{PO}$$

$$A_{12}{}^{T} = A_{PE}{}^{T}P_{P}A_{PI}, \quad A_{22} = A_{PE}{}^{T}P_{P}A_{PE}, \quad A_{23} = A_{PE}{}^{T}P_{P}A_{PO}$$

$$A_{13}{}^{T} = A_{PO}{}^{T}P_{P}A_{PI}, \quad A_{23}{}^{T} = A_{PO}{}^{T}P_{P}A_{PE}, \quad A_{33} = A_{PO}{}^{T}P_{P}A_{PO} + A_{OB}{}^{T}P_{O}A_{OB}$$

$$u_1 = A_{PI}{}^{T}P_{P}w_P + A_{II}{}^{T}P_{I}w_I$$

$$u_2 = A_{PE}{}^{T}P_{P}w_P$$

$$u_3 = A_{PO}{}^{T}P_{P}w_P + A_{OB}{}^{T}P_{O}w_O$$

Reversing the sequence of rows and rearranging the columns in equ. (5.63) we get

$$\left[\begin{array}{c|cc} A_{33} & A_{23}{}^{T} & A_{13}{}^{T} \\ \hline A_{23} & A_{22} & A_{12}{}^{T} \\ A_{13} & A_{12} & A_{11} \end{array}\right] \left[\begin{array}{c} \delta x_O \\ \hline \delta x_E \\ \delta x_I \end{array}\right] + \left[\begin{array}{c} u_3 \\ \hline u_2 \\ u_1 \end{array}\right] = \left[\begin{array}{c} 0 \\ \hline 0 \\ 0 \end{array}\right] \qquad (5.64)$$

The direct solution of normal equations (equ. (5.64)) requires either the inversion of a (16m + 3n) matrix or the solution for (16m + 3n) unknowns of the linear system, where m is the number of photographs and n is the number of object points. This also requires storage space allocation for the (16m + 3n) x (16m + 3n) sparce coefficient matrix of the unknown parameters. However, using the rules for inverting partitioned matrices, it is possible to eliminate δx_O from the solution and solve for δx_E and δx_I. This is desireable since the arithmetic value 16m is usually much smaller than the value of 3n. The largest matrix to be inverted in this process is the 3x3 symmetric matrix A_{33}. Once the expression for δx_E and δx_I is obtained, it is back-substituted to obtain the expression for δx_O.

Elimination of the vector δx_O from equ. (5.64) results in the reduced normal equations for the determination of the camera parameters

$$\begin{bmatrix} \mathbf{N}_{11} & \mathbf{N}_{21}{}^{T} \\ \mathbf{N}_{21} & \mathbf{N}_{22} \end{bmatrix} \begin{bmatrix} \delta x_E \\ \delta x_I \end{bmatrix} + \begin{bmatrix} u_{11} \\ u_{21} \end{bmatrix} = \begin{bmatrix} 0 \\ 0 \end{bmatrix} \qquad (5.65)$$

or $$\mathbf{N}\delta\mathbf{x} + \mathbf{u} = \mathbf{0} \qquad (5.66)$$

where

$$\underset{(6m,6m)}{\mathbf{N}_{11}} = A_{22} - A_{23}A_{33}^{-1}A_{23}^{T} =$$

$$= A_{PE}^{T}P_{P}A_{PE} - A_{PE}^{T}P_{P}A_{PO}(A_{PO}^{T}P_{P}A_{PO} + A_{OB}^{T}P_{O}A_{OB})^{-1}A_{PO}^{T}P_{P}A_{PE}$$

$$\underset{(6m,10m)}{\mathbf{N}_{21}^{T}} = A_{12}^{T} - A_{23}A_{33}^{-1}A_{13}^{T} =$$

$$= A_{PE}^{T}P_{P}A_{PI} - A_{PE}^{T}P_{P}A_{PO}(A_{PO}^{T}P_{P}A_{PO} + A_{OB}^{T}P_{O}A_{OB})^{-1}A_{PO}^{T}P_{P}A_{PI}$$

$$\underset{(10m,6m)}{\mathbf{N}_{21}} = A_{12} - A_{13}A_{33}^{-1}A_{23}^{T} =$$

$$= A_{PI}^{T}P_{P}A_{PE} - A_{PI}^{T}P_{P}A_{PO}(A_{PO}^{T}P_{P}A_{PO} + A_{OB}^{T}P_{O}A_{OB})^{-1}A_{PO}^{T}P_{P}A_{PE}$$

$$\underset{(10m,10m)}{\mathbf{N}_{22}} = A_{11} - A_{11}A_{33}^{-1}A_{13}^{T} =$$

$$= (A_{PI}^{T}P_{P}P_{PI}+A_{II}^{T}P_{I}A_{II}) - A_{PI}^{T}P_{P}A_{PO}(A_{PO}^{T}P_{P}A_{PO}+A_{OB}^{T}P_{O}A_{OB})^{-1}A_{PO}^{T}P_{P}A_{PI}$$

$$\underset{(6m,1)}{\mathbf{u}_{11}} = u_2 - A_{23}A_{33}^{-1}u_3 =$$

$$= A_{PE}^{T}P_{P}w_{P} - A_{PE}^{T}P_{P}A_{PO}(A_{PO}^{T}P_{P}A_{PO}+ A_{OB}^{T}P_{O}A_{OB})^{-1}(A_{PO}^{T}P_{P}w_{P}+ A_{OB}^{T}P_{O}w_{O})$$

$$\underset{(10m,1)}{\mathbf{u}_{21}} = u_1 - A_{13}A_{33}^{-1}u_3 =$$

$$= (A_{PI}^{T}P_{P}w_{P}+A_{II}^{T}P_{I}w_{I}) - A_{PI}^{T}P_{P}A_{PO}(A_{PO}^{T}P_{P}A_{PO}+A_{OB}^{T}P_{O}A_{OB})^{-1}(A_{PO}^{T}P_{P}w_{P}+A_{OB}^{T}P_{O}w_{O})$$

Due to the sparce structure of the design matrices and due to

the fact that all object points do not appear on all photographs, we proceed to the formation of the **N** matrix and the **u** vector of equ.(5.66) based on the contribution of each individual photo-observation.

The elements of $\mathbf{N}_{11}$ are formed as follows:

-- Main-diagonal elements: $\mathbf{N}_{11}(i,i)$, i=1,2,3,...,m

$$\mathbf{N}_{11}(i,i) = \sum_{k=1}^{n}[(\mathbf{E}_{ki}^{T}\mathbf{P}_{P}\mathbf{E}_{ki}) - [(\mathbf{E}_{ki}^{T}\mathbf{P}_{P}\mathbf{A}_{ki})\mathbf{C}_{kk}(\mathbf{A}_{ki}^{T}\mathbf{P}_{P}\mathbf{E}_{ki})]] \quad (5.67)$$

-- Elements below the main-diagonal: $\mathbf{N}_{11}(i,j)$, i=2,3,...,m; j=1,2,3,...,(i-1)

$$\mathbf{N}_{11}(i,j) = -\sum_{k=1}^{n}[(\mathbf{E}_{ki}^{T}\mathbf{P}_{P}\mathbf{A}_{ki})\ \mathbf{C}_{kk}(\mathbf{A}_{kj}^{T}\mathbf{P}_{P}\mathbf{E}_{kj})] \quad (5.68)$$

-- Elements above the main-diagonal: $\mathbf{N}_{11}(j,i)$

$$\mathbf{N}_{11}(j,i) = (\mathbf{N}_{11}(i,j))^{T} \quad (5.69)$$

The elements of $\mathbf{N}_{22}$ are formed as follows:

-- Main-diagonal elements: $\mathbf{N}_{22}(i,i)$, i=1,2,3,...,m

$$\mathbf{N}_{22}(i,i) = \sum_{k=1}^{n}[[(\mathbf{P}_{ki}^{T}\mathbf{P}_{P}\mathbf{P}_{ki})+\mathbf{P}_{Ii}]-[(\mathbf{P}_{ki}^{T}\mathbf{P}_{P}\mathbf{A}_{ki})\mathbf{C}_{kk}(\mathbf{A}_{ki}^{T}\mathbf{P}_{P}\mathbf{P}_{ki})]] \quad (5.70)$$

-- Elements below the main-diagonal: $\mathbf{N}_{22}(i,j)$, i=2,3,...,m; j=1,2,3,...,(i-1)

$$\mathbf{N}_{22}(i,j) = -\sum_{k=1}^{n}[(\mathbf{P}_{ki}^{T}\mathbf{P}_{P}\mathbf{A}_{ki})\mathbf{C}_{kk}(\mathbf{A}_{kj}^{T}\mathbf{P}_{P}\mathbf{P}_{kj})] \quad (5.71)$$

-- Elements above the main-diagonal: $\mathbf{N}_{22}(j,i)$

$$\mathbf{N}_{22}(j,i) = (\mathbf{N}_{22}(i,j))^{T} \quad (5.72)$$

The elements of $\mathbf{N}_{21}$ are formed as follows:

-- Main-diagonal elements: $\mathbf{N}_{21}(i,i)$, i=1,2,3,...,m

$$\mathbf{N}_{21}(i,i) = \sum_{k=1}^{n}[(\mathbf{P}_{ki}^{T}\mathbf{P}_{P}\mathbf{E}_{ki})-[(\mathbf{P}_{ki}^{T}\mathbf{P}_{P}\mathbf{A}_{ki})\mathbf{C}_{kk}(\mathbf{A}_{ki}^{T}\mathbf{P}_{k}\mathbf{E}_{ki})]] \qquad (5.73)$$

-- Elements below the main-diagonal: $\mathbf{N}_{21}(i,j)$, i=2,3,...,m; j=1,2,3,...,(i-1)

$$\mathbf{N}_{21}(i,j) = \sum_{k=1}^{n}[(\mathbf{P}_{ki}^{T}\mathbf{P}_{P}\mathbf{A}_{ki})\mathbf{C}_{kk}(\mathbf{A}_{kj}^{T}\mathbf{P}_{P}\mathbf{E}_{kj})] \qquad (5.74)$$

-- Elements above the main-diagonal: $\mathbf{N}_{21}(i,j)$, j=2,3,...,m; i=1,2,3,...,(j-1)

$$\mathbf{N}_{21}(i,j) = \sum_{k=1}^{n}[(\mathbf{P}_{ki}^{T}\mathbf{P}_{P}\mathbf{A}_{ki})\mathbf{C}_{kk}(\mathbf{A}_{kj}^{T}\mathbf{P}_{P}\mathbf{E}_{kj})] \qquad (5.75)$$

The elements of **C** matrix are formed as follows:

-- Main-diagonal elements: C(k,k), k=1,2,3,...,n

$$\mathbf{C}(k,k) = [(\sum_{i=1}^{m}(\mathbf{A}_{ki}^{T}\mathbf{P}_{P}\mathbf{A}_{ki}) + \mathbf{P}_{Ok}]^{-1} \qquad (5.76)$$

-- Off-diagonal elements are equal to zero.

The elements of the constant vector **u** are determined next.

The elements of $\mathbf{u}_{11}(i,1)$, i=1,2,3,...,m are formed as follows:

$$\mathbf{u}_{11}(i,1) = \sum_{k=1}^{n}[(\mathbf{E}_{ki}^{T}\mathbf{P}_{P}\mathbf{w}_{Pki}) - (\mathbf{E}_{ki}^{T}\mathbf{P}_{P}\mathbf{A}_{ki})\mathbf{C}_{kk} \cdot [\sum_{j=1}^{m}(\mathbf{A}_{kj}^{T}\mathbf{P}_{P}\mathbf{w}_{Pkj}) + \mathbf{P}_{Ok}\mathbf{w}_{Ok}]] \qquad (5.77)$$

The elements of $\mathbf{u}_{21}(i,1)$, i=1,2,3,...,m are formed as follows:

$$\mathbf{u}_{21}(i,1) = \sum_{k=1}^{n}[(\mathbf{P}_{ki}^{T}\mathbf{P}_{P}\mathbf{w}_{Pki} + \mathbf{P}_{Ii}\mathbf{w}_{Ii}) - (\mathbf{P}_{ki}^{T}\mathbf{P}_{P}\mathbf{A}_{ki})\mathbf{C}_{kk} [\sum_{j=1}^{m}(\mathbf{A}_{kj}^{T}\mathbf{P}_{P}\mathbf{w}_{Pkj}) + \mathbf{P}_{Ok}\mathbf{w}_{Ok}]] \qquad (5.78)$$

The dimensions of the vector **u** are (16m,1) while the dimensions of $\mathbf{u}_{11}$ and $\mathbf{u}_{21}$ are (6m,1) and (10m,1) respectively. The symmetric structure of the matrix **N** enables us to reduce storage space requirements. This is possible by using the symmetric storage mode, where only the elements on and below the main diagonal are stored by rows. Thus, an 1 by 1 symmetric matrix is reduced to a vector of length 1(1+1)/2, where the location (i,j) can be found as the location (b) of the vector **b**. For i≥j b=(i(i-1)/2)+j. For i<j, the element in location (i,j) is identical to the one in location (j,i). The saving of memory space is 1(1-1)/2 locations by storing the matrix in such a mode. For our case we therefore need about half of the $(16m)^2$ locations required. From Fig. (5.7) it is inferred that: for matrices $\mathbf{N}_{11}$ and $\mathbf{N}_{22}$ only the main diagonal and elements below the main diagonal need to be formed and stored; for matrix $\mathbf{N}_{21}$ all elements are required to be formed and stored.

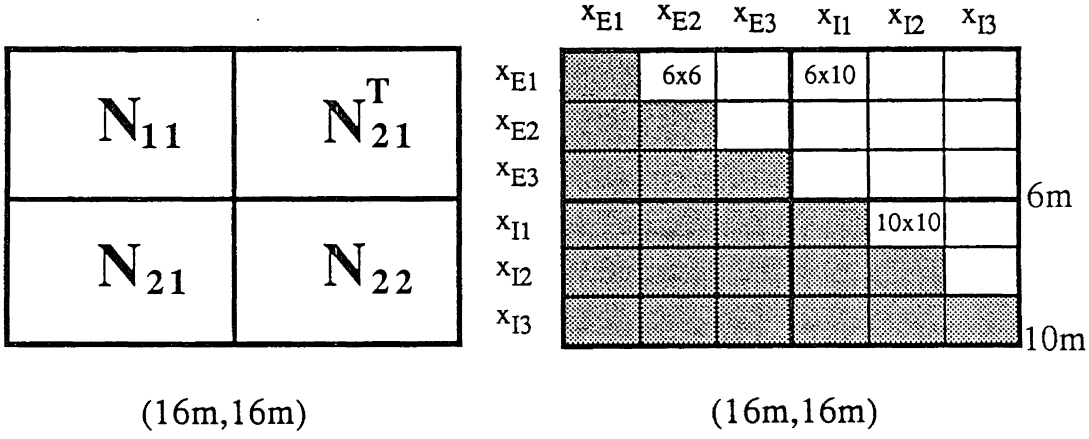

Figure 5.7: Structure of the cofactor matrix **N** of the reduced normal equations (m=3).

The direct simultaneous solution of the system of normal equations (equ.(5.66)) is obtained by using the Cholesky or square-root method

(Fadeeva, 1959), because it is very effective from the computational point of view (Lawson and Hanson, 1974; Knight and Mepham, 1978; Junkins and Steeves, 1986). In the beginning, the cofactor matrix **N** is factorized as

$$\mathbf{N} = \mathbf{L}\,\mathbf{L}^T \tag{5.79}$$

where **L** is a lower triangular matrix.

The solution of the system (5.66) of normal equations is reduced to the solution of two triangular systems. That is, it is equivalent to

$$\mathbf{L}\,\mathbf{L}^T\boldsymbol{\delta x} + \mathbf{u} = \mathbf{0} \tag{5.80}$$

or

$$\mathbf{L}\,\mathbf{g} = -\mathbf{u} \tag{5.81a}$$

and

$$\mathbf{L}^T\boldsymbol{\delta x} = \mathbf{g} \tag{5.81b}$$

The solution of **g** is obtained from equ.(5.81a) using a "forward substitution" process, since the matrix **L** is of a triangular type. Once **g** is known, $\boldsymbol{\delta x}$ is solved for, by using a "backward substitution" process on equ.(5.81b). It is worth mentioning that the solution $\boldsymbol{\delta x}$ is derived without inversion of the matrix **N**.

Having solved for the unknown camera parameters $\boldsymbol{\delta x}_E$ and $\boldsymbol{\delta x}_I$, the solution of the unknown coordinates is obtained from the system of equ.(5.64) if we solve it for $\boldsymbol{\delta x}_O$. Thus,

$$\underset{(3n,1)}{\boldsymbol{\delta x}_O} = -\mathbf{A}_{33}^{-1}\left[\left[\mathbf{A}_{23}^T \,\middle|\, \mathbf{A}_{13}^T\right]\begin{bmatrix}\boldsymbol{\delta x}_E \\ \hline \boldsymbol{\delta x}_I\end{bmatrix} + \mathbf{u}_3\right] \tag{5.82}$$

To reduce storage requirements due to the sparse nature of the matrices and to simplify the computational process, the solution is

computed for each individual object point. The correction δx_{Oi} for point i appearing on m photographs is obtained as

$$\delta x_{Oi} = -[\sum_{j=1}^{m}(A_{ij}^T P_P A_{ij}) + P_{Oj}]^{-1} \cdot$$

$$\cdot [\sum_{j=1}^{m}(A_{ij}^T P_P E_{ij} \cdot \delta x_{Ej}) + \sum_{j=1}^{m}(A_{ij}^T P_P P_{ij} \cdot \delta x_{Ij}) +$$

$$+ [\sum_{j=1}^{m}(A_{ij}^T P_P w_{Pij}) + P_{Oi} w_{Oi}]] \qquad (5.83)$$

The total solution vector δx_O will then be

$$\delta x_O = [\delta x^T_{O1}, \delta x^T_{O2}, \ldots, \delta x^T_{On}]^T$$

where n is the number of points.

5.5.2 Weights of the Observations and Initial Approximate Values of the Unknown Parameters

The weight matrix of the observations is very important because it expresses their precision and their effect on the final accuracy of the estimated parameters. For the sake of simplicity and due to lack of extensive and verified information about their precision, the observations are treated as uncorrelated. Therefore, the submatrices of the weight matrix P (equ.(5.58)) are also of diagonal form and act as scale factors during the formation of the normal equations. Since the variances of the observations involved have small numerical values, the diagonal elements of the weight matrices have large values, inversely proportional to these variances.

Thus, the summations given in the previous subsection tend to have very large numerical values if a great number of points exists or if a point appears on many photographs. This situation creates

numerical problems, particularly when the inverse of a matrix is required. It is therefore practical that the groups of observations be assigned relative weights with respect to the weights of the photo-observations. That is if,

$$p_p = \frac{\sigma_o^2}{\sigma_p^2} \quad \text{and} \quad p_g = \frac{\sigma_o^2}{\sigma_g^2} \tag{5.84}$$

then

$$p_g = \frac{\sigma_p^2}{\sigma_g^2} p_p \tag{5.85}$$

where

p_p : is the weight corresponding to the photo-observation p

p_g : is the weight corresponding to observation g

σ_o^2 : is the common a-priori variance factor

σ_p^2 : is the variance of the photo-observation p

σ_g^2 : is the variance of the observation g

Since the precision of the measured photo-coordinates is very high- in the range of micrometers- it is found practical to set the weight p_p equal to unity ($p_p = 1$). Thus, equ.(5.85) becomes

$$p_g = \frac{\sigma_p^2}{\sigma_g^2} \tag{5.86}$$

Equ.(5.86) is used to determine the relative weights for the other sets of observations (e.g., object space control points).

In order to linearize the non-linear photogrammetric model, initial approximate values for all the parameters are required. The least squares solution is obtained in an iterative manner, linearizing each time at the updated values of the parameters.

Moreover, the values of the initial approximations affect the numerical behaviour of the system. Poor initial values may cause erroneous results or divergence of the solution (El-Hakim, 1979). The influence of unstable initial approximations may also create ill-conditioning problems in the photo-variant self-calibration approach (Moniwa, 1981).

Generally, there is not a unique algorithm for obtaining approximate values. The initial approximations of the three groups of unknown parameters in the <PTBV> (Photogrammetric Triangulation by Bundles, Photo-Variant) bundle block adjustment system are derived as follows:

a) Elements of interior orientation.

- Camera constant c: The given (nominal) focal length is used as input.
- Coordinates x_o, y_o of the principal point: The centroid of the photo-format is used. Normally, it is sufficient to set $x_o=y_o=0$ and have all the photo-observations refer to this origin with the photo-format defining the directions of the coordinate system.
- Additional parameters $a_1,\ldots,a_7$: They are set equal to zero at the beginning. To avoid ill-conditioning or indeterminancy (Moniwa, 1977), the additional parameters are introduced as weighted unknown parameters at a later stage of the iterative procedure.

b) Elements of exterior orientation.

The position of the camera stations and the orientation of the camera axes are also entered in the program. For convenience,

the subprogram <RESECT> developed as part of the <APOLO> software can be initially used to perform a space resection and then provide initial values.

c) Coordinates of the object points.

The approximate coordinates of the object points are computed by space intersection from the first two photographs on which any object point appears. Since approximate values of the elements of interior and exterior orientation for all camera stations are available, the approximate coordinates of an object point P can be determined as (Moffit and Mikhail, 1980)

$$\begin{bmatrix} XP \\ YP \\ ZP \end{bmatrix} = \begin{bmatrix} XC_1 \\ YC_1 \\ ZC_1 \end{bmatrix} + s_1 \begin{bmatrix} u_1 \\ v_1 \\ w_1 \end{bmatrix} + 0.5d \begin{bmatrix} e_x \\ e_y \\ e_z \end{bmatrix} \qquad (5.87)$$

where

$[XP, YP, ZP]^T$:are the approximate coordinates of an object point

$[XC_1, YC_1, ZC_1]^T$:are the coordinates of the first camera station

$[u_1, v_1, w_1]^T$:are the rotated values of the photo-vector $[x_1, y_1, -c_1]^T$

$[e_x, e_y, e_z]^T$:are the direction components of vector **e**, which represents the minimum distance between two corresponding photo-rays.

s_1, d :are the proper scalar multipliers.

A detailed decscription of the procedure and the associated formulation are given in Armenakis, (1983).

It should be emphasized that independent of the method adopted for obtaining initial approximate values, better approximations require less iterations.

5.5.3 Estimation of the Variance-Covariance Matrix of the Object Points

The accuracy of the unknown parameters at the zero epoch is also required in order to predict the covariance matrix of the state vector at current time t. The state vector is restricted now to the coordinates of the object detail points. The accuracy of the camera parameters is also part of the computational process, since it affects the accuracy of the estimated coordinates.

The least squares solution of the object coordinates is given by equ.(5.82), as it has been shown. Using the matrix elements from equ.(5.63), equ.(5.82) can be written in a more extended form as

$$\delta\mathbf{x}_0 = -\mathbf{A}_{33}^{-1}\left[\begin{array}{cc|c|c} \mathbf{A}_{23}^T & \mathbf{A}_{13}^T & \mathbf{A}_{PO}^T\mathbf{P}_P & \mathbf{A}_{OB}^T\mathbf{P}_O \end{array}\right] \left[\begin{array}{c} \delta\mathbf{x}_E \\ \delta\mathbf{x}_I \\ \hline \mathbf{w}_P \\ \hline \mathbf{w}_O \end{array}\right] \qquad (5.88)$$

Equ.(5.88) can be reduced to a more concise expression

$$\delta\mathbf{x}_0 = \mathbf{D}\mathbf{y} \qquad (5.89a)$$

with

$$\mathbf{D} = -\mathbf{A}_{33}^{-1}\left[\begin{array}{cc|c|c} \mathbf{A}_{23}^T & \mathbf{A}_{13}^T & \mathbf{A}_{PO}^T\mathbf{P}_P & \mathbf{A}_{OB}^T\mathbf{P}_O \end{array}\right] \qquad (5.89b)$$

and

$$\mathbf{y} = [\,\delta\mathbf{x}_E^T\ \delta\mathbf{x}_I^T\,|\,\mathbf{w}_P^T\,|\,\mathbf{w}_O^T\,]^T \qquad (5.89c)$$

The final solution of the parameters is

$$\hat{\mathbf{x}}_0 = \mathbf{x}^{(o)} + \delta\mathbf{x}_0 = \mathbf{x}^{(o)} + \mathbf{D}\mathbf{y} \qquad (5.90)$$

The relative variance-covariance matrix $\mathbf{C}_{\hat{\mathbf{x}}}$ of the parameters $\hat{\mathbf{x}}_0$ is obtained by applying the covariance law to the above equ.(5.90)

$$C_{\hat{x}} = D\, C_y\, D^T \tag{5.91}$$

C_y is the covariance matrix of the vector **y** and is defined as

$$C_y = \begin{bmatrix} C_1 & 0 & 0 \\ 0 & C_2 & 0 \\ 0 & 0 & C_3 \end{bmatrix} \tag{5.92}$$

where

C_1 is the covariance matrix of the estimated camera parameters, that is

$$C_1 = N^{-1} \tag{5.93}$$

C_2 is the covariance matrix of the misclosure vector w_P, that is

$$C_2 = C_{wP} = P_P{}^{-1} \tag{5.94}$$

C_3 is the covariance matrix of the misclosure vector w_O, that is

$$C_3 = C_{wO} = P_O{}^{-1} \tag{5.95}$$

While matrices C_2 and C_3 can be computed easily, matrix C_1 cannot be determined without extra computational effort. The computation of the inverse of the **N** matrix is based again on its Cholesky decomposition (equ.(5.79)).

Thus,

$$N^{-1} = (L\, L^T)^{-1} = (L^{-1})^T\, L^{-1} \tag{5.96a}$$

or

$$N^{-1} = \left[\begin{array}{c|c} Q_{11} & Q_{21}{}^T \\ \hline Q_{21} & Q_{22} \end{array}\right] \tag{5.96b}$$

In the case where a point does not appear on all photographs, the necessary elements are extracted from N^{-1}.

Substituting equs.(5.92)-(5.95) into equ.(5.91), and considering equs.(5.89) we have

$$\underset{\sim}{C}_{\mathbf{x}} = A_{33}^{-1}[(A_{23}^T \,\vdots\, A_{13}^T)\, N^{-1} \begin{bmatrix} A_{23} \\ \cdots \\ A_{13} \end{bmatrix} + A_{PO}^T P_P A_{PO} + P_O](A_{33}^{-1})^T =$$

$$= A_{33}^{-1}\,[\,H + A_{PO}^T P_P A_{PO} + P_O\,]\,(A_{33}^{-1})^T \qquad (5.97)$$

Equ.(5.97) represents the general form of the variance-covariance matrix $\hat{C_x}$ of the coordinates of the object points.

Subsequently, the terms in equ.(5.97) are defined explicitly for each point k appearing on m photographs.

The term H is the summation of four terms

$$H = H_1 + H_2 + H_3 + H_4 \qquad (5.98)$$

where

$$H_1 = (A_{PO}{}^T P_P A_{PE})\, Q_{11}\, (A_{PE}{}^T P_P A_{PO})$$

$$H_2 = (A_{PO}{}^T P_P A_{PI})\, Q_{21}\, (A_{PE}{}^T P_P A_{PO})$$

$$H_3 = (A_{PO}{}^T P_P A_{PE})\, Q_{21}{}^T\, (A_{PI}{}^T P_P A_{PO})$$

$$H_4 = (A_{PO}{}^T P_P A_{PI})\, Q_{22}\, (A_{PI}{}^T P_P A_{PO})$$

The diagonal matrix elements of the terms H_i (i=1,2,3,4) are formed as follows:

$$H_1 = \sum_{l=1}^{m} [\sum_{j=1}^{m} [(A_{kj}^T P_P E_{kj})\, Q_{11}(j,l)]\, E_{kl}^T P_P A_{kl}] \qquad (5.99)$$

$$H_2 = \sum_{l=1}^{m} [\sum_{j=1}^{m} [(A_{kj}^T P_P P_{kj})\, Q_{21}(j,l)]\, E_{kl}^T P_P A_{kl}] \qquad (5.100)$$

$$H_3 = \sum_{l=1}^{m} [\sum_{j=1}^{m} [(A_{kj}^T P_P E_{kj})\, Q_{21}^T(l,j)]\, P_{kl}^T P_P A_{kl}] \qquad (5.101)$$

$$H_4 = \sum_{l=1}^{m} [\sum_{j=1}^{m} [(A_{kj}^T P_P P_{kj})\, Q_{22}(j,l)]\, P_{kl}^T P_P A_{kl}] \qquad (5.102)$$

The term $A_{PO}^T P_P A_{PO} + P_O$ is formed as

$$A_{PO}^T P_P A_{PO} + P_O = \sum_{j=1}^{m} (A_{kj}^T P_P A_{kj}) + P_{Ok} \qquad (5.103)$$

Finally, the term A_{33}^{-1} is formed as the inverse of the above equ.(5.103).

Due to the use of relative weights, the estimated variance-covariance matrix $\hat{C}_{\hat{x}}$ expresses the measure of accuracy of the parameters. Thus,

$$\hat{C}_{\hat{x}} = \hat{\sigma}_o^2 \, C_{\hat{x}} \quad , \tag{5.104}$$

where $\hat{\sigma}_o^2$ is the a-posteriori variance factor determined as

$$\hat{\sigma}_o^2 = \frac{v_P^T P_P v_P + v_I^T P_I v_I + v_O^T P_O v_O}{df} \tag{5.105}$$

with df denoting the degrees of freedom of the least squares adjustment.

$$v_O^T P_O v_O = v_{CN}^T P_{CN} v_{CN} + v_{OB}^T P_{OB} v_{OB}$$

where the subscript (CN) refers to the control points and the subscript (OB) refers to any other weighted object points.

Only the diagonal matrix elements of the estimated covariance matrix $\hat{C}_{\hat{x}}$ need to be computed (Fig.5.8). This was considered to be the best solution for two main reasons:

a) The computational effort should be kept as low as possible without losing significant information.

b) The estimated covariance matrix $\hat{C}_{\hat{x}}$ will play the role of weighting the predicted object coordinates and is not used for any global statistical testing.

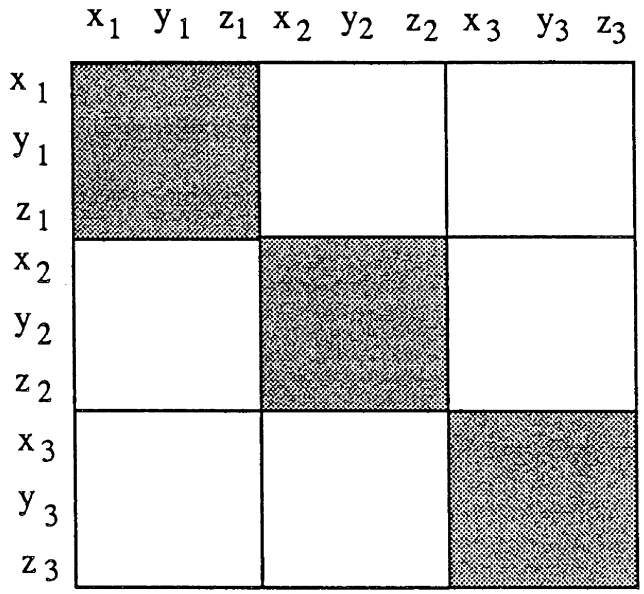

Figure 5.8: Structure of the estimated variance-covariance matrix $\hat{C}_{\hat{x}}$ (for 3 object points).

5.6 Sequential Estimation of the State Information

With the parameter vector and its covariance matrix known at the zero epoch t_o, it is possible to anticipate changes of the state information at time t ($t \neq t_o$). This information is obtained with the prediction model.

At the same time t a subset of observations becomes available. To attain an optimal estimate of the state information at time t, the updated sequential filtering mechanism -equs.(5.35) and (5.36)- is invoked. Consideration is given to the nature of the parameters $\mathbf{x}_E$, $\mathbf{x}_I$, $\mathbf{x}_O$, their evolution with time and their mathematical

relations with the observations in the measurement model.

5.6.1 Practical Considerations and Selection of the State Parameters

In the physical world the updated sequential filtering algorithm can be applied as is, if in addition to the predicted positions of the object points, the parameters of interior and exterior orientation of the camera stations can be predicted at each monitoring campaign. Let us assume logically, that no interrelation exists among the three groups due to their heterogeneous nature. Then, the transition matrix $\mathbf{T}$ is partitioned into the following diagonal form.

$$\mathbf{T} = \begin{bmatrix} \mathbf{T}_I & \mathbf{0} & \mathbf{0} \\ \mathbf{0} & \mathbf{T}_E & \mathbf{0} \\ \mathbf{0} & \mathbf{0} & \mathbf{T}_O \end{bmatrix} \qquad (5.106)$$

where $\mathbf{T}_I$, $\mathbf{T}_E$, $\mathbf{T}_O$ are individual transition matrices corresponding to each group of parameters.

In each photogrammetric campaign we have:

a) Known (or fixed) exposure stations using the same or different cameras. This case applies mainly to terrestrial photogrammetric projects. The transition and the predicted covariance matrices will then be:

- For the exterior orientation parameters $\mathbf{x}_E$:

  $\mathbf{T}_E = \mathbf{I}$ since $\hat{\mathbf{x}}_{E,t} \approx \hat{\mathbf{x}}_{E,t-1}$, with $\mathbf{C}_E(\cdot)$ = constant

- For the interior orientation (IO) parameters $\mathbf{x}_I$ we distinguish three cases:

  i) $\mathbf{T}_I = \mathbf{I}$ using the same metric cameras (stable interior

orientation) with $\mathbf{C}_I(-)$ = constant.

ii) $\mathbf{T}_I$ = $\mathbf{T}(IO(t),\delta t)$ using the same non-metric cameras (unstable interior orientation), with $\mathbf{C}_I(-)$ = f(t).

iii) $\mathbf{T}_I$ = $\mathbf{I}$ for different cameras and reinitialization of $\hat{\mathbf{x}}_I$, with $\mathbf{C}_I(-)$ = constant.

- For the trajectories of the object points:

$\mathbf{T}_O$ = $\mathbf{T}_O(\mathbf{p},\delta t)$ (cf.equ.(5.26)) with $\mathbf{C}_{O,t}(-)$ = f(t) (cf. equ.(5.28)).

b) Unknown (different) exposure stations with either the same or different cameras. This situation applies to aerial photogrammetry and many terrestrial situations. The transition and the predicted covariance matrices will then be:

- For the parameters $\mathbf{x}_E$ of the exterior orientation:

$\mathbf{T}_E = \mathbf{T}_E$ (flight parameters, δt) with $\mathbf{C}_E(-)$ = f(t)

- For the parameters $\mathbf{x}_I$ of the interior orientation:

$\mathbf{T}_I$ and $\mathbf{C}_I(-)$ are defined as in case a).

-For the trajectories of the object points:

$\mathbf{T}_O$ and $\mathbf{C}_O(-)$ are defined as in case a)

Naturally both arrangements can be handled using the final updated equs.(5.35) and (5.36) of the general sequential photogrammetric model. However, two points must be stressed:

1) Most of the times we are interested in monitoring the object. Camera stations are more or less subject to design criteria. Thus, the parameter vector $\mathbf{x}_O$ and its accuracy is the final product of the photogrammetric campaign.

2) In the general situation, i.e. case b), it is difficult in

practice to obtain appropriate and accurate information for the definition T_E and perhaps T_I, when they are not equal to unity. With the new technological developments, (e.g,. Global Positioning System; Lucas, 1987) more accurate information on the elements of exterior orientation will become available.

Three alternative solutions have been investigated by the author. The first two utilize the existing control points to solve for the extended set of space resection parameters. The third is a special case of the first two.

First Approach (Use of the complete measurement model).

This approach is designed to handle the lack of proper information regarding the transition matrices T_E and T_I in epoch t. Steps 1 to 4 have been designed to alleviate this shortcoming by creating "artificial" transition and prediction covariance matrices. Step 5 is a direct application of equs.(5.35) and (5.36).

Step 1. Use only the observation model and partition δx as

$$\delta x = [\ \delta x_{E,I}{}^T \ \vdots\ \delta x_O{}^T\ ]^T$$

Step 2. Eliminate δx_O.

Step 3. Solve the reduced normal equations for $\delta x_{E,I}$, and compute the estimated camera parameters.

$$\hat{x}_{E,I,(t)} = \left[\ \hat{x}_{E,(t)}^T \ \vdots\ \hat{x}_{I,(t)}^T\ \right]^T$$

and their covariance matrix $C_{E,I,(t)}$

Step 4. Use $\hat{x}_{E,(t)}$ and $\hat{x}_{I,(t)}$ as predicted pseudo-observations for time t and their covariance $C_{E,I,(t)}$ as their

predicted accuracy. Thus, it is possible to set

$$T_{I,(t)} = I \text{ and } T_{E,(t)} = I$$

and overcome the problems related to case b).

Step 5. Integrate the predicted information of the camera stations with the predicted model of the object. Use both the prediction- and the measurement models for the combined determination of the updated parameters and their covariance at the current time t.

Second Approch (Use of the reduced measurement model).

This approach originates from the fact that we are mainly interested in determining the trajectories of the object points. If there is a way to know a priori the camera parameters at time t, then the coordinates of the object points are obtained via a general intersection solution. However, the propagation of the errors of the camera parameters to the accuracy of the object points is very important and should not be overlooked.

Bearing that in mind and realizing the heavy computational effort required in the first approach after having solved for the extended space resection, it was decided to apply the updated mechanism for the unknown object coordinates only.

This approach is described in the following steps:

Steps 1 to 3 are the same as in the first approach. That is, the extended space resection problem is solved for.

Step 4. Since the parameters $\hat{x}_E$ and $\hat{x}_I$ are considered known, the remaining unknown parameter is the vector $\hat{x}_O$. The general form of the reduced observation model will then

be:

- For the photogrammetric observations (cf. equ.(5.52))

$$F_1 (\hat{x}_0) = l_p, \; P_P \tag{5.107}$$

which, when linearized, becomes

$$A_{P0}\delta x_0 + w_P - v_P = 0, \; P_P \tag{5.108}$$

- For the terrestrial observations of the object points, (including control points (cf. equ.(5.48))

$$F_3 (\hat{x}_0) = l_0, \; P_0 \tag{5.109}$$

or in linearized form:

$$A_{0B}\delta x_0 + w_0 - v_0 = 0, \; P_0 \tag{5.110}$$

Combining equs.(5.108) and (5.110) the reduced observation model is expressed as

$$\begin{bmatrix} A_{P0} \\ A_{0B} \end{bmatrix} [\, \delta x_0 \,] + \begin{bmatrix} w_P \\ w_0 \end{bmatrix} - \begin{bmatrix} v_P \\ v_0 \end{bmatrix} = \begin{bmatrix} 0 \\ 0 \end{bmatrix} \tag{5.111}$$

and the weight matrix P of the observations is given as

$$P = \begin{bmatrix} P_P & 0 \\ 0 & P_0 \end{bmatrix} \tag{5.112}$$

To conform with the notation of equs.(5.35) and (5.36), the observation model of equ. (5.111) is written for time t as

$$A_t \, \delta x_0 + w_t - v_t = 0 \tag{5.113}$$

and the covariance matrix C_t of the observations is defined from equ.(5.112) as

$$C_t = P^{-1} = \begin{bmatrix} P_P^{-1} & 0 \\ 0 & P_0^{-1} \end{bmatrix} \tag{5.114}$$

Step 5. Now we can use the prediction model for the object space and for the reduced measurement model (equs.(5.113),(5.114)) to find optimal estimations of the current coordinates of the object points and their covariance matrix at time t. This means that the updated equations (5.35) and (5.36) are applied only to the object points.

Third Approach (Use of the reduced observation model with known (or fixed) camera parameters).

This approach is applied directly to terrestrial (close-range, laboratory) photogrammetry. It serves the situation where the monitoring of the trajectory of the object is performed from known camera positions with known and stable interior orientation parameters of the camera(s) used. The procedure of the second approach is also followed here, disregarding of course steps 1 to 3. Therefore, this approach requires only steps 4 and 5 of the previously presented second approach.

5.6.2 Estimation of the Updated Object Parameters

The analysis performed for each of the three alternative solutions not only illustrated the nature of the problem, but also led to selection of the second approach, and the corresponding software for the sequential state estimation has been developed by the author. It is called <SPDM> (Sequential Photogrammetric

Displacement Monitoring). This solution is considered most appropriate from the practical point of view as it does not require additional information for the parameters of the camera stations. The initial approximations of these parameters are normally updated during the iterative procedure, while the predicted coordinates of the object points are updated with the sequential filtering expressions (equs.(5.35)). To avoid datum indeterminacies, the necessary number and distribution of control points must be available especially if the predicted object coordinates have large uncertainties.

This method is also computationally effective. The first approach requires operations with the full matrix of normal equations of the bundle block adjustment case for the updated solution of the complete model. Then the computations for the extended space resection have to be added. Extensive partitioning and elimination processes of matrices are unavoidable. From the modelling point of view, step 5 of the first approach is equivalent to a model which -in addition to the already described observation model- considers the elements of exterior orientation as weighted unknown parameters. It is obvious that the third approach can be incorporated into the second approach by holding the camera parameters equal to their initial values.

The expression for the updated estimated object parameters for the second approach is presented next.

First, equ.(5.35) is rewritten in a condensed form, as

$$\hat{\mathbf{x}}_t\,(+) = \hat{\mathbf{x}}_t(-) - \mathbf{s} \qquad (5.115)$$

where

$\hat{x}_t(+)$: is the updated vector of the coordinates of the object points

$\hat{x}_t(-)$: is the predicted vector of the coordinates of the object points

s : is the correction term due to the contribution of the reduced observation model.

The correction term **s** for each point k (k=1,...,n) appearing on m photographs is derived in detail as

$$\begin{aligned} s_k = \sum_{i=1}^{m} [& (C_{t,kk} A_{ki}^T P_P).[(I - A_{ki} C_{kk} A_{ki}^T P_P).(A_{ki}\delta x_k + w_{Pki}) + \\ & + \sum_{j=1, j\neq i}^{m} [(-A_{ki} C_{kk} A_{kj}^T P_P).(A_{kj}\delta x_k + w_{Pkj})] + \\ & + (-A_{ki} C_{kk} P_O).(\delta x_k + w_O)]] + \\ & + (C_{t,kk} P_O).[(I - C_{kk} P_O).(\delta x_k + w_O) + \\ & + \sum_{i=1}^{m} [(-C_{kk} A_{ki}^T P_P).(A_{ki}\delta x_k + w_{Pki})]] \end{aligned} \qquad (5.116)$$

The matrices involved have already been defined in the previous sections.

5.6.3 Estimation of the Updated Variance-Covariance Matrix of the Object Parameters

The accuracy of the parameters in every estimation process is an indispensable part of the solution. Thus, the last stage of the sequential photogrammetric approach is the estimation of the updated covariance matrix $C_t(+)$ of the object coordinates. This matrix $C_t(+)$ has been derived in equ.(5.36). It is given here in a shorter version:

$$C_t(+) = (I - G \cdot A_t) \cdot C_t(-) \qquad (5.117)$$

with G being the already defined gain matrix.

Again, only the diagonal elements of the updated covariance matrix $C_t(+)$ are computed. The matrix structure of equ.(5.117) is illustrated in Fig.5.9.

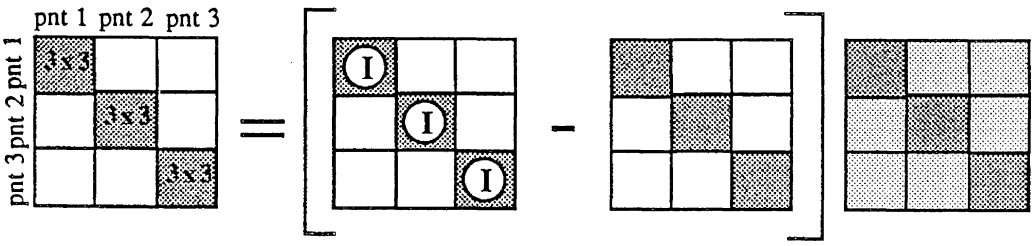

Figure 5.9: Structure of the expression for the updated variance-covariance matrix $C_t(+)$ (for 3 object points).

The diagonal elements of the term $G \cdot A_t$ are given explicitly for each point k appearing on m photographs:

$$\begin{aligned} G \cdot A_{t,k} = \sum_{i=1}^{m} [& (C_{t,kk} A_{ki}^T P_P) \cdot [(I - A_{ki} C_{kk} A_{ki}^T P_P) A_{ki} + \\ & + \sum_{j=1, j \neq i}^{m} [(-A_{ki} C_{kk} A_{kj}^T P_P) \cdot A_{kj}] + (-A_{ki} C_{kk} P_O)] + \\ & + (C_{t,kk} P_O) \cdot [(I - C_{kk} P_O) + \sum_{i=1}^{m} [(-C_{kk} A_{ki}^T P_P) A_{ki}]] \end{aligned} \qquad (5.118)$$

After substituting the term for $G \cdot A_t$ into equ.(5.117), the complete updated covariance matrix $C_t(+)$ can be found.

Because the updating mechanism is applied only to the object points, it is advisable to include in their accuracy the uncertainty of the camera parameters. This can be done -if required- in the following two ways:

- By computing the variance-covariance matrix of the object points using only the photogrammetric observation model (equ.(5.97)) and then add it to the predicted covariance matrix $\mathbf{C}_t(-)$,
- Or by incorporating any expected uncertainty of the object coordinates into the uncertainty $\mathbf{Q}$ of the prediction model (equ.(5.28)). Then, this uncertainty is contained in the predicted covariance matrix $\mathbf{C}_t(-)$ of the current estimation time t.

6. EXAMPLES OF APPLICATIONS

The developements related to data collection and processing (Chapters 4 and 5) for photogrammetric monitoring of displacements were applied to real and simulated cases. The findings of these applications are presented in this chapter. The <APOLO> measuring system has been used to measure photo-coordinates of targetted and natural points. The sequential photogrammetric approach was then applied to three cases. In case one, simulated data were used to demonstrate clearly the capabilities of the method. Cases two and three are real applications of close-range and aerial photogrammetry respectively. The results are discussed and evaluated for both data collection and data processing operations.

6.1 On-line Semi-Automatic System <APOLO>

The <MONO>- and <STEREO>-mode branches of the developed measuring system have been examined and assessed during practical tests. The theoretical aspects of the evaluation have been presented in section 4.7.

6.1.1 Data Collection and Evaluation Using the <MONO>-mode Subsystem

The photo-coordinates of discrete targetted image points were measured using the on-line mono-comparator option of the <APOLO> semi-automatic measuring system. The intersections of grid test plates were selected to represent the signalized images points. This serves two purposes: a) the calibrated coordinates of the grid nodes are well known, thus providing a rigorous measure of comparison, and b) the results of the measurements could be used to evaluate the performance of the measuring devices of the analytical plotter.

Twenty-one (21) well distributed grid intersections were measured in three sets. Their calibrated coordinates were disturbed and stored to simulate the digitized table coordinates of the image points. Three aspects were examined: repeatability, accuracy of measurements,and overall execution time.

The computations for the repeatability of the measurements gave the following results for the average overall standard deviations:

for the left photo-carrier $\bar{s}_x = \pm 2.7$ μm, $\bar{s}_y = \pm 2.6$ μm

for the right photo-carrier $\bar{s}_x = \pm 1.9$ μm, $\bar{s}_y = \pm 2.6$ μm.

The evaluation of the accuracy was based on the estimated parameters and the statistical information derived from the least squares solution for the six parameter transformation (Appendix IV).

The estimated parameters for the left photo-carrier were:

scale factors $k_x = 0.99990$, $k_y = 0.99995$

angle of non-orthogonality $\beta_L = -0.00171$ deg

translations c = -108.696 mm, f = -111.280mm

The a-posteriori variance factors with df = 18 were:

$\hat{\sigma}_{o,}{}^{2}{}_{x}$ = 3.25 E-06, $\hat{\sigma}_{o,}{}^{2}{}_{y}$ = 3.27 E-06

The X^2-test on the reference variance factor $\sigma_o{}^2$ = 4.0 E-06 passed at the 0.95 confidence level for both the x- and y-observations.

The estimated variance-covariance matrices of the transformation parameters were also computed. The variances are given here:

var (a) = 6.46 E-11 rad^2 var (d) = 5.99 E-11 rad^2

var (b) = 6.46 E-11 rad^2 var (e) = 5.99 E-11 rad^2

var (c) = 1.91 E-06 mm^2 var (f) = 1.77 E-06 mm^2

The estimated parameters for the right photo-carrier were:

scale factors k_x = 0.99998, k_y = 0.99993

angle of non-orthogonality β_R = -0.00288 deg

translations c = -109.865 mm, f = -110.119mm

The a-posteriori variance factors with df = 18 were:

$\hat{\sigma}_{o,}{}^{2}{}_{x}$ = 1.82 E-06, $\hat{\sigma}_{o,}{}^{2}{}_{y}$ = 3.09 E-06

Again, the X^2-test on the reference variance factor $\sigma_o{}^2$ = 4.0 E-06 passed at the 0.95 confidence level for both the x- and y-observations.

The estimated variance-covariance matrices of the transformation parameters were also computed and the variances were:

var (a) = 3.20 E-11 rad^2 var (d) = 5.99 E-11 rad^2

var (b) = 3.20 E-11 rad^2 var (e) = 5.99 E-11 rad^2

var (c) = 9.46 E-07 mm^2 var (f) = 1.77 E-06 mm^2

The residuals of the photo-observations were plotted for both

carriers (Fig. 6.1 and 6.2). Visual inspection of the distribution of the residual vectors does not reveal a systematic trend. It should be noted here that the magnitude of the residuals for the right photo-carrier is smaller than the one for the left carrier. This is attributed to the fact that the right measuring mark appears to have a slightly smaller size than the left one.

The total time to run the program, that is responding to the prompts and measuring the points (21 points x 3 obs/point = 63 obs) was done in about 10 minutes. The travelling speed of the measuring mark was estimated to be approximately 12-13 mm/s.

The <MONO>-mode system proved to be an excellent tool for measuring images of characteristic natural point features from small scale photography taken from the Space Shuttle with the Large Format Camera (LFC), where approximately 4500 photo-observations were made (Derenyi and Newton, 1987). According to Newton, (1986) the measuring system proved to be extremely beneficial because manual tasks and manual data entry are eliminated, the location of image points under computer control was quick, while the measuring mark was driven to within approximately 1 mm of all points, and finally the operator's fatigue was quite low, while the data collection was very rapid. Time-wisely, the rule-of-thumb given (ibid) was that all measurements on a diapositive, that is digitization and three measurement sets, consisting of 100 image points could be completed in 4 hours. For targetted points, shorter measuring times would be achievable, since for most of the natural detail points their location sketches had to be reviewed prior to measurements.

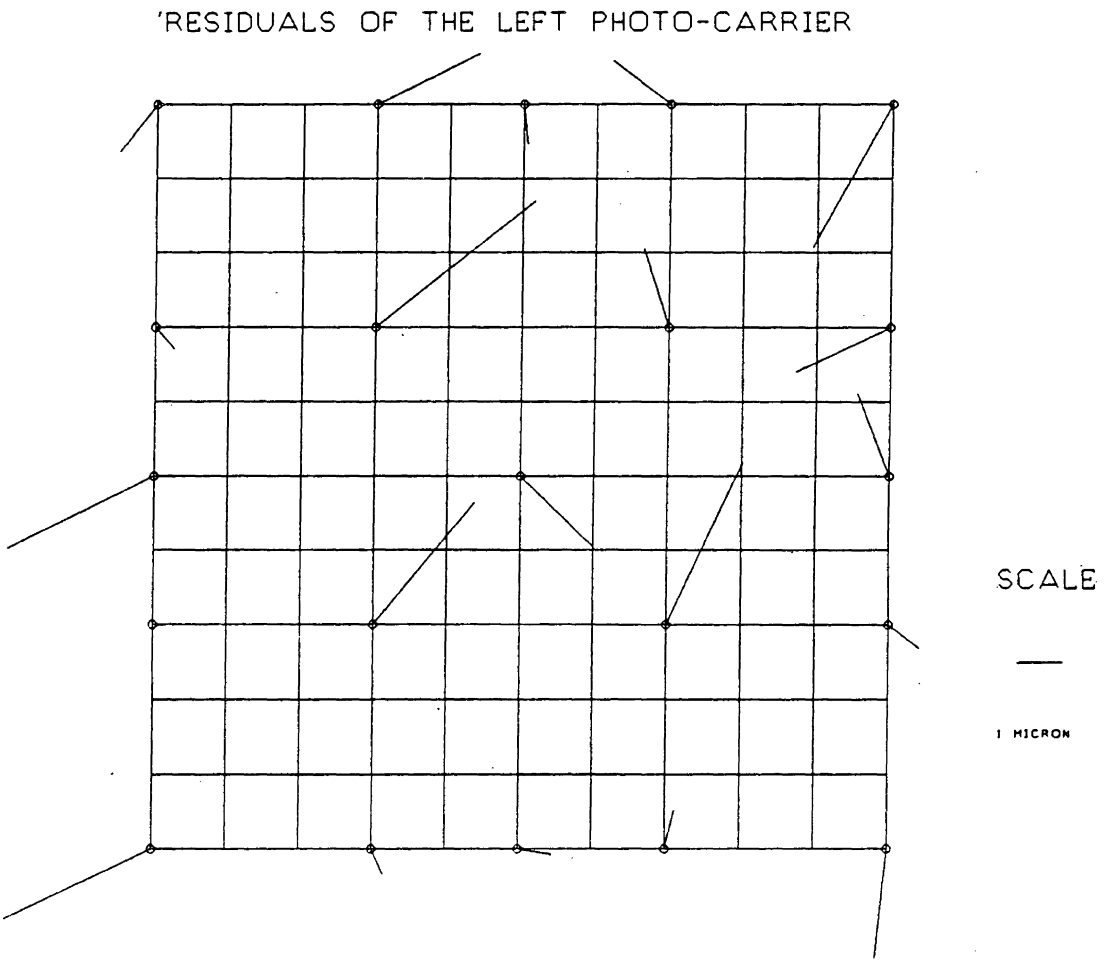

Figure 6.1: Residual vectors of the photo-observations at the grid nodes (left photo-carrier).

Judging from the results of the practical tests, the usefulness of the on-line semi-automatic measuring system for targetted points has been established. The introduced automation reduces drastically the measuring time while the on-line editing capabilities offer flexibility and confidence to the operator. At the same time the

accuracy of the photo-coordinates is maintained at the precision level of the measuring devices (rotary encoders) of the analytical plotter.

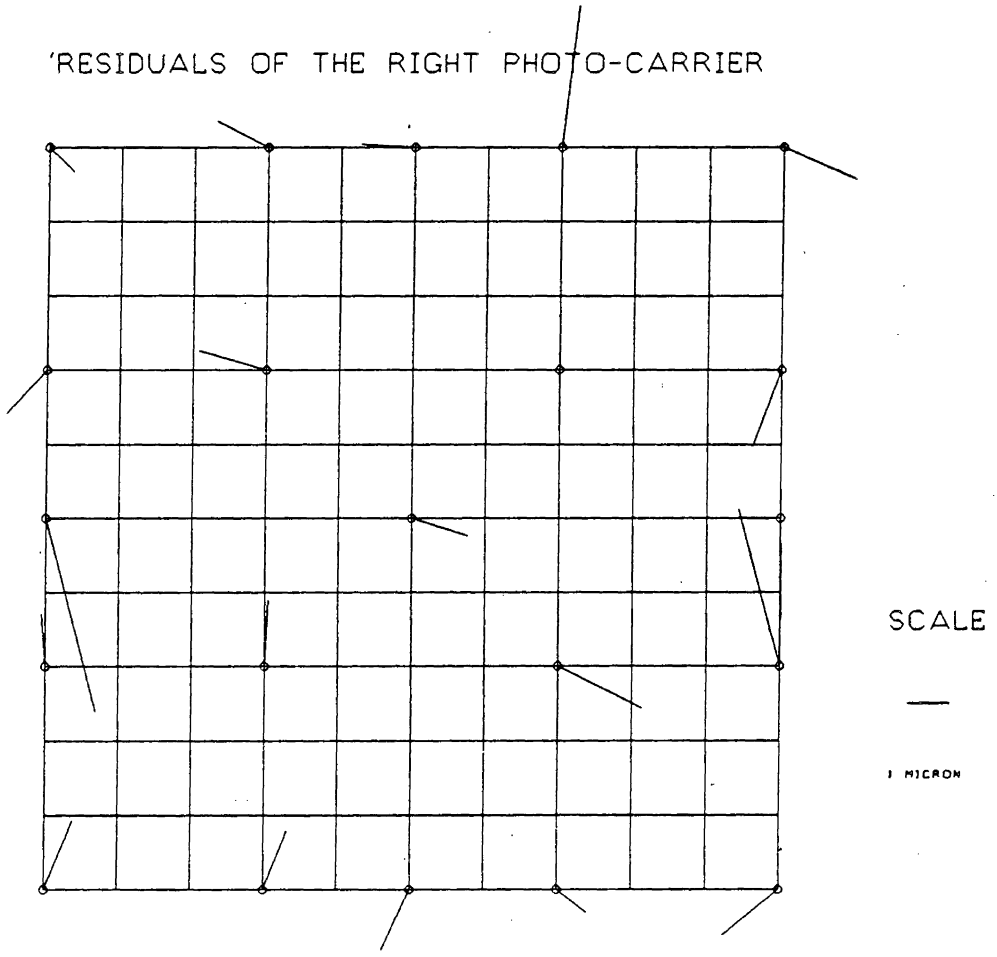

Figure 6.2: Residual vectors of the photo-observations at the grid nodes (right photo-carrier).

6.1.2 Data Collection and Evaluation Using the <STEREO>-mode Subsystem

The <STEREO>-mode option of the <APOLO> semi-automatic measuring system was employed to measure the image coordinates of natural points from multi-temporal photographs. The analytical plotter was used in three on-line modes of operation: as plotter, as stereo-comparator and as combined plotter/comparator.

The study area was a 1 km x 1 km mountain slope with elevation differences of about 500 m. A standard aerial camera (f = 152.48mm) was used for both photographic campaigns at a photo-scale of approximately 1:6000. The magnitude of expected ground displacements was in the range of 1 to 1.5 metres.

At this initial stage, the measuring procedures were examined with respect to the required time for data collection, the ease of operations and the quality of the measured photo-coordinates. The evaluation of the photo-coordinates was performed independently of the object space, thus providing a direct assessment of the measuring system. It was originally planned to examine all aspects by comparing results between the conventional photogrammetric mensuration scheme, which involves point transfer via marking prior to taking stereo-comparator readings, and the on-line measuring system, which employs the analytical stereo-plotter OMI AP-2C. However, due to temporary unavailability of the stereo-comparator, all measurements for this test were performed on the analytical plotter with the <STEREO>-mode subsystem. The comparisons for time and convenience were based on the author's previous experience with the conventional approach. While the difficulties of the manual

operations and the operator's fatigue and eye-strain were drastically reduced, the total time for data collection is estimated to have been cut at least in half.

Two pairs of aerial photographs were measured corresponding to the two different time periods. Most of the points were natural details on the ground, and for epoch 2 these points were marked on the emulsion of one of the photographs because of the previous conventional use of this stereo-pair. The photo-coordinates of 34 points were measured for each epoch with the two-step procedure of the <STEREO>-mode method. The point transfer for the photo-pair of epoch 1 was performed "digitally" using <STEREO>, thus physical point marking became unneccessary. The same 15 well distributed points were chosen on each stereo-pair to determine the elements of the dependent-pair relative orientation.

The stochastic model was defined empirically based on preliminary photo-observations. The observations were considered uncorrelated and of equal weight. The inverse of the variances of the observations was scaled to obtain a diagonal relative weight matrix **P** which was used to avoid numerical problems. Thus,

$$\mathbf{P} = \sigma_o^2 \, \mathbf{C}_l^{-1}$$

where

$$\sigma_o^2 = 9.0 \text{ E-06}$$

$$\mathbf{C}_l^{-1} = d \cdot \mathbf{I} \quad (\mathbf{I} \text{ is the identity matrix})$$

and

$$d = (\sigma_l^2)^{-1} \quad \text{with } \sigma_l = 0.006 \text{ mm.}$$

The magnitude of the residuals for epoch 2 (containing a premarked

photograph) was larger than for epoch 1. This is reflected in the corresponding a-posteriori variance factors where

$$\hat{\sigma}_{o,2}^2 = 5.44 \text{ E-05} \quad > \quad \hat{\sigma}_{o,1}^2 = 8.53 \text{ E-06}$$

with $df_1 = df_2 = df$ and $\mathbf{P}_1 = \mathbf{P}_2 = 0.25\ \mathbf{I}\ mm^{-2}$.

The X^2-test was performed on the ratio $\sigma_o^2/\hat{\sigma}_o^2$. The two tailed confidence interval for σ_o^2 was calculated for each epoch for df = 10 degrees of freedom and a significance level $\alpha = 0.05$. For epoch 1, and thus for the photo-pair without premarked points the null hypothesis $H_{o,1}$: $\hat{\sigma}_{o,1}^2 = \sigma_{o,1}^2$ versus the alternative hypothesis $H_{A,1}$: $\hat{\sigma}_{o,1}^2 \neq \sigma_{o,1}^2$ was not rejected (4.1 E-06 < 9.0 E-06 < 2.6 E-05). This is a global indication of the appropriateness of the functional and stochastic models. However, for epoch 2, containing the premarked points, $H_{o,2}$: $\hat{\sigma}_{o,2}^2 = \sigma_{o,2}^2$ was rejected in favour of $H_{A,2}$: $\hat{\sigma}_{o,2}^2 \neq \sigma_{o,2}^2$ (2.6 E-05 $\not<$ 9.0 E-06 < 1.6 E-04).

Since it is unlikely that the functional model (coplanarity condition) is incorrect, it can be said that either the weight matrix may be improper, or that there may be outlying observations, or that untreated systematic errors may exist. The former two situations were investigated at the present time while the third was not considered at this stage of evaluation of the collected data. The influence of systematic errors was not examined here because of two reasons: a) a well calibrated metric (aerial) camera was used thus resulting in small and controllable effects of the systematic errors, and b) the incorporation of additional parameters in the coplanarity condition for a single pair of photographs can lead to ill-conditioning problems and computational inefficiency (Moniwa, 1977).

The collected photo-coordinates were then examined for possible blunders due to poor stereoscopy which was noticed at some points of epoch 2. For df=10, $\alpha = 0.05$ and $\alpha_o \approx 0.001$, the critical value c is equal to 3.29. While all points from epoch 1 were accepted, two points from epoch 2 were flagged as their absolute standardized residuals ($|w_6| = 6.27$, $|w_9| = 3.66$) exceeded the value of c.

Nevertheless, the weight matrix of the observations for the marked photo-pair was reconsidered as one of the possibilites for the failure of the test on the variance factor. The precision of the observations was reevaluated and, based on additional tests, it was considered worse by a factor of two. That is, $\sigma_{1,2}{}' = 2\sigma_{1,2}$ and consequently $\mathbf{P}'_2 = 0.25\ \mathbf{P}_2$. The computations for epoch 2 were repeated with the new weight matrix $\mathbf{P}'_2$ and this time the test on the variance factor passed at the 0.95 confidence level (6.6 E-06 < 9.0 E-06 <4.2 E-05). It should be noted here that $\hat{\sigma}_{o,1}{}^2$ was still smaller than the new $\hat{\sigma}_{o,2}{}^{2'}$ (= 1.36 E-05). In addition, no point was flagged as containing outlying observations although again one of the earlier rejected points showed the largest standardized residual value and passed only marginally ($|w_6| = 3.13 < 3.29$).

The computed redundancy numbers corresponding to the x components of the photo-coordinates were very close to zero as expected, while for the y components the corresponding values were in the range of 0.2 - 0.4. Therefore, pointing gross errors could rather be detected through the controllability of the y observations.

Another indicator for assessing the measurements was the computation of the residual parallaxes (RP) at each model point for

both epochs. Their expected accuracies, represented by their mean values and their standard deviations, were:

for the unmarked photo-pair $\overline{RP}_1$ = -0.0005mm, $s_{RP,1} = \pm 0.0070$mm

for the marked photo-pair $\overline{RP}_2$ = 0.0001mm, $s_{RP,2} = \pm 0.0163$mm

While the difference of the mean values can be considered insignificant (<1μm) with respect to the capabilites of the measuring instrument, the standard deviation of the residual parallaxes for epoch 2 is about 2.2 times larger than its corresponding value in epoch 1. Therefore, it can be said that the model coordinates of epoch 1 have been estimated more efficiently than the ones from epoch 2.

The measuring experiment showed a significant increase of the productivity due to the higher speed of execution in certain operations and due to the integration of certain photogrammetric data collection phases. The approach is flexible because it offers on-line editing capabilities and options. The quality of the measured coordinates has also been improved, not only because of the preservation of stereoscopic observations, but also because the photo-coordinates establish directly the point location on the multi-temporal photographs. This has been demonstrated by the higher precision of the photo-coordinates and the lower risk of contamination by blunders.

6.2 Sequential Photogrammetric Approach

The combination of the photogrammetric observations with external information related to the position of the object at the

time of exposure was tested with three examples. The definitions and mathematical derivations have been given in chapters 2 and 5.

6.2.1 Case 1: Test with simulated data

A grid of 600m x 600m with an interval of 200m was created. Sixteen points of various elevations located at the nodes of the grid were considered to be detail points representing the object. The area was covered by five convergent photographs. Their photo-format was 230mm x 230mm, while the focal length was set to be equal to 150mm, thus providing an average photo-scale of about 1:2800. The positions and orientations of the camera stations are given in Table 6.1.

Table 6.1: Camera stations - Epoch 1

Photo #	XC(m)	YC(m)	ZC(m)	$w^{(o)}$	$\varphi^{(o)}$	$k^{(o)}$
1	500.0	750.0	625.0	-15.0	0.0	0.0
2	500.0	500.0	600.0	0.0	0.0	0.0
3	500.0	250.0	625.0	15.0	0.0	0.0
4	250.0	500.0	625.0	0.0	-15.0	0.0
5	750.0	500.0	625.0	0.0	15.0	0.0

The detail points and the locations of the camera stations are illustrated in Fig. 6.3.

For the first epoch the photo-coordinates of the images of the sixteen points on the five photographs were generated using the collinearity equations.

For the second epoch predicted object coordinates were generated using two different displacement matrices **T** (the program

SPDM can accomodate up to five matrices T). The parameters used to determine the displacement matrices are given in Table 6.2.

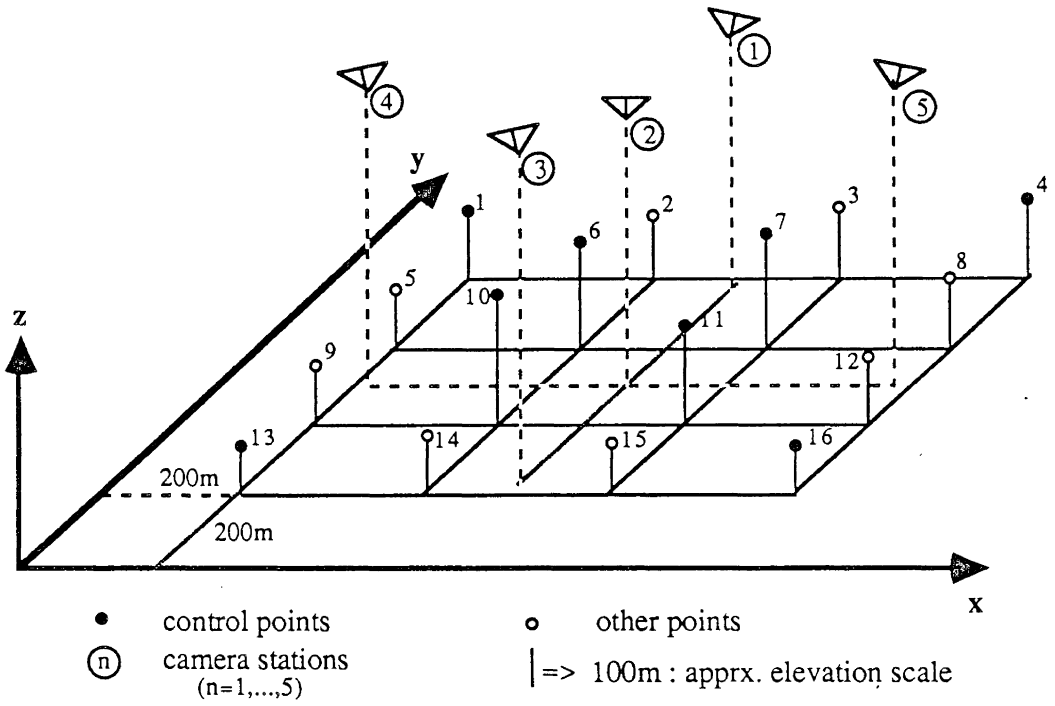

Figure 6.3: Geometric configuration of the simulated test field.

Table 6.2: Actual parameters of the displacement matrices

	Actual Parameters												
T	scale	rotations(deg)			strain			shear					
	s	r_X	r_Y	r_Z	e_Z	e_Y	e_Z	a	b	c	d	e	f
T_1	1.0	0.0	0.0	0.2	1.0	1.0	1.0	0.0	0.0	0.0	0.0	0.0	0.0
T_2	0.998	0.0	0.0	-0.1	1.0	1.0	1.0	0.0	0.0	0.0	0.0	0.0	0.0

These parameters were used to compute the elements of the two matrices **T**. Thus,

$$\mathbf{T}_1 = \begin{bmatrix} 0.99999 & -3.4907E\text{-}07 & 0.0 \\ 3.4907E\text{-}03 & 0.99999 & 0.0 \\ 0.0 & 0.0 & 1.0 \end{bmatrix}$$

and

$$\mathbf{T}_2 = \begin{bmatrix} 0.99800 & 1.7418E\text{-}03 & 0.0 \\ -1.7418E\text{-}03 & 0.99800 & 0.0 \\ 0.0 & 0.0 & 0.99800 \end{bmatrix}$$

Premultiplying the coordinates of points 1, 2, 5, 6, 9, and 10 with matrix $\mathbf{T}_1$ and the coordinates of points 3, 4, 7, 8, 11, 12, 13, 14, 15, and 16 with matrix $\mathbf{T}_2$ the object point coordinates after the displacements are computed. Simulating again a photographic campaign similar to the first epoch, the photo-coordinates of the images of the displaced detail points for the second epoch are generated using the collinearity equations. The exterior orientation elements of the five photographs for this campaign are given in Table 6.3.

Table 6.3: Camera stations - Epoch 2

Photo #	XC(m)	YC(m)	ZC(m)	$w^{(o)}$	$\varphi^{(o)}$	$k^{(o)}$
1	500.0	755.0	630.0	-15.0	0.0	0.0
2	495.0	500.0	605.0	0.0	0.0	0.0
3	505.0	245.0	630.0	15.0	0.0	0.0
4	245.0	495.0	630.0	0.0	-15.0	0.0
5	755.0	500.0	620.0	0.0	15.0	0.0

The two stages of the sequential photogrammetric approach were examined. At the first stage, that is the initial estimation of the

state information, the bundle adjustment program PTBV was tested. It was used to determine the object coordinates of the detail points and their covariances for the zero (first) epoch. The simulated photo-coordinates and the coordinates of the control points were used as observations. The coordinates of the remaining object points were left as free parameters. Approximate values of the elements of exterior orientation for the five camera stations were determined by distorting the simulated values given in Table 6.1 (about ± 5 metres for the position and about ± 0.5 degrees for the orientation parameters). The simulated object coordinates and the parameters of exterior orientation were completely recovered. The statistical information necessary for the evaluation of the photogrammetric adjustment is given in Table 6.4.

Table 6.4: Statistical information of the photogrammetric adjustment - Epoch 1

Residuals	Mean Value	Standard Deviation
photo x (mm)	0.000	$\pm$ 0.001
photo y (mm)	-0.001	$\pm$ 0.003
check-points X(m)	0.001	$\pm$ 0.002
check-points Y(m)	0.000	$\pm$ 0.007
check-points Z(m)	-0.002	$\pm$ 0.004
control-points X(m)	0.000	$\pm$ 0.000
control-points Y(m)	0.000	$\pm$ 0.000
control-points Z(m)	0.000	$\pm$ 0.000
a-posteriori variance factor: 0.645 E-11		
mean value of the standard deviations of the non-control points		
$\bar{\sigma}_X = \pm 6.1$ mm	$\bar{\sigma}_Y = \pm 6.0$ mm	$\bar{\sigma}_Z = \pm 11.0$ mm

The positions and the symmetric elements of the covariance matrices of the points of this initial state were stored in order to define the predicted information required for the second stage of the approach.

The stability of the matrix **N** of the normal equations for the estimation of the camera paameters was expressed by computing its condition number, cond (**N**), where

$$\text{cond}\ (\mathbf{N}) = \frac{\text{maximum singular value of } \mathbf{N}}{\text{minimum singular value of } \mathbf{N}} \qquad (6.1)$$

Without additional parameters, the cond (**N**) equals 1,071,285.999 (≈1.0 E+06). When additional parameters were introduced at the last iteration, then the cond (**N**) became 305,828,284.708 (≈3.0 E+08). The deterioration of the stability of the system shows that the introduction of different additional parameters for each photograph and their weighting must be done very cautiously.

The second stage of the process, that is the sequential estimation of the information, is introduced at this point. The prediction model for the second epoch was generated by distorting the actual parameters of the displacement matrices **T** (Table 6.2), and by forming an artificial uncertainty matrix $\mathbf{Q}_t$ due to these distorted (predicted) parameters. The distorted parameters of the matrices **T** are given in Table 6.5.

Table 6.5: Distorted parameters of the displacement matrices

	Distorted Parameters											
T	scale	rotations(deg)			strain			shear				
	s	r_X	r_Y	r_Z	e_Z	e_Y	e_Z	a	b	c	d	e	f
T_1	1.0	0.0	0.0	0.1	1.0	1.0	0.998	0.0	0.0	0.0	0.0	0.0	0.0
T_2	0.998	0.0	0.0	-0.2	1.0	1.0	1.0	0.0	0.0	0.0	0.0	0.0	0.0

The computed distorted elements of the two matrices are:

$$T_1 = \begin{bmatrix} 1.0 & -1.7453E\text{-}03 & 0.0 \\ 1.7453E\text{-}03 & 1.0 & 0.0 \\ 0.0 & 0.0 & 0.998 \end{bmatrix}$$

and

$$T_2 = \begin{bmatrix} 0.99799 & 3.4837E\text{-}03 & 0.0 \\ -3.4837E\text{-}03 & 0.99799 & 0.0 \\ 0.0 & 0.0 & 0.998 \end{bmatrix}$$

Premultiplying the coordinates of the corresponding points with the distorted matrices T_1 and T_2 respectively, the predicted state information is obtained. The differences in the coordinates between the predicted values generated by the distorted displacement matrices and the values generated by the actual displacement matrices ranged from 0.10m to 1.60m. Thus, these new object points did not correspond to the generated photo-images for epoch 2. The uncertainty of the parameters of the prediction model was intentionaly exaggerated to permit additional freedom to the predicted values. Therefore matrix Q_t was set to be equal to 16I, allowing thus a circular uncertainty of 4m at each point in addition

to the propagated uncertainty from epoch 1.

The program SPDM for the sequential photogrammetric monitoring of displacements was used to estimate the updated object parameters, the updated variance-covariance matrices and to assess the significance of displacements. Again, approximate camera parameters were used. The combination of the photogrammetric measurements with the predicted state information using the extended filtering technique derived in chapter 5 recovered successfully the actual values of the camera parameters and of the detail points. The movements of the points were verified at the 0.95 confidence level using the single and global congruency test on the displacements.

In addition, the bundle adjustment program PTBV was successfully run for epoch two as well. The statistical information from the two adjustment approaches, that is the sequential photogrammetric approach and the single bundle approach is given in Table 6.6.

The comparison and evaluation of the two approaches based on presented and non-presented experiments led to two significant conclusions.

1) When a strong and well-controlled bundle geometry exists, the estimation of the positional parameters is almost identical using the two approaches. This is illustrated in Table 6.6, where the mean values and the standard deviations of the examined residuals, and the a-posteriori variance factors do not significantly differ. On the other hand, the accuracies of the estimated object coordinates have been improved using the sequential photogrammetric approach (smaller values of the elements of the corresponding

covariance matrices). This is shown by the mean values of the standard deviations of the non-control points (Table 6.6).

2) In cases where either poor geometry or insufficient number and/or inappropriate distribution of the control points exist, the sequential photogrammetric approach performed better in both aspects (position and accuracy) than the bundle adjustment. This was anticipated because all the object points act as control with various weights, although of course the updated sequential extended filtering mechanism is applied differently than the updating procedure used in the bundle adjustment.

Table 6.6: Statistical information of two photogrammetric adjustments. (S): SPDM , (P): PTBV

Residuals	Mean Value (S)	Mean Value (P)	Standard Deviation (S)	Standard Deviation (P)
photo x (mm)	0.000	0.000	±0.001	±0.001
photo y (mm)	0.000	0.000	±0.002	±0.002
check-points X(m)	0.001	0.001	±0.004	±0.004
check-points Y(m)	-0.001	-0.001	±0.006	±0.008
check-points Z(m)	0.002	0.002	±0.007	±0.004
control-points X(m)	0.000	0.000	±0.000	±0.000
control-points Y(m)	0.000	0.000	±0.000	±0.000
control-points Z(m)	0.000	0.000	±0.000	±0.000

a-posteriori variance factor
(S): 0.304 E-11 (P): 0.308 E-11

mean value of the standard deviations of the non-control points

(S): $\bar{\sigma}_X$ = ±2.7 mm $\bar{\sigma}_Y$ = ±2.8 mm $\bar{\sigma}_Z$ = ±5.3 mm
(P): $\bar{\sigma}_X$ = ±4.0 mm $\bar{\sigma}_Y$ = ±4.0 mm $\bar{\sigma}_Z$ = ±7.6 mm

This was verified with additional experimental computer runs using program PTBV. Two examples are given here. In the first the relative weight of the control points was w_{g1} = 1.0E-03 while the

relative weight for the other object points used was w_{g2} = 1.0E-06. In the second example the corresponding values were 1.0E-03 and 1.0 E-07. While the estimated location parameters were similar, the accuracies of the object points were better for the first case. The computed condition numbers were cond $(\mathbf{N})_1$ equals 1,007,350.220 (≈1.0 E+6) and cond $(\mathbf{N})_2$ equals 1,032,640.521 (≈1.0 E+6), respectively. The latter leads to the conclusion that the sequential photogrammetric approach reduces the value of the condition number of the coefficient matrix of the normal equations, thus contributing to the improvement of the stability of the system. Two factors support this, namely a) the freedom of movement of the point is restricted within the space of the predicted covariance matrices, and b) the weights which are introduced for all object points for the simultaneous space resection.

This improvement may also provide a more flexible handling of additional parameters, and possibly make it easier to discover outlying photo-observations due to the previously mentioned first factor.

6.2.2 Case 2: Test with real data (close-range photogrammetry)

This test was conducted in a laboratory environment using close-range photogrammetry and real data. The test field model consists of five parts and has the following dimensions: 1.40m x 0.90m x 0.25m. Each part can accomodate different deformations, while several points can be moved individually to provide single point movements. More details about the model and the measuring

procedures can be found in Shi (1985), where this model was initially utilized.

Two photogrammetric observation epochs were used. In the second epoch, single point displacement and subsidence deformation had been introduced in parts of the model. Convergent photography with 100% overlap was taken from the four corners of the test field with a Cannon AE-1 non-metric (35mm) camera. A standard lens (f = 50mm) was used and the approximate photo-scale was equal to 1:45. The location of the object points and the camera stations are shown in Fig.6.4.

The photo-coordinates of the image points from the eight photographs had been measured on the precision analogue stereo-plotter Wild A-10 because a precision comparator was unavailable at the time of measurements. Two sets of measurements from both epochs were performed, resulting in an average accuracy for both x and y photo-coordinates of about $\pm$12μm. The accuracy of the object coordinates measured by geodetic means was $\pm$1–2mm.

The bundle adjustment program PTBV with additional parameters was utilized to estimate the necessary information of the initial stage (epoch 1). As a check, the bundle adjustment program GEBAT-V (El-Hakim, 1982) was run as well. The total number of object points was 45, of which 9 points were used as control- and 3 as check points. The necessary statistical information from both programs is given in Table 6.7.

It is very interesting to notice in Table 6.7 that the program GEBAT-V results in obviously smaller mean values of the standard deviaton of all non-control points than the ones obtained from the

program PTBV. This was observed in the two examples with the real data. From Table 6.7 we can also notice that the results of the residual values from program PTBV are slightly smaller than the ones from GEBAT-V.

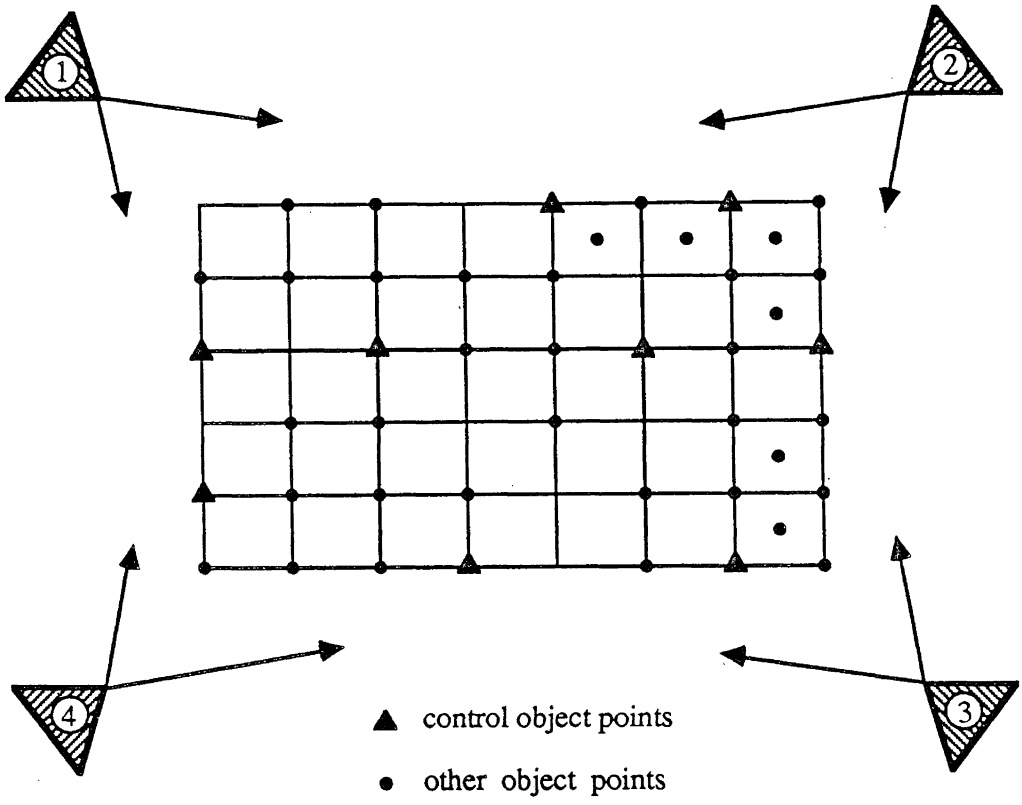

Figure 6.4: Plan diagram (not to scale) of the object-camera configuration of the laboratory model.

One of the major factors affecting the absolute variance-covariance matrix of the object points is the scale factor by which the weight cofactor matrix of the object coordinates is multiplied. The scale factor is the a-posteriori variance factor $\hat{\sigma}_o^2$ (equs. (5.104) and (5.105)). Unmodelled or uncompensated sytematic errors increase the value of the estimate $\hat{\sigma}_o^2$ which renders higher values

to the variance-covariance matrix of the object coordinates. It is the author's understanding that the estimate $\hat{\sigma}_o^2$ from GEBAT-V is not computed as in equ. (5.104), but is based on the quality of the image coordinates only (El-Hakim, 1981). In addition, the average standard deviations of the position parameters for the four camera stations computed by GEBAT-V were $\bar{\sigma}_{XC} = \pm 3.50$mm, $\bar{\sigma}_{YC} = \pm 3.75$mm, $\bar{\sigma}_{ZC} = \pm 4.00$mm, which can be used as indicative information of the absolute accuracy. An international test showed also that absolute accuracies may differ by a factor varying between 2 and 10 (Förstner, 1984). Therefore, this report (ibid) recommends that further investigation about the absolute accuracy is necessary through measures of external reliability.

Table 6.7: Statistical information of photogrammetric adjustments
Epoch 1, Case 2

Residuals	Mean Value (PTBV)	Mean Value (GEBATV)	Standard Deviation (PTBV)	Standard Deviation (GEBATV)
photo x (mm)	0.000	-	±0.013	±0.016
photo y (mm)	-0.001	-	±0.013	±0.018
check-points X(m)	0.002	0.014	±0.008	±0.016
check-points Y(m)	-0.002	0.005	±0.001	±0.006
check-points Z(m)	0.001	-0.010	±0.007	±0.012
control-points X(m)	0.000	0.011	±0.003	±0.004
control-points Y(m)	0.000	0.009	±0.002	±0.002
control-points Z(m)	0.000	0.010	±0.004	±0.002

a-posteriori variance factor
(PTBV): 0.405 E-09 (GEBATV): -

mean value of the standard deviations of the non-control points

(PTBV): $\bar{\sigma}_X = \pm 1.1$ mm $\bar{\sigma}_Y = \pm 1.2$ mm $\bar{\sigma}_Z = \pm 1.7$ mm
(GEBATV): $\bar{\sigma}_X = \pm 0.3$ mm $\bar{\sigma}_Y = \pm 0.3$ mm $\bar{\sigma}_Z = \pm 0.5$ mm

Due to the lack of a systematic and controlled mechanism causing the displacements it was extremely difficult to predict the positions and accuracies of the object points. The available information was that some of the displacements had values slightly over 1cm. Two alternatives then were examined. For both of them the displacement matrix **T** was considered to be equal to the unit matrix. In the first alternative, the object coordinates of the first epoch were assumed to be the predicted values with the uncertainty matrix **Q** equal to 2.25E-04**I**. However, during the execution of the sequential estimation process (program SPDM) problems of divergency occured at the step of simultaneous space resection. This was attributed to the fact that a 1cm displacement in the object space causes approximately 200μm image displacements in the photo space due to the large photo scale of 1:45. It was then impossible for the bundle adjustment part of the program SPDM to handle such a large image error or in other words such poor approximate values.

In the second alternative, approximate object coordinates with their accuracies were determined using PTBV without incorporating the additional parameters. These values played the role of the predicted information for the sequential photogrammetric approach (program SPDM). A large uncertainty matrix **Q** was set, i.e., **Q** was equal to 0.0225**I**. Besides program SPDM, programs PTBV and GEBAT-V were used to provide additional measures of comparison. The statistical results from the three approaches for epoch 2 are given in Table 6.8.

Table 6.8: Statistical information of photogrammetric adjustments
Epoch 2, Case 2

Residuals	Mean Value (SPDM)	(PTBV)	(GEBATV)	Standard Deviation (SPDM)	(PTBV)	(GEBATV)
photo x (mm)	-0.001	0.000	-	±0.010	±0.007	±0.014
photo y (mm)	-0.002	0.000	-	±0.012	±0.010	±0.015
check-points X(m)	0.000	0.000	-0.002	±0.002	±0.002	±0.003
check-points Y(m)	0.001	0.001	-0.002	±0.002	±0.002	±0.003
check-points Z(m)	0.002	0.002	0.000	±0.009	±0.009	±0.008
control-points X(m)	0.000	0.000	-0.002	±0.001	±0.001	±0.001
control-points Y(m)	0.000	0.000	-0.002	±0.001	±0.001	±0.001
control-points Z(m)	0.000	0.000	-0.002	±0.003	±0.004	±0.002

a-posteriori variance factor
(SPDM): 0.181E-09 (PTBV): 0.191E-09 (GEBATV):

mean value of the standard deviations of the non-control points

(SPDM): $\overline{\sigma}_X = \pm 0.3$ mm $\overline{\sigma}_Y = \pm 0.3$ mm $\overline{\sigma}_Z = \pm 0.4$ mm
(PTBV): $\overline{\sigma}_X = \pm 0.8$ mm $\overline{\sigma}_Y = \pm 0.8$ mm $\overline{\sigma}_Z = \pm 1.2$ mm
(GEBATV): $\overline{\sigma}_X = \pm 0.3$ mm $\overline{\sigma}_Y = \pm 0.3$ mm $\overline{\sigma}_Z = \pm 0.3$ mm

Again, it should be pointed out that the values provided by GEBAT-V are smaller than the ones from PTBV. GEBAT-V's output listing shows that the average of the standard deviations of the position parameters from the four camera stations were $\overline{\sigma}_{XC} = \pm 2.6$mm, $\overline{\sigma}_{YC} = \pm 2.8$mm, $\overline{\sigma}_{ZC} = \pm 3.4$mm. These values can provide an indication of the actual accuracy.

Finally, the differences in displacements between geodetic results and photogrammetric ones (SPDM) were compared at 16 points. The average differences were:

$\overline{\delta X} = -0.4$mm, $\overline{\delta Y} = 0.1$mm, $\overline{\delta Z} = -0.9$mm

The application of the sequential photogrammetric approach for monitoring displacements in a real case photogrammetric laboratory project demonstrated that both programs PTBV and SPDM performed

successfully. As in the example with simulated data the method proposed in this study showed a significant improvement in accuracy of the object coordinates (Table 6.8), while at the same time under strong bundle geometry (4 bundle rays per point at good angles of intersection) the estimated coordinates are almost identical with the ones from the independent bundle adjustment.

The independent comparison with the geodetic results showed submillimetre overall discrepancies. Consequently, this approach can be used for such types of experiments, where high accuracies are required, and the estimation of the point coordinates by non-photogrammetric methods can be a tedious and time-consuming operation.

6.2.3 Case 3: Test with real data (aerial photogrammetry)

The final test was performed using a practical case involving aerial photography. The area and the information related to the data acquisition phase have already been described in section 6.1.2 where the quality of the measured photo-coordinates was evaluated.

This case is a classical example of a practical situation, where we were faced with two significant weaknesses. The first is related to the photo-coverage of the area. Only two aerial photographs with 60% overlap were available for each epoch, thus resulting in the determination of the object points from only two intersecting rays. The second problem is associated with the distribution and accuracy of the control points. A cluster of control points was available at the peak of the mountain slope and

only one point was available at the foot of the mountain. This configuration provides a very poor geometry for a bundle adjustment solution. Therefore, densification was attempted using the independent model adjustment program PAT-M43 (Ackermann et al., 1973) because its mathematical model is less susceptible to "weak" geometry. The models were formed analytically from the image coordinates. One additional control point could then be utilized near the bottom of the mountain slope. Finally, the accuracy of the reference points was not completely known (between 10 and 20 cm approximately). For the bundle adjustment solutions five full control points and four check points were used. (Fig. 6.5).

The two stages of the sequential photogrammetric approach were applied and examined. For the initial (epoch 1) estimation of the position and accuracy of the detail points the program PTBV was used. Program GEBAT-V was also utilized . The results from the two bundle adjustment programs are shown in Table 6.9.

While the performance of PTBV at the check points is slightly better than that of GEBAT-V, the latter provides slightly smaller photo-residuals and significantly better absolute accuracy. However, the standard deviations may be considered as optimistic because the standard deviations of the camera position parameters alone amounted to:

For photo 1: $\overline{\sigma}_{XC} = \pm 0.087$m, $\overline{\sigma}_{YC} = \pm 0.097$m, $\overline{\sigma}_{ZC} = \pm 0.227$m

For photo 2: $\overline{\sigma}_{XC} = \pm 0.078$m, $\overline{\sigma}_{YC} = \pm 0.130$m, $\overline{\sigma}_{ZC} = \pm 0.269$m

This appears to confirm that different scale factors are applied to obtain the absolute accuracy of the object points from the relative variance-covariance matrix.

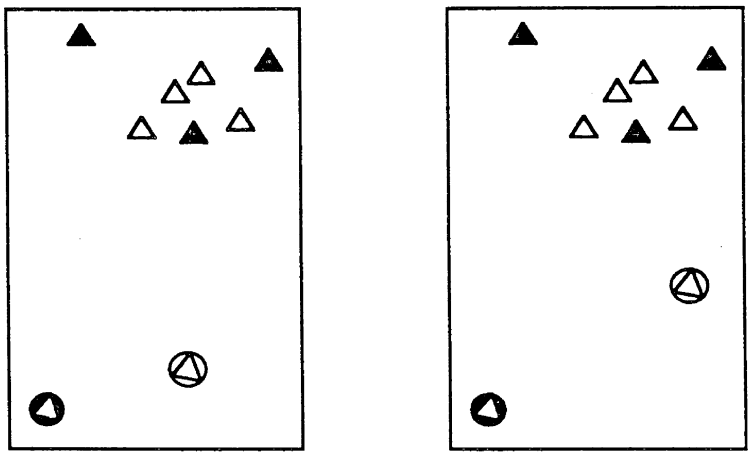

Figure 6.5: Configuration of the control and check points in the overlapping area (not to scale).

The position and the accuracy of the points were stored in order to predict the corresponding information from the next observation campaign. Due to underground mining operations, the deformation model of the mountain slope was not exactly known. However, movements of approximately 1m to 1.5m had been predicted for some areas based on certain subsidence theories. Therefore, the displacement matrix **T** was set equal to the unit matrix, while the uncertainty matrix **Q** was set equal to 3.0I. Thus, the predicted

coordinates and their predicted accuracies were computed for the second photogrammetric campaign.

Table 6.9: Statistical information of photogrammetric adjustments
Epoch 1, Case 3

Residuals	Mean Value (PTBV)	Mean Value (GEBATV)	Standard Deviation (PTBV)	Standard Deviation (GEBATV)
photo x (mm)	0.000	-	±0.006	±0.002
photo y (mm)	0.000	-	±0.007	±0.004
check-points X(m)	-0.021	-0.084	±0.096	±0.115
check-points Y(m)	0.028	-0.078	±0.088	±0.112
check-points Z(m)	-0.093	-0.136	±0.067	±0.194
control-points X(m)	0.000	0.062	±0.048	±0.055
control-points Y(m)	0.000	-0.034	±0.043	±0.017
control-points Z(m)	0.000	-0.024	±0.015	±0.017
a-posteriori variance factor (PTBV): 0.199 E-09		(GEBATV): -		
mean value of the standard deviations of the non-control points				
(PTBV):	$\bar{\sigma}_X$ = ±0.089mm	$\bar{\sigma}_Y$ = ±0.086mm	$\bar{\sigma}_Z$ = ±0.197mm	
(GEBATV):	$\bar{\sigma}_X$ = ±0.017mm	$\bar{\sigma}_Y$ = ±0.013mm	$\bar{\sigma}_Z$ = ±0.043mm	

The quality of the photo-coordinates in this second epoch was not as good as in epoch 1 because premarked photo-points were involved (section 6.1.2). The photogrammetric sequential state estimation was performed with the program SPDM, while the bundle adjustment programs PTBV and GEBAT-V were used as well. The statistical results of the three photogrammetric approaches are given in Table 6.10.

Again GEBAT-V shows the best absolute accuracy. However, the standard deviations of the camera position parameters computed by this program were:

For photo 1: $\overline{\sigma}_{XC} = \pm 0.188m$, $\overline{\sigma}_{YC} = \pm 0.151m$, $\overline{\sigma}_{ZC} = \pm 0.422m$

For photo 2: $\overline{\sigma}_{XC} = \pm 0.192m$, $\overline{\sigma}_{YC} = \pm 0.195m$, $\overline{\sigma}_{ZC} = \pm 0.484m$

The large discrepancies at the check points are attributed to the poor quality of the provided ground control coordinates. For example, there is an apparent systematic shift in the X-direction, while the differences in the Z-direction show large dispersion.

Table 6.10: Statistical information of photogrammetric adjustments
Epoch 2, Case 3

Residuals	Mean Value (SPDM)	(PTBV)	(GEBATV)	Standard Deviation (SPDM)	(PTBV)	(GEBATV)
photo x (mm)	-0.002	0.000	-	±0.006	±0.006	±0.004
photo y (mm)	0.001	0.000	-	±0.013	±0.008	±0.006
check-points X(m)	0.281	0.215	0.167	±0.141	±0.095	±0.174
check-points Y(m)	0.069	0.044	-0.041	±0.055	±0.049	±0.074
check-points Z(m)	0.010	-0.010	-0.149	±0.277	±0.290	±0.301
control-points X(m)	-0.008	-0.008	0.000	±0.141	±0.140	±0.000
control-points Y(m)	-0.005	-0.005	0.000	±0.073	±0.073	±0.000
control-points Z(m)	0.000	0.000	0.000	±0.009	±0.009	±0.000

a-posteriori variance factor
(SPDM): 0.138E-09 (PTBV): 0.263E-09 (GEBATV): -

mean value of the standard deviations of the non-control points

(SPDM):	$\overline{\sigma}_X = \pm 0.049m$	$\overline{\sigma}_Y = \pm 0.047m$	$\overline{\sigma}_Z = \pm 0.102m$
(PTBV):	$\overline{\sigma}_X = \pm 0.118m$	$\overline{\sigma}_Y = \pm 0.120m$	$\overline{\sigma}_Z = \pm 0.231m$
(GEBATV):	$\overline{\sigma}_X = \pm 0.025m$	$\overline{\sigma}_Y = \pm 0.025m$	$\overline{\sigma}_Z = \pm 0.082m$

Comparing now the combined sequential photogrammetric approach (SPDM) with the single bundle approach (PTBV) the following can be observed for this particular case from Table 6.10:

a) Due to constraints imposed on the amount of movements of the object points, the mean values of the photo-residuals for SPDM are not zero. This small deviation (1 to 2μm) is attributed to

the existence of outlying observations. (cf. with section 6.1.2) under the condition that most systematic errors have been compensated. For the same reason and because of the use of only two overlapping photographs, the standard deviation of the photo-residuals in the Y-direction are larger for program SPDM, as anticipated.

b) The combined sequential photogrammetric approach led again to better absolute accuracies. For this example the improvement was more than 50% with respect to the corresponding accuracy resulting from the single bundle approach.

c) The differences between the absolute coordinate values were in the range of 2 to 8 cm. Only three points showed differences in elevation of about 20cm but it was found that they also had a lower absolute accuracy than the other points.

Despite the fact that certain requirements were not fulfilled, the third example confirmed the potential of the combined sequential photogrammetric procedure for monitoring displacements. As in the previous two examples, significant improvement of the absolute accuracy is achieved. The coordinate differences observed are due to weak bundle geometry and the distribution and quality of the reference points. The preservation of position elements with simultaneous enhancement of the accuracy measures suggests that the proposed approach can be an attractive alternative and a useful tool in photogrammetric research on monitoring methods and techniques.

7. CONCLUSIONS AND RECOMMENDATIONS

7.1 Final Remarks and Conclusions

Monitoring movements of natural or man-made environments over time is one of the most important contributions of the surveying engineering profession to society.

Usually, a deformable body is depicted by a number of detail points through a representation process. Multiple observation campaigns monitor the movements of these points. The displacements of the detail points provide the information on the deformation of the body through a generalization process.

This study has focused on the geometry represented by the position of the detail points with respect to a reference system over time. Although displacements can be expressed as coordinate differences, it was found that the simplest motion theorem (rotation and scale change of the position vector) expressed by the displacement matrix **T**, offers certain advantages. It provides direct information about the deformity and the attitude of the position vector, and it can group together areas of the deformable body with similar deformation characteristics. The displacement vector can be directly determined from the actual displacement

matrix **D** and the initial position vector, if the deformation properties of the body are known.

The displacement matrix **T** has been derived through a series of affine transformations, which represent the possible movements of the position vector in space. The relationship between the displacement matrix and the parameters of the simplest path theorem has been proven. This also establishes the interrelation of displacement and deformation. The analysis of the geometric behaviour of the position vector was necessary because the functional relationship of the detail points between different time epochs is based on it.

Photogrammetry has been selected as the geometric monitoring method in this study. Its advantages and its applications to date show that under certain circumstances photogrammetry provides the only feasible solution for determining displacements.

Extensive analysis has been performed on the factors affecting the significance of displacement. It is very crucial to know that the detected movements are due to deformation causes and not a result of instability of the datum, inaccuracies and/or blunders in the observations, and poor reliability and sensitivity of the photogrammetric network. The optimization of the photogrammetric networks has been examined with respect to accuracy (precision, fidelity, reliability), testability and economy. The proper design of a monitoring network, considering the peculiarity of the photogrammetric factors, renders the results to be within preset specifications.

Various photogrammetric approaches were examined, and areas

where further research was needed were identified. The research in this study concentrated on:

a) improving the conditions of mensuration for photo-coordinates with simultaneous enhancement of their quality because the measuring phase is the most laborious, time-consuming and critical part of any photogrammetric system;

b) incorporating additional external information about the object into the photogrammetric observation model aiming towards a combined functional model which would provide better positional and accuracy information.

Various photogrammetric measuring systems were examined. With respect to versatility, accuracy, mathematical rigour, speed of execution, and convenience there is no doubt that the closed-loop on-line photogrammetric systems are most suitable. The analytical photogrammetric stereo-plotter belongs in this category. Fortunately, the Department of Surveying Engineering at the University of New Brunswick has one, the OMI AP-2C, interfaced with a DEC PDP 11/60 as control computer.

For the development of the measuring system proposed in this study, several existing settings for the operations of the analytical plotter had to be examined and redesigned. The existing process of interior orientation was only a procedure of centering, thus ignoring the non-alignment (or kappa rotation) between the fiducial (or photo) axes and the stage axes. That is, the origin of the stage system was placed at the fiducial centre. As a result, the real-time program computes stage coordinates instead of photo-coordinates. It is then impossible to relocate photo-points using

the computer-controlled capabilities of the analytical plotter if a photograph has been removed from the photo-carrier and reset again. An affine transformation has been utilized to transfer coordinates from the stage- to photo-coordinate systems and vice-versa. Another aspect considered was the location of the origin of the model (machine) coordinate system. The existing setup has the origin located in the model space. For this particular study the origin was shifted to the perspective center of the stationary photograph to facilitate the operations.

The proposed on-line semi-automatic photogrammetric measuring system consists of two branches. The first one handles photo-measurements of signalized points. The developed system works as an on-line mono-comparator. The measuring process has been automated to a great extent by driving the measuring mark to predetermined image locations. These locations are computed either from digitized table coordinates of the photo-points or from approximate object coordinates. On-line editing capabilities are available during the measuring process.

For natural points, photo-measurements are more complex. Thus, the second branch represents an integrated "cross-identification" and measuring procedure, that has been designed and implemented. It is based on the fact that the location of a point on multi-temporal photographs needs to be independent of external reference systems. This analytical method utilizes "real" and "pseudo" photogrammetric models which depend on the relative positions of the photographs at the same or at different time epochs respectively. The formation of "pseudo" models provides a means for point selection, measurement,

and storage of photo-coordinates of the detail points for one photograph of each epoch. The corresponding coordinates on photographs of the same epoch are then determined by restituting the "real" photogrammetric models and using the iterative positioning process developed for this purpose. On-line editing capabilites are available to the user at certain stages of the process.

The measuring system and the quality of the measured coordinates have been tested and evaluated with the aid of specifically developed software. The results of these tests are summarized here. The high degree of automation introduced into the photogrammetric mensuration phases has significantly improved productivity and has increased the speed of execution. The approach provides flexibility by offering certain options and on-line editing capabilities. It reduces the operator's inconvenience and offers man-machine interaction allowing continuous control and insight into the measuring process. Moreover, the quality of the measured photo-coordinates remains high for the targetted points and has been significantly improved in the case of natural points because the photo-coordinates themselves establish directly the point location. The latter is evident from the residuals of the observations and from the estimated a-posteriori variance factors which are smaller for the photo-pair without marked points. The smaller standard deviation of the residual parallaxes in the model space for the same stereo-pair demonstrates better consistency of the photo-measurements. Finally, the values of the absolute standardized residuals for the unmarked stereo-pair are much smaller than the ones from the other stereo-pair containing marked points, and

consequently smaller than the critical value. Therefore, the observations are less susceptible to blunders.

The other major aspect which has been investigated in this research was the possibility of extending the single-epoch static photogrammetric observation model. The proposed sequential photogrammetric approach over time combines both prediction and geometric (photogrammetric) methods which so far have been used separately and independently. The development of combined sequential processing of photogrammetric and object observations has been based on the principles of sequential least squares. The philosophy of dynamic filtering from the optimal estimation theory offered a better insight into the perception of the problem. The merging of the additional object information was possible with a more generalized view of the least squares problem. Thus, all the variables involved in the mathematical formulation are considered as observations with the unknown parameters becoming "pseudo" observations. The parameter vector changes not only as new observations become available but also over time.

The author's philosophy was that each observation model involved must maintain its individuality. Thus the mathematical model consists of two component models: the photogrammetric and the prediction model. The photogrammetric model comprises three observation equations with their relevant weight matrices: the extended collinearity equations, the elements of interior orientation, and the coordinates of the control points. The prediction model is composed of the prediction equation that maps the object coordinates of epoch (t) onto epoch (t+1) with the

displacement matrix **T**, and the predicted variance-covariance matrix of the predicted coordinates. For practical, numerical and computational reasons the prediction model was limited to the object points, although three alternative solutions were examined.

The recursive formulae of the combined mathematical model have been derived. Attention has been paid to the linearization process, where linearization is applied each time about the most recent estimate. The updated sequential formulae are of the iterated extended form meaning that iterative linearization occurs also within the correction term due to new observations. This improves the results and is very useful for highly non-linear systems.

Problems related to the divergence of the algorithm have been discussed along with some remedies. The consideration of computational limitations led to the final forms of the updated estimated parameter vector and the updated covariance matrix. These formulae are the backbone of the sequential estimation of the state information over time. The necessary information for the initial estimation of the state estimation is obtained through the single photogrammetric model. Details of its derivation and of algorithmic and computational procedures have been extensively discussed in this study.

Appropriate software has been developed to implement the proposed methodology. This software made it possible to test the combined sequential photogrammetric approach for monitoring displacements in three examples. Simulated data were used in the first example, while the other two were cases of close-range and aerial photogrammetric applications with real data. From these

limited applications the following conclusions were drawn with respect to the proposed approach:

1) The redundant information about the object space which is included in the combined sequential photogrammetric approach contributes to the partial or complete removal of datum deficiency and/or configuration defects, and also to accuracy improvements.
2) The estimated positional parameters (orientations of the photographs and object coordinates) are almost identical between the single bundle adjustment and the combined sequential photogrammetric approach when a strong and well-controlled bundle geometry exists. The differences are more apparent in the estimated elements of interior orientation due to imposition of different types of constraints.
3) The estimated positional parameters tend to be different for the two approaches in cases of weak bundle geometry and poor datum definition. If the predicted information (object coordinates and their accuracies) is reliable, then the combined sequential photogrammetric process provides better absolute results.
4) The use of the combined sequential photogrammetric approach showed a significant improvement (up to 50%) in the absolute accuracy of the object coordinates compared to the single bundle adjustment.
5) The combination of the photogrammetric and prediction approaches contributes to a better estimation of position and accuracy, since each method plays the role of a safeguard and complements the other. How powerful this role is, depends of course on the

uncertainties in the deterministic and stochastic parts of each model.

6) Finally, the combined sequential photogrammetric process together with the on-line measuring scheme can enhance the contribution of photogrammetry to deformation studies.

7.2 Recommendations

Naturally, a solution to a problem creates new questions. The findings of this research are not an exception. The complexity of the problem of deformation surveys definitely requires interdisciplinary cooperation and knowledge. For example, this will result in a more accurate definition of the displacement matrix **T** and also will increase the reliability of the determined displacements through the appropriate interpretations.

There is no doubt that the ultimate goal of the measuring system is complete automation. This requires special equipment and the recently introduced digital image technology for pattern-target recognition. However, the existing system as it stands can also be improved. The measurements of physical points on multi-temporal photographs are based on one "pseudo" and two "real" photogrammetric models. Extension to a multi-model system will be definitely useful for future applications. While the theoretical aspects will remain as derived in this study, the present software has to undergo minor modifications. Also, more editing freedom should be offered during the measurements of "real" models.

Although positive results were obtained on a practical project,

further tests involving a controlled deformable body are desirable to investigate thoroughly the measuring accuracies of the natural points.

The measuring system for targetted points can support photo-measurements of characteristic natural point features (e.g., road intersections, corners of buildings) from small scale photography.

The characteristic capability of the <STEREO> mode to automatically relocate photo-points and lock on them utilizing the iterative positioning routine can find applications in data collection for aerotriangulation projects. Minor changes have to be made to the software design since only the common pass points between models need to be automatically relocated during strip development, but not all the measured points. It should be mentioned here that part of the <STEREO> mode functions as an on-line stereo-comparator.

The software can be improved with additional safeguards to protect the user from wrong entries and abnormal exits.

The derivation of the combined sequential photogrammetric approach was entirely built on the concept that there is no correlation between the two sets of measurements. This provided the block diagonal form of the combined weight matrix and made possible the derivation of the recursive sequential formulae and algorithms. However, further investigation is needed to either verify or reject this assumption. If the latter is the case, then the effect of the correlations on the formulae and algorithms should be investigated. Whatever the case, further numerical and computational considerations can improve the existing software.

The scaling of covariance (or weight) matrices still needs further investigation. In particular, the operations where the absolute predicted covariance matrix of the object points has to be rescaled in order to be consistent with the relative weight matrices. Erroneous scaling will affect both the solution and the accuracy. The expression $(\mathbf{C}_1^{-1} + \mathbf{A}_2^T \mathbf{P}_2 \mathbf{A}_2)^{-1}$ can cause significant problems due to loss of numerical rigour. The estimation of variance components of the heterogeneous data may provide an answer.

The interaction between the predicted accuracies of the object points and their accuracies from the photogrammetric determination must also be investigated.

Problems with divergence of the algorithms can be partially controlled by fixing the control points. Such an option is provided in the software.

The proposed method is applied in two steps: initial estimation and sequential estimation of the state information. The feasibility of combining them into a simultaneous process should be investigated.

The derived recursive algorithms and procedures can find applications in the rapidly growing field of real-time photogrammetry. Attention should be paid to the computer memory and accuracy requirements. For example the gain matrix $\mathbf{G}$ can be computed off-line and stored in a computer if the mean position parameter $\overline{\mathbf{x}}(t)$ where the linearization occurs, is known a-priori (case of losing the iterated extended property of the algorithm).

This research has dealt with absolute photogrammetric monitoring networks. Perhaps the method suggested in section 2.6

with reweighting the reference points can offer a practical alternative for relative networks.

Finally, the photogrammetric model must be formulated according to the contemporary trends of the photogrammetric science, art, and technology.

REFERENCES

Abbreviations:

ACSM: American Congress of Surveying and Mapping
ASME: American Society of Mechanical Engineers
ASP(RS): American Society of Photogrammetry (and Remote Sensing)
CIS(M): Canadian Institute of Surveying (and Mapping)
FIG: Federation Internationale des Geometres
IAG: International Association of Geodesy
IAP(RS): International Archives of Photogrammetry (and Remote Sensing)
IEEE: Institute of Electrical and Electronic Engineers
ISP(RS): International Society for Photogrammetry (and Remote Sensing)
PEDS: Precise Engineering and Deformation Surveys
PE(&RS): Photogrammetric Engineering (and Remote Sensing)
SIAM: Society for Industrial and Applied Mathematics

Ackermann, F., H. Ebner, H. Klein (1973). "Block Triangulation with Independent Models", PE, Vol. 39, pp. 967-981.

Anton, H. (1984). "Elementary Linear Algebra", John Wiley & Sons, Ltd. New York. 403 pp.

Armenakis, C. (1983). "Subsidence Determination by Aerial Photogrammetry", Technical Report No. 93, Dept. of Surveying Engineering, Univ. of New Brunswick, Fredericton, N.B., Canada, 104 pp.

Armenakis, C. (1984). "Deformation Measurements from Aerial Photographs", IAP(RS), Vol. XXV, Part A5, Com. V, Rio de Janeiro, Brazil, pp. 39-48.

Baarda, W. (1968). "A Testing Procedure for Use in Geodetic Networks", Netherlands Geodetic Commission, Publications on Geodesy, Vol. 2, No. 5, Delft, Netherlands.

Barnett, B., T. Lewis (1984). "Outliers in Statistical Data", John Wiley & Sons Ltd., New York, 463 pp.

Beckman, R.J., R.D. Cook (1983). "Outlier....s", Technometrics, Vol. 25, No. 2, May, pp. 119-163.

Beggs, J.S. (1983). "Kinematics", Hemisphere Publishing Corporation, Washington, 223 pp.

Bernini, F., M. Cunietti, R. Galetto (1968). "A Photogrammetric Method for Assessing the Displacements under Stress of Large Structure Models - Experimental Application", Bulletino di Geodesia e Scienze Affini, Anno XXVII, No. 3.

Blaha, G. (1982). "Free Networks: Minimum Norm Solution as Obtained by the Inner Adjustment Constraint Method", Bulletin Geodesique, Vol. 56, pp. 209-219.

Borutta, H., J. Peipe (1986). "Deformation Analysis of Three-Dimensional Photogrammetric Point Fields", IAP(RS), Vol. 26, Part 5, Com. V, Ottawa, Canada, pp. 165-175.

Brandenberger, A.J., M.T. Erez (1972). "Photogrammetric Determination of Displacement and Deformations in Large Engineering Structures", The Canadian Surveyor, Vol. 26, No. 2, pp. 163-169.

Brandenberger, A.J., S.K. Ghosh, M. Bougouss (1983). "Deformation Measurements of Power Dams with Aerial Photogrammetry", PE&RS, Vol. 49, No. 11, November, pp. 1561-1567.

Brown, D.C. (1969). "Advanced Methods for the Calibration of Metric Cameras", ASP Symposium on Computational Photogrammetry, Syracuse University.

Brown, D.C. (1973). "Accuracies of Analytical Triangulation in Applications to Cadastral Surveying", Journal of Surveying and Mapping, ACSM, Vol. 33, No. 3, September, pp. 281-302.

Brown, D.C. (1980). "Application of Close-Range Photogrammetry to Measurements of Structures in Orbit", Geodetic Services Incorporated Technical Report, Vol. 1, 131 pp.

Brown, D.C. (1984). "Tools of the Trade", State-of-the-Art in Close Range Photogrammetry and Surveying, Workshop Handbook, Vol. 1, ASP-ACSM Fall Convention, San Antonio, TX, USA, pp. 1-157.

Chen, Y.Q. (1983). "Analysis of Deformation Surveys - A Generalized Method", Technical Report No. 94, Dept. of Surveying Engineering, Univ. of New Brunswick, Fredericton, N.B., Canada, 262 pp.

Christensen, J.R. (1980). "Observation of Displacements of a Bridge Loaded to Failure, Using Analytical Photogrammetry", IAP, Vol. XXIII, Part B5, Com. V, Hamburg, W. Germany, pp. 129-136.

Chrzanowski, A. (1981). "Engineering Surveys - Part I, Collection of Selected Papers and Hand-outs", Dept. of Surveying Engineering, Univ. of New Brunswick, Fredericton, N.B., Canada.

Chrzanowski, A. (with the contributions by members of FIG ad hoc committee on the Analysis of Deformation Surveys) (1981). "A Comparison of Different Approaches into the Analysis of Deformation Measurements", Proc. of FIG XVI Inter. Congress, Montreux, Switzerland, Paper No. 602.3.

Chrzanowski, A., W. Faig, M.Y. Fisekci, B. Kurz (1982). "Telemetric Monitoring of Ground Subsidence over a Hydraulic Mining Operation in the Canadian Rocky Mountains", Inter. Symposium for Mine Surveying, Vol. 3, September, Varna, Bulgaria.

Cooper, M.A.R., M.R. Shortis (1978). "Photogrammetric Measurements of Small Components for Motor Vehicles", Proc. of the Inter-Congress Symposium: Photogrammetry for Industry, Com. V, Stockholm, Sweden, pp. 69-71.

Cooper, M.A.R. (1984). "Deformation Measurement by Photogrammetry". Photogrammetric Record, Vol. 11, No. 63, pp. 291-301.

Cooper, M.A.R., N.E. Lindsey, D.M. Stirling (1984). "Monitoring the Three Dimensional Movement of a Large Stone Structure", IAP(RS), Vol. XXV, Part A5, Com. V, Rio de Janeiro, Brazil, pp. 214-222.

Crossfield, J.K. (1979). "Ground Settlement Monitoring by Digital Photogrammetry", Proc. of ASP 45th Annual Convention, Washington, D.C., USA, Vol. 2, pp. 600-606.

Dauphin, E., K. Torlegard (1977). "Displacement and Deformation Measurements over Longer Periods of Time", Photogrammetria, 33: pp. 225-239.

Derenyi, E., L. Newton (1987). "Control Extension Utilizing Large Format Camera Photography", PE&RS, Vol. 53, No. 5, pp. 495-499.

Dorrer, E. (1981). "Real Time Orientation and Integral Part of On-line Analytical Aerial Triangulation", Photogrammetria, Vol.36, pp. 111-118.

Dorrer, E. (1986). "Operational Aspects of On-Line Phototriangulation", Photogrammetria, Vol. 40, pp. 257-298.

Dowideit, B.R. (1980). "An On-line Bundle Block Adjustment for Analytical Plotter", IAP, Vol. XXIII, B3, Com. III, pp. 168-177.

Dowman, I.J. (1977). "Developments in On-Line Techniques for Photogrammetry and Digital Mapping", Photogrammetric Record, 9 (49), pp. 41-54.

El-Hakim, S.F. (1979). "Potentials and Limitations of Photogrammetry for Precision Surveying", Technical Report No. 63, Dept. of Surveying Engineering, Univ. of New Brunswick, Fredericton, N.B., Canada, 168 pp.

El-Hakim, S.F. (1981). "An Evaluation of the Different Criteria to Express Photogrammetric Accuracy", Proc. of the ASP Fall Technical Meeting, September, San Francisco, CA, USA, pp.292-298.

El-Hakim, S.F. (1982). "The General Bundle Adjustment Triangulation (GEBAT) System - Theory and Applications", Photogrammetric Research, Division of Physics, National Research Council, Ottawa, Canada, 47 pp.

El-Hakim, S.F. (1985). "Photogrammetric Measurement of Microwave Antennae", PE&RS, Vol. 51, No. 10, pp. 1577-1581.

Erlandson, J.P., S.A. Veress (1975). "Monitoring Deformations of Structures", PE&RS, Vol. 41, No. 11, pp. 1375-1384.

Fadeeva, V.N. (1959). "Computational Methods of Linear Algebra", Dover Publications Inc., 252 pp.

Faig, W. (1965). "Photogrammetry Applied to Arctic Glacier Surveys", M.Sc.E. Thesis, Dept. of Surveying Engineering, Univ. of New Brunswick, Fredericton, N.B., Canada.

Faig, W. (1978). "The Utilization of Photogrammetry in the Determination of Deformations of Structural Parts in the Ship Building Industry", Proc. of the II Inter. Symposium of Deformation Measurements by Geodetic Methods, Bonn, Germany, Edited by Konrad Wittwer, 1981, Stuttgart, pp. 218-223.

Faig, W. (1980). "Precision Photogrammetry for Industrial Purposes", IAP, Vol. XXIII, Part B5, Com. V, Hamburg, W. Germany, pp. 183-190.

Faig, W. (1984a). "Aerial Triangulation and Digital Mapping", Monograph 10, School of Surveying, Univ. of New South Wales, Kensington, Australia, 107 pp.

Faig, W. (1984b). "Subsidence Monitoring in Mountainous Terrain-An Example of Four Dimensional Photogrammetry", IAP(RS), Vol. XXV, Part A5, Com. V, Rio de Janeiro, Brazil, pp.276-285.

Faig, W. (1984c). "The Use of Photogrammetry for Mining Subsidence Determination", Australian Journal of Geod., Photog., Surv., No. 41, December, pp. 21-35.

Faig, W. (1986). "Deformation Measurements: Why and How?", Opening Address, Proc. of the Deformation Measurement Workshop PEDS II, Dept. of Earth, Atmospheric and Planetary Sciences, Massachusetts Institute of Technology, USA, pp. 1-6.

Faux, I.D. and M.J. Pratt (1983). "Computational Geometry for Design and Manufacture", Ellis Horwood Limited, England, 331 pp.

Fenton, P. (1982). "Digital Terrain Modelling Techniques for Volume Calculations and Road Design", Proc. of the 4th Canadian Symposium on Mining Surveying and Deformation Measurements, June 7-9, Banff, Alberta, Canada, pp. 97-114.

Florek, R. (1975). "Modern Techniques in Investigations of High-Speed Deformations", I Inter. Symposium on Deformation Measurements by Geodetic Methods, Krakow, Poland, 22-24/9, pp. 129-133.

Förstner, W. (1979). "On the Internal and External Reliability of Photogrammetric Coordinates", Presented paper at the Annual ASP-ACSM Convention, Washington, DC, USA.

Förstner, W., R. Schroth (1981). "On the Estimation of Covariance Matrices for Photogrammetric Image Coordinates", Proc. of the Inter. Symposium on Geodetic Networks and Computations of IAG,München, Deutsche Geodätische Kommission, Heft Nr. 258/VI, pp. 43-70.

Förstner, W. (1984). "Results of Test 2 on Gross Error Detection of ISP WG III/1 and OEEPE", IAP(RS), Vol. XXV, Part A3a, Comm. III, Rio de Janeiro, Brazil, pp. 220-233.

Förstner, W. (1985). "The Reliability of Block Triangulation", PE&RS, Vol. 51, No. 8, pp. 1137-1149.

Fraser, C.S. (1982). "The Potential of Analytical Close-Range Photogrammetry for Deformation Monitoring", Proc. of the 4th Canadian Symposium on Mining, Surveying and Deformation Measurements, Banff, Alberta, Canada, June 7-9, pp. 183-196.

Fraser, C.S., P.C. Stoliker (1983). "Deformation Monitoring of a Landslide Area by High-Precision Photogrammetry", Presented paper, FIG XVIII International Congress, Sofia, Bulgaria.

Fraser, C.S. (1984a). "Network Design Optimization in Non-Topographic Photogrammetry", PE&RS, Vol. 50, No. 8, 1984, pp. 1115-1126.

Fraser, C.S. (1984b). "Monitoring Mining Subsidence by Photogrammetry - Three Practical Examples", Workshop Handbook, ASP-ACSM Fall Convention, Vol. II, San Antonio, TX, USA.

Fraser, C.S., P.C. Gustafson, M.A. Chapman (1984). "The Monitoring of Movement of Brick and Precast Panels on the Jubillee Auditorium, Calgary, Canada", Workshop Handbook, ASP-ACSM Fall Convention, Vol. II, San Antonio, TX, USA.

Fraser, C.S. (1985). "Photogrammetric Measurement of Thermal Deformation of a Large Process Compressor", PE&RS, Vol. 51, No. 10, pp. 1569-1575.

Fraser, C.S. and L. Gruendig (1985). "The Analysis of Photogrammetric Deformation Measurements on Turtle Mountain", PE&RS, Vol. 51, No. 2, pp. 207-216.

Fraser, C.S. (1986a). "Microwave Antenna Measurement", PE&RS, Vol. 52, No. 10, pp. 1627-1635.

Fraser, C.S. (1986b). "Industrial Applications of Photogrammetry for Deformation Measurement", Proc. of the Deformation Measurements Workshop PEDS II, Dept. of Earth, Atsmospheric and Planetary Sciences, Massachusetts Institute of Technology, USA, pp. 336-360.

Fraser, C.S., D.C. Brown (1986). "Industrial Photogrammetry: New Developments and Recent Applications", Photogrammetric Record, Vol. 12, No. 68, pp. 197-217.

Fritsch, D. (1986). "Photogrammetry as a Tool for Detecting Recent Crustal Movements", Tectonophysics, Vol. 130, pp. 407-420.

Fritz, L.W. (1982). "Testing Procedures for Analytical Plotters", PE&RS, Vol. 48, No. 6, pp. 885-889.

Gelb, A. (1974). "Applied Optimal Estimation", The M.I.T. Press, Massachusetts Institute of Technology, Cambridge, Massachusetts, USA, 374 pp.

Gerstenecker, C., E. Groten, G. Hein (1978). "The Application of Modern Geodetic Techniques in Monitoring Translocations", Proc. of the II Inter. Symposium of Deformation Measurements by Geodetic Methods, Bonn, Germany, Konrad Wittwer 1981, Stuttgart, pp. 113-127.

Grafarend, E.W. (1974). "Optimization of Geodetic Networks", The Canadian Surveyor, Vol. 28, No. 5, December, pp. 716-723.

Grant, S. (1976). "Integration of Passive Ranging Loran-C, Satellite Navigation, Ship's Log, and Ship's Gyrocompass", M.Sc.E. Thesis, Dept. of Surveying Engineering, Univ. of New Brunswick, Fredericton, N.B., Canada.

Grün, A.W. (1979). "Gross Error Detection in Bundle Adjustment", Presented paper at Aerial Triangulation Symposium, Dept. of Surveying, Univ. of Queensland, Brisbane, Australia.

Grün, A.W. (1985). "Algorithmic Aspects in On-Line Triangulation", PE&RS, Vol. 51, No. 4, pp. 419-436.

Gustafson, P.C., J.D. Brown (1985). "Interactive Photogrammetric Network Design on a Microcomputer", Technical papers ASP Vol. 1, ASP-ACSM Annual Convention, Washington, DC, USA, pp. 195-203.

Haggren, Martikaine, Salmenperä, Vehkaperä, Väätäinen (1978). "Three-Dimensional Control of Ship Construction", Proc. of the Inter-Congress Symposium: Photogrammetry for Industry, Com. V, Stockholm, Sweden, pp. 72-79.

Helmering, R.J. (1977). "A General Sequential Algorithm for Photogrammetric On-Line Processing", PE&RS, Vol. 43, No. 4, pp. 469-474.

Henderson, H.V., S.R. Searle (1981). "On Deriving the Inverse of a Sum of Matrices", SIAM Review, Vol. 23, No. 1, pp. 53-60.

Jacobi, O. (1980). "Photogrammetric Tracking of a Moving Particle in Running Water", IAP, Vol. XXIII, Part B5, Com. V, Hamburg, W. Germany, pp. 368-374.

Jacobsen, K. (1984). "Data Collection for Bundle Block Adjustment on Analytical Plotters", IAP(RS), Vol. XXV, Part A3a, Com. III, Rio de Janeiro, Brazil, pp. 435-439.

Johnson, W. (1982). "Monitoring Volcanic Hazards", Bulletin Kern, No. 32, pp. 11-13.

Johnson, S., F. Grube (1982). "Photogrammetric Applications in Surface Mining in the United States", Inter. Symposium for Mine Surveying, Vol. 2, Sept. 19-25, Varna, Bulgaria, pp. 225-234.

Jaksic, Z. (1967). "Solution of Aerial Triangulation Problem using the NRC Analytical Plotter", Photogrammetria, Vol. 22, No. 2.

Jaksic, Z. (1979). "Conceptual Principle and Architecture of the ANAPLOT System", The Canadian Surveyor, Vol. 33, No. 2, June, pp. 95-106.

Junkins, J.L. (1978). "An Introduction to Optimal Estimation of Dynamical Systems", Sijthoff & Noordhoff International Publishers, B.V., Alphen aan den Rijn, The Netherlands, 339 pp.

Junkins, D.R., R.R. Steeves (1986). "Accumulation of the Cholesky Square Root in Helmert Blocking", The Canadian Surveyor, Vol. 40, No. 3, pp. 297-314.

Janusz, W. (1983). "Determination of Horizontal Displacements of Control Network Points", Proc. of the Institute of Geodesy and Cartography, Poland, Vol. XXX, No. 1, pp. 16-29.

Kalman, R.E. (1960). "A New Approach to Linear Filtering and Prediction Problems", ASME Transactions - Journal of Basic Engineering, Vol. 82, Series D, pp. 35-45.

Kavouras, M. (1982). "On the Detection of Outliers and the Determination of Reliability in Geodetic Networks", Technical Report No. 87, Dept. of Surveying Engineering, Univ. of New Brunswick, Fredericton, Canada, 121 pp.

Khachaturyan, A.G. (1983). "Theory of Structural Transformations in Solids", John Wiley & Sons, Inc., New York, 574 pp.

Kilburg, R.F., S.J. Rathburn (1984). "Applications of Close-Range Photogrammetry at General Dynamics Fort Worth Division", Workshop Handbook, ASP-ACSM Fall Convention, Vol. II, San Antonio, TX, USA.

Kilpelä, E. (1980). "Compensation of Systematic Errors of Image and Model Coordinates", Report of Working Group III/3, IAP, Vol. 23, Part B9, Com. III, Hamburg, W. Germany, pp. 407-427.

Knight, W., M.P. Mepham (1978). "Report on Computer Programs for Solving Large Systems of Normal Equations". Proc. of the 2nd Inter. Symposium on Problems to the Redefinition of North American Geodetic Networks, Arlington, VA, pp. 357-363.

Koch, K.R., D. Fritsch (1981). "Multivariate Hypothesis Tests for Detecting Recent Crustal Movements", Tectonophysics, Vol. 71, pp. 301-313.

Kölbl, O., J.J. Stuby (1982). "Mesure de Deplacement du Terrain a l'Aide de Photographies Multi-temporaires", Mensuration Photogrammetric Genie Rural 11/82, Ecole Polytechnique Federale de Lausanne.

Konecny, G. (1980). "How the Analytical Plotter Works and Differs from an Analog Plotter", Proc. of the ASP Analytical Plotter Symposium and Worshop, Reston, VA, USA, pp. 30-75.

Krakiwsky, E.J. (1975). "A Synthesis of Recent Advances in the Method of Least Squares", Lecture Notes No. 42, Dept. of Surveying Engineering, Univ. of New Brunswick, Fredericton, N.B., Canada.

Krakiwsky, E.J. (1986). "An Overview of Deformations Measurement, Technologies, and Modeling and Analysis", Proc. of the Deformation Measurements Workshop PEDS II, Dept. of Earth, Atmospheric and Planetary Sciences, Massachusetts Institute of Technology, USA, pp. 7-33.

Kratky, V. (1972). "Image Transformations", PE, Vol. 38, pp.463-471.

Kratky, V. (1976). "Analytical On-Line Systems in Close-Range Photogrammetry", PE&RS, Vol. 42, No. 1, pp. 81-90.

Kratky, V. (1979). "On-Line Analytical Triangulation", The Canadian Surveyor, Vol. 33, No. 2, pp. 162-176.

Kratky, V. (1980). "Present Status of On-Line Analytical Triangulation", IAP, Vol. XXIII, B3, Com. III, Hamburg, W. Germany, pp. 379-388.

Kratky, V. S.F. El-Hakim (1983). "Quality Control for NRC On-Line Triangulation", PE&RS, Vol. 49, No. 6, pp. 763-769.

Kratky, V. (1984). "On-Line Triangulation Performance of the NRC Anaplot", IAP(RS), Vol. XXV, Part A3a, Com. III, Rio de Janeiro, Brazil, pp. 561-573.

Kratzsch, H. (1983). "Mining Subsidence Engineering", Springer-Verlag, Berlin, 543 pp.

Lawson, C.L., R.J. Hanson (1974). "Solving Least Squares Problems", Prentice-Hall, Inc., Englewood Cliffs, New Jersey, 340 pp.

LeMay, J.L. (1984). Coordinator of "Kalman Filtering Lecture Notes", Vol. I and II, Univ. of California, Los Angeles-University Extension, Dept. of Engineering, Science and Mathematics, Copyright St. Joseph Sciences, Inc.

Liebelt, P.B. (1967). "An Introduction to Optimal Estimation", Addison-Wesley Publishing Company, Don Mills, Ontario, Canada, pp. 273.

Lucas, J.R. (1987). "Aerotriangulation without Ground Control", PE&RS, Vol. 53, No. 3, pp. 311-314.

"Manual of Photogrammetry" (1980). 4th edition. Published by the American Society of Photogrammetry and Remote Sensing.

Martin, G.E. (1982). "Transformation Geometry. An Introduction to Symmetry", Springer-Verlay, New York, Inc., pp. 237.

Masry, S.E., G. Konecny (1970). "Flowcharts and Description of the Real-Time Program of the Analytical Plotter AP-2C", Technical Report No. 2, Dept. of Surveying Engineering, Univ. of New Brunswick, Fredericton, N.B., Canada.

Masry, S.E. (1972). "Real-time Digitizing and Editing from Photogrammetric Instruments", Technical Report No. 12, Dept. of Surveying Engineering, Univ. of New Brunswick, Fredericton, N.B., Canada, 55 pp.

Masry, S.E., W. Faig (1977). "The Analytical Plotter in Close Range Applications", PE&RS, Vol. 43, No. 1, pp. 89-94.

Mehto, L., E. Viitanen (1976). "On the Use of Numerical Photogrammetry in an I-girder Loading Experiment", Applications of Numerical Photogrammetry, Tampere University, 25 pp.

Mertikas, S.P. (1987). "A Statistical Investigation Pertaining to Accuracy of the GPS in Navigation", Ph.D. Dissertation, Dept. of Surveying Engineering, Univ. of New Brunswick, Fredericton, N.B., Canada.

Mierlo van, J. (1978). "A Testing Procedure for Analysing Geodetic Deformation Measurements", Proc. of the 2nd Inter. Symposium on Deformation Measurements by Geodetic Methods, Bonn, W. Germany, Konrad Wittwer 1981, pp. 321-353.

Mikhail, E.M., R.J. Helmering (1973). "Recursive Methods in Photogrammetric Data Reduction", PE, Vol. 39, No. 9, pp. 983-989.

Mikhail, E.M. (1976). "Observations and Least Squares", Harper & Row, Publishers, Inc., New York, 497pp.

Moffit, F.H., E.M. Mikhail (1980). "Photogrammetry", 3rd Edition, Harper & Row, Inc., New York, USA, 648 pp.

Molenaar, M. (1981). "Several Aspects on the Sequential Processing of Photogrammetric Bundle Blocks", Seminar on Mathematical Models of Geodetic/Photogrammetric Point Determination with Regard to Outliers and Systematic Errors, edited by F.E. Ackermann, Deutsche Geodätische Kommission, Reihe A, Heft Nr. 98, Stuttgart, pp. 105-130.

Moniwa, H. (1977). "Analytical Photogrammetric System with Self-Calibration and its Applications", Ph.D. Dissertation, Dept. of Surveying Engineering, Univ. of New Brunswick, Fredericton, N.B., Canada, 120 pp.

Moniwa, H. (1981). "The Concept of Photo-Variant Self-Calibration and its Application in Block Adjustment with Bundles", Photogrammetria, Vol. 36, pp. 11-29.

Morrison, N. (1969). "Introduction to Sequential Smoothing and Prediction", McGraw-Hill, Inc., 645 pp.

Murai, S., R. Matsuoka, T. Okuda (1984). "A Study on Analytical Calibration for Non-Metric Cameras and Accuracy of Three-Dimensional Measurement", IAP, Vol. 25, Part A5, Com. V, Rio de Janeiro, Brazil, pp. 570-579.

Newton, L. (1986). "Control Extension Utilizing Large Format Camera Photography", M.Eng. Report, Dept. of Surveying Engineering, Univ. of New Brunswick, Fredericton, N.B., Canada, 94 pp.

Niemeier, W. (1981). "Statistical tests for Detecting Movements in Repeatedly Measured Geodetic Networks", Tectonophysics, Vol. 71, pp. 335-351.

Niemeier, W. (1982). "Design, Diagnosis and Optimization of Monitoring Networks in Engineering Surveying", Proc. of the CIS Centennial Convention, Ottawa, Canada, Vol. 2, pp. 228-246.

Okang, J.P. (1971). "Errors in Point Marking", PE, Vol. 37, No. 10. pp. 1069-1074.

Papo, H.B. (1985). "Deformation Analysis by Close-Range Photogrammetry", PE&RS, Vol. 51, No. 10, pp. 1561-1567.

Perelmuter, A. (1979). "Adjustment of Free Networks", Bulletin Geodesique, Vol. 53, pp. 291-296.

Perry, L.H. (1984). "Photogrammetric Summary of the Ada County Project", PE&RS, Vol. 50, No. 5, pp. 563-567.

Peterson, J.C. (1976). "Photogrammetric Monitoring of Structural Displacement", Proc. of the ASP Annual Convention, Seattle, USA.

Pope, A.J. (1976). "The Statistics of Residuals and the Detection of Outliers", U.S. Dept. of Commerce, NOAA Technical Report NOS. 65 NGS 1, Rockville, MD., USA.

Reichenbach von, K. (1984). "Terrestrisch-Photogrammetrische Vermessung von Grossbaggern im Tagebau", Presented paper at the Inter. Congress for Photog. and Rem. Sen., Com. V/4, Rio de Janeiro, Brazil.

Reinhardt, W., H. Rentsch (1986). "Determination of Changes in Volume and Elevation of Glaciers using Digital Elevation Models for the Vernagtferner, Ötztal Alps, Austria", Annals of Glaciology, No. 8, pp. 151-155.

Robertson, G. (1982). "Measuring Component Movements of a Cable Reeler using a Photogrammetric Method", IAP, Vol. 24, Part V/2, Com. V, York, England, pp. 405-411.

Robertson, G.R., A.M.R. Macrae, J. Tribe, D.W. Sibley, D.H. Smith (1982). "Use of Photogrammetric Methods for Mine Slope Deformation Surveys", Proc. of the 4th Canadian Symposium on Mining Surveying and Deformation Measurements, Banff, Alberta, Canada, 7-9 June, pp. 223-231.

Rosculet, D. (1980). "Recursive Methods for the Simultaneous Adjustment of Photogrammetric and Geodetic Observations in Analytical Aerotriangulation", IAP, Vol. XXIII, Part B3, Com. III, Hamburg, W. Germany, pp. 617-625.

Schmitt, G. (1982). "Optimal Design of Geodetic Networks", Proc. of the Inter. Symposium on Geodetic Networks and Computations of the IAG, Vol. III, Deutsche Geodätische Kommission, Reihe B, Heft Nr. 258/III, pp. 7-12.

Schoeler, H. (1978). "New Equipment for Point Transfer and Point Marking in Photogrammetric Strips and Blocks", Proc. of the ASP 44th Annual Meeting, Washington, DC, pp. 21-27.

Schwarz, K.-P. (1983). "Kalman Filtering and Optimal Smoothing", Papers for CIS Adjustment and Analysis Seminars, edited by E.J. Krakiwsky, CISM, pp. 230-264.

Secord, J.M. (1985). "Implementation of a Generalized Method for the Analysis of Deformation Surveys", Technical Report No. 117, Dept. of Surveying Engineering, Univ. of New Brunswick, Fredericton, N.B., Canada, 161 pp.

Seymour, R.H. (1980). "Analytical Plotter Interfaces", Proc. of the ASP Analytical Plotter Symposium and Workshop, Reston, VA, USA, pp. 277-283.

Shi, Z. (1985). "Application of an Integrated Method in Deformation Analysis", M.Sc.E. Thesis, Dept. of Surveying Engineering, Univ. of New Brunswick, Fredericton, N.B., Canada, 127 pp.

Shih, T.Y. (1987). "The Fundamental Review of Additional Parameters", Internal paper, Dept. of Surveying Engineering, Univ. of New Brunswick, Fredericton, N.B., Canada.

Shortis, M.R., L.J. Price, P.J. Turner (1986). "Photogrammetric Monitoring of the Excavation of a Trunk Sewer Pumping Station", IAP(RS), Vol. 26, Part 5, Com. V, Ottawa, Canada, pp. 241-249.

Somogyi, J. (1982). "Die Rolle der Photogrammetrie im ungarischen Bergbau", Neue Bergbautechnik, 12 Jg, Heft 7, Juli, pp. 380-384.

Sorenson, H.W. (1970). "Least-Squares Estimation: from Gauss to Kalman", IEEE Spectrum, July, pp. 63-68.

Stirling, D.M. (1982). "Measuring Short Term Glacial Fluctuations by Aerial and Terrestrial Photogrammetry - A Comparative Study", IAP, Vol. 24, Part V/2, Com. V, York - England, pp. 484-496.

Strang, G. (1980). "Linear Algebra and its Applications", Academic Press, Inc., New York, 414 pp.

Swerling, P. (1971). "Modern State Estimation Methods from the Viewpoint of the Method of Least Squares", IEEE Transactions on Automatic Control, Vol. AC-16, No. 6, December, pp. 707-719.

Szczechowski, B. (1980). "The Photogrammetric Measurements of the Ship Deformations", IAP, Vol. XXIII, Part B5, Com. V, Hamburg, W. Germany, pp. 714-723.

Thompson, E.H. (1969). "Introduction to the Algebra of Matrices with Some Applications", The University of Toronto Press, Canada, 229 pp.

Tobin, P. (1983). "Examination of Deformation Measurements Using Invariant Functions of Displacements", M.Sc.E. Thesis, Dept. of Surveying Engineering, Univ. of New Brunswick, Fredericton, N.B., Canada, 72 pp.

Toomey, M.A.G. (1982). "The Application of Digital Terrain Models to Mine Development Mapping", Proc. of the 4th Canadian Symposium on Mining Surveying and Deformation Measurements, Banff, Alberta, pp. 89-94.

Torlegard, K., E. Dauphin (1976). "Displacement between Building Elements using an Amateur Camera", Presented paper, ISP Congress, Com. V, Helsinki, Finland.

Torlegard, K. (1978). "Photogrammetric Methods for Deformation Measurements", Proc. of the II Inter. Symposium on Deformation Measurements by Geodetic Methods, Konrad Wittwer 1981, Bonn, W. Germany.

Torlegard, K. (1981). "Accuracy Improvement in Close-Range Photogrammetry", Wissenschaftlicher Studiengang Vermessungswesen Hochschule der Bundeswehr München, Schriftenreihe, 5, 68 pp.

Trinder, J.C. (1984). "Pointing Precisions on Aerial Photography", PE&RS, Vol. 50, No. 10, pp. 1449-1462.

Trinder, J.C. (1986). "Potential of Monocular and Stereoscopic Observations on Aerial Photographs", Photogrammetria, No. 41, pp. 17-27.

Uzi, E. (1984). "Measuring Deformations of a Multi-Storey Building with a Non-Metric Camera", IAP(RS), Vol. XXV, Part A5, Com. V, Rio de Janeiro, Brazil, pp. 683-689.

Vanicek, P., E. Krakiwsky (1986). "Geodesy: The Concepts", 2nd edition, Elsevier Science Publishing Company, Inc., New York, USA, 697 pp.

Veress, S.A. (1980). "Photogrammetry for Dimensional Control of Bridges", IAP, Vol. XXIII, Part B5, Com. V, Hamburg, W. Germany, pp. 746-754.

Veress, S.A., J.N. Hatzopoulos (1981). "A Combination of Aerial and Terrestrial Photogrammetry for Monitoring", PE&RS, Vol. 47, No. 12, pp. 1725-1731.

Veress, S.A. (1982a). "Deformation Measurements by Aerial and Terrestrial Photogrammetry", III Inter. Symposium on Deformation Measurement by Geodetic Methods, FIG - Com. 6, Budapest, August, Vol. 1.

Veress, S.A. (1982b). "Photogrammetric Analysis of Deformation of Transmission Lines", IAP, Vol. 24, Part V/2, Com. V, York, England, pp. 516-523.

Wells, D.E. (1971). "Matrices", Technical Report No. 15, Dept. of Surveying Engineering, Univ. of New Brunswick, Fredericton, N.B., Canada, 87 pp.

Wells, D.E., E.J. Krakisky (1971). "The Method of Least Squares", Lecture Notes No. 18, Dept. of Surveying Engineering, Univ. of New Brunswick, Fredericton, N.B., Canada.

Wells, D.E., K. Frankich (1983). "Review of Linear Algebra", Papers for the CIS Adjustment and Analysis Seminars edited by E.J. Krakiwsky, CISM, pp. 32-78.

Welsch, W. (1981). "Gegenwärtiger Stand der geodätischen Analyse und Interpretation geometrischer Deformationen", Allgemeine Vermessungs - Nachrichten, Heft 2, pp. 41-51.

Wijk van, M.C., H. Ziemann (1976). "The Use of Non-Metric Cameras in Monitoring High Speed Processes", Invited paper, XIII Congress of the ISP, Com. V/2. Helsinki, Finland, pp. 91-102.

Wong, K.W., A.P. Vonderohe (1981). "Planar Displacements by Motion Parallax", PE&RS, Vol. 47, No. 6, pp. 769-777.

Wrobel, B., W. Weise (1980). "Deformation Measurements by High-Frequency Photography during Crash Tests of Steel Concrete Plates", IAP, Vol. XXIII, Part B5, Com. V, Hamburg, W. Germany, pp. 834-846.

Ziemann, H. (1985). "System Calibration and Self-Calibration with Fully-Controlled Vertical Aerial Photography", Technical Papers, 51st Annual Meeting ASP, Vol. 2, Washington, DC, pp. 736-745.

APPENDIX I

Flowcharts of the <APOLO> System

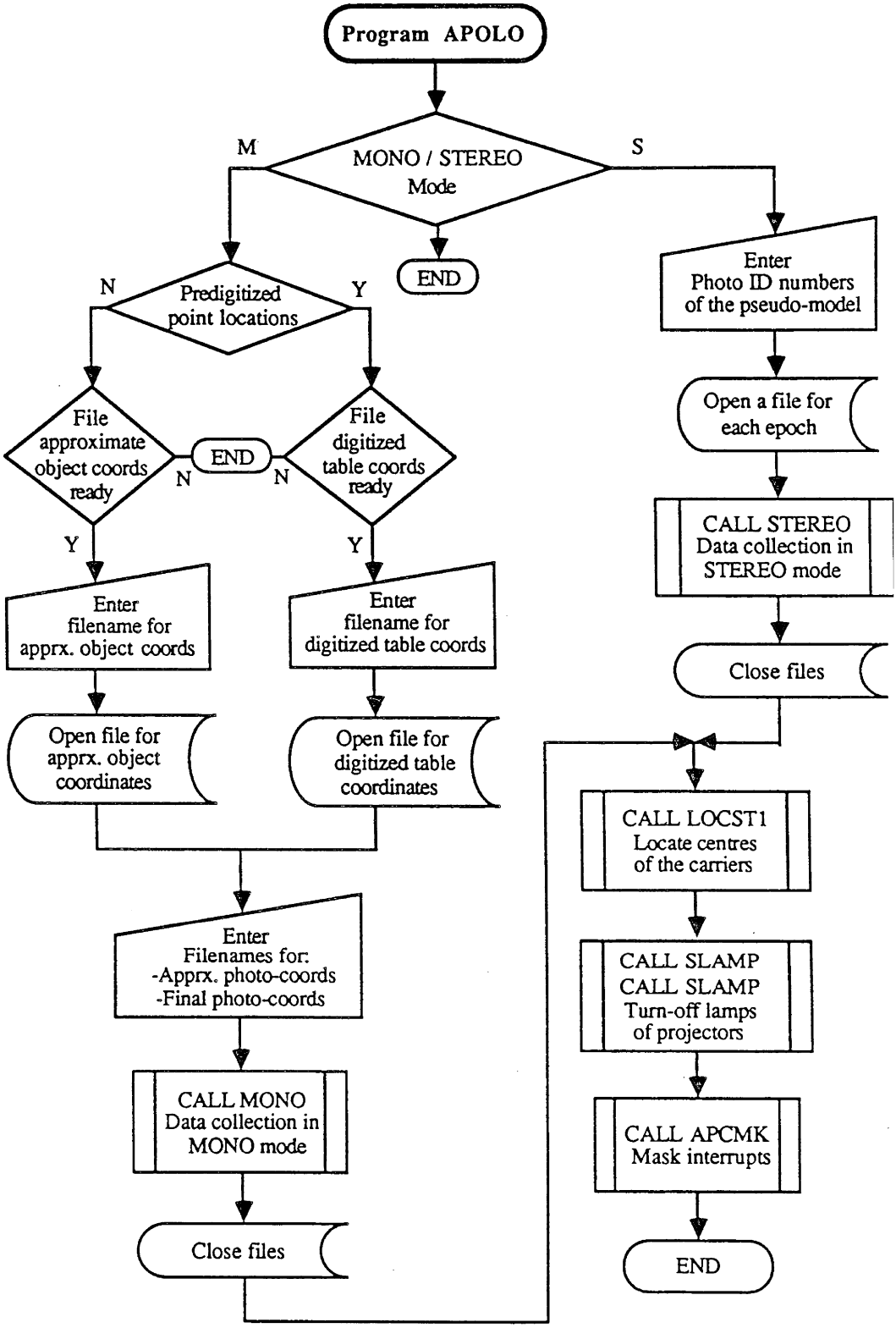
Program APOLO
MONO / STEREO Mode
M
S
END
Predigitized point locations
N
Y
File approximate object coords ready
END
N
File digitized table coords ready
N
Y
Y
Enter filename for apprx. object coords
Enter filename for digitized table coords
Open file for apprx. object coordinates
Open file for digitized table coordinates
Enter Filenames for: -Apprx. photo-coords -Final photo-coords
CALL MONO Data collection in MONO mode
Close files
Enter Photo ID numbers of the pseudo-model
Open a file for each epoch
CALL STEREO Data collection in STEREO mode
Close files
CALL LOCST1 Locate centres of the carriers
CALL SLAMP CALL SLAMP Turn-off lamps of projectors
CALL APCMK Mask interrupts
END

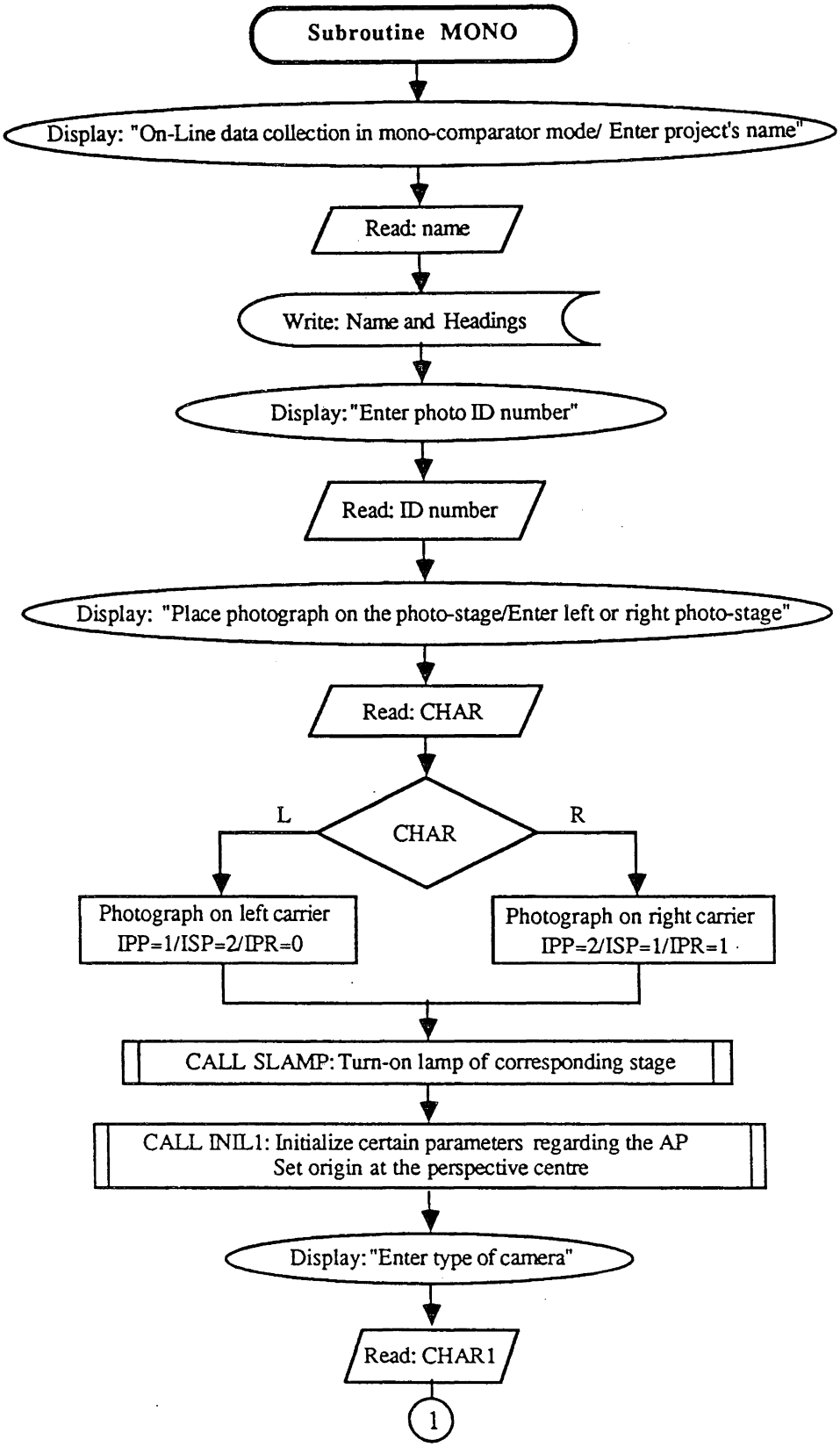
Subroutine MONO
Display: "On-Line data collection in mono-comparator mode/ Enter project's name"
Read: name
Write: Name and Headings
Display: "Enter photo ID number"
Read: ID number
Display: "Place photograph on the photo-stage/Enter left or right photo-stage"
Read: CHAR
CHAR
L
R
Photograph on left carrier
IPP=1/ISP=2/IPR=0
Photograph on right carrier
IPP=2/ISP=1/IPR=1
CALL SLAMP: Turn-on lamp of corresponding stage
CALL INIL1: Initialize certain parameters regarding the AP
Set origin at the perspective centre
Display: "Enter type of camera"
Read: CHAR1
1

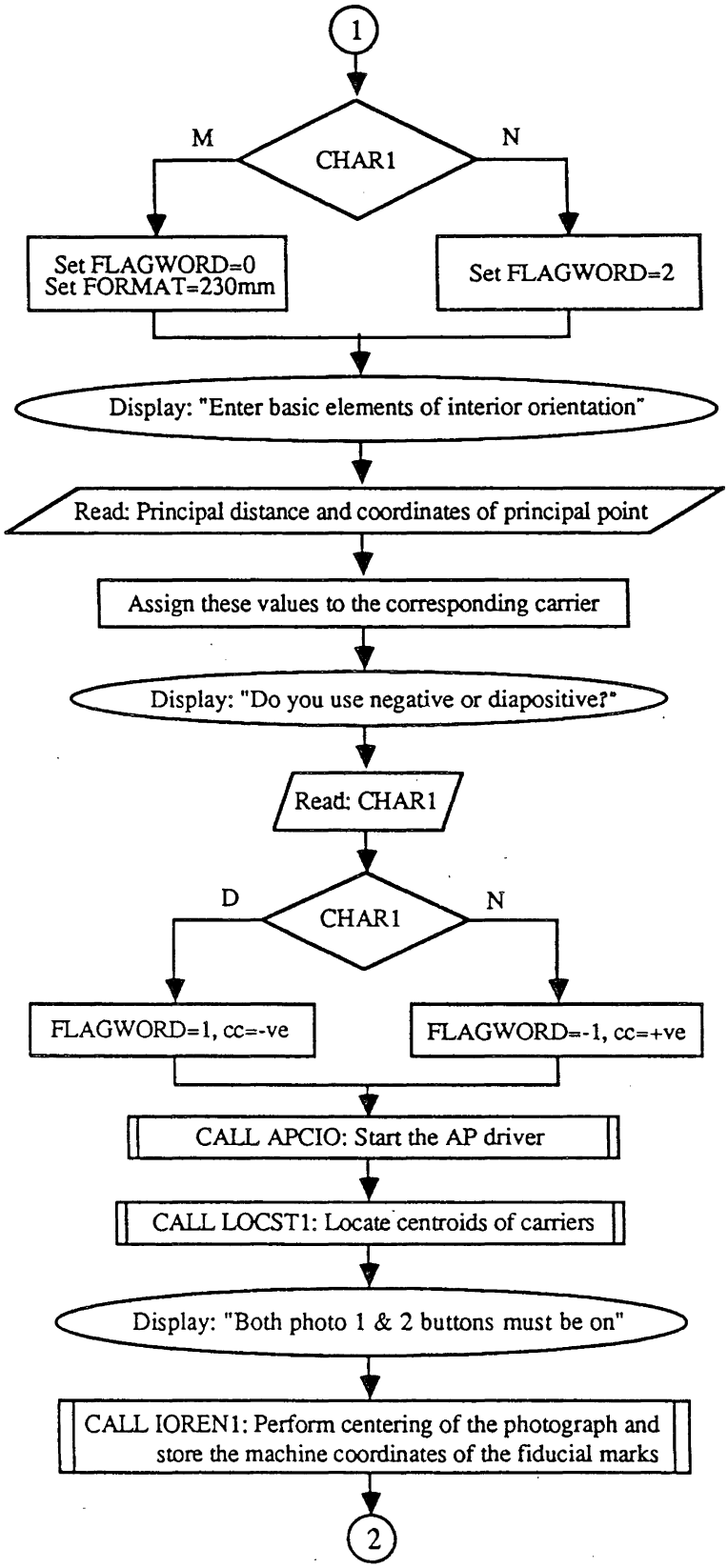
1
M
CHAR1
N
Set FLAGWORD=0
Set FORMAT=230mm
Set FLAGWORD=2
Display: "Enter basic elements of interior orientation"
Read: Principal distance and coordinates of principal point
Assign these values to the corresponding carrier
Display: "Do you use negative or diapositive?"
Read: CHAR1
D
CHAR1
N
FLAGWORD=1, cc=-ve
FLAGWORD=-1, cc=+ve
CALL APCIO: Start the AP driver
CALL LOCST1: Locate centroids of carriers
Display: "Both photo 1 & 2 buttons must be on"
CALL IOREN1: Perform centering of the photograph and store the machine coordinates of the fiducial marks
2

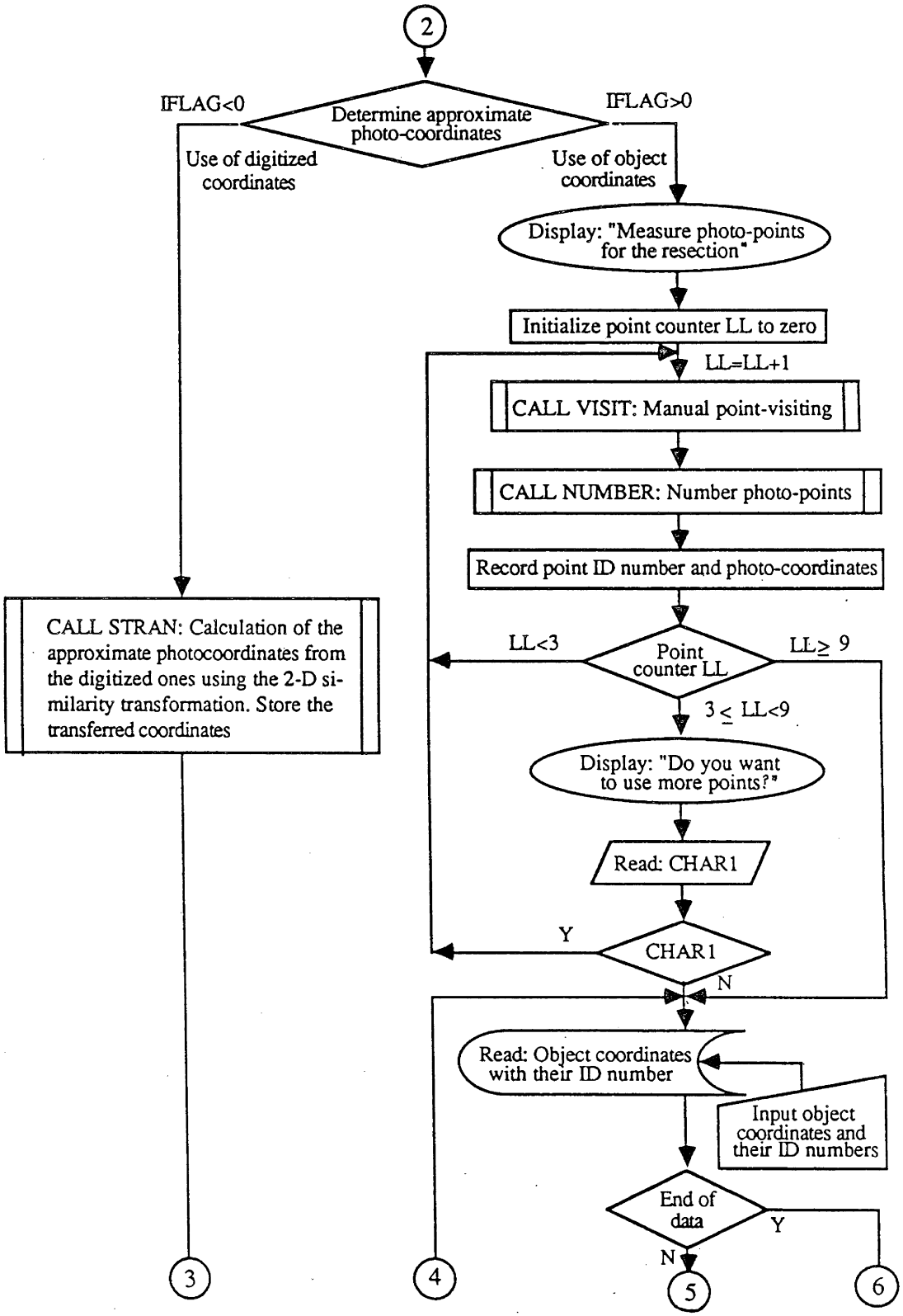
2
IFLAG<0
Determine approximate photo-coordinates
IFLAG>0
Use of digitized coordinates
Use of object coordinates
Display: "Measure photo-points for the resection"
Initialize point counter LL to zero
LL=LL+1
CALL VISIT: Manual point-visiting
CALL NUMBER: Number photo-points
Record point ID number and photo-coordinates
CALL STRAN: Calculation of the approximate photocoordinates from the digitized ones using the 2-D similarity transformation. Store the transferred coordinates
LL<3
Point counter LL
LL≥ 9
3 ≤ LL<9
Display: "Do you want to use more points?"
Read: CHAR1
Y
CHAR1
N
Read: Object coordinates with their ID number
Input object coordinates and their ID numbers
End of data
Y
N
3
4
5
6

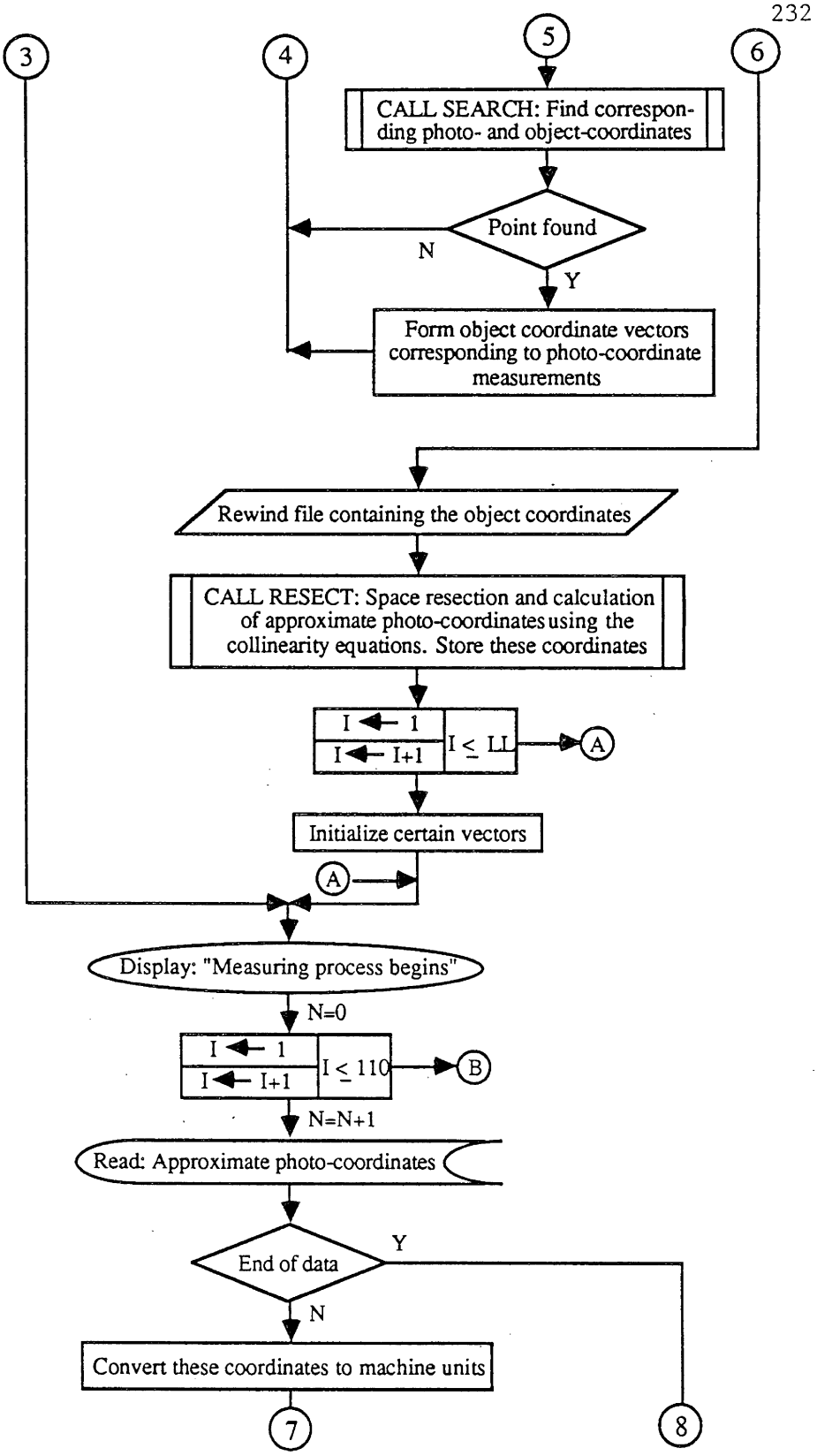
3
4
5
6
CALL SEARCH: Find corresponding photo- and object-coordinates
Point found
N
Y
Form object coordinate vectors corresponding to photo-coordinate measurements
Rewind file containing the object coordinates
CALL RESECT: Space resection and calculation of approximate photo-coordinates using the collinearity equations. Store these coordinates
I ← 1
I ← I+1
I ≤ LL
A
Initialize certain vectors
A
Display: "Measuring process begins"
N=0
I ← 1
I ← I+1
I ≤ 110
B
N=N+1
Read: Approximate photo-coordinates
End of data
Y
N
Convert these coordinates to machine units
7
8

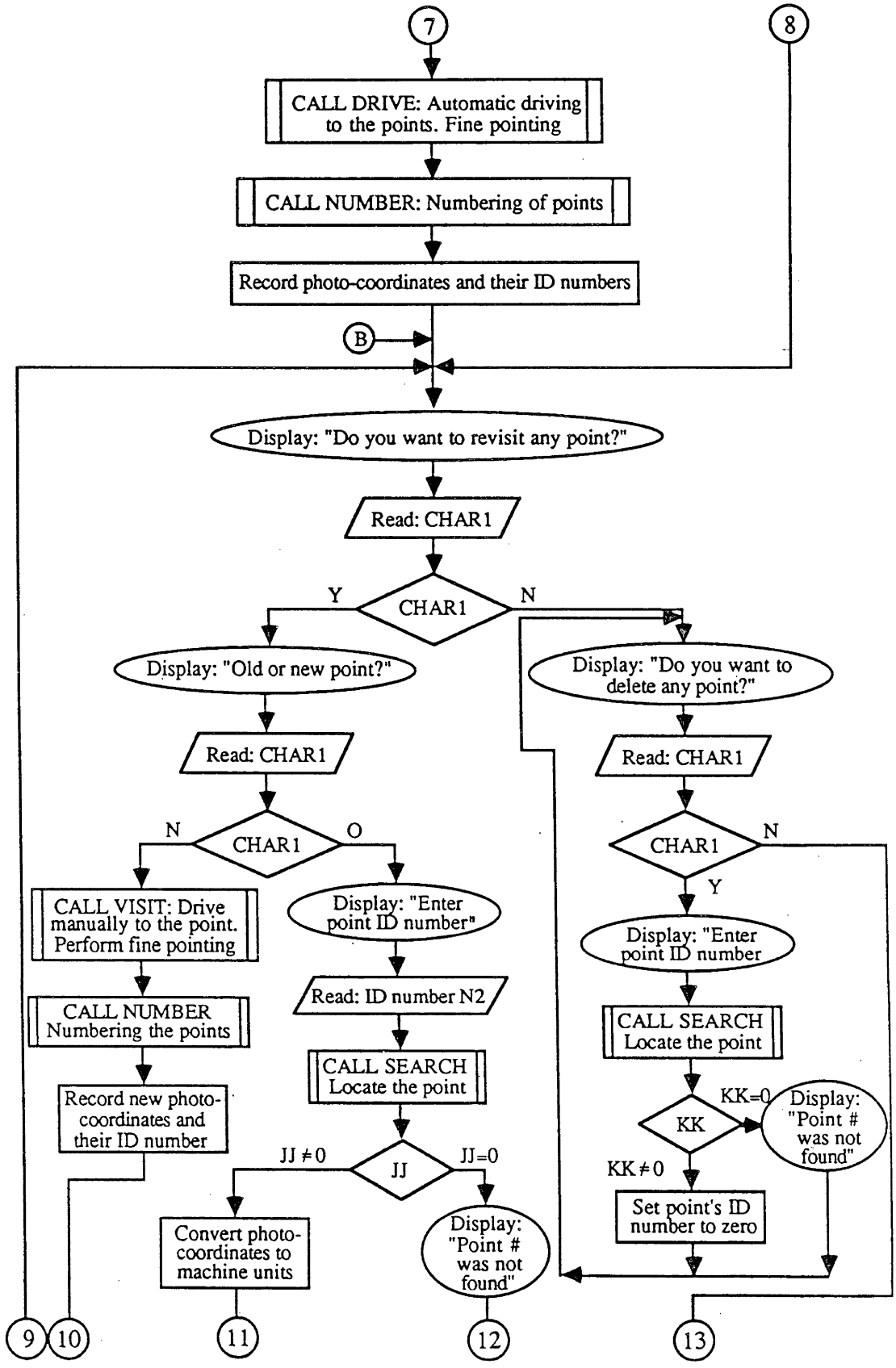
7
8
CALL DRIVE: Automatic driving to the points. Fine pointing
CALL NUMBER: Numbering of points
Record photo-coordinates and their ID numbers
B
Display: "Do you want to revisit any point?"
Read: CHAR1
CHAR1
Y
N
Display: "Old or new point?"
Read: CHAR1
CHAR1
N
O
CALL VISIT: Drive manually to the point. Perform fine pointing
CALL NUMBER Numbering the points
Record new photo-coordinates and their ID number
Display: "Enter point ID number"
Read: ID number N2
CALL SEARCH Locate the point
JJ
JJ ≠ 0
JJ=0
Convert photo-coordinates to machine units
Display: "Point # was not found"
Display: "Do you want to delete any point?"
Read: CHAR1
CHAR1
N
Y
Display: "Enter point ID number
CALL SEARCH Locate the point
KK
KK=0
Display: "Point # was not found"
KK ≠ 0
Set point's ID number to zero
9
10
11
12
13

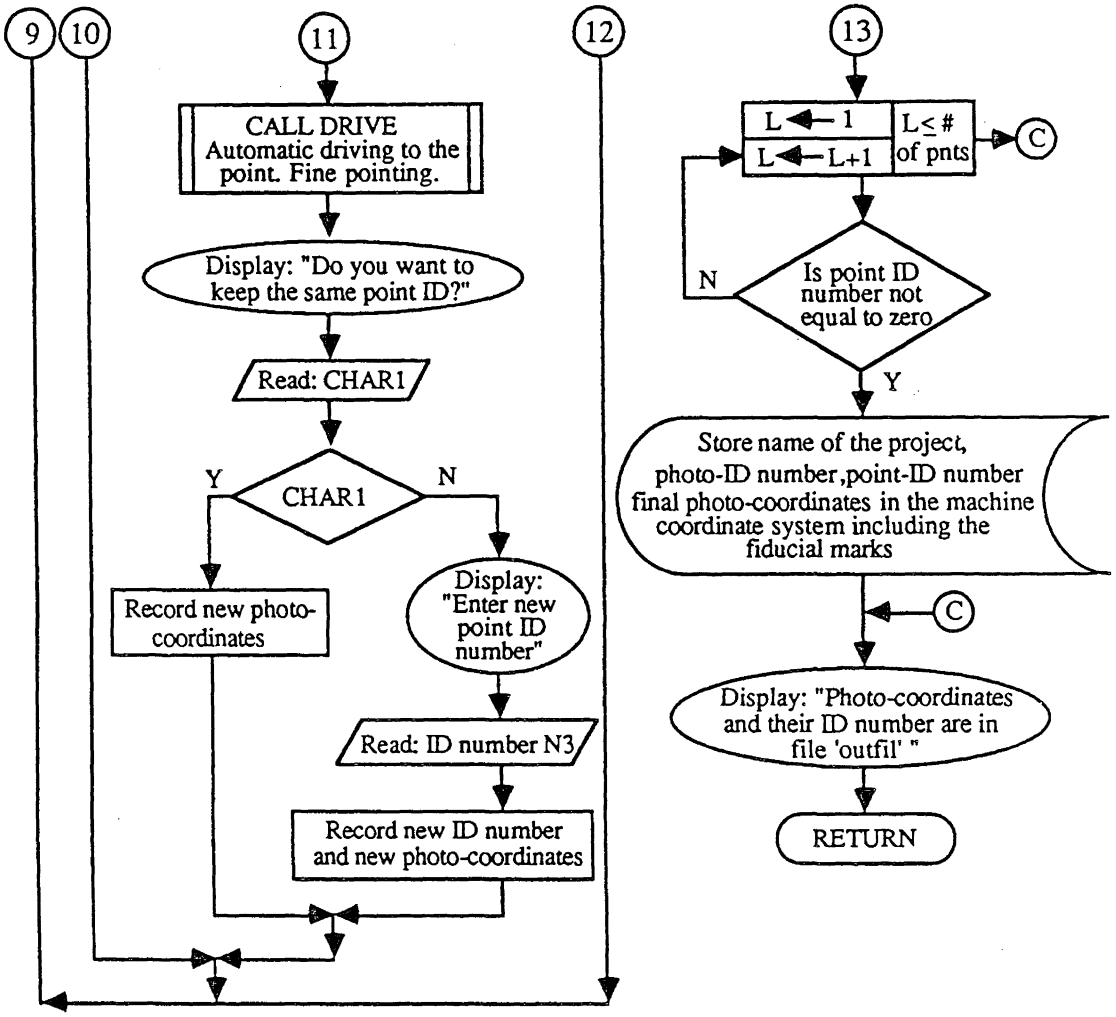
9
10
11
12
13
CALL DRIVE
Automatic driving to the point. Fine pointing.
Display: "Do you want to keep the same point ID?"
Read: CHAR1
Y
CHAR1
N
Record new photo-coordinates
Display: "Enter new point ID number"
Read: ID number N3
Record new ID number and new photo-coordinates
L ← 1
L ← L+1
L ≤ # of pnts
C
N
Is point ID number not equal to zero
Y
Store name of the project, photo-ID number, point-ID number final photo-coordinates in the machine coordinate system including the fiducial marks
C
Display: "Photo-coordinates and their ID number are in file 'outfil' "
RETURN

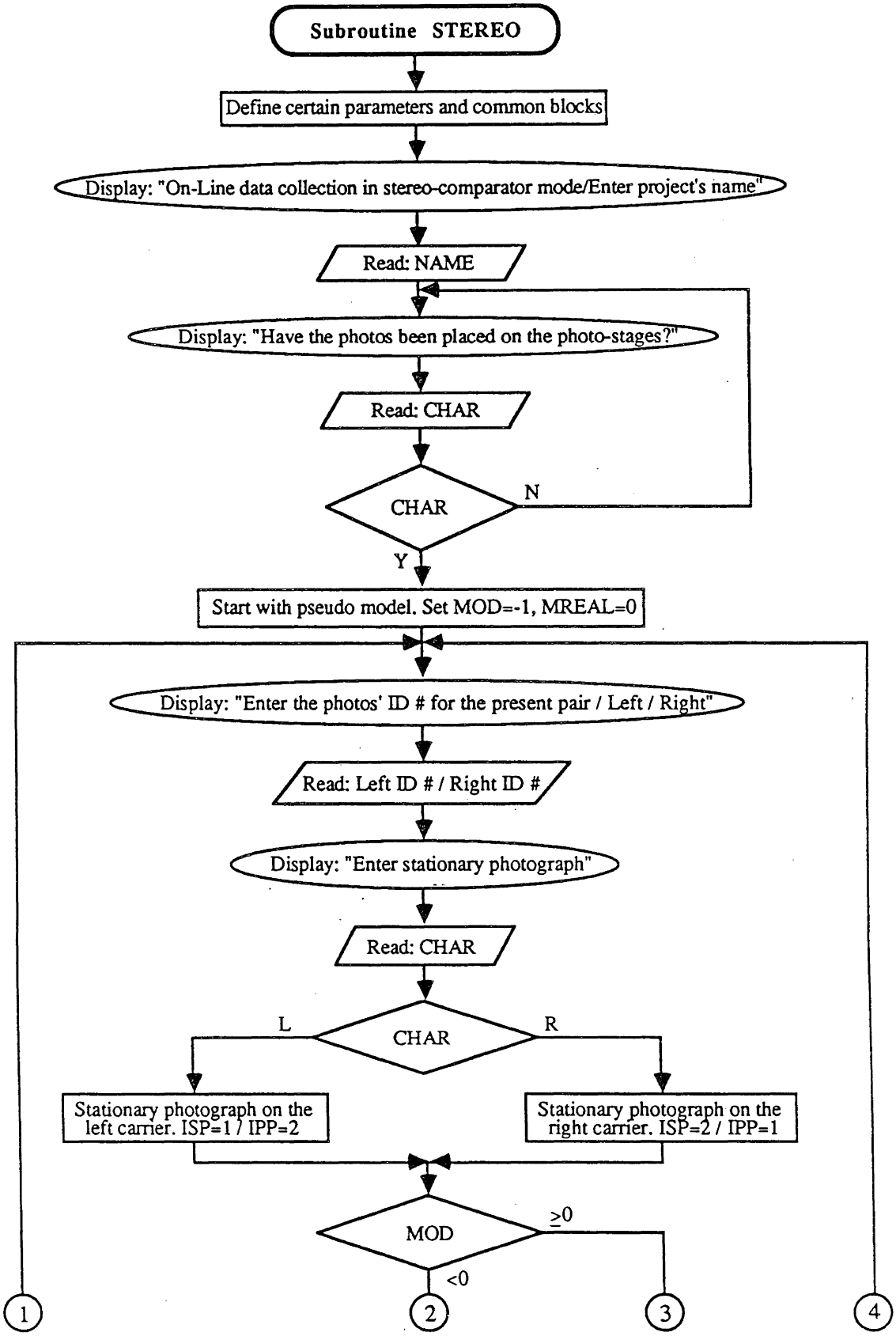
Subroutine STEREO
Define certain parameters and common blocks
Display: "On-Line data collection in stereo-comparator mode/Enter project's name"
Read: NAME
Display: "Have the photos been placed on the photo-stages?"
Read: CHAR
CHAR
N
Y
Start with pseudo model. Set MOD=-1, MREAL=0
Display: "Enter the photos' ID # for the present pair / Left / Right"
Read: Left ID # / Right ID #
Display: "Enter stationary photograph"
Read: CHAR
L
CHAR
R
Stationary photograph on the left carrier. ISP=1 / IPP=2
Stationary photograph on the right carrier. ISP=2 / IPP=1
MOD
≥0
<0
1
2
3
4

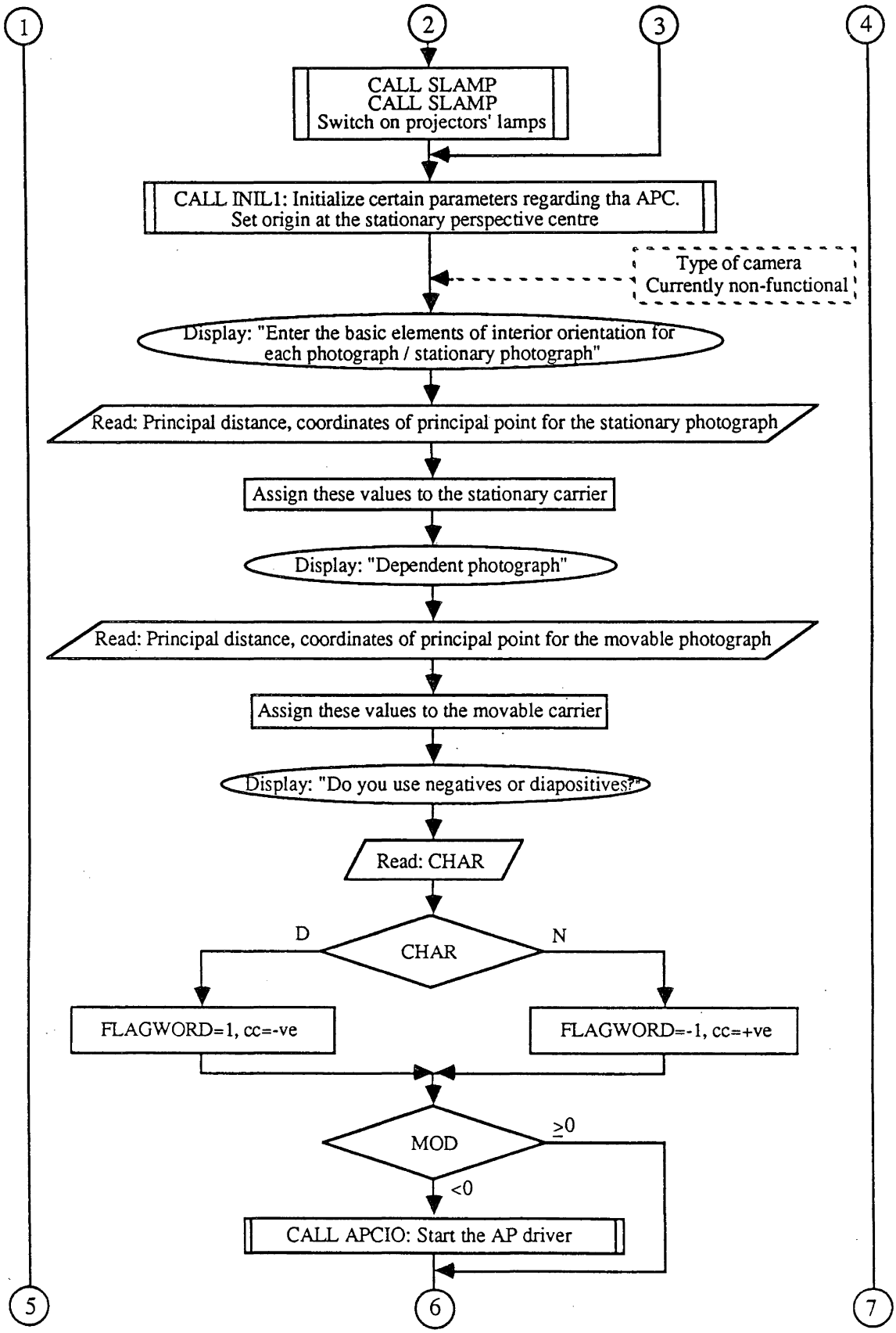
1
2
3
4
CALL SLAMP
CALL SLAMP
Switch on projectors' lamps
CALL INIL1: Initialize certain parameters regarding tha APC.
Set origin at the stationary perspective centre
Type of camera
Currently non-functional
Display: "Enter the basic elements of interior orientation for each photograph / stationary photograph"
Read: Principal distance, coordinates of principal point for the stationary photograph
Assign these values to the stationary carrier
Display: "Dependent photograph"
Read: Principal distance, coordinates of principal point for the movable photograph
Assign these values to the movable carrier
Display: "Do you use negatives or diapositives?"
Read: CHAR
D
CHAR
N
FLAGWORD=1, cc=-ve
FLAGWORD=-1, cc=+ve
MOD
≥0
<0
CALL APCIO: Start the AP driver
5
6
7

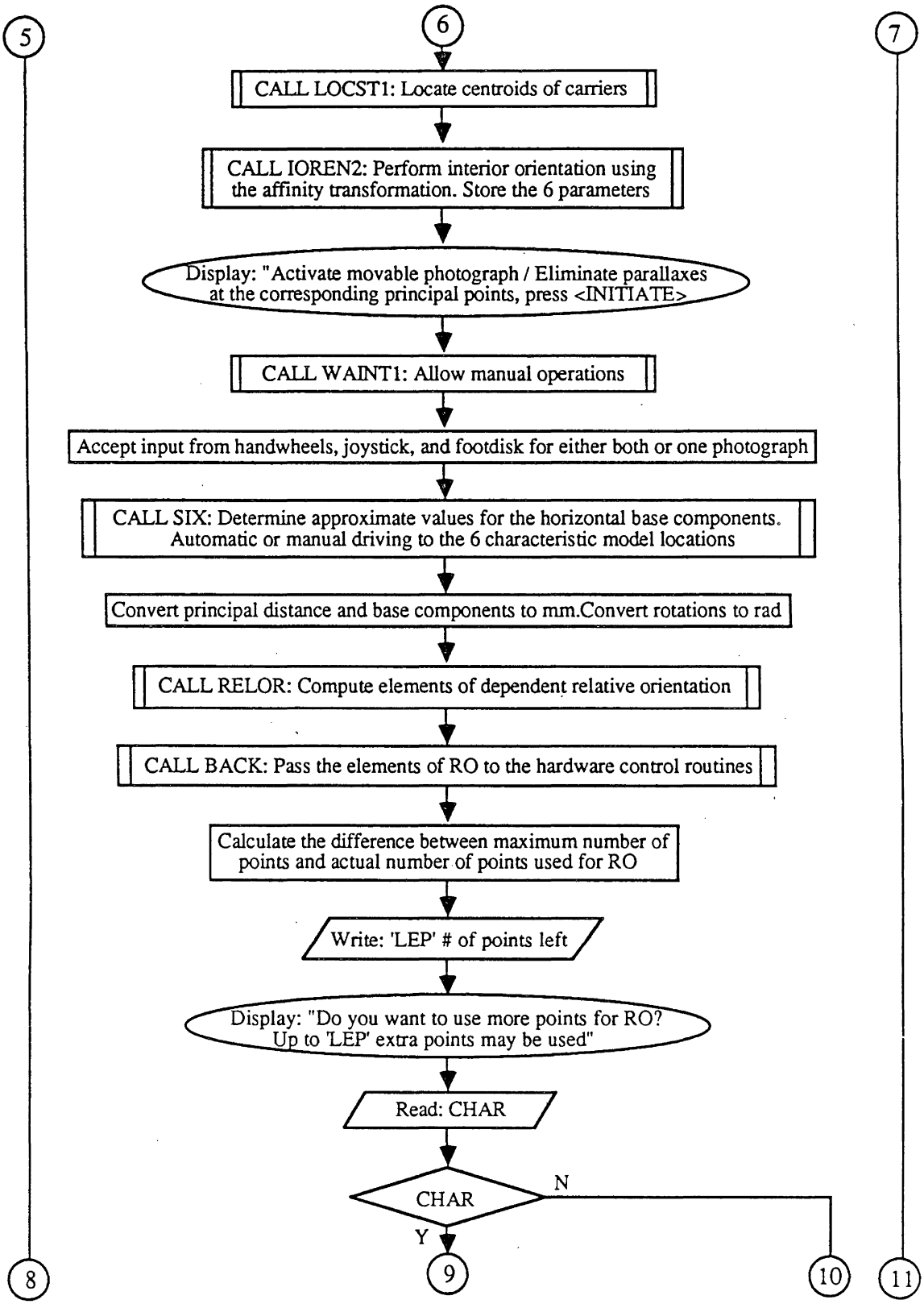
5
6
7
CALL LOCST1: Locate centroids of carriers
CALL IOREN2: Perform interior orientation using the affinity transformation. Store the 6 parameters
Display: "Activate movable photograph / Eliminate parallaxes at the corresponding principal points, press <INITIATE>
CALL WAINT1: Allow manual operations
Accept input from handwheels, joystick, and footdisk for either both or one photograph
CALL SIX: Determine approximate values for the horizontal base components. Automatic or manual driving to the 6 characteristic model locations
Convert principal distance and base components to mm.Convert rotations to rad
CALL RELOR: Compute elements of dependent relative orientation
CALL BACK: Pass the elements of RO to the hardware control routines
Calculate the difference between maximum number of points and actual number of points used for RO
Write: 'LEP' # of points left
Display: "Do you want to use more points for RO? Up to 'LEP' extra points may be used"
Read: CHAR
CHAR
N
Y
8
9
10
11

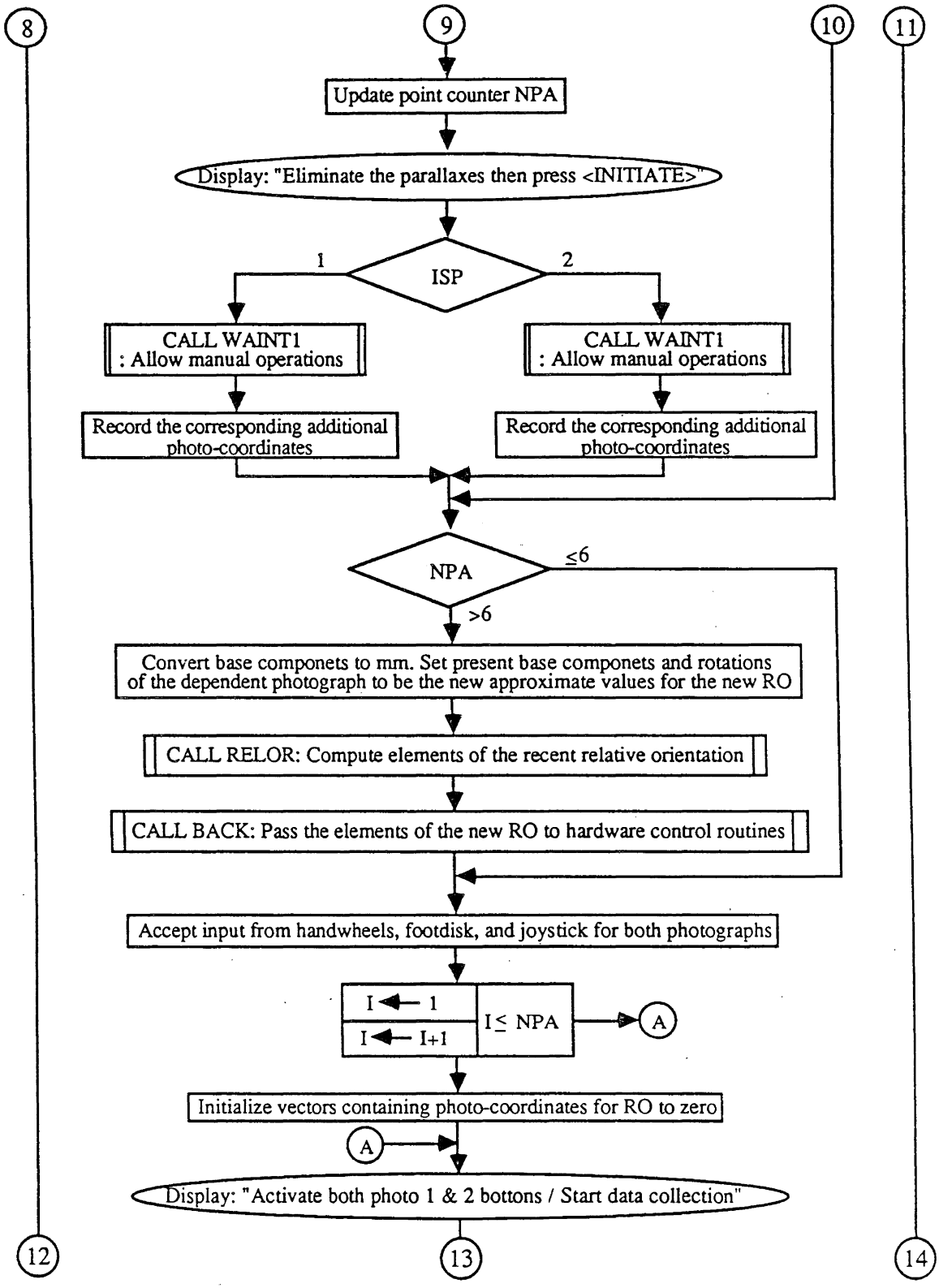
8
9
10
11
Update point counter NPA
Display: "Eliminate the parallaxes then press <INITIATE>"
1
ISP
2
CALL WAINT1
: Allow manual operations
CALL WAINT1
: Allow manual operations
Record the corresponding additional photo-coordinates
Record the corresponding additional photo-coordinates
NPA
≤6
>6
Convert base componets to mm. Set present base componets and rotations of the dependent photograph to be the new approximate values for the new RO
CALL RELOR: Compute elements of the recent relative orientation
CALL BACK: Pass the elements of the new RO to hardware control routines
Accept input from handwheels, footdisk, and joystick for both photographs
I ← 1
I ← I+1
I≤ NPA
A
Initialize vectors containing photo-coordinates for RO to zero
A
Display: "Activate both photo 1 & 2 bottons / Start data collection"
12
13
14

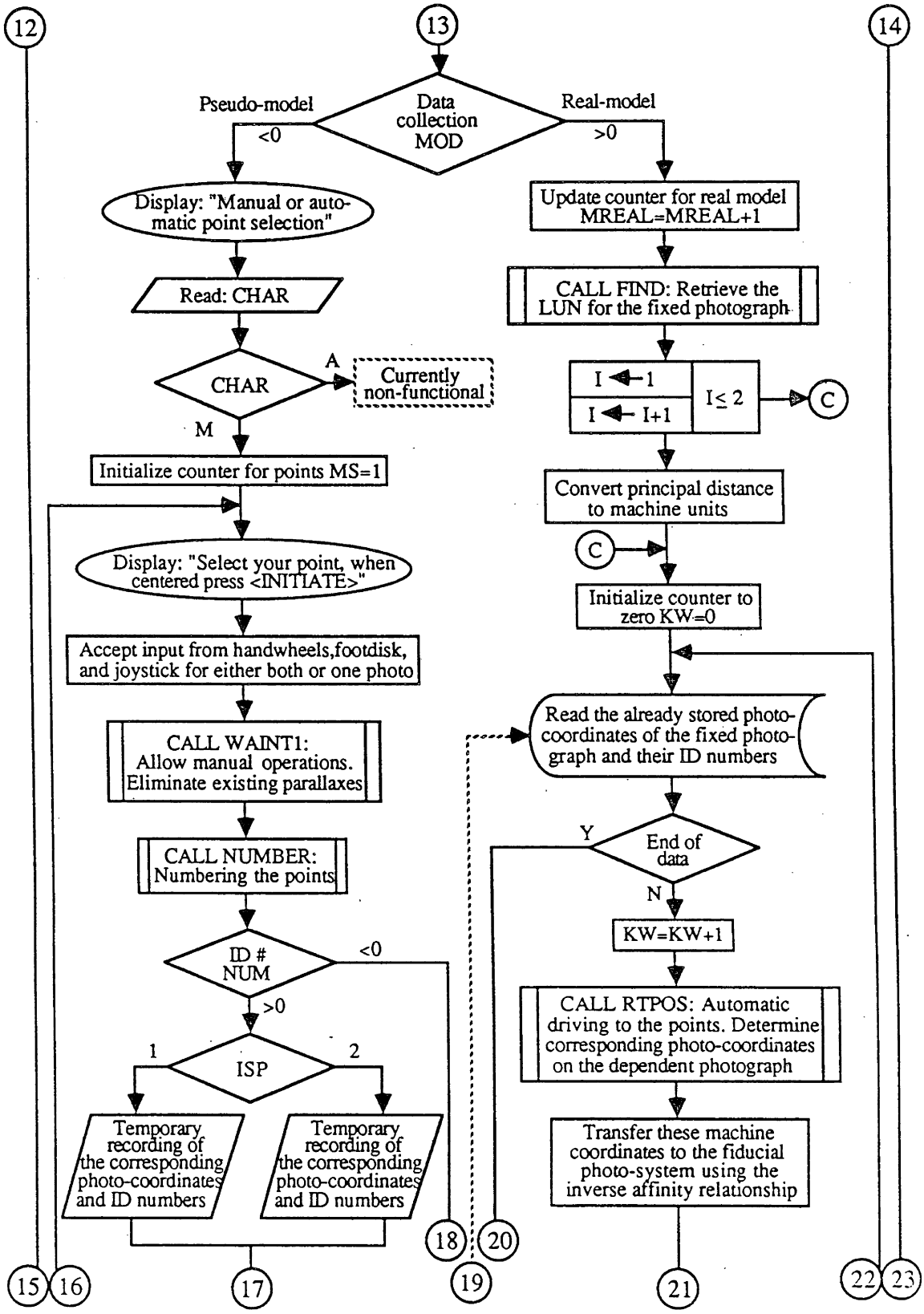
12
13
14
Data collection MOD
Pseudo-model
<0
Real-model
>0
Display: "Manual or automatic point selection"
Read: CHAR
CHAR
A
Currently non-functional
M
Initialize counter for points MS=1
Display: "Select your point, when centered press <INITIATE>"
Accept input from handwheels,footdisk, and joystick for either both or one photo
CALL WAINT1: Allow manual operations. Eliminate existing parallaxes
CALL NUMBER: Numbering the points
ID # NUM
<0
>0
1
ISP
2
Temporary recording of the corresponding photo-coordinates and ID numbers
Temporary recording of the corresponding photo-coordinates and ID numbers
Update counter for real model MREAL=MREAL+1
CALL FIND: Retrieve the LUN for the fixed photograph
I ← 1
I ← I+1
I≤ 2
C
Convert principal distance to machine units
C
Initialize counter to zero KW=0
Read the already stored photo-coordinates of the fixed photograph and their ID numbers
Y
End of data
N
KW=KW+1
CALL RTPOS: Automatic driving to the points. Determine corresponding photo-coordinates on the dependent photograph
Transfer these machine coordinates to the fiducial photo-system using the inverse affinity relationship
15
16
17
18
19
20
21
22
23

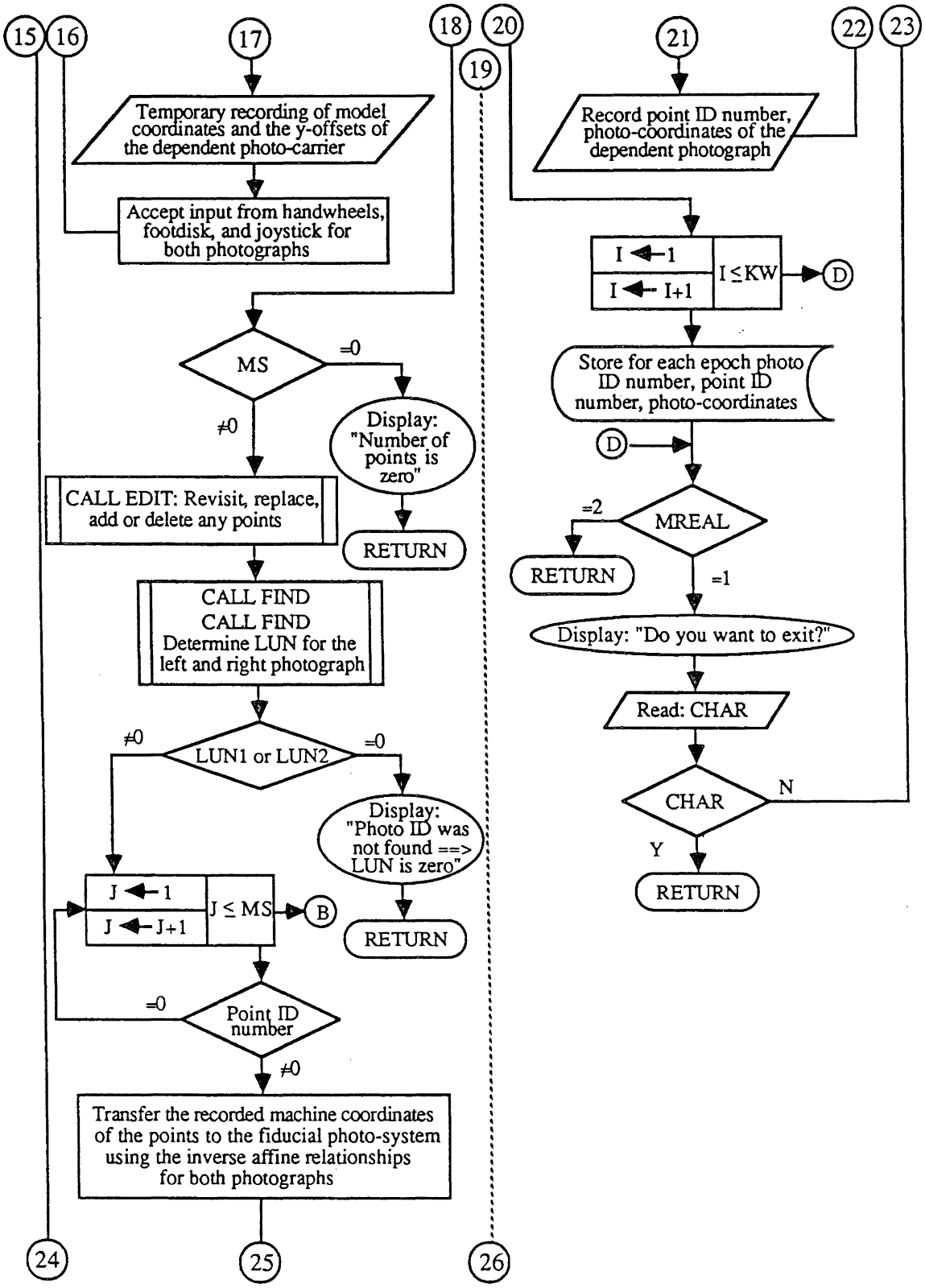
15
16
17
18
19
20
21
22
23
Temporary recording of model coordinates and the y-offsets of the dependent photo-carrier
Accept input from handwheels, footdisk, and joystick for both photographs
MS
=0
≠0
Display: "Number of points is zero"
RETURN
CALL EDIT: Revisit, replace, add or delete any points
CALL FIND
CALL FIND
Determine LUN for the left and right photograph
≠0
LUN1 or LUN2
=0
Display: "Photo ID was not found ==> LUN is zero"
RETURN
J ← 1
J ← J+1
J ≤ MS
B
=0
Point ID number
≠0
Transfer the recorded machine coordinates of the points to the fiducial photo-system using the inverse affine relationships for both photographs
Record point ID number, photo-coordinates of the dependent photograph
I ← 1
I ← I+1
I ≤ KW
D
Store for each epoch photo ID number, point ID number, photo-coordinates
D
=2
MREAL
RETURN
=1
Display: "Do you want to exit?"
Read: CHAR
CHAR
N
Y
RETURN
24
25
26

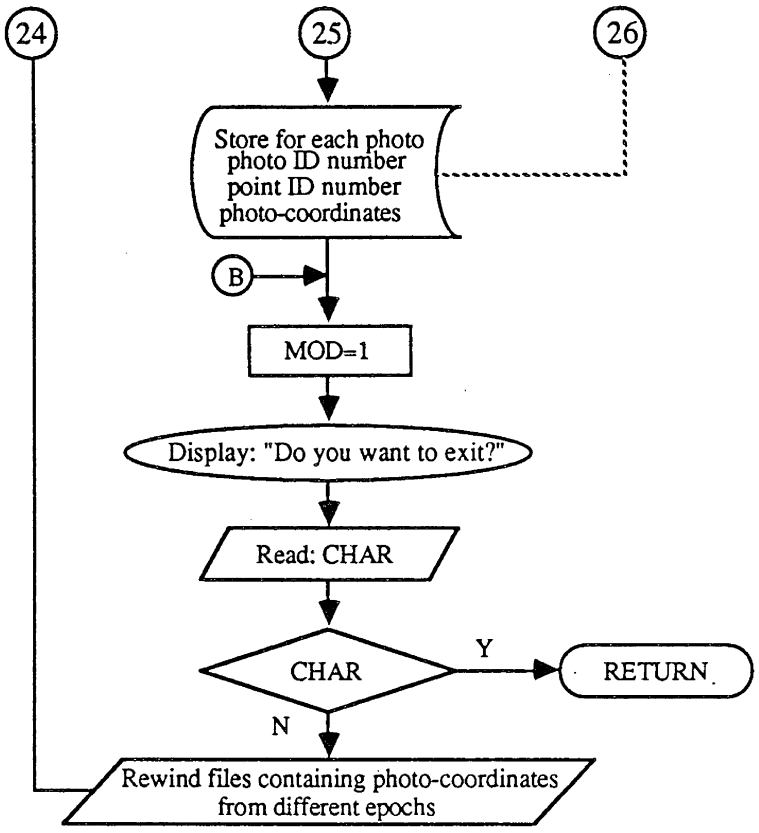
24
25
26
Store for each photo
photo ID number
point ID number
photo-coordinates
B
MOD=1
Display: "Do you want to exit?"
Read: CHAR
CHAR
Y
RETURN
N
Rewind files containing photo-coordinates
from different epochs

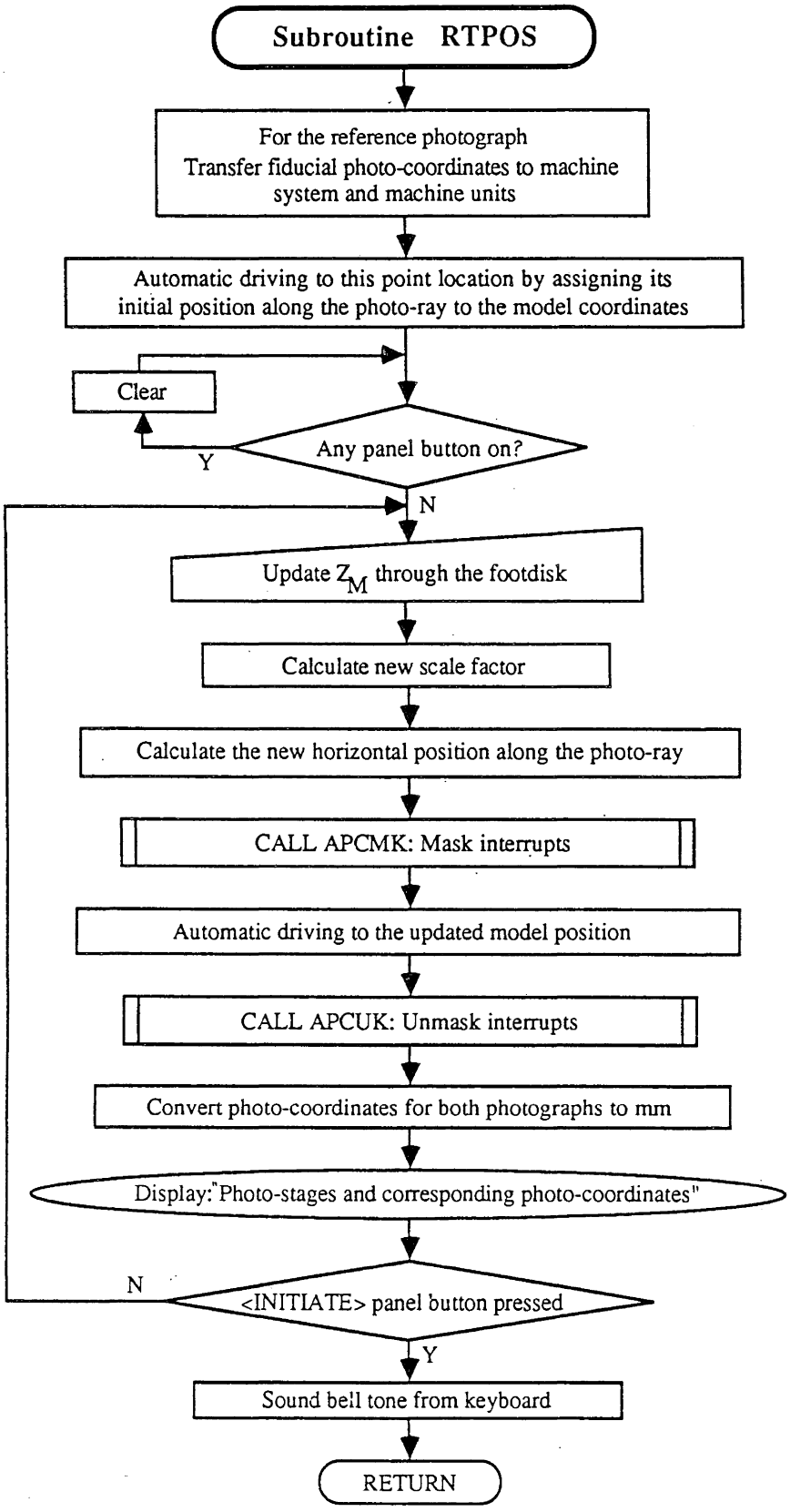
Subroutine RTPOS
For the reference photograph
Transfer fiducial photo-coordinates to machine system and machine units
Automatic driving to this point location by assigning its initial position along the photo-ray to the model coordinates
Clear
Any panel button on?
Y
N
Update Z_M through the footdisk
Calculate new scale factor
Calculate the new horizontal position along the photo-ray
CALL APCMK: Mask interrupts
Automatic driving to the updated model position
CALL APCUK: Unmask interrupts
Convert photo-coordinates for both photographs to mm
Display:"Photo-stages and corresponding photo-coordinates"
N
<INITIATE> panel button pressed
Y
Sound bell tone from keyboard
RETURN

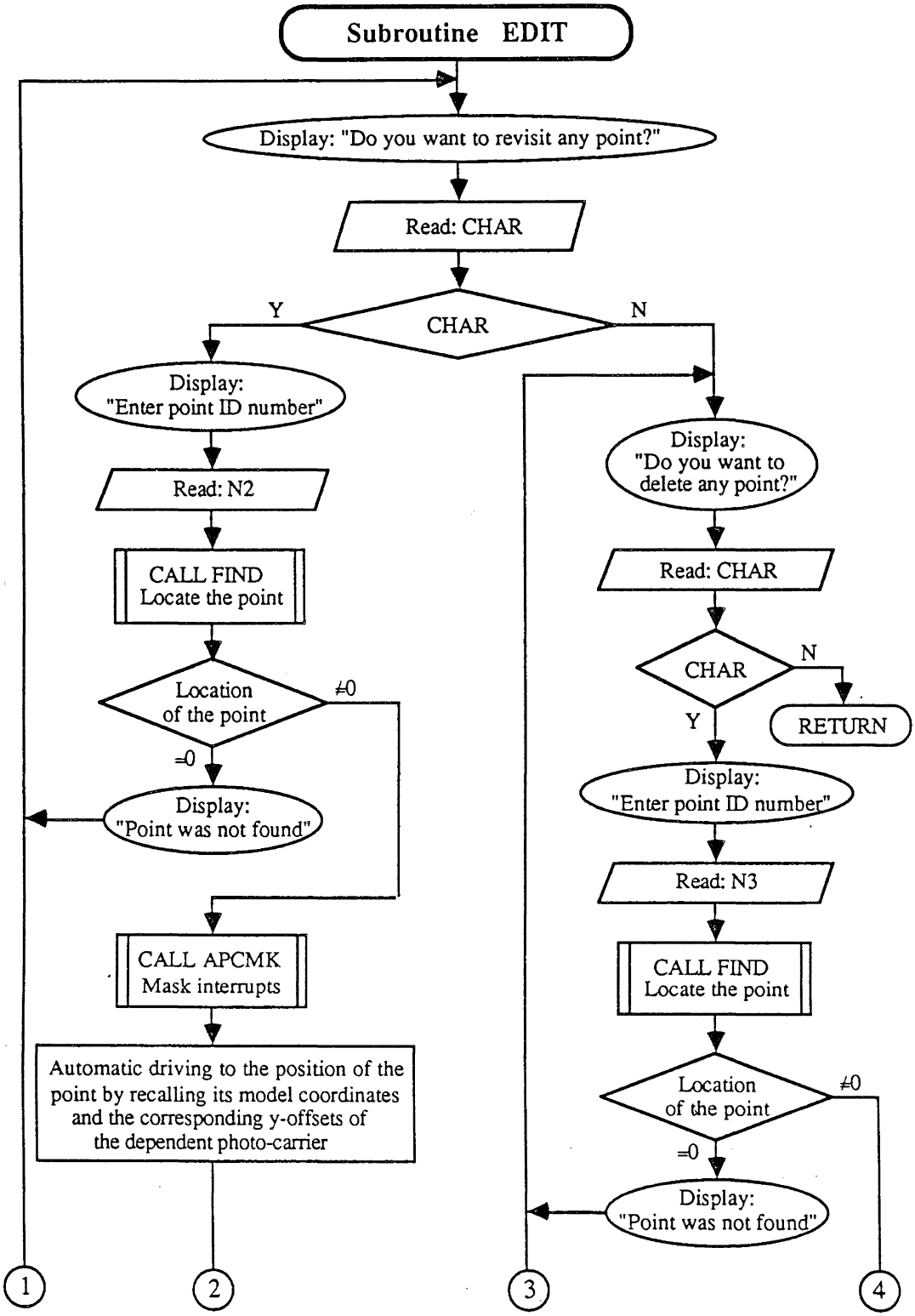
Subroutine EDIT
Display: "Do you want to revisit any point?"
Read: CHAR
CHAR
Y
N
Display: "Enter point ID number"
Read: N2
CALL FIND Locate the point
Location of the point
≠0
=0
Display: "Point was not found"
CALL APCMK Mask interrupts
Automatic driving to the position of the point by recalling its model coordinates and the corresponding y-offsets of the dependent photo-carrier
Display: "Do you want to delete any point?"
Read: CHAR
CHAR
N
Y
RETURN
Display: "Enter point ID number"
Read: N3
CALL FIND Locate the point
Location of the point
≠0
=0
Display: "Point was not found"
1
2
3
4

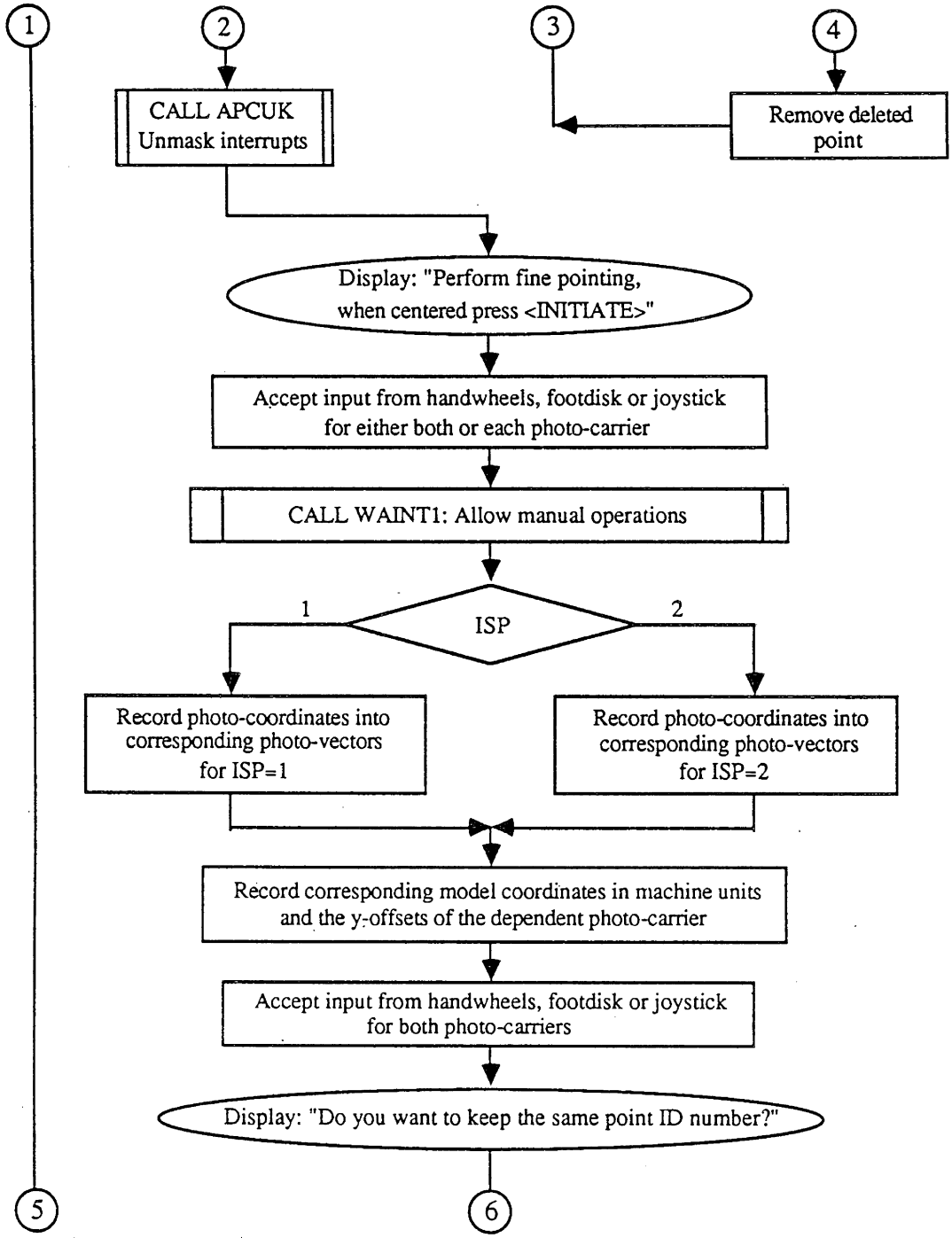
1
2
3
4
CALL APCUK
Unmask interrupts
Remove deleted
point
Display: "Perform fine pointing,
when centered press <INITIATE>"
Accept input from handwheels, footdisk or joystick
for either both or each photo-carrier
CALL WAINT1: Allow manual operations
1
ISP
2
Record photo-coordinates into
corresponding photo-vectors
for ISP=1
Record photo-coordinates into
corresponding photo-vectors
for ISP=2
Record corresponding model coordinates in machine units
and the y-offsets of the dependent photo-carrier
Accept input from handwheels, footdisk or joystick
for both photo-carriers
Display: "Do you want to keep the same point ID number?"
5
6

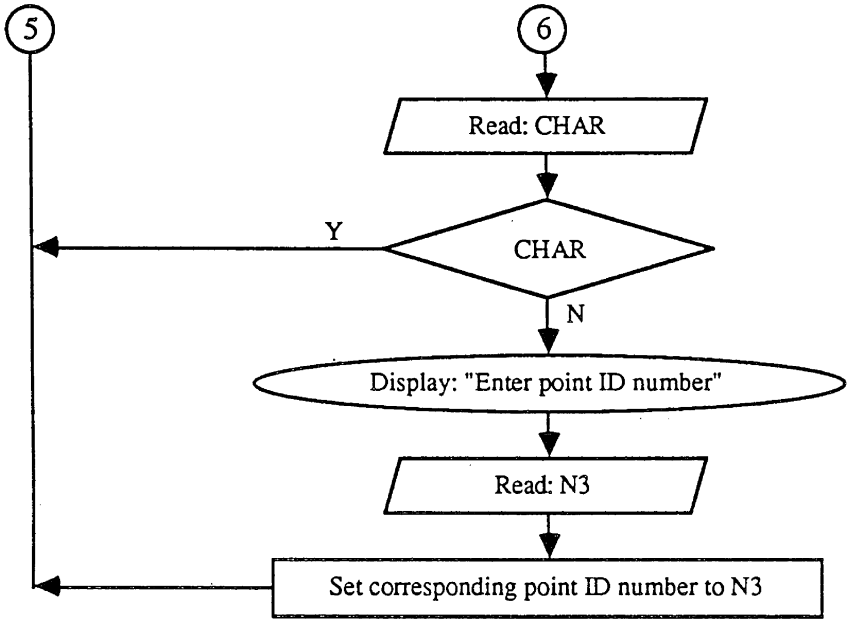
5
6
Read: CHAR
Y
CHAR
N
Display: "Enter point ID number"
Read: N3
Set corresponding point ID number to N3

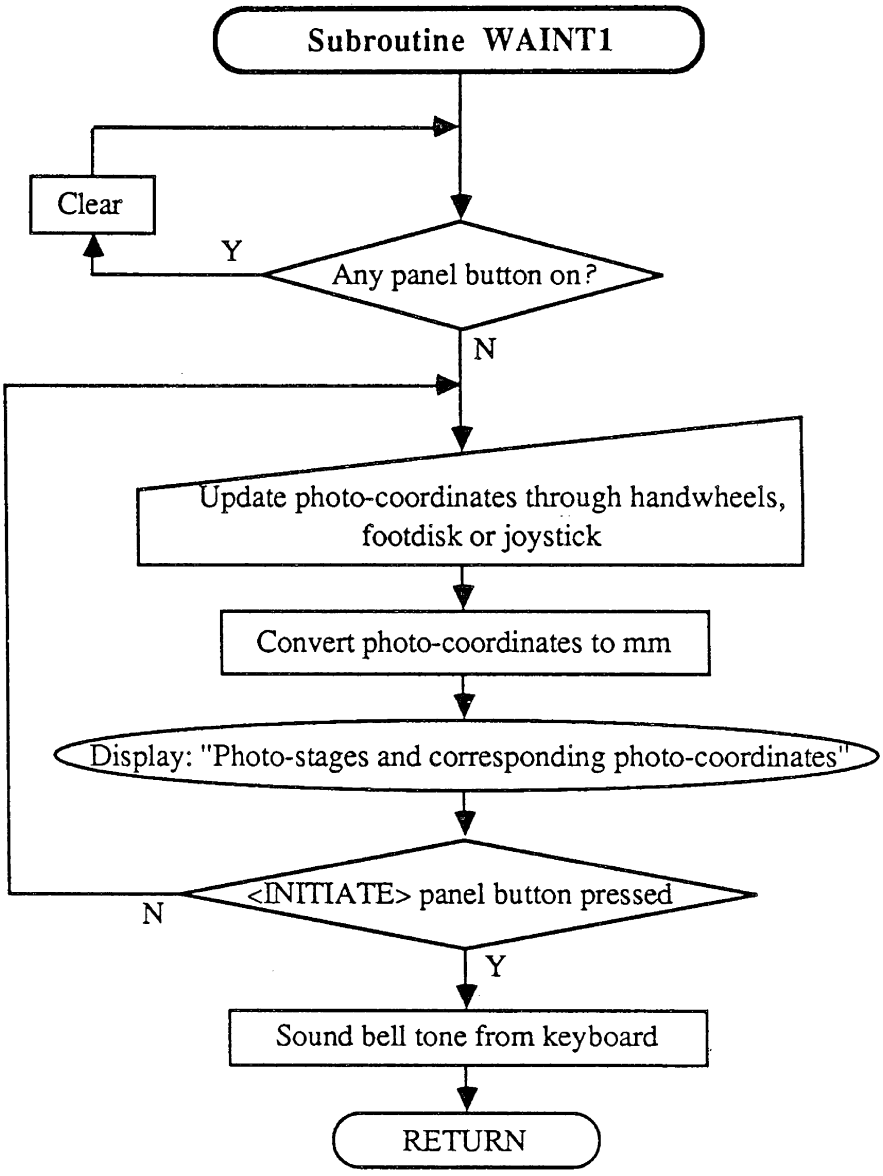
Subroutine WAINT1
Clear
Y
Any panel button on?
N
Update photo-coordinates through handwheels, footdisk or joystick
Convert photo-coordinates to mm
Display: "Photo-stages and corresponding photo-coordinates"
<INITIATE> panel button pressed
N
Y
Sound bell tone from keyboard
RETURN

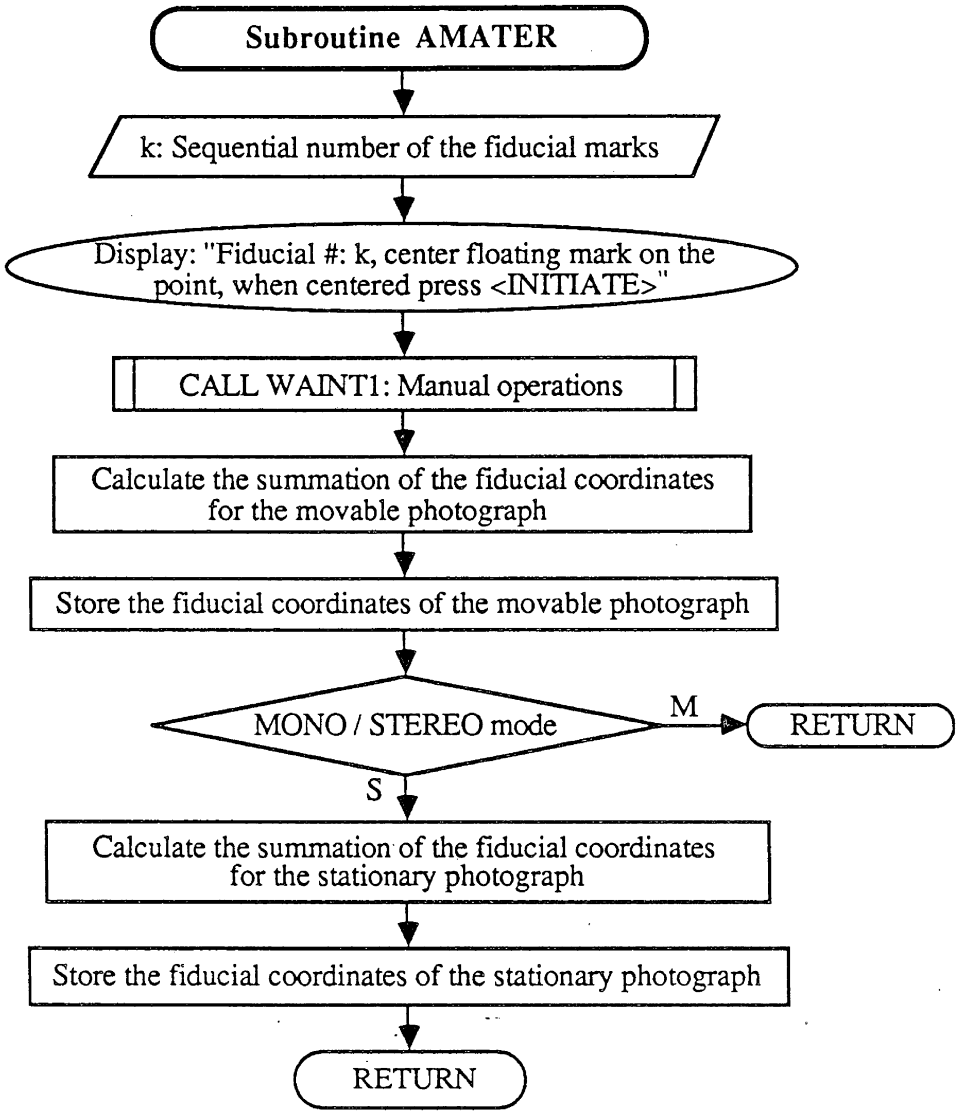
Subroutine AMATER
k: Sequential number of the fiducial marks
Display: "Fiducial #: k, center floating mark on the point, when centered press <INITIATE>"
CALL WAINT1: Manual operations
Calculate the summation of the fiducial coordinates for the movable photograph
Store the fiducial coordinates of the movable photograph
MONO / STEREO mode
M
RETURN
S
Calculate the summation of the fiducial coordinates for the stationary photograph
Store the fiducial coordinates of the stationary photograph
RETURN

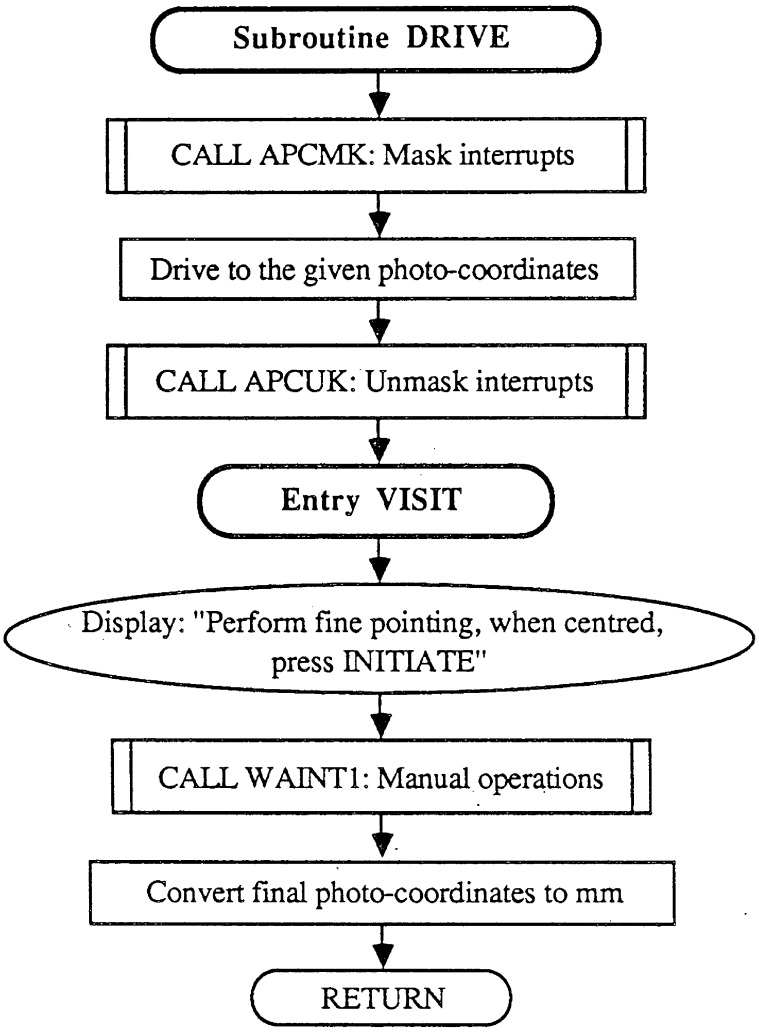
Subroutine DRIVE
CALL APCMK: Mask interrupts
Drive to the given photo-coordinates
CALL APCUK: Unmask interrupts
Entry VISIT
Display: "Perform fine pointing, when centred, press INITIATE"
CALL WAINT1: Manual operations
Convert final photo-coordinates to mm
RETURN

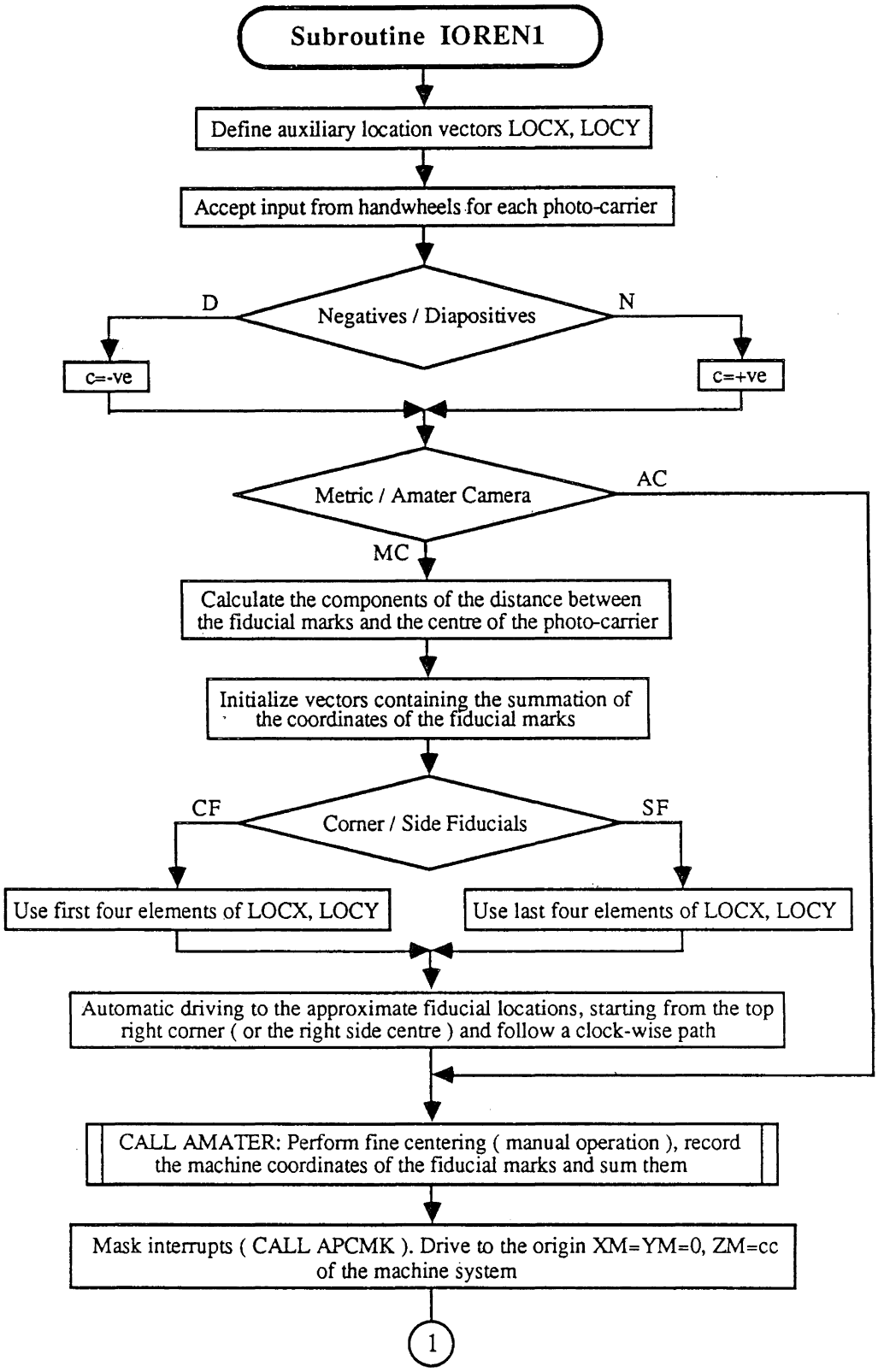
Subroutine IOREN1
Define auxiliary location vectors LOCX, LOCY
Accept input from handwheels for each photo-carrier
D
Negatives / Diapositives
N
c=-ve
c=+ve
Metric / Amater Camera
AC
MC
Calculate the components of the distance between the fiducial marks and the centre of the photo-carrier
Initialize vectors containing the summation of the coordinates of the fiducial marks
CF
Corner / Side Fiducials
SF
Use first four elements of LOCX, LOCY
Use last four elements of LOCX, LOCY
Automatic driving to the approximate fiducial locations, starting from the top right corner (or the right side centre) and follow a clock-wise path
CALL AMATER: Perform fine centering (manual operation), record the machine coordinates of the fiducial marks and sum them
Mask interrupts (CALL APCMK). Drive to the origin XM=YM=0, ZM=cc of the machine system
1

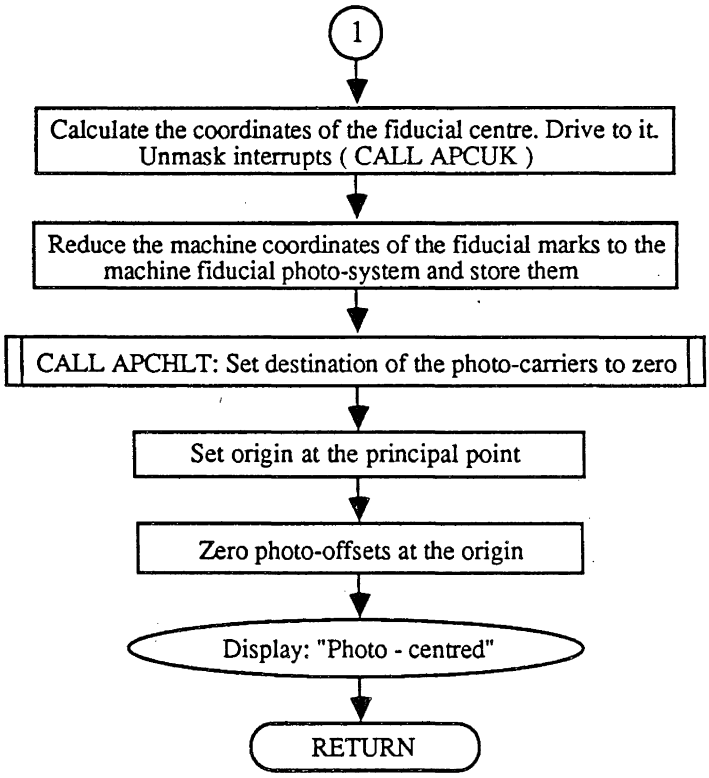
1
Calculate the coordinates of the fiducial centre. Drive to it. Unmask interrupts (CALL APCUK)
Reduce the machine coordinates of the fiducial marks to the machine fiducial photo-system and store them
CALL APCHLT: Set destination of the photo-carriers to zero
Set origin at the principal point
Zero photo-offsets at the origin
Display: "Photo - centred"
RETURN

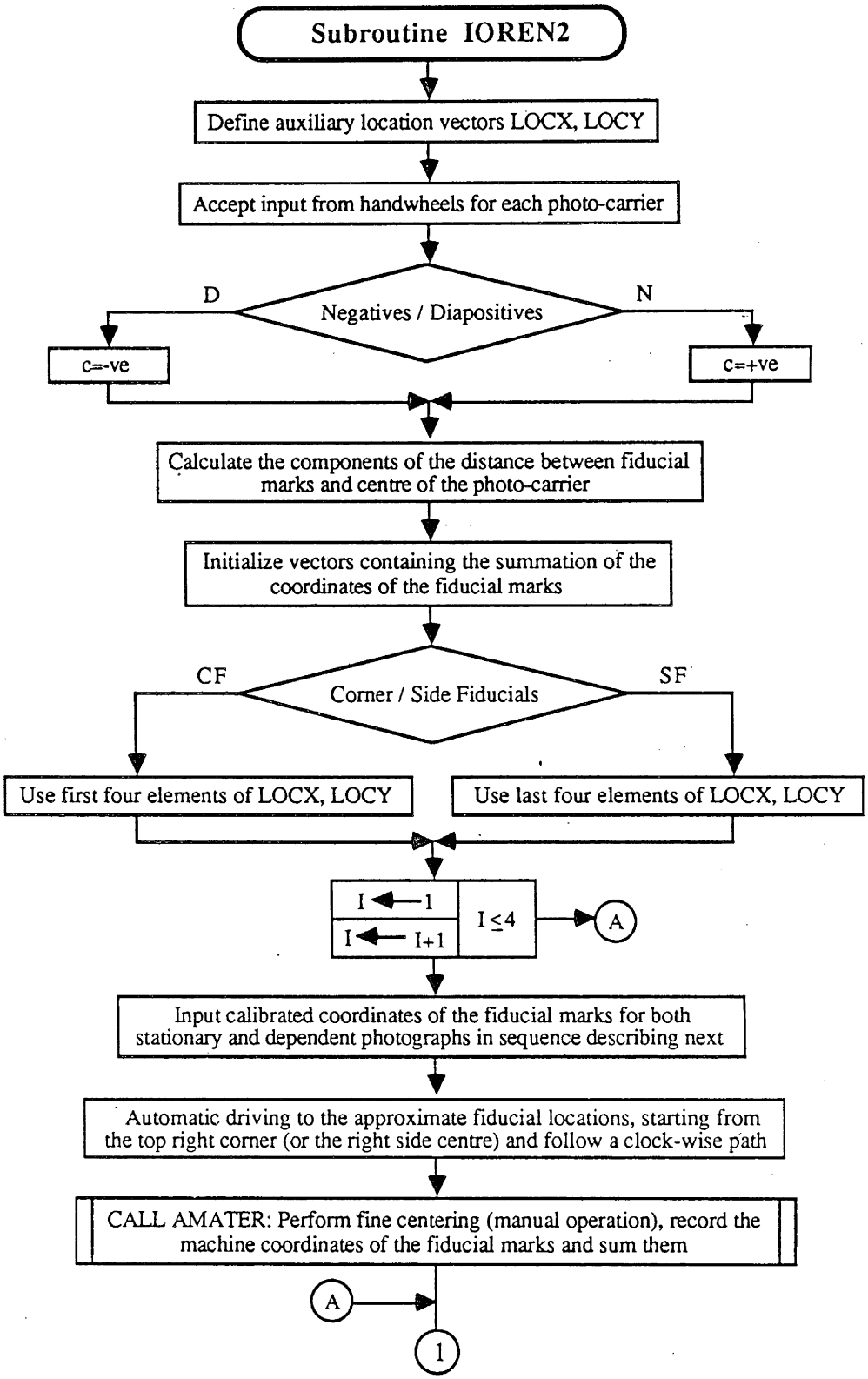
Subroutine IOREN2
Define auxiliary location vectors LOCX, LOCY
Accept input from handwheels for each photo-carrier
D
Negatives / Diapositives
N
c=-ve
c=+ve
Calculate the components of the distance between fiducial marks and centre of the photo-carrier
Initialize vectors containing the summation of the coordinates of the fiducial marks
CF
Corner / Side Fiducials
SF
Use first four elements of LOCX, LOCY
Use last four elements of LOCX, LOCY
I ← 1
I ← I+1
I ≤ 4
A
Input calibrated coordinates of the fiducial marks for both stationary and dependent photographs in sequence describing next
Automatic driving to the approximate fiducial locations, starting from the top right corner (or the right side centre) and follow a clock-wise path
CALL AMATER: Perform fine centering (manual operation), record the machine coordinates of the fiducial marks and sum them
A
1

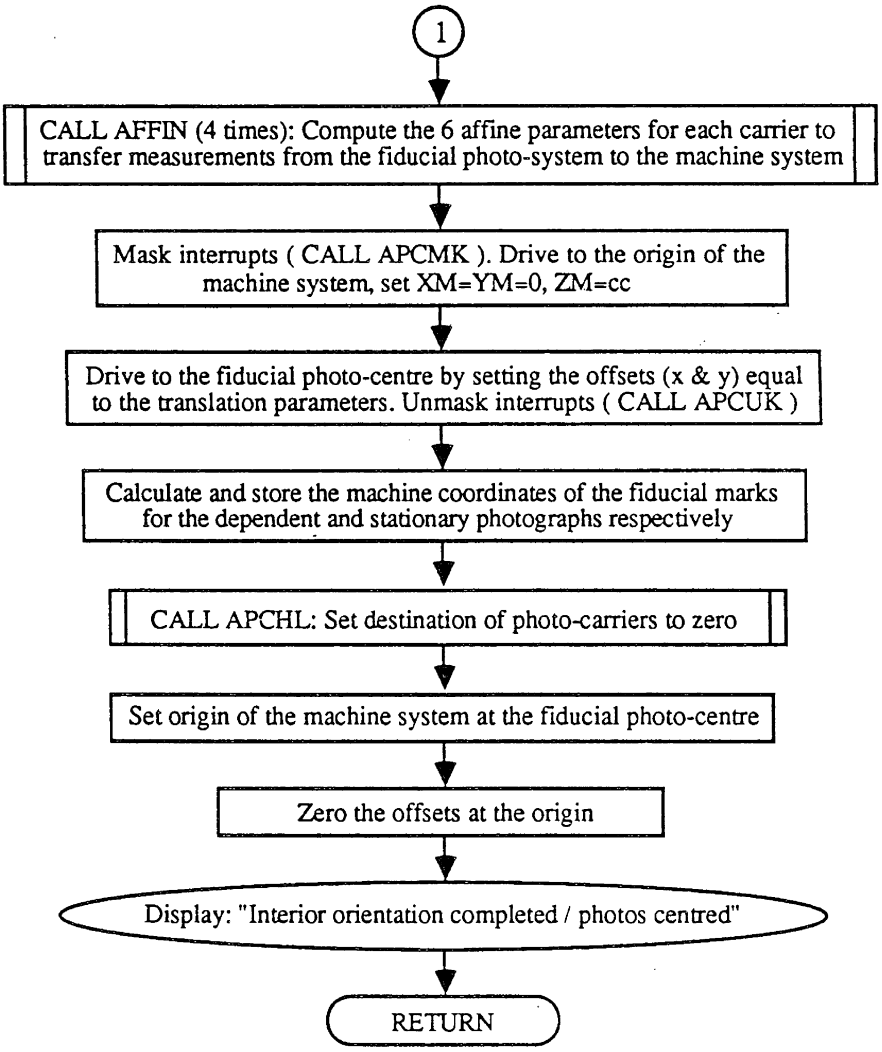
1
CALL AFFIN (4 times): Compute the 6 affine parameters for each carrier to transfer measurements from the fiducial photo-system to the machine system
Mask interrupts (CALL APCMK). Drive to the origin of the machine system, set XM=YM=0, ZM=cc
Drive to the fiducial photo-centre by setting the offsets (x & y) equal to the translation parameters. Unmask interrupts (CALL APCUK)
Calculate and store the machine coordinates of the fiducial marks for the dependent and stationary photographs respectively
CALL APCHL: Set destination of photo-carriers to zero
Set origin of the machine system at the fiducial photo-centre
Zero the offsets at the origin
Display: "Interior orientation completed / photos centred"
RETURN

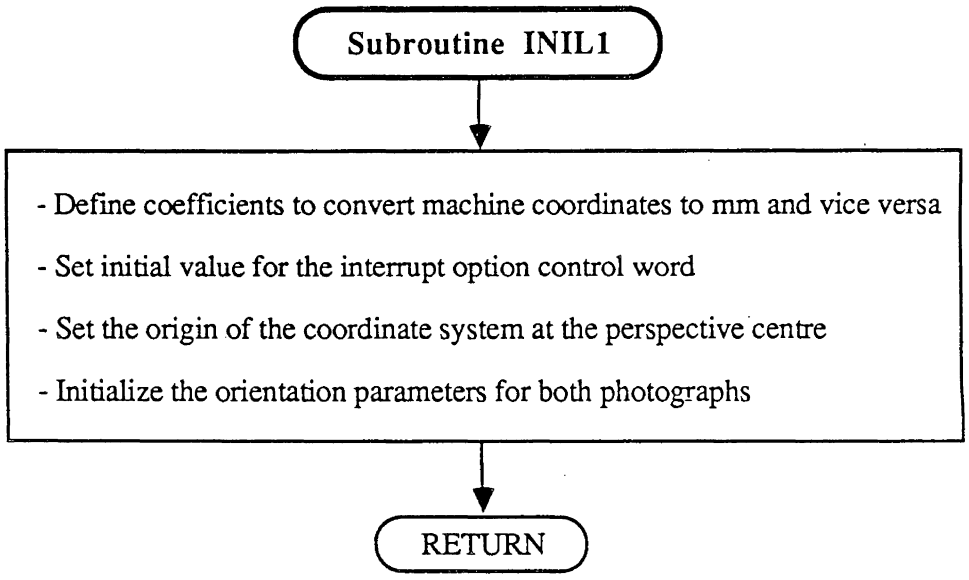
Subroutine INIL1
- Define coefficients to convert machine coordinates to mm and vice versa
- Set initial value for the interrupt option control word
- Set the origin of the coordinate system at the perspective centre
- Initialize the orientation parameters for both photographs
RETURN

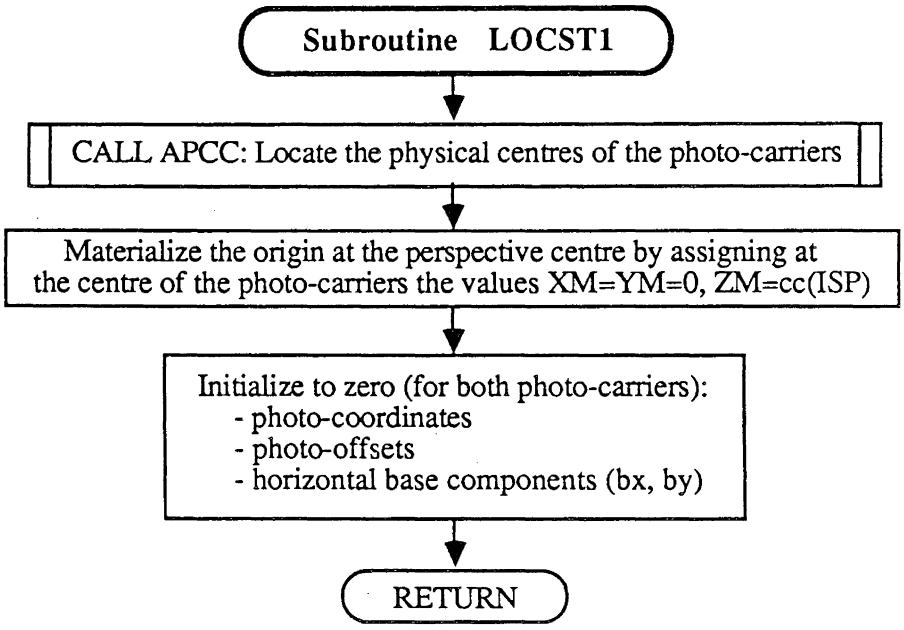
Subroutine LOCST1
CALL APCC: Locate the physical centres of the photo-carriers
Materialize the origin at the perspective centre by assigning at the centre of the photo-carriers the values XM=YM=0, ZM=cc(ISP)
Initialize to zero (for both photo-carriers):
- photo-coordinates
- photo-offsets
- horizontal base components (bx, by)
RETURN

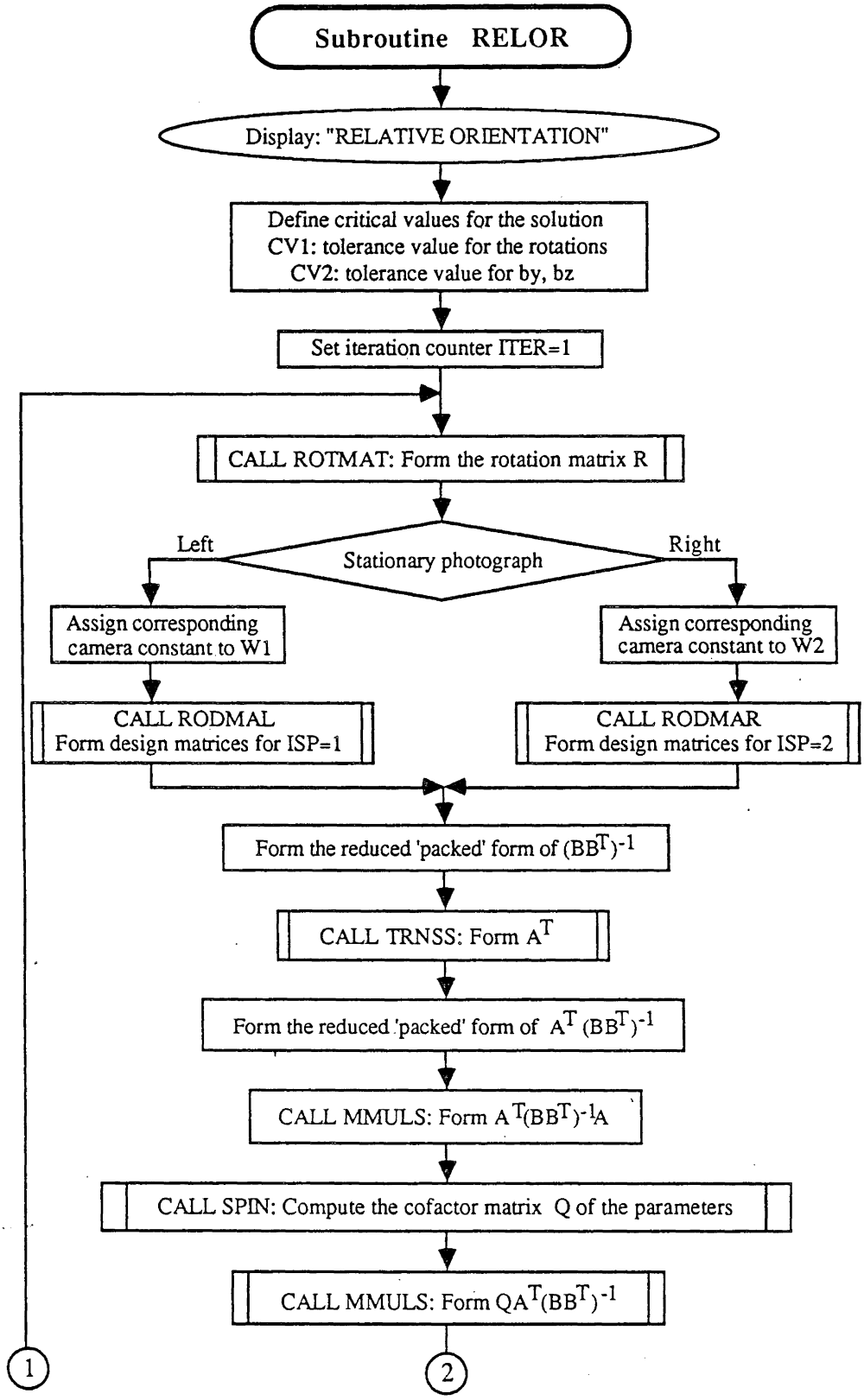
Subroutine RELOR
Display: "RELATIVE ORIENTATION"
Define critical values for the solution
CV1: tolerance value for the rotations
CV2: tolerance value for by, bz
Set iteration counter ITER=1
CALL ROTMAT: Form the rotation matrix R
Left
Stationary photograph
Right
Assign corresponding camera constant to W1
Assign corresponding camera constant to W2
CALL RODMAL
Form design matrices for ISP=1
CALL RODMAR
Form design matrices for ISP=2
Form the reduced 'packed' form of $(BB^T)^{-1}$
CALL TRNSS: Form A^T
Form the reduced 'packed' form of $A^T(BB^T)^{-1}$
CALL MMULS: Form $A^T(BB^T)^{-1}A$
CALL SPIN: Compute the cofactor matrix Q of the parameters
CALL MMULS: Form $QA^T(BB^T)^{-1}$
1
2

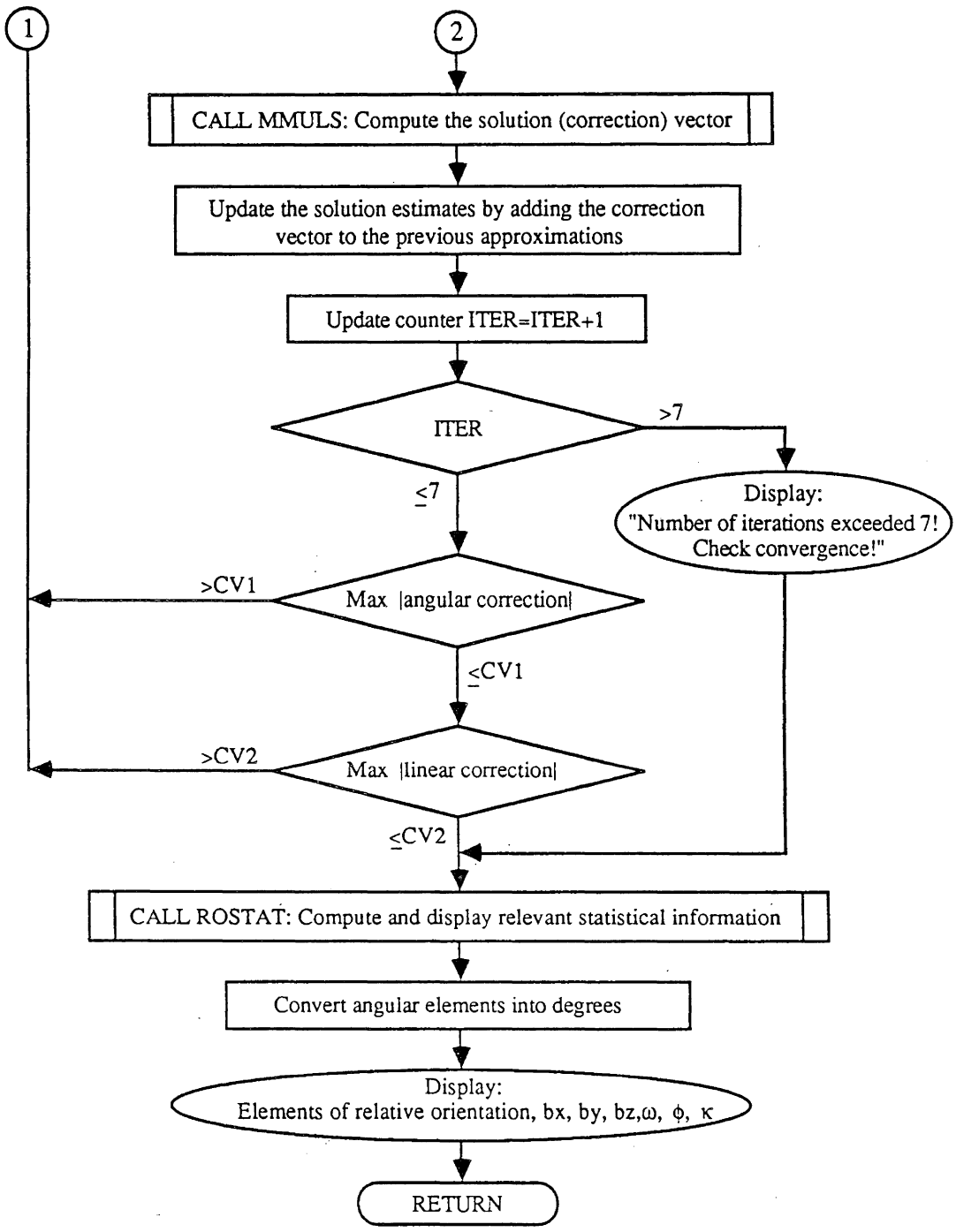
1
2
CALL MMULS: Compute the solution (correction) vector
Update the solution estimates by adding the correction vector to the previous approximations
Update counter ITER=ITER+1
ITER
>7
≤7
Display: "Number of iterations exceeded 7! Check convergence!"
>CV1
Max |angular correction|
≤CV1
>CV2
Max |linear correction|
≤CV2
CALL ROSTAT: Compute and display relevant statistical information
Convert angular elements into degrees
Display: Elements of relative orientation, bx, by, bz,ω, ϕ, κ
RETURN

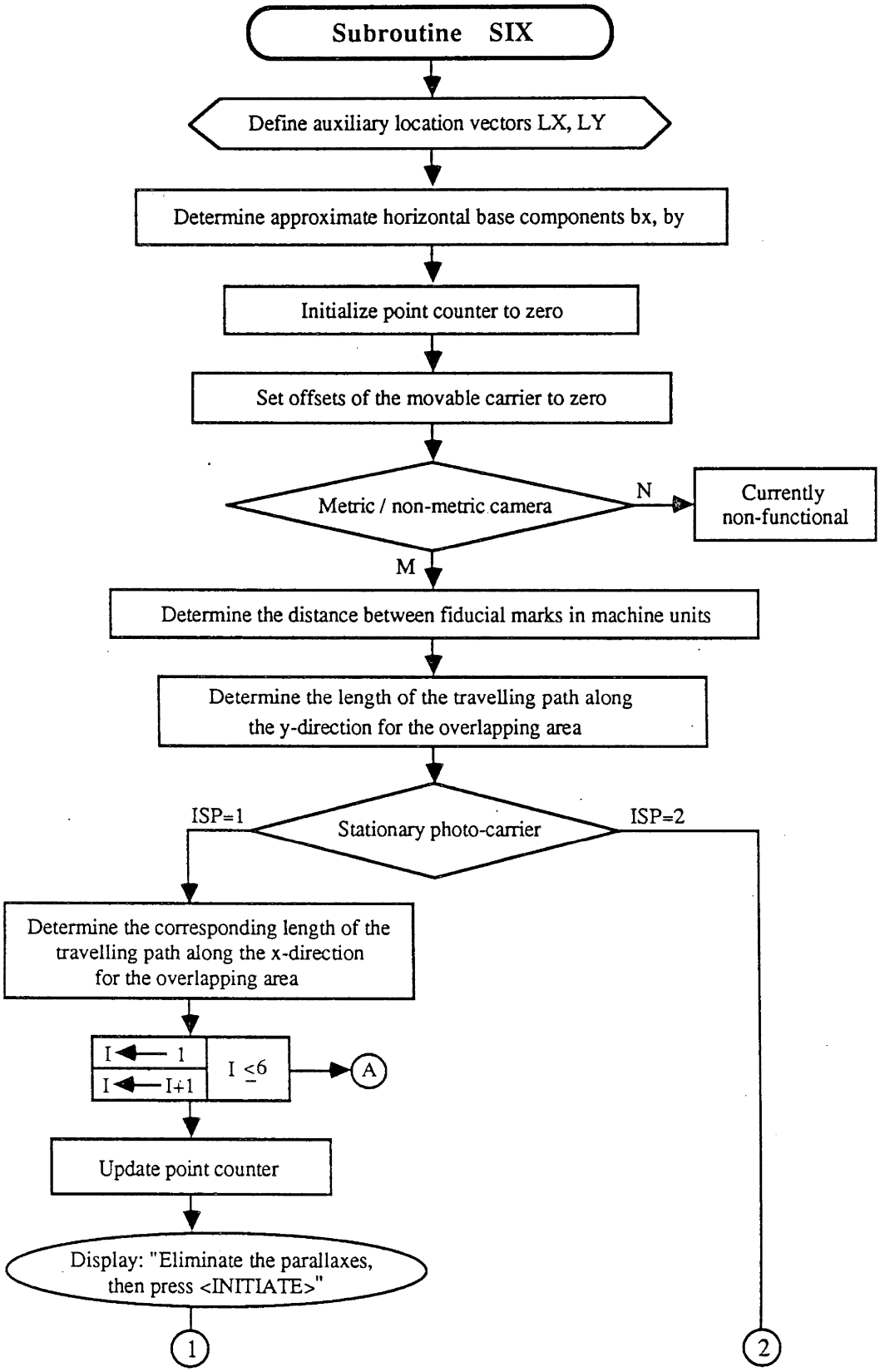
Subroutine SIX
Define auxiliary location vectors LX, LY
Determine approximate horizontal base components bx, by
Initialize point counter to zero
Set offsets of the movable carrier to zero
Metric / non-metric camera
N
Currently non-functional
M
Determine the distance between fiducial marks in machine units
Determine the length of the travelling path along the y-direction for the overlapping area
ISP=1
Stationary photo-carrier
ISP=2
Determine the corresponding length of the travelling path along the x-direction for the overlapping area
I ← 1
I ← I+1
I ≤6
A
Update point counter
Display: "Eliminate the parallaxes, then press <INITIATE>"
1
2

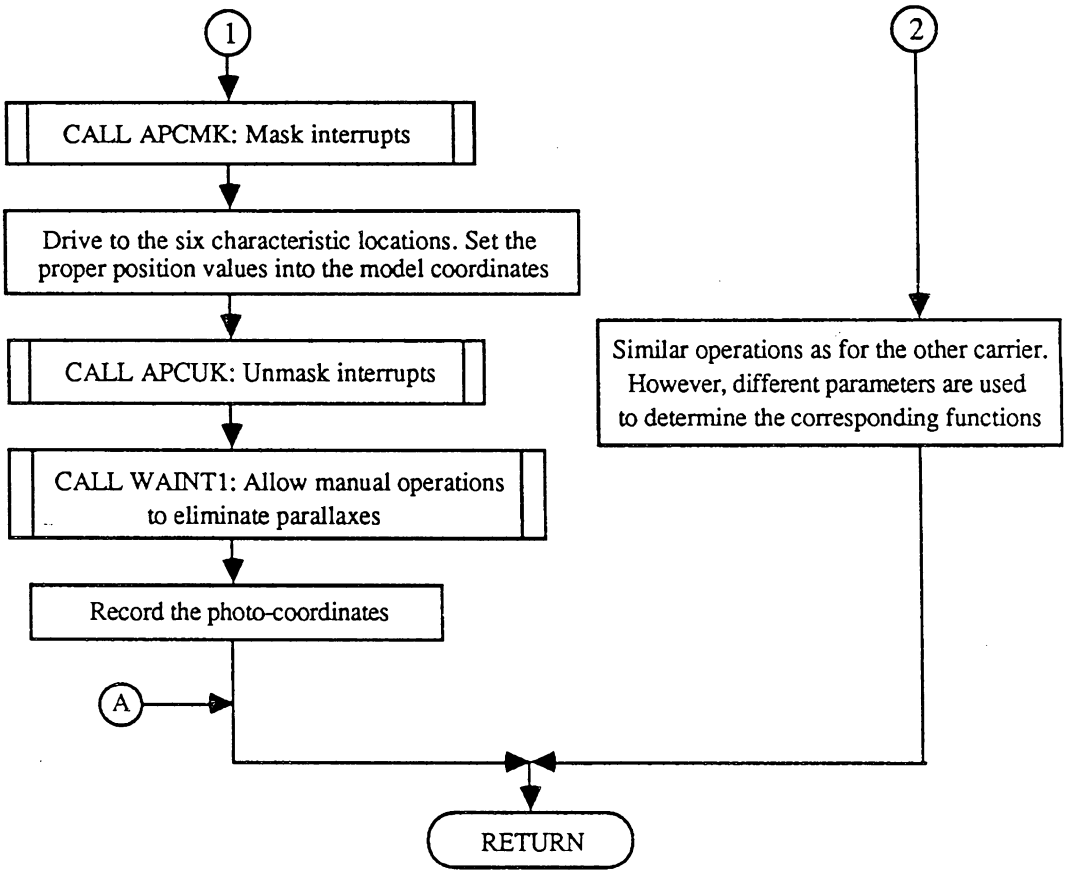
1
CALL APCMK: Mask interrupts
Drive to the six characteristic locations. Set the proper position values into the model coordinates
CALL APCUK: Unmask interrupts
CALL WAINT1: Allow manual operations to eliminate parallaxes
Record the photo-coordinates
A
2
Similar operations as for the other carrier. However, different parameters are used to determine the corresponding functions
RETURN

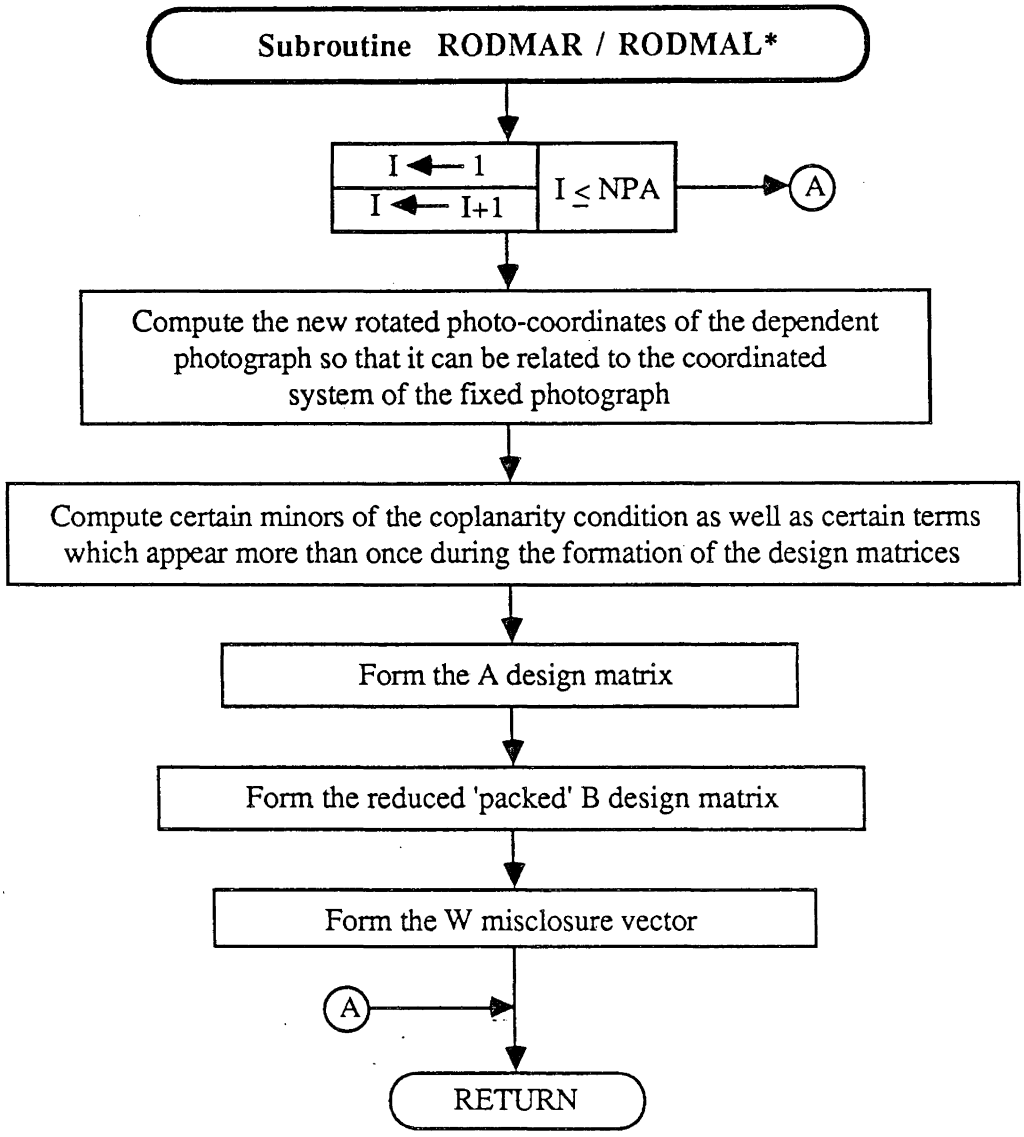

* Note: <RODMAL> is used when the dependent photograph is placed on left photo-carrier during the RO procedure. Otherwise <RODMAR> is used to form the design matrices.

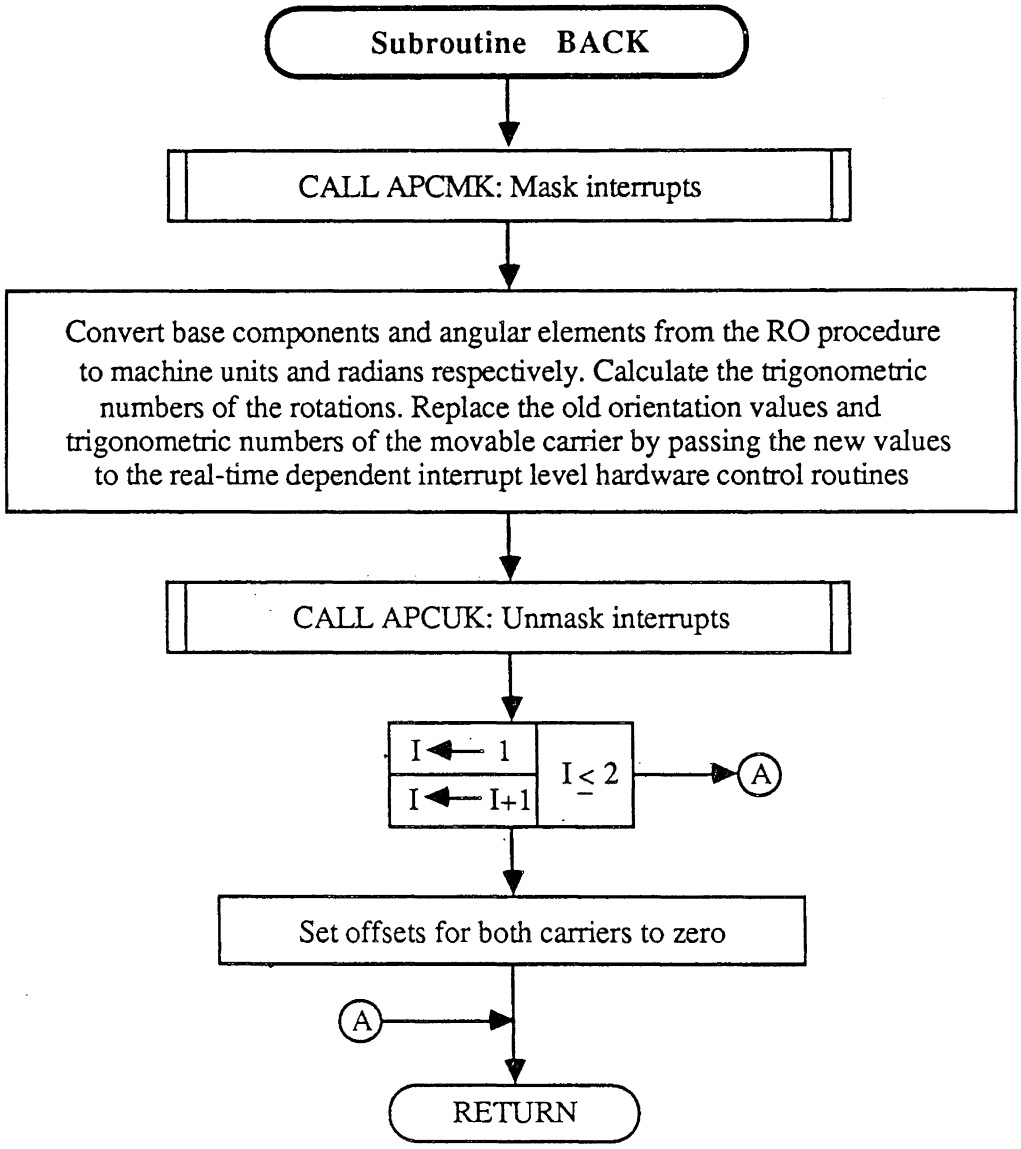
Subroutine BACK
CALL APCMK: Mask interrupts
Convert base components and angular elements from the RO procedure to machine units and radians respectively. Calculate the trigonometric numbers of the rotations. Replace the old orientation values and trigonometric numbers of the movable carrier by passing the new values to the real-time dependent interrupt level hardware control routines
CALL APCUK: Unmask interrupts
I ← 1
I ← I+1
I ≤ 2
A
Set offsets for both carriers to zero
A
RETURN

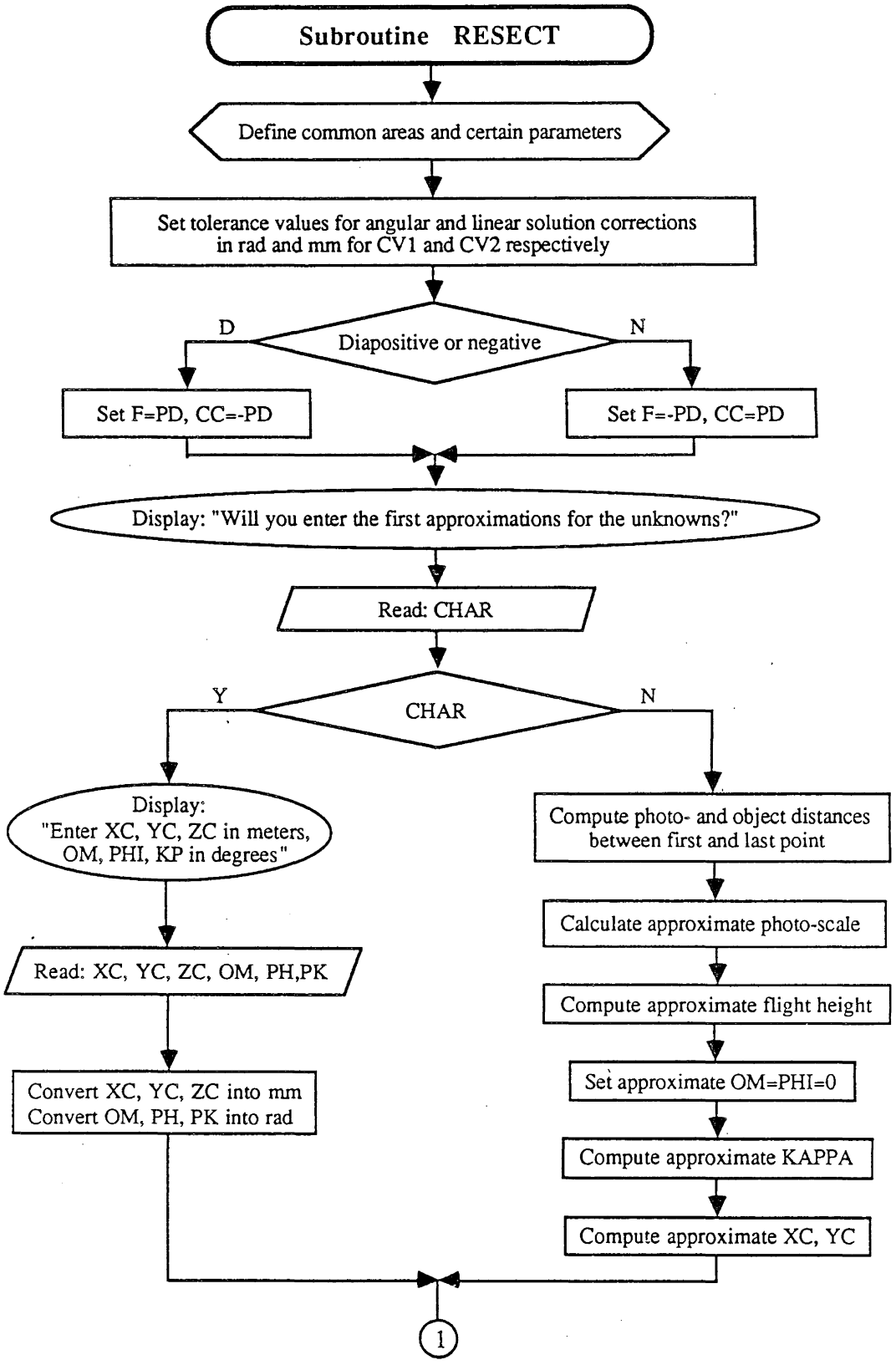
Subroutine RESECT
Define common areas and certain parameters
Set tolerance values for angular and linear solution corrections in rad and mm for CV1 and CV2 respectively
D
Diapositive or negative
N
Set F=PD, CC=-PD
Set F=-PD, CC=PD
Display: "Will you enter the first approximations for the unknowns?"
Read: CHAR
Y
CHAR
N
Display: "Enter XC, YC, ZC in meters, OM, PHI, KP in degrees"
Read: XC, YC, ZC, OM, PH,PK
Convert XC, YC, ZC into mm
Convert OM, PH, PK into rad
Compute photo- and object distances between first and last point
Calculate approximate photo-scale
Compute approximate flight height
Set approximate OM=PHI=0
Compute approximate KAPPA
Compute approximate XC, YC
1

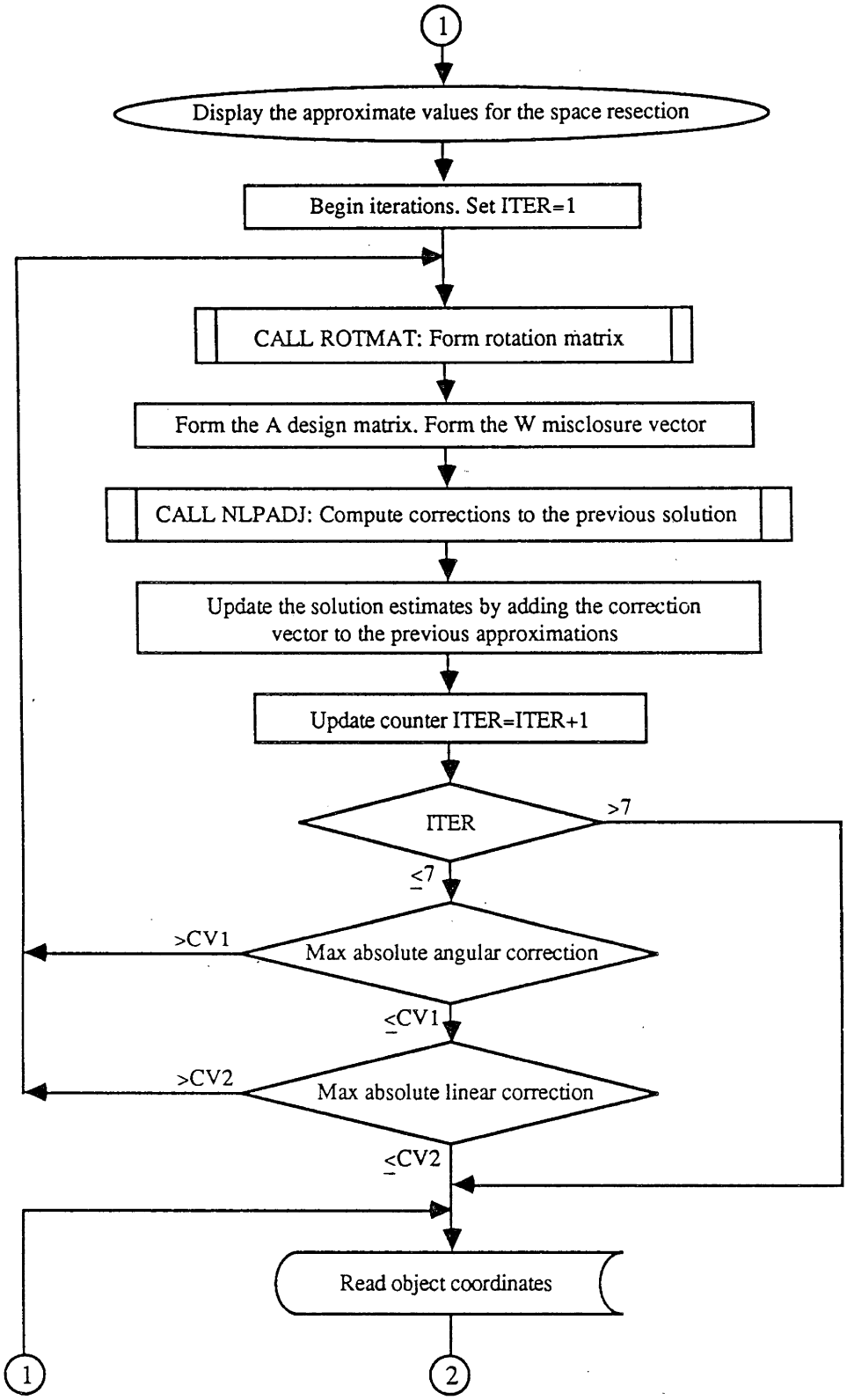
1
Display the approximate values for the space resection
Begin iterations. Set ITER=1
CALL ROTMAT: Form rotation matrix
Form the A design matrix. Form the W misclosure vector
CALL NLPADJ: Compute corrections to the previous solution
Update the solution estimates by adding the correction vector to the previous approximations
Update counter ITER=ITER+1
ITER
>7
≤7
>CV1
Max absolute angular correction
≤CV1
>CV2
Max absolute linear correction
≤CV2
Read object coordinates
1
2

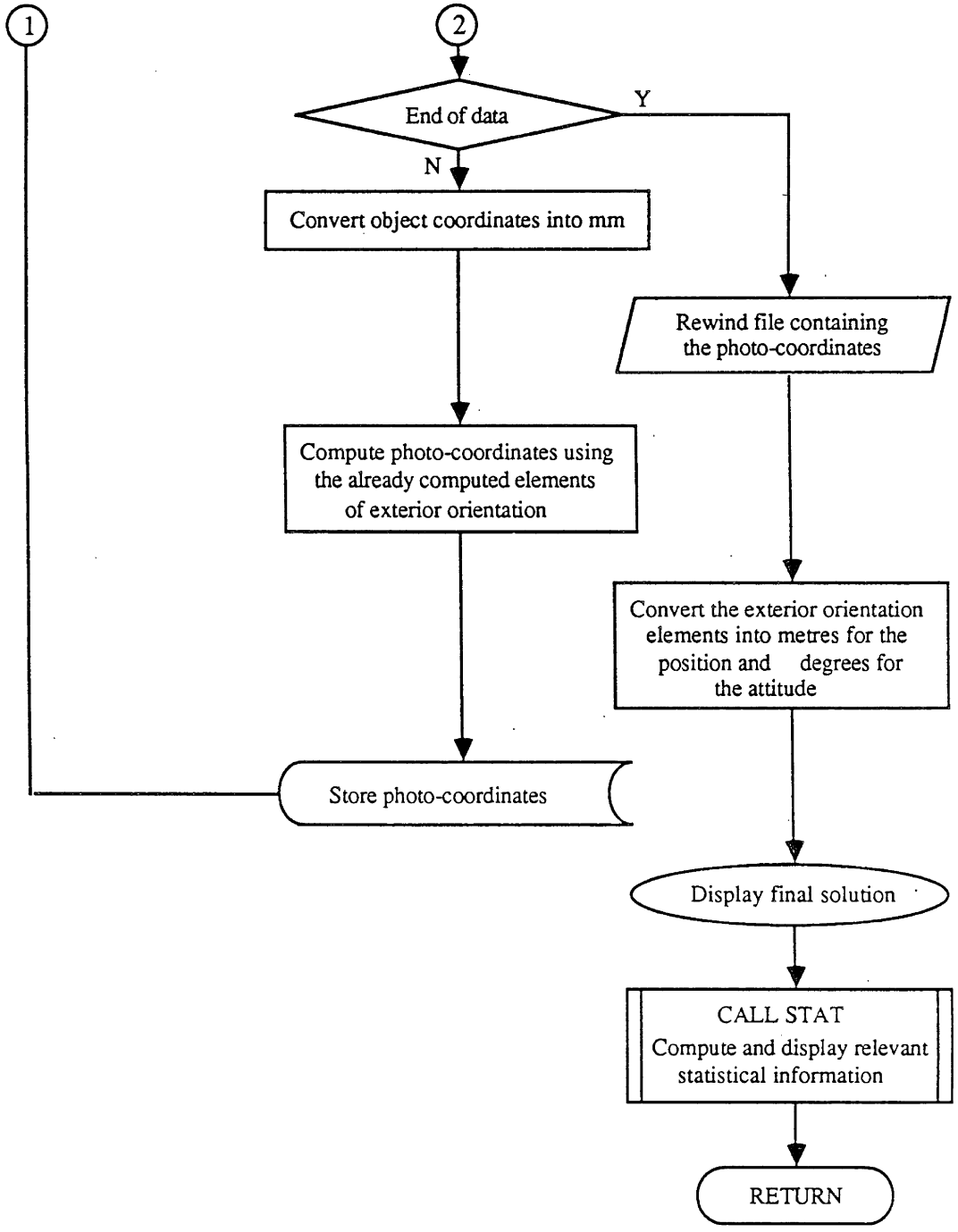
1
2
End of data
Y
N
Convert object coordinates into mm
Rewind file containing the photo-coordinates
Compute photo-coordinates using the already computed elements of exterior orientation
Convert the exterior orientation elements into metres for the position and degrees for the attitude
Store photo-coordinates
Display final solution
CALL STAT
Compute and display relevant statistical information
RETURN

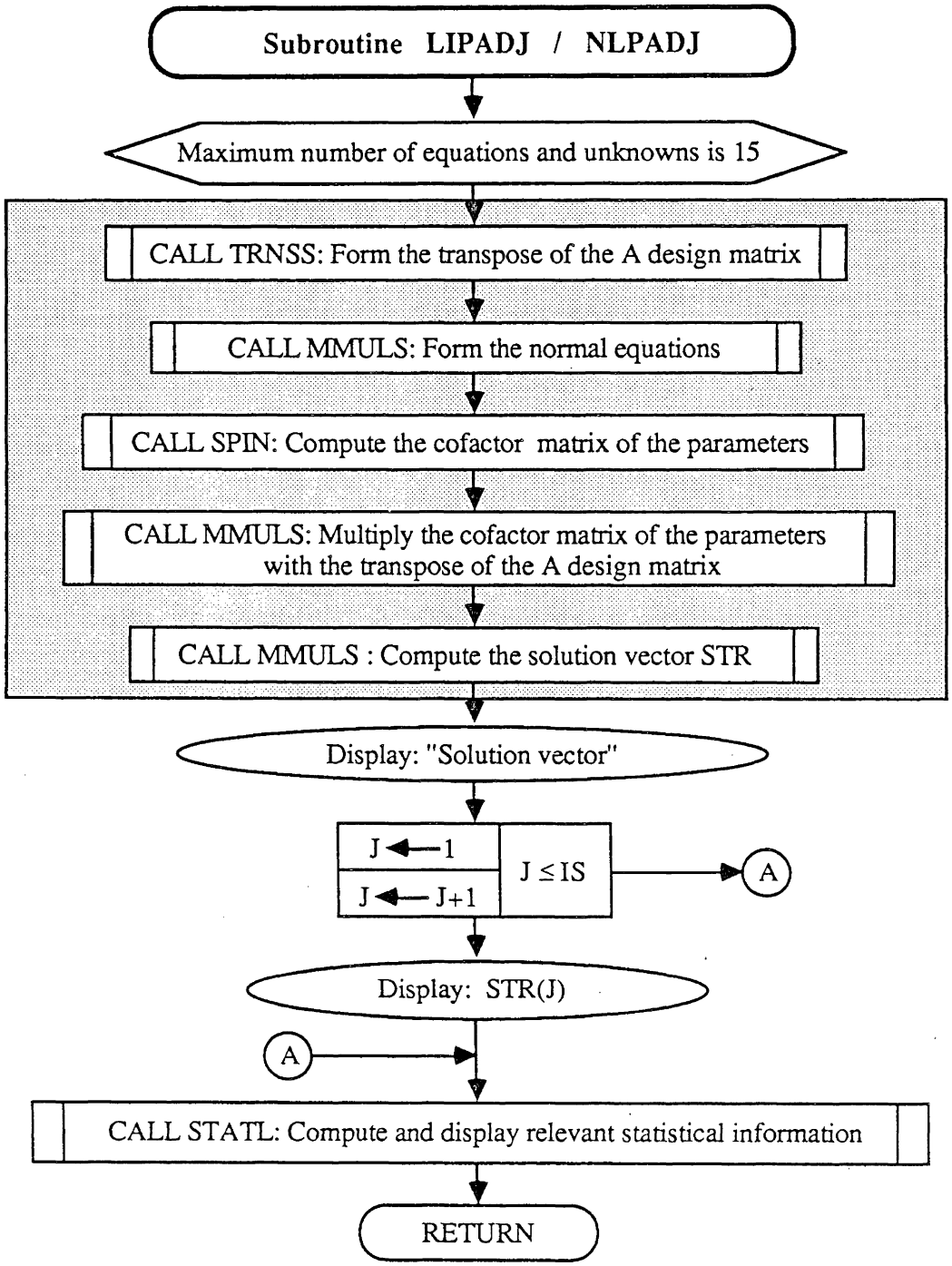

Contains operations for subroutine NLPADJ

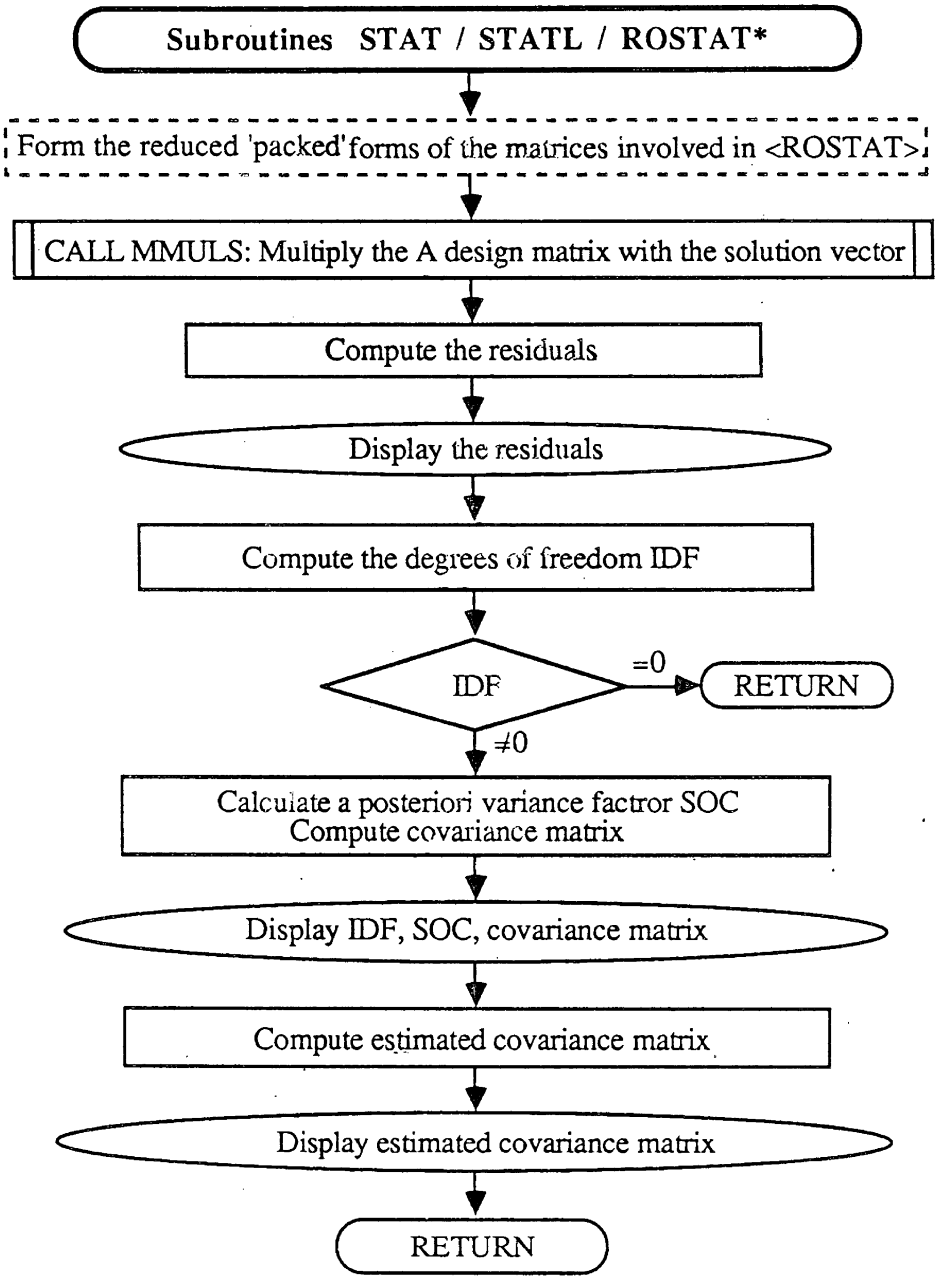

* STATL is called by <LIPADJ>, STAT is call by <NLPADJ>
ROSTAT is called by <RELOR>

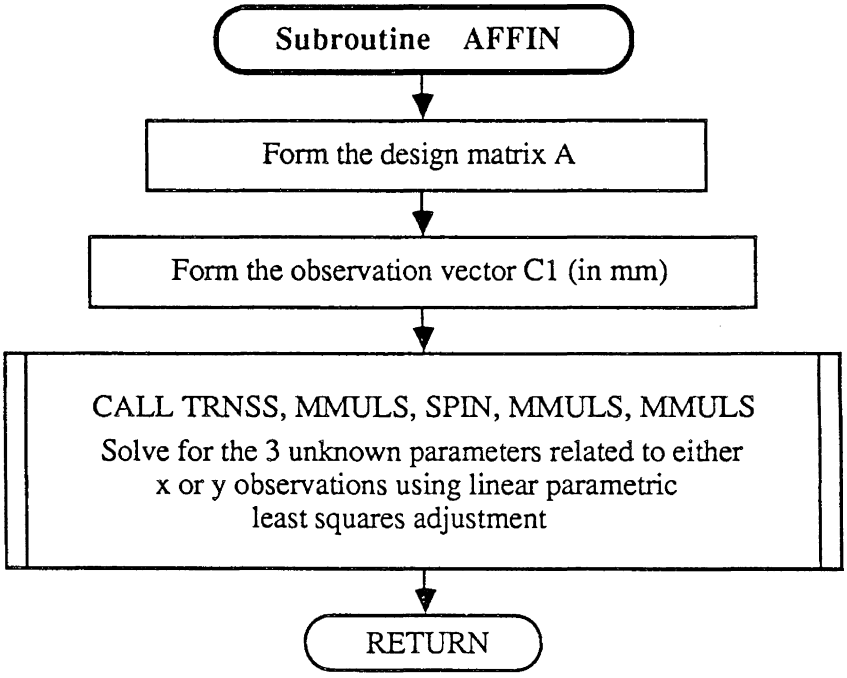
Subroutine AFFIN
Form the design matrix A
Form the observation vector C1 (in mm)
CALL TRNSS, MMULS, SPIN, MMULS, MMULS
Solve for the 3 unknown parameters related to either
x or y observations using linear parametric
least squares adjustment
RETURN

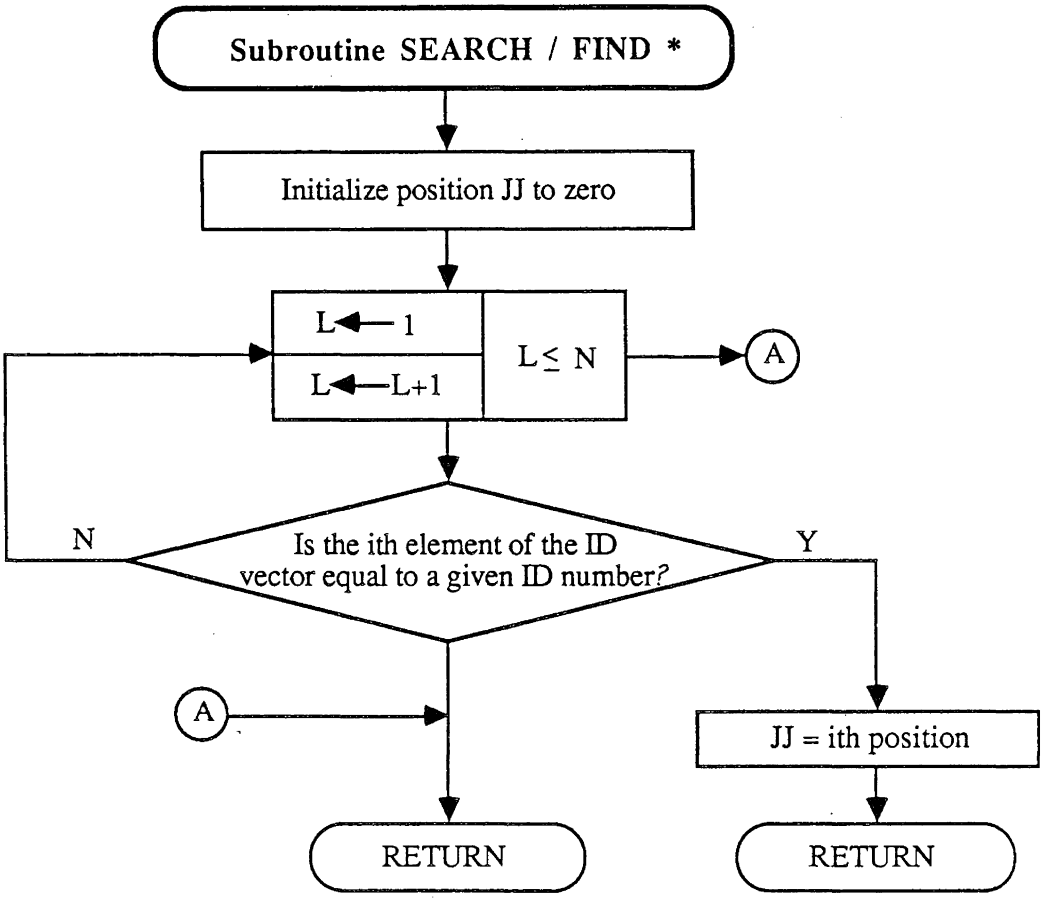

* While they perform the same task, < SEARCH > includes a blank COMMON area

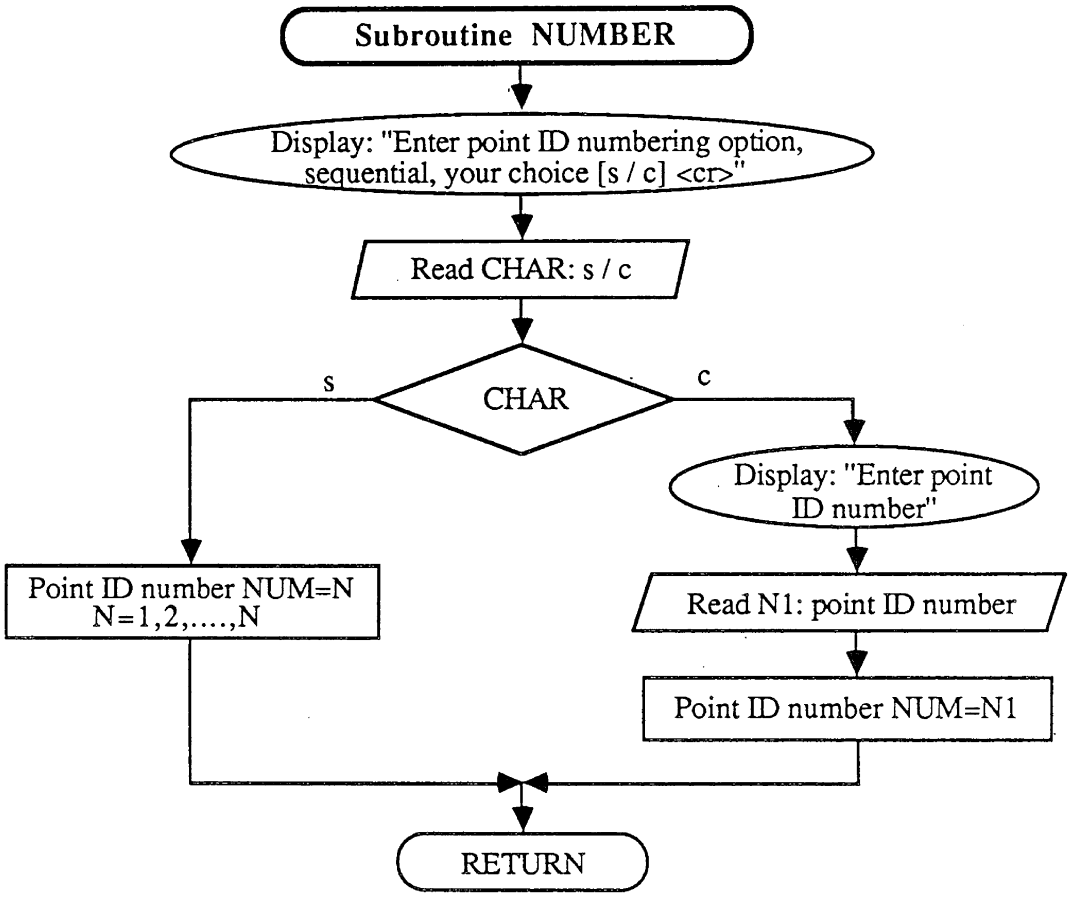
Subroutine NUMBER
Display: "Enter point ID numbering option, sequential, your choice [s / c] <cr>"
Read CHAR: s / c
CHAR
s
c
Point ID number NUM=N
N=1,2,....,N
Display: "Enter point ID number"
Read N1: point ID number
Point ID number NUM=N1
RETURN

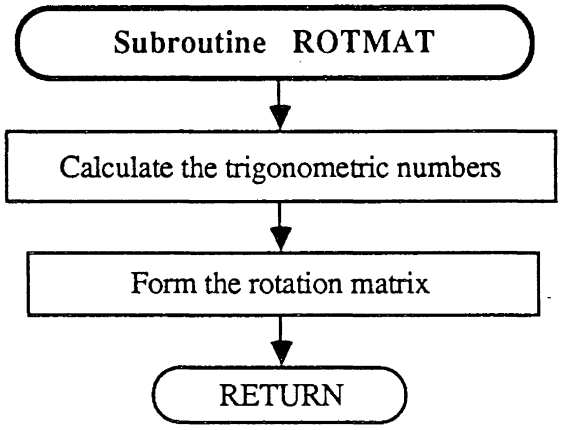
Subroutine ROTMAT
Calculate the trigonometric numbers
Form the rotation matrix
RETURN

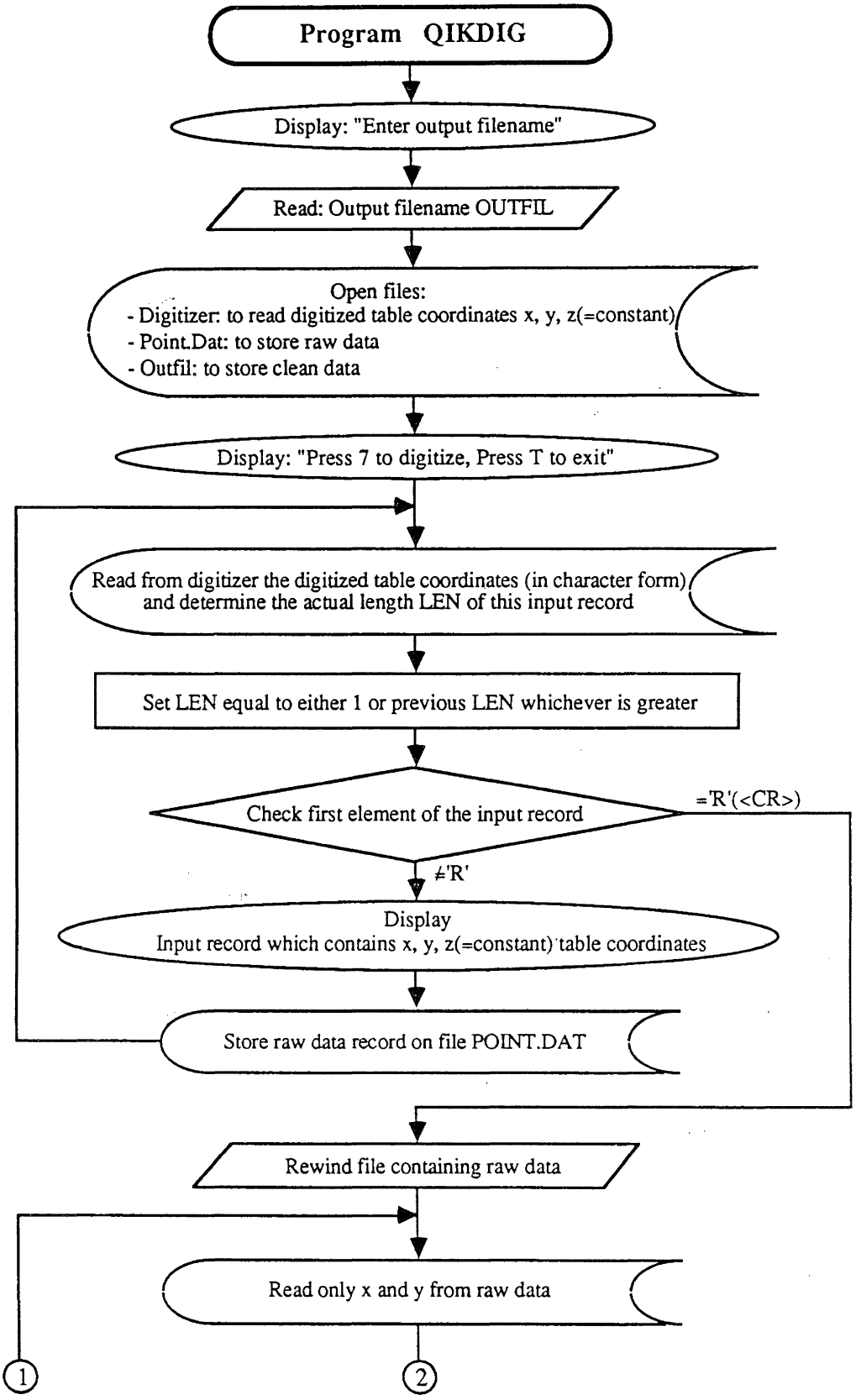
Program QIKDIG
Display: "Enter output filename"
Read: Output filename OUTFIL
Open files:
- Digitizer: to read digitized table coordinates x, y, z(=constant)
- Point.Dat: to store raw data
- Outfil: to store clean data
Display: "Press 7 to digitize, Press T to exit"
Read from digitizer the digitized table coordinates (in character form)
and determine the actual length LEN of this input record
Set LEN equal to either 1 or previous LEN whichever is greater
Check first element of the input record
='R'(<CR>)
≠'R'
Display
Input record which contains x, y, z(=constant) table coordinates
Store raw data record on file POINT.DAT
Rewind file containing raw data
Read only x and y from raw data
1
2

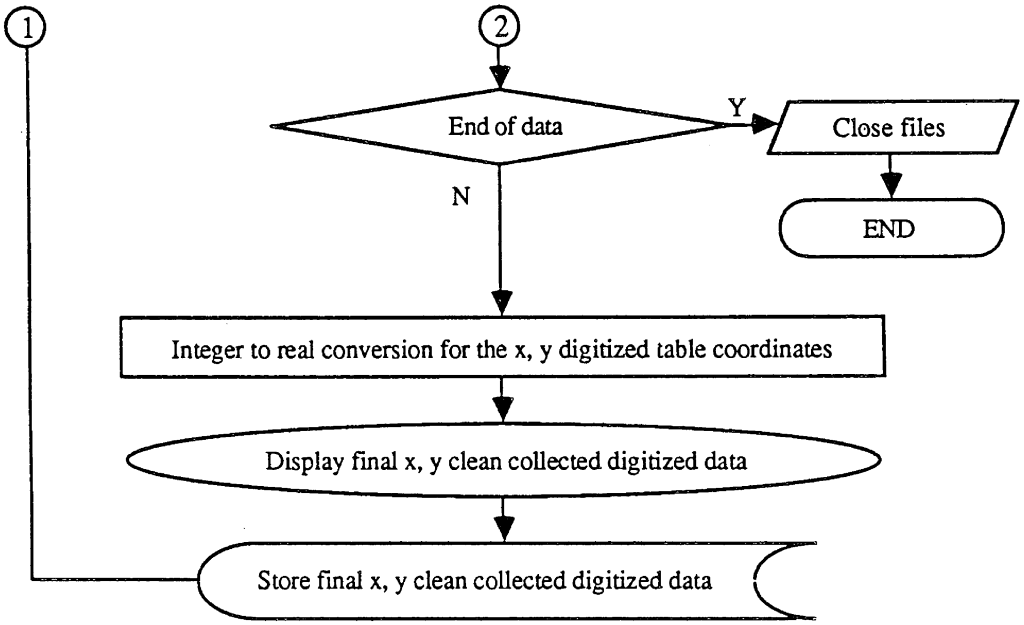

Note: Prior to the execution of program <QIKDIG> type:
ASSIGN TT7: DC:

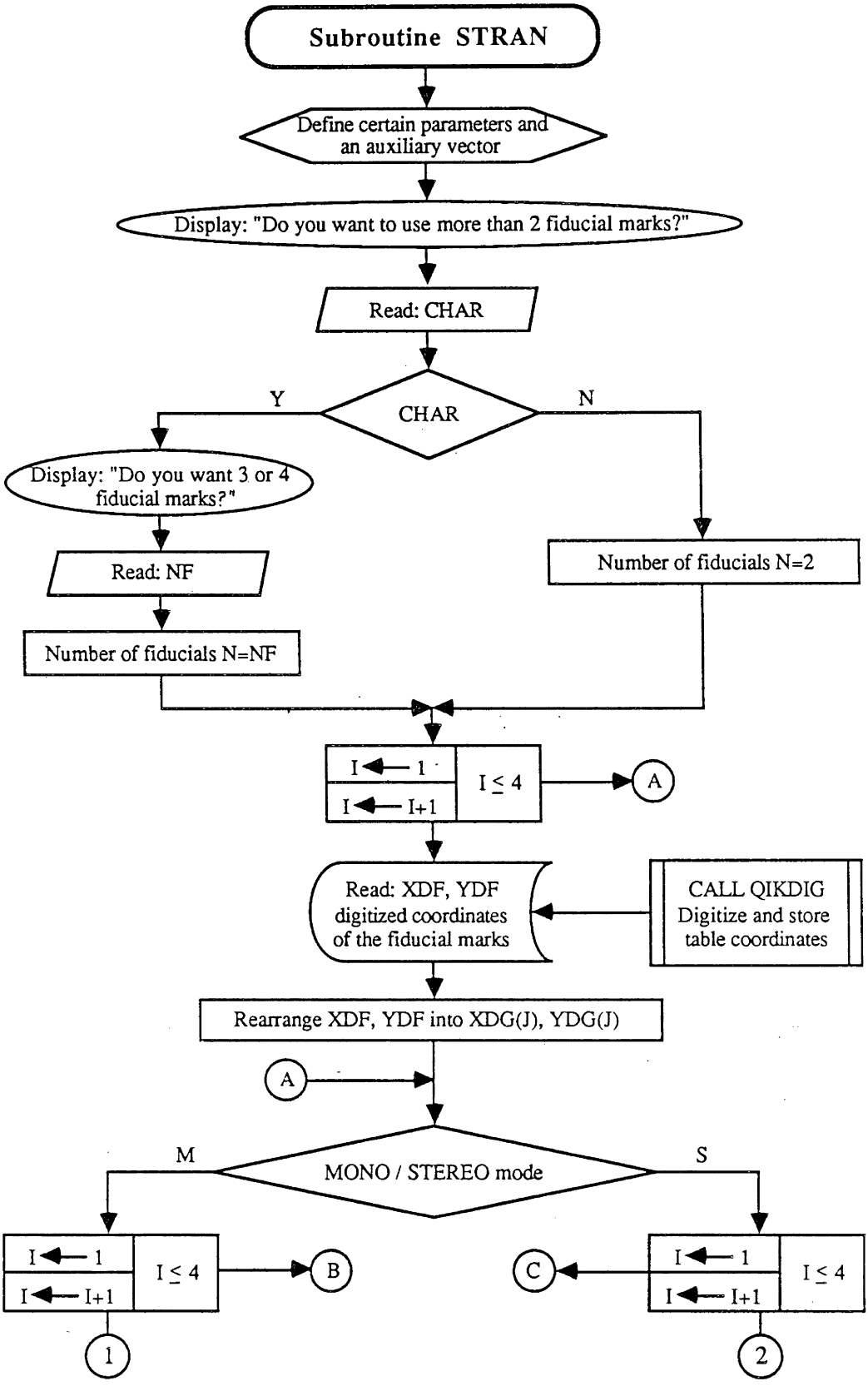
Subroutine STRAN
Define certain parameters and an auxiliary vector
Display: "Do you want to use more than 2 fiducial marks?"
Read: CHAR
CHAR
Y
N
Display: "Do you want 3 or 4 fiducial marks?"
Read: NF
Number of fiducials N=NF
Number of fiducials N=2
I ← 1
I ← I+1
I ≤ 4
A
Read: XDF, YDF digitized coordinates of the fiducial marks
CALL QIKDIG Digitize and store table coordinates
Rearrange XDF, YDF into XDG(J), YDG(J)
A
MONO / STEREO mode
M
S
I ← 1
I ← I+1
I ≤ 4
B
1
C
I ← 1
I ← I+1
I ≤ 4
2

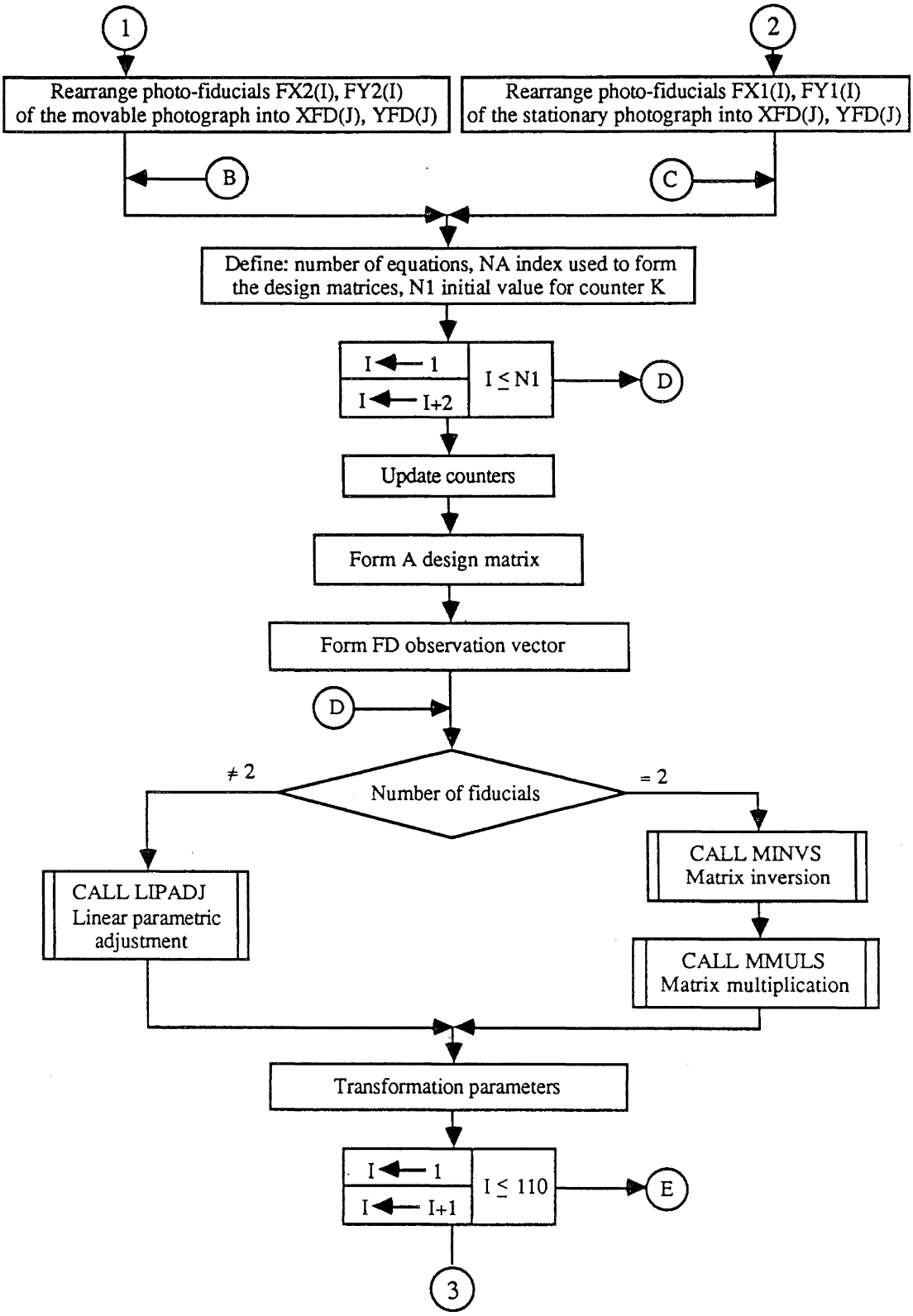
1
2
Rearrange photo-fiducials FX2(I), FY2(I) of the movable photograph into XFD(J), YFD(J)
Rearrange photo-fiducials FX1(I), FY1(I) of the stationary photograph into XFD(J), YFD(J)
B
C
Define: number of equations, NA index used to form the design matrices, N1 initial value for counter K
I ← 1
I ← I+2
I ≤ N1
D
Update counters
Form A design matrix
Form FD observation vector
D
≠ 2
Number of fiducials
= 2
CALL LIPADJ Linear parametric adjustment
CALL MINVS Matrix inversion
CALL MMULS Matrix multiplication
Transformation parameters
I ← 1
I ← I+1
I ≤ 110
E
3

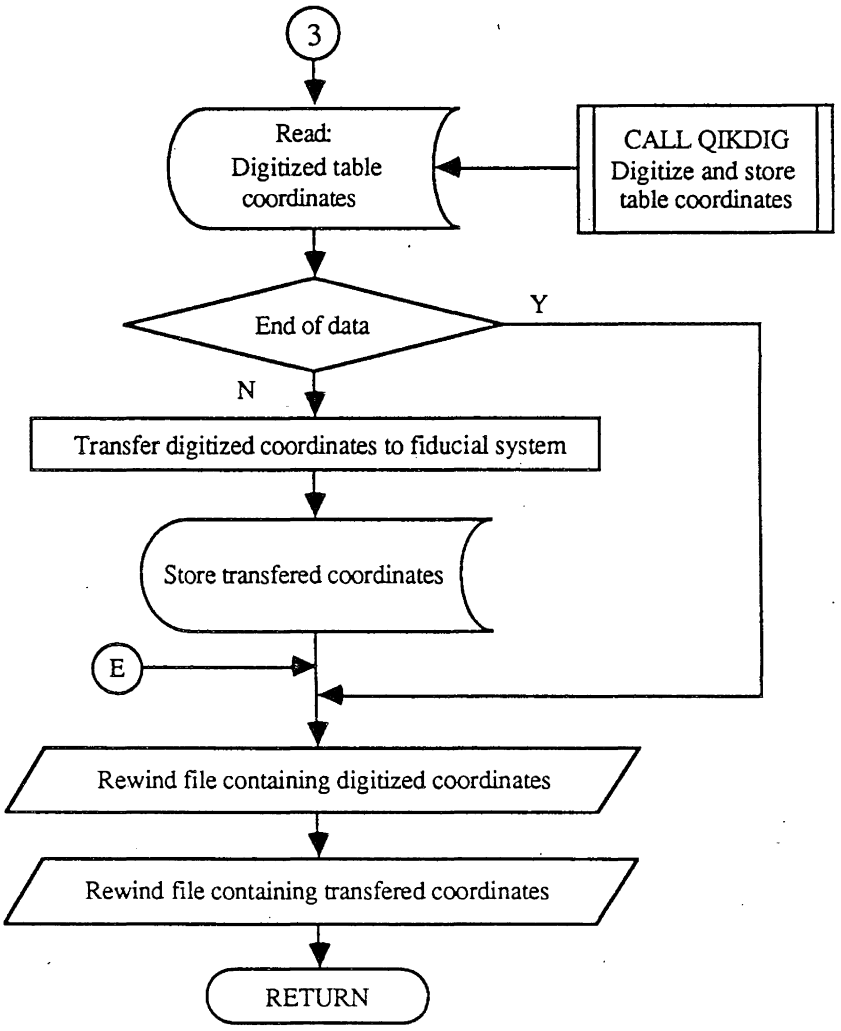
3
Read:
Digitized table
coordinates
CALL QIKDIG
Digitize and store
table coordinates
End of data
Y
N
Transfer digitized coordinates to fiducial system
Store transfered coordinates
E
Rewind file containing digitized coordinates
Rewind file containing transfered coordinates
RETURN

APPENDIX II

Subroutines of Program <PTBV>

(Photogrammetric Triangulation by Bundles - Photo Variant)

MAIN: Performs initialization and calls various main routines.

PHOTO: Processes photo-information. Computes approximate object coordinates.

ROTMAT: Forms the rotation matrix.

FIND: Performs searching operations.

SORTD: Performs sorting operations.

OBJECT: Processes object information. Performs necessary checks. Computes degrees of freedom.

ADJUST: Performs the bundle adjustment.

EMAT: Forms the design matrix of the unknown exterior orientation parameters.

AMAT: Forms the design matrix of the unknown object coordinates.

PMAT: Forms the design matrix of the unknown interior orientation parameters.

WPMAT: Forms the misclosure vector of the photogrammetric observations.

WIMAT: Forms the misclosure vector of the observations of the interior orientation elements.

OBCOR: Computes the corrections (solution) to the object coordinates.

PHORES: Computes the residuals of the photogrammetric observations. Computes the quadratic forms of the photo- and interior orientation- residuals. Computes pertinent statistical information.

CEKRES: Computes the differences at check points. Computes pertinent statistical information.

COVAR: Computes the variance-covariance matrix of the object coordinates.

CEKCON: Computes the residuals at the control points, their quadratic form, and pertinent statistical information. Computes the a-posteriori variance factor.

SPIN: Matrix inversion subroutine for symmetric positive-definite matrices.

SYMSYS: Solves the normal equations for the least squares when the coefficient matrix is positive-definite and in symmetric storage mode.

CHOLDP: Performs the Cholesky decomposition of a positive-definite matrix in symmetric storage mode.

ELIM: Performs forward and backward substitution.

MESAG: Prints messages for error conditions.

MMULD: Matrix multiplication subroutine.

TRNSD: Matrix transposition subroutine.

APPENDIX III

Subroutines of Program <SPDM>

(Sequential Photogrammetric Displacement Monitoring)

MAIN: Performs initialization and calls various main routines.

PHOTOP: Processes photo -and predicted- information.

PREDIC: Computes the predicted object coordinates and their predicted variance-covariance matrix.

ROTMAT: Forms the rotation matrix.

FIND: Performs searching operations.

SORTD: Performs sorting operations.

DISMAT: Forms the displacement transformation matrix **T**.

OBJECT: Modified version of the corresponding routine in <PTBV>. Processes object information. Performs necessary checks. Computes the degrees of freedom.

ADJUST: Modified version of the corresponding routine in <PTBV>. Performs the bundle and sequential adjustment.

EMAT: Forms the design matrix of the unknown exterior orientation parameters.

AMAT: Forms the design matrix of the unknown object coordinates.

PMAT: Forms the design matrix of the unknown interior orientation parameters.

WPMAT: Forms the misclosure vector of the photogrammetric observations.

WIMAT: Forms the misclosure vector of the observations of the interior orientation elements.

FILTER: Computes the updated object coordinates.

UPCOVF: Computes the updated variance-covariance matrix of the updated object coordinates.

SIGDIS: Computes and examines the significance of the displacements.

PHORES: Computes the residuals of the photogrammetric observations. Computes the quadratic forms of the photo -and interior orientation- residuals. Computes pertinent statistical information.

CEKRES: Computes the differences at check points. Computes pertinent statistical information.

COVAR: Modified version of the corresponding routine in <PTBV>. Computes variance-covariance matrix of the object coordinates.

CEKCON: Modified version of the corresponding routine in <PTBV>. Computes the residuals at the control points, their quadratic form, and pertinent statistical information. Computes the a-posteriori variance factor.

SPIN: Matrix inversion subroutine for symmetric positive definite matrices.

SYMSYS: Solves the normal equations of the least squares when the coefficient matrix is positive-definite and in symmetric storage mode.

CHOLDP: Performs the Cholesky decomposition of a positive-definite matrix in symmetric storage mode.

ELIM: Performs forward and backward substitution.

MESAG: Prints messages for error conditions.

MMULD: Matrix multiplication subroutine.

TRNSD: Matrix transposition subroutine.

APPENDIX IV

Affine or Six-Parameter Transformation

The affine transformation between two coordinate systems is defined by the following six parameters (Fig.IV-1):

1) Rotation of the axes through an angle Θ
2) Translation of the origin in x-direction by c
3) Translation of the origin in y-direction by f
4) Uniform scale change K_x along the x-direction
5) Uniform scale change K_y along the y-direction
6) Non-orthogonality of the axes of one system expressed by a small angle β.

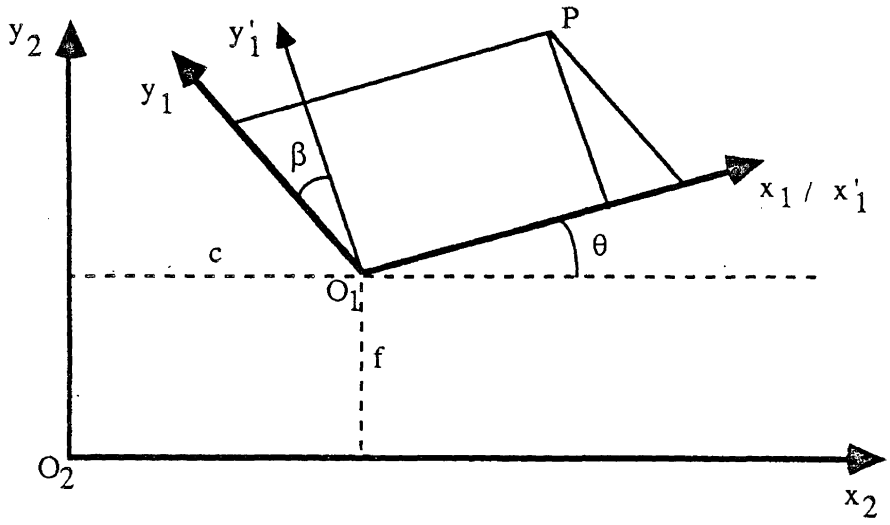

Figure IV-1: Geometry of the affine transformation between two coordinate systems (x_1,y_1 -> x_2,y_2).

The general form of the affine transformation equations can be derived from Figure IV-1 and is :

$$\mathbf{x}_2 = \mathbf{R}_\Theta \, \mathbf{R}_\beta \, \mathbf{K} \, \mathbf{x}_1 + \mathbf{t} \qquad \text{(IV-1)}$$

or explicitly

$$\begin{bmatrix} x_2 \\ y_2 \end{bmatrix} = \begin{bmatrix} \cos\Theta & -\sin\Theta \\ \sin\Theta & \cos\Theta \end{bmatrix} \begin{bmatrix} 1 & -\sin\beta \\ 0 & \cos\beta \end{bmatrix} \begin{bmatrix} k_x & 0 \\ 0 & k_y \end{bmatrix} \begin{bmatrix} x_1 \\ y_1 \end{bmatrix} + \begin{bmatrix} c \\ f \end{bmatrix} \qquad \text{(IV-2)}$$

where

x_1, y_1 represent the measuring system (e.g.,comparator axes)

x_2, y_2 represent the reference system (e.g.,calibrated axes)

Equation (IV-2) can also be written in linear form, which is the one used for practical and computational reasons. Thus,

$$\begin{aligned} x_2 &= a\, x_1 + b\, y_1 + c \\ y_2 &= d\, x_1 + e\, y_1 + f \end{aligned} \qquad \text{(IV-3)}$$

where

$$a = k_x \cos\Theta \qquad \text{(IV-4.1)}$$

$$b = -\, k_y \sin(\Theta + \beta) = -\, k_y \sin\alpha \qquad \text{(IV-4.2)}$$

$$d = k_x \sin\Theta \qquad \text{(IV-4.3)}$$

$$e = k_y \cos(\Theta + \beta) = k_y \cos\alpha \qquad \text{(IV-4.4)}$$

The parameters a, b, c, d, e, and f of equ.(IV-3) are usually estimated by the method of least squares. While the translation parameters c and f are directly determined, the remaining four physical parameters are explicitly determined using equs.(IV-4). Therefore,

$$K_x = (a^2 + d^2)^{1/2}$$

$$K_y = (b^2 + e^2)^{1/2}$$

$$\Theta = \left[\cos^{-1}\left[-\frac{a}{K_x}\right] + \sin^{-1}\left[-\frac{d}{K_x}\right] \right] /2$$

$$\alpha = \left[\sin^{-1}\left[-\frac{b}{K_y}\right] + \cos^{-1}\left[-\frac{e}{K_y}\right] \right] /2$$

$$\beta = \alpha - \Theta$$

APPENDIX V

Proof of Matrix Inversion Identity

We need to show that:

$$(A + BDB^T)^{-1} = A^{-1} - A^{-1}B\,(D^{-1} + B^TA^{-1}B)^{-1}B^TA^{-1} \qquad (V\text{-}1)$$

Proof:

Post multiplying the right hand side of the above expression by $(A + BDB^T)$ we have

$$A^{-1}(A + BDB^T) - A^{-1}B\,(D^{-1}+B^TA^{-1}B)^{-1}B^TA^{-1}(A + BDB^T) =$$

$$=A^{-1}A + A^{-1}BDB^T - A^{-1}B(D^{-1}+B^TA^{-1}B)^{-1}B^TA^{-1}A -$$

$$-A^{-1}B(D^{-1} + B^TA^{-1}B)^{-1}B^TA^{-1}BDB^T=$$

$$= I + A^{-1}BDB^T - A^{-1}B(D^{-1} + B^TA^{-1}B)^{-1}B^TI -$$

$$-A^{-1}B(D^{-1} + B^TA^{-1}B)^{-1}B^TA^{-1}BDB^T \qquad (V\text{-}2)$$

Factoring out the terms $A^{-1}B$ and B^T in equ.(V-2) we obtain

$$I + A^{-1}B[D - (D^{-1} + B^TA^{-1}B)^{-1}]\,B^T-$$

$$-A^{-1}B[\,(D^{-1} + B^TA^{-1}B)^{-1}B^TA^{-1}BD\,]\,B^T \qquad (V\text{-}3)$$

Post multiplying also the left hand side of equ.(V-1) by $(A + BDB^T)$ results in the unit matrix I. Therefore, the matrix identity is valid if the expression (V-3) is equal to the unit matrix I. This is true if

$$D - (D^{-1} + B^T A^{-1} B)^{-1} = (D^{-1} + B^T A^{-1} B)^{-1} B^T A^{-1} BD \qquad \text{(V-4)}$$

Pre-multiplying both sides of equ.(V-4) by $(D^{-1} + B^T A^{-1} B)$ we have:

For the left hand side

$$(D^{-1} + B^T A^{-1} B)\ [D - (D^{-1} + B^T A^{-1} B)^{-1}] =$$

$$= D^{-1} D + B^T A^{-1} BD - (D^{-1} + B^T A^{-1} B)\ (D^{-1} + B^T A^{-1} B)^{-1} =$$

$$= B^T A^{-1} BD \qquad \text{(V-5)}$$

For the right hand side

$$(D^{-1} + B^T A^{-1} B)\ [(D^{-1} + B^T A^{-1} B)^{-1} B^T A^{-1} BD] =$$

$$= (D^{-1} + B^T A^{-1} B)\ (D^{-1} + B^T A^{-1} B)^{-1} B^T A^{-1} BD =$$

$$= B^T A^{-1} BD \qquad \text{(V-6)}$$

Thus, equ.(V-4) is valid because its left hand side term is equal to its right hand side term because of equs. (V-5) and (V-6). Therefore, the matrix expression (V-1) is true.